

University of Missouri, St. Louis

IRL @ UMSL

---

Dissertations

UMSL Graduate Works

---

10-26-2010

## Activation of the Innate Immune Response by the Alzheimer's Amyloid Beta Protein Via Toll-Like Receptors

Udan Lourdes Maria

University of Missouri-St. Louis, malou\_u@yahoo.com

Follow this and additional works at: <https://irl.umsl.edu/dissertation>

 Part of the [Chemistry Commons](#)

---

### Recommended Citation

Maria, Udan Lourdes, "Activation of the Innate Immune Response by the Alzheimer's Amyloid Beta Protein Via Toll-Like Receptors" (2010). *Dissertations*. 460.

<https://irl.umsl.edu/dissertation/460>

This Dissertation is brought to you for free and open access by the UMSL Graduate Works at IRL @ UMSL. It has been accepted for inclusion in Dissertations by an authorized administrator of IRL @ UMSL. For more information, please contact [marvinh@umsl.edu](mailto:marvinh@umsl.edu).

ACTIVATION OF THE INNATE IMMUNE RESPONSE BY  
THE ALZHEIMER'S AMYLOID BETA PROTEIN  
VIA TOLL-LIKE RECEPTORS

A Dissertation

Submitted to the Faculty

of

University of Missouri-Saint Louis

by

Maria L.D. Udan

In Partial Fulfillment of the

Requirements for the Degree

of

Doctor of Philosophy

Chemistry and Biochemistry

August 2009

University of Missouri-Saint Louis

Saint Louis, Missouri

For my mama and papa...

## ACKNOWLEDGEMENTS

My sincerest gratitude goes to my advisor, Dr. Michael R. Nichols, for giving me continuous support and encouragement throughout my PhD, and for challenging me to think outside the box.

I would also like to thank my committee members, Dr. Alexei Demchenko, Dr. Chung Wong and Dr. Bethany Zolman for all the comments and suggestions in my dissertation.

My five years in the lab wouldn't be as exciting if not for my present and previous labmates- Deepa Ajit, Nikkilina Crouse, Geeta Paranjape, Laura Williams and Darcy Denner. I deeply appreciate all the brainstorming sessions and stimulating discussions that we had. My dissertation wouldn't be complete without all your help.

To my colleagues at the Department of Chemistry and Biochemistry, thank you all for being so helpful, cheerful and very supportive, and to the Center for Nanoscience for letting us use the microscopy facility.

I would like to thank all my friends and relatives who continue to encourage, support and believe in me, especially Deepa not only for the AFM images but also for the strong bond that we have built throughout the years, Darcy for being the best friend ever, and my uncle Nato for encouraging me to be the best that I can be.

In addition, my sincerest thanks to the Johns family, Larry, Debby, Lauren and Ryan, for becoming my second family here in St. Louis. Thank you for your prayers and encouragements. Ryan, thank you for loving me and for believing in me. I appreciate all the things that you've done for me. I want you to know that you're a big part of my success. You are my inspiration.

And lastly, I would like to thank my family, for always having faith in me. Without your love and prayers, I wouldn't be able to reach this far. I am who I am now because of you. My success is your success. Mama and Papa, I dedicate this dissertation to you both.

## TABLE OF CONTENTS

	PAGE
LIST OF TABLES .....	vii
LIST OF FIGURES .....	viii
LIST OF ABBREVIATIONS .....	x
ABSTRACT .....	xiv
PUBLICATION .....	xvi
<b>1 INTRODUCTION</b>	
1.1 Alzheimer’s Disease: Comprehending the etiology of the disease .....	1
1.1.1 Neurofibrillary Tangles .....	2
1.1.2 Senile plaques .....	3
1.2 Probing the molecular mechanism of AD: Focus on amyloid $\beta$ -Protein ( $A\beta$ ).....	4
1.2.1 Amyloid precursor protein processing and generation of $A\beta$ ....	5
1.2.2 Missense mutations in APP and other mutations cause autosomal dominant AD .....	9
1.2.3 Amyloid- $\beta$ peptide .....	13
1.2.4 Amyloid $\beta$ fibrillogenesis .....	17
1.2.5 Correlation between $A\beta$ assembly and AD .....	23
1.3 AD and inflammation .....	26
1.4 Toll-like receptors and innate immunity .....	32
1.4.1 Toll-like receptors (TLR) .....	34
1.4.1.1 TLR4 .....	39
1.4.1.2 TLR2, TLR1, TLR6 .....	45
1.4.2 TLRs and $A\beta$ : What is the connection? .....	47
1.5 Bibliography .....	50
<b>2 GENERAL METHODS</b>	
2.1 Cell Culture .....	66
2.1.1 THP-1 monocytes .....	66
2.1.1.1 THP-1 storage, growth and culture .....	66
2.1.1.2 THP-1 preparation for experimentation .....	68
2.1.2 Human Embryonic Kidney (HEK293) cells .....	69
2.2 Preparation of $A\beta$ peptides .....	73
2.3 Activation of cell model systems .....	73
2.4 Conversion of non-adherent THP-1 monocytes to adhering cells .....	75

2.5 LPS contamination assay .....	76
2.6 TLR antibody neutralization assay .....	76
2.7 Measurement of proinflammatory products .....	77
2.8 Cell viability assay .....	78
2.9 Atomic Force Microscopy .....	81
2.10 Statistical analysis .....	81
2.11 Bibliography .....	82
3 MODULATION OF AMYLOID BETA AGGREGATION MORPHOLOGY AND ITS EFFECT ON PROINFLAMMATORY RESPONSE OF THP-1 MONOCYTES	
3.1 Introduction .....	84
3.2 Results .....	86
3.2.1 A $\beta$ aggregation and proinflammatory response .....	86
3.2.2 Modulation of A $\beta$ aggregation .....	92
3.3 Discussion .....	96
3.4 Bibliography .....	103
4 THE ROLE OF TOLL-LIKE RECEPTORS IN AMYLOID BETA(1-42) ACTIVATION OF THE INNATE IMMUNE RESPONSE	
4.1 Introduction .....	109
4.2 Results .....	111
4.2.1 Mammalian cell model system: THP-1 monocytes .....	111
4.2.1.1 Toll-like receptor ligands activate the proinflammatory response in THP-1 monocytes .....	111
4.2.1.2 Amyloid beta (1-42) is devoid of any contamination .....	112
4.2.1.3 Toll-like receptor antibody neutralization assay was effective in blocking the activity of known TLR agonists bacterial LPS and synthetic Pam <sub>3</sub> CSK <sub>4</sub> .....	116
4.2.1.4 TLR2 and TLR4 play a role in fibrillar A $\beta$ (1-42)- induced TNF $\alpha$ response in THP-1 monocytes .....	120
4.2.1.5 TLR1 and TLR6 may also be involved in fibrillar A $\beta$ (1-42)-induced activation of the innate immune response .....	127
4.2.2 Mammalian cell system: Human Embryonic Kidney (HEK) cells .....	131
4.2.2.1 Induction of proinflammatory IL-8 production in transfected HEK 293 cells with known TLR agonists .....	131
4.2.2.2 Induction of proinflammatory IL-8 production in transfected HEK 293 cells with fibrillar A $\beta$ (1-42) .....	135
4.3 Discussion .....	136
4.4 Bibliography .....	143

5 THE ROLE OF MONOCYTE MATURATION AND ITS RELATIONSHIP TO A $\beta$ AND INFLAMMATION	
5.1 Introduction .....	148
5.2 Results .....	149
5.2.1 TNF $\alpha$ production induced by known TLR agonists in differentiated and undifferentiated THP-1 cells .....	149
5.2.2 A $\beta$ -induced TNF $\alpha$ production is augmented in PMA-derived THP-1 macrophages .....	150
5.3 Discussion .....	153
5.4 Bibliography .....	157
6 CONCLUSION .....	160
VITA .....	162

## LIST OF TABLES

	PAGE
1.1 Cytotoxic actions of amyloid- $\beta$ peptide .....	24
1.2 Microglial antigens and inflammatory mediators elevated in Alzheimer's disease .....	31
1.3 Human TLRs and ligands .....	37

## LIST OF FIGURES

	PAGE
1.1 Processing of Amyloid precursor protein (APP) .....	7
1.2 APP mutations genetically linked to familial Alzheimer's disease .....	10
1.3 Structural studies of A $\beta$ .....	15
1.4 Mechanism of A $\beta$ fibril formation .....	19
1.5 The toll-like receptor signaling pathway .....	38
1.6 Chemical structure of known TLR agonists .....	41
1.7 TLR2 and TLR4 signaling pathway .....	43
2.1 Schematic diagram of the subculture of HEK293 cells .....	70
2.2 Optimization of HEK 293 adhesion time prior to stimulation With Pam <sub>3</sub> CSK <sub>4</sub> .....	72
2.3 Effect of HEK293 passage number on fibrillar A $\beta$ (1-42) response .....	74
2.4 Conversion of XTT to a water-soluble formazan salt by viable cells .....	80
3.1 Proinflammatory activity of synthetic A $\beta$ (1-42) at different aggregation .....	87
3.2 Morphological studies of A $\beta$ (1-42) aggregated species .....	90
3.3 Effect of exposure time on A $\beta$ (1-42)-, LPS- and Pam <sub>3</sub> CSK <sub>4</sub> - induced TNF $\alpha$ response in THP-1 cells .....	91
3.4 Proinflammatory activity and morphological studies of Concentrated A $\beta$ (1-42) sample .....	93
3.5 Accelerated aggregation of A $\beta$ (1-42) by increasing the incubation temperature failed to invoke TNF $\alpha$ response in THP-1 monocytes .....	95
3.6 A $\beta$ (1-40) failed to induce proinflammatory activity on THP-1 cells .....	97
4.1 Known TLR agonists induce TNF $\alpha$ production in a dose-dependent manner .....	113
4.2 PMX-B is a powerful tool for ruling out the presence of small traces of contaminating bacterial LPS .....	115
4.3 Toll-like receptor (TLR) neutralization of bacterial lipopolysaccharide .....	117
4.4 TLR antibody neutralization of bacterial lipopolysaccharide and Pam <sub>3</sub> CSK <sub>4</sub> .....	119
4.5 TLR2, TLR4 and CD14 play an active role in A $\beta$ -induced innate immune response activation .....	122
4.6 Dose-dependent neutralizing ability of TLR antibodies against A $\beta$ (1-42) .....	123
4.7 Combination TLR antibody neutralization of A $\beta$ (1-42)-induced TNF $\alpha$ response .....	126
4.8 TLR2 complex antibody neutralization of known TLR2 agonists, synthetic	

diacylated or triacylated lipopeptide .....	128
4.9 Combination TLR2 complex antibody neutralization of A $\beta$ (1-42)-induced TNF $\alpha$ response .....	130
4.10 PAMP activity on HEK 293 cells .....	133
4.11 TLR2 complex antibody neutralization of TLR2 ligands .....	134
4.12 Fibrillar A $\beta$ (1-42) activity on HEK 293 cells .....	137
5.1 LPS-induced TNF $\alpha$ production from differentiated and undifferentiated THP-1 cells .....	151
5.2 Dose response of TNF $\alpha$ production by known TLR agonists .....	152
5.2 Fibrillar A $\beta$ (1-42)- induced TNF $\alpha$ secretion from differentiated and undifferentiated THP-1 cells .....	154

## LIST OF ABBREVIATIONS

A $\beta$	Amyloid beta
AD	Alzheimer's Disease
ADDL	A $\beta$ -derived diffusible ligands
AFM	Atomic force microscopy
APP	Amyloid precursor protein
BBB	Blood-brain barrier
BPI	Bactericidal/permeability-increasing protein
CD	Circular dichroism
cdk5	Cyclin-dependent kinase 5
CHO	Chinese hamster ovary
CK1	Casein kinase 1
CNS	Central nervous system
CSF	Cerebrospinal fluid
DC	Dendritic cells
DMSO	Dimethyl sulfoxide
ELISA	Enzyme-linked immunosorbent assay
EM	Electron microscopy
EOAD	Early onset Alzheimer's disease
FAD	Familial Alzheimer's disease

FBS	Fetal bovine serum
FSL	Pam <sub>2</sub> CGDPKHPKSF; synthetic diacylated lipoprotein
FTD	Fronto-temporal dementia
FTIR	Fourier transform infrared spectroscopy
GS	<i>Griffonia simplicifolia</i>
GSK-3	Glycogen synthase kinase-3
HEK	Human embryonic kidney
HFIP	Hexafluoroisopropanol
IFN	Interferon
IgG	Immunoglobulin G
IL	Interleukin
IRAK	IL-1R associated kinase
KC	Keratinocyte chemoattractant
K <sub>D</sub>	Dissociation constant
LBP	Lipid-binding protein
LMW	Low molecular weight
LP	Lipoproteins
LPS	Lipopolysaccharide
LPT	Lipopeptide
LRR	Leucine-rich repeats
LTA	Lipoteichoic acid
MAP	Mitogen-activated protein
MCP	Monocyte chemoattractant

MHC	Major histocompatibility complex
MIP	Macrophage inflammatory protein
MS	Mass spectrometry
MTT	3-(4,5-dimethylthiazol-2-yl)-2-diphenyltetrazolium bromide
MyD88	Myeloid differentiation factor 88
NF- $\kappa$ B	Nuclear factor- $\kappa$ B
NFT	Neurofibrillary tangles
NMR	Nuclear magnetic resonance
NO	Nitric oxide
NSAID	Non-steroidal anti-inflammatory drug
PAMP	Pathogen-associated molecular pattern
Pam <sub>3</sub> CSK <sub>4</sub>	Tripalmytoyl cysteinyl seryl tetralysine
Pam <sub>3</sub> Cys	Tripalmytoyl-S-glyceryl-cysteine
PBM	Peripheral blood monocytes
PBS	Phosphate buffered saline
PGN	Peptidoglycan
PKA	cyclic AMP-dependent kinase
PMA	Phorbol 12-myristate 13-acetate
PMS	Phenazine methosulfate
PMX-B	Polymyxin-B sulfate
PRR	Pattern recognition receptor
QLS	Quasielastic light scattering spectroscopy
RAGE	Receptor for advanced glycation end products

R <sub>H</sub>	Hydrodynamic radius
rIgG	Rat immunoglobulin G
ROS	Reactive oxygen species
sAPP $\alpha$	soluble APP cleaved by $\alpha$ secretase
sAPP $\beta$	soluble APP cleaved by $\beta$ secretase
SD	Standard deviation
SE	Standard error
SEC	Size exclusion chromatography
SPR	Surface plasmon resonance
TGF	Transforming growth factor
TIR	Toll/IL-1 receptor
TIRAP	Toll-1L-1 receptor associated protein
TLR	Toll-like receptor
TNF $\alpha$	Tumor necrosis factor alpha
TRAF	TNF-receptor associated factor 6
TRAM	Toll receptor-associated molecule
TRIF	Toll-associated activator of IFN
WT	Wildtype
XTT	2,3-bis(2-methoxy-4-nitro-5-sulfohenyl)-2H-tetrazolium-5-carboxanilide
293-hRTLR2	HEK 293 cells transfected with TLR2
293-hTLR2/CD14	HEK 293 cells transfected with TLR2 and CD14

## ABSTRACT

Udan, Maria L.D. PhD., University of Missouri-Saint Louis, August 2009. Activation of the innate immune response by the Alzheimer's amyloid beta protein via Toll-like receptors. Major Professor: Michael R. Nichols

Alzheimer's Disease (AD) is the most common form of neurodegenerative disease characterized by the generation and deposition of amyloid beta plaques and the formation of neurofibrillary tangles. A wealth of data now demonstrate that inflammation is a prominent feature in AD pathology and a potential therapeutic target for the treatment and prevention of the disease. The emergence of evidence linking amyloid beta protein (A $\beta$ ), the primary component of senile plaques, to inflammation has led to new insights into understanding AD pathology. A $\beta$ , a protein fragment resulting from cleavage of human amyloid precursor protein (APP), primarily exists in two forms: a slower-aggregating 40-amino acid long peptide (A $\beta$ (1-40)), and a faster-aggregating 42-residue peptide A $\beta$ (1-42). This investigation focused on elucidating the mechanism by which A $\beta$  provokes an inflammatory response in AD. For this study, we utilized THP-1 human monocytes/macrophages as an inflammatory model system due to their sensitivity to A $\beta$ . We hypothesized that fibrillar A $\beta$ (1-42) may utilize Toll-like receptors (TLRs), a family of transmembrane receptors that mediate recognition of certain conserved structural motifs in pathogens, for production of proinflammatory products and activation of the innate immune response. Biophysical characterization of the bioactive species of A $\beta$ (1-42) revealed that a soluble yet fibrillar species of A $\beta$ (1-42) invokes tumor necrosis factor alpha (TNF $\alpha$ ) production in THP-1 monocytes/macrophages. Moreover, using a TLR antibody neutralization assay, whereby receptor blockade inhibits cell responsiveness to TLR ligands, we showed that both TLR2 and TLR4 were highly involved in A $\beta$ (1-42)-induced TNF $\alpha$  production. The role of TLR2 in A $\beta$ -induced innate immune response was further substantiated by the production of proinflammatory interleukin-8 (IL-8) in transfected HEK293 cells, a mammalian cell line that does not express TLR2, after stimulation with A $\beta$ (1-42). Furthermore, our results suggest the possible involvement of TLR2/TLR1 or TLR2/TLR6 for the A $\beta$ -induced activation of TLR downstream signaling. Taken together, our findings provide strong correlation between A $\beta$  and innate immune response activation via TLR2 and TLR4. The identification of TLRs that recognize A $\beta$  has opened new venues for understanding the mechanism of A $\beta$ -induced inflammatory response and may thus be a new therapeutic target for AD.

## PUBLICATION

## Toll-like receptors 2 and 4 mediate A $\beta$ (1-42) activation of the innate immune response in a human monocytic cell line

Maria L. D. Udan, Deepa Ajit, Nikkilina R. Crouse and Michael R. Nichols

Department of Chemistry and Biochemistry, University of Missouri, St Louis, Missouri, USA

### Abstract

The primary molecules for mediating the innate immune response are the Toll-like family of receptors (TLRs). Recent work has established that amyloid-beta (A $\beta$ ) fibrils, the primary components of senile plaques in Alzheimer's disease (AD), can interact with the TLR2/4 accessory protein CD14. Using antibody neutralization assays and tumor necrosis factor alpha release in the human monocytic THP-1 cell line, we determined that both TLR2 and TLR4 mediated an inflammatory response to aggregated A $\beta$ (1-42). This was in contrast to exclusive TLR ligands lipopolysaccharide (LPS) (TLR4) and tripalmitoyl cysteinyl seryl tetralysine (Pam<sub>3</sub>CSK<sub>4</sub>) (TLR2). Atomic force microscopy imaging showed a fibrillar morphology for the proinflammatory A $\beta$ (1-42) species. Pretreatment of the cells with 10  $\mu$ g/mL of a TLR2-specific antibody blocked ~50% of the cell response to fibrillar A $\beta$ (1-42), completely blocked the Pam<sub>3</sub>CSK<sub>4</sub> response, and had no ef-

fect on the LPS-induced response. A TLR4-specific antibody (10  $\mu$ g/mL) blocked ~35% of the cell response to fibrillar A $\beta$ (1-42), completely blocked the LPS response, and had no effect on the Pam<sub>3</sub>CSK<sub>4</sub> response. Polymyxin B abolished the LPS response with no effect on A $\beta$ (1-42) ruling out bacterial contamination of the A $\beta$  samples. Combination antibody pretreatments indicated that neutralization of TLR2, TLR4, and CD14 together was much more effective at blocking the A $\beta$ (1-42) response than the antibodies used alone. These data demonstrate that fibrillar A $\beta$ (1-42) can trigger the innate immune response and that both TLR2 and TLR4 mediate A $\beta$ -induced tumor necrosis factor alpha production in a human monocytic cell line.

**Keywords:** aggregation, Alzheimer's disease, amyloid- $\beta$  peptide, inflammation, innate immunity, Toll-like receptors.

*J. Neurochem.* (2008) **104**, 524-533.

Alzheimer's disease (AD) is a progressive neurodegenerative illness diagnosed clinically by cognitive decline and pathologically by the presence of extracellular neuritic plaques in limbic brain regions and intracellular neurofibrillary tangles (Selkoe 2001). The primary component of neuritic plaques is amyloid-beta (A $\beta$ ) (Glennner and Wong 1984), a 40- or 42-residue peptide derived from proteolysis of the amyloid- $\beta$  precursor protein. A large body of evidence supports the fundamental role of A $\beta$  in AD etiology. The monomeric form of A $\beta$  circulates ubiquitously in plasma and cerebrospinal fluid yet an aggregated insoluble fibrillar form comprises the characteristic AD deposits (Selkoe 2004). *In vitro* studies have shown that A $\beta$  monomer will undergo non-covalent self-assembly (Jarrett *et al.* 1993) to form a polydisperse mixture of soluble oligomers (Dahlgren *et al.* 2002) and protofibrils (Harper *et al.* 1999) that are enriched in  $\beta$ -sheet structure (Walsh *et al.* 1999) and ultimately insoluble fibrils (Harper *et al.* 1997a). The types of intermediates formed during fibrillogenesis are dependent on the solution conditions (Harper *et al.* 1999; Dahlgren *et al.* 2002). Cellular

studies have shown that fibrillar forms of A $\beta$  are toxic to neurons compared with the benign monomer (Yankner 1996) yet difficulties have been encountered trying to correlate insoluble fibrillar A $\beta$  with memory loss in a transgenic mouse model (Westerman *et al.* 2002). Therefore, much of the recent investigative focus has shifted to soluble A $\beta$  aggregates as early toxic agents (Haass and Selkoe 2007). Further research will clarify if one species can be implicated

Received May 17, 2007; revised manuscript received September 14, 2007; accepted September 17, 2007.

Address correspondence and reprint requests to Michael R. Nichols, PhD, Department of Chemistry and Biochemistry, University of Missouri, One University Blvd., St Louis, MO 63121, USA.  
E-mail: nicholsmic@umsl.edu

**Abbreviations used:** AD, Alzheimer's disease; AFM, atomic force microscopy; A $\beta$ , amyloid- $\beta$ ; BSA, bovine serum albumin; LPS, lipopolysaccharide; Pam<sub>3</sub>CSK<sub>4</sub>, tripalmitoyl cysteinyl seryl tetralysine; PAMPs, pathogen-associated molecular patterns; PBS, phosphate-buffered saline; PMX-B, polymyxin B; TLRs, Toll-like receptors; TNF $\alpha$ , tumor necrosis factor alpha; XTT, 2,3-bis (2-methoxy-4-nitro-5-sulphophenyl)-2H-tetrazolium-5-carboxanilide.

as the primary toxic agent in AD but it is becoming evident that morphologically diverse aggregation species can cause different harmful effects (Deshpande *et al.* 2006). The overall findings suggest that distinct toxic and biological mechanisms are dependent on a specific A $\beta$  structure or the extent of oligomerization.

One such biological activity of A $\beta$  is as a proinflammatory stimulus. It has been well documented that inflammatory markers such as activated microglia and proinflammatory cytokines have been observed surrounding A $\beta$  lesions in the human AD brain (McGeer *et al.* 1987). The parenchymal microglia are believed to originate from peripheral cells of the monocyte/microglial lineage which infiltrate the parenchyma and differentiate into microglial cells (Wegiel *et al.* 2004). The *in vivo* inflammatory response to A $\beta$  has been recapitulated in numerous *in vitro* cell model systems including both microglial and monocyte cells (Klegeris *et al.* 1997; Yates *et al.* 2000; Combs *et al.* 2001).

The mechanism by which A $\beta$  evokes a proinflammatory response appears to be quite complex. Fibrillar A $\beta$  serves as a ligand for both the scavenger receptor class A (El Khoury *et al.* 1996; Paresce *et al.* 1996) and receptor for advanced glycation end products (Yan *et al.* 1996) although neither is linked to a proinflammatory response. A multireceptor complex comprising the scavenger receptor class B receptor CD36,  $\alpha_5\beta_1$ -integrin, and the integrin-associated protein CD47 has been identified in mediating fibrillar A $\beta$  initiation of human THP-1 monocyte and murine microglial proinflammatory events (Bamberger *et al.* 2003) and phagocytosis of fibrillar A $\beta$  via atypical phagocytic mechanisms (Koenigsnecht and Landreth 2004).

Increasing evidence suggests that the human innate immune response may be triggered by aggregated A $\beta$ . Human innate immunity is an important line of defense during bacterial, fungal, or viral invasion and can involve production of proinflammatory cytokines, anti-microbial peptides (Hoffmann *et al.* 1999), and proteases (Mun-Bryce *et al.* 2002) to neutralize pathogens. The ability of phagocytic and immune cells to recognize these pathogens is due to motifs called pathogen-associated molecular patterns (PAMPs) which bind pattern recognition receptors. The primary mediators of the innate immune response are a family of transmembrane pattern recognition receptors termed Toll-like receptors (TLRs) which recognize PAMPs [reviewed in Hoffmann *et al.* (1999); Aderem and Ulevitch (2000)]. There are currently 11 human TLRs and they vary in their cellular localization and ability to detect distinct pathogens (Aderem and Ulevitch 2000; Boehme and Compton 2004). The most widely studied PAMP is bacterial lipopolysaccharide (LPS), an outer-membrane component of Gram-negative bacteria. LPS can activate TLR4 via complex formation with LPS-binding protein and CD14, a glycosylphosphatidylinositol-anchored but not membrane-spanning receptor (Boehme and Compton 2004). The function of

CD14 appears to be ligand-binding and presentation to membrane TLR4 and/or TLR2 (Kielian 2006), which transduce the signal through the membrane and initiate the intracellular innate immune response pathways. More recently, CD14 was shown to mediate uptake of double-stranded RNA and directly interact with intracellular TLR3 (Lee *et al.* 2006).

A growing number of endogenous human molecules now appear to activate the innate immune response (Kielian 2006) including the A $\beta$  peptide. A physical and functional interaction was demonstrated between fibrillar A $\beta$ (1–42) and CD14 that resulted in the release of inflammatory products in primary murine microglial cells and human peripheral blood mononuclear cells (Fassbender *et al.* 2004). Furthermore, CD14-mediated internalization of fibrillar A $\beta$ (1–42) by a phagocytic mechanism in microglia and increased CD14 immunostaining was observed in AD brain slices compared with age-matched controls (Liu *et al.* 2005). As CD14 can interact with both TLR4 and TLR2, we sought to determine which transmembrane TLR plays a functional role in transducing the A $\beta$ -induced innate immune signal through the membrane.

## Materials and methods

### Cell culture and cellular assays

The THP-1 cells were obtained from ATCC (Manassas, VA, USA) and maintained in RPMI-1640 culture medium (HyClone, Logan, UT, USA) containing 2 mmol/L L-glutamine, 25 mmol/L HEPES, 1.5 g/L sodium bicarbonate, 10% fetal bovine serum (HyClone), 50 U/mL penicillin, 50  $\mu$ g/mL streptomycin (HyClone), and 50  $\mu$ mol/L  $\beta$ -mercaptoethanol at 37°C in 5% CO<sub>2</sub>. For cellular assays, THP-1 cells were centrifuged, washed, and resuspended in reduced fetal bovine serum (2%) growth medium. Cell concentrations were adjusted to  $1.0 \times 10^6$  cells/mL and 0.3 mL was added to individual wells of a 48-well sterile culture plate. Proinflammatory modulators ultrapure bacterial LPS (*Escherichia coli* K12) and synthetic bacterial lipoprotein tripalmitoyl cysteinyl seryl tetralysine (Pam<sub>3</sub>CSK<sub>4</sub>) (InvivoGen, San Diego, CA, USA), and polymyxin B (PMX-B) sulfate (Sigma, St Louis, MO, USA) were added directly to cells and incubated at 37°C. Following incubation, the content of each well was removed, centrifuged at 2500 g for 10 min, and the supernatant was frozen at –20°C for subsequent analysis. Concentration-dependence data for TLR agonists were fit to a sigmoidal three-parameter equation using SigmaPlot graphing program to determine EC<sub>50</sub> values. A $\beta$ (1–42)-induced THP-1 cell adherence was measured by direct counting. At various time points the medium containing remaining suspension cells was removed, adherent cells were washed with phosphate-buffered saline (PBS) and removed with 0.25% trypsin-EDTA (HyClone). The medium, PBS wash, and removed adherent cells were counted under a microscope using a hemocytometer.

### Preparation of A $\beta$ peptides

A $\beta$ (1–42) peptides (rPeptide, Bogart, GA, USA) were dissolved in 100% hexafluoroisopropanol (Sigma) for 1 h, aliquotted into sterile

microcentrifuge tubes, dried in a vacuum centrifuge, and stored at  $-20^{\circ}\text{C}$ . Prior to cell treatment the lyophilized peptides were resuspended in sterile water to 100  $\mu\text{mol/L}$  peptide concentration and incubated at  $4^{\circ}\text{C}$ . Freshly reconstituted  $\text{A}\beta(1-42)$  in water was allowed to incubate at  $4^{\circ}\text{C}$  prior to cell application. Numerous experiments indicated that the peak cell response occurred between 48 and 96 h of  $\text{A}\beta(1-42)$  aggregation. Cells were exposed to a final concentration of 15  $\mu\text{mol/L}$   $\text{A}\beta(1-42)$ . Commercial  $\text{A}\beta$  lots were endotoxin-tested prior to shipment and determined to be 0.35 EU/mg. This translates into an effective LPS concentration of 8 pg/mL based on the calculations described in (Gao and Tian 2003). LPS concentrations at this level were ineffective at stimulating THP-1 cells. Hexafluoroisopropanol-treatment of  $\text{A}\beta$  peptide lots prior to shipment rendered the endotoxin levels undetectable.  $\text{A}\beta(1-42)$  preparations were also routinely tested for contamination using an 2,3-bis (2-methoxy-4-nitro-5-sulphophenyl)-2H-tetrazolium-5-carboxamide (XTT) cell proliferation assay (Scudiero *et al.* 1988). The presence of bacterial growth was probed by mitochondrial-mediated reduction of XTT (Sigma). Briefly,  $\text{A}\beta(1-42)$  aliquots and water controls were incubated for 72 h at  $37^{\circ}\text{C}$  with XTT (0.3 mg/mL) and phenazine methosulfate (8.3  $\mu\text{mol/L}$ ). Reduced XTT absorbance was measured at 467 nm. Minimal XTT reduction was observed in the cell-free  $\text{A}\beta(1-42)$  samples or sterile water controls and no differences were noted between the two.

#### Determination of TNF $\alpha$ levels

Measurement of secreted tumor necrosis factor alpha (TNF- $\alpha$ ) in the supernatants was determined by ELISA. Briefly, 100  $\mu\text{L}$  of 4  $\mu\text{g/mL}$  monoclonal anti-human TNF $\alpha$ /TNFSF1A capture antibody (R&D Systems, Minneapolis, MN, USA) was added to 96-well plates for overnight incubation at  $24^{\circ}\text{C}$ . Wells were washed with PBS (HyClone) containing 0.05% Tween-20 and blocked with 300  $\mu\text{L}$  PBS containing 1% bovine serum albumin (BSA), 5% sucrose, and 0.05%  $\text{NaN}_3$  for 1 h at  $24^{\circ}\text{C}$ . After washing, successive additions of 50  $\mu\text{L}$  samples or standards (2 h), 100  $\mu\text{L}$  biotinylated polyclonal anti-human TNF- $\alpha$ /TNFSF1A detection antibody (R&D Systems) in 20 mmol/L Tris with 150 mmol/L NaCl and 0.1% BSA (2 h), 100  $\mu\text{L}$  streptavidin-horseradish peroxidase (R&D Systems) diluted 200 times with PBS containing 1% BSA (20 min), and 100  $\mu\text{L}$  of equal volumes of 3,3',5,5'-tetramethylbenzidine and hydrogen peroxide (KPL, Gaithersburg, MD, USA) (30 min). The reaction was stopped by the addition of 1%  $\text{H}_2\text{SO}_4$  solution. The optical density of each sample was analyzed at 450 nm with a reference reading at 630 nm using a SpectraMax 340 absorbance plate reader (Molecular Devices, Union City, CA, USA). The concentration of TNF- $\alpha$  in the experimental samples was calculated from a TNF- $\alpha$  standard curve of 15–2000 pg/mL. When necessary, samples were diluted to fall within the standard curve.

#### Antibody neutralization assay

THP-1 cells ( $1.0 \times 10^6$  cells/mL) were added to a 48-well cell culture plate and pre-treated with 5–20  $\mu\text{g/mL}$  TLR antibodies, IgG isotype control, or PBS for 1 h at  $37^{\circ}\text{C}$  in 5%  $\text{CO}_2$ . Antibodies and isotype controls used were functional grade anti-human TLR2 (clone T2.5), TLR4 (clone HTA125), CD14 (clone G1D3) antibodies, mouse IgG2a $\kappa$  and IgG1 $\kappa$  isotype controls from eBioscience (San Diego, CA, USA), polyclonal anti-TLR2 and TLR4 antibodies from InvivoGen, and rat IgG isotype control from Sigma. Following

the 1 h incubation,  $\text{A}\beta(1-42)$  or TLR agonists were applied in the continuing presence of neutralizing antibodies and the cells were further incubated for 6 h in the same conditions. TNF $\alpha$  from cell supernatants was determined as described above. Statistical analysis was performed for selected experiments to determine the confidence limit at which two measurements were statistically different. A *t*-test was applied to each data set and *p*-values were obtained and reported in the figure legends.

#### Atomic force microscopy

$\text{A}\beta$  (1–42) aggregation solutions (100  $\mu\text{mol/L}$ ) were diluted to 1  $\mu\text{mol/L}$  in water. Grade V1 mica (Ted Pella, Inc., Redding, CA, USA) was cut into 11 mm circles and affixed to 12 mm metal discs. Aliquots (50  $\mu\text{L}$ ) were applied to freshly cleaved mica, allowed to adsorb for 15 min, washed twice with water, air dried, and stored in a container with desiccant. Images were obtained with a Nanoscope III multimode atomic force microscope (Digital Instruments, Santa Barbara, CA, USA) in TappingMode<sup>TM</sup>. Height analysis was performed using Nanoscope III software on flattened height mode images.

## Results

Human THP-1 monocytic cells have been a useful model for  $\text{A}\beta$  proinflammatory activity (Klegeris *et al.* 1997; Yates *et al.* 2000) and exhibit responses to stimuli similar to those of microglia (Combs *et al.* 2001). These cells play a critical role in the innate immune response and phagocytic cells express the largest repertoire of TLRs (Boehme and Compton 2004). Our initial studies confirmed the sensitivity of the THP-1 monocytes to TLR agonists. Commercial preparations of the TLR4 agonist LPS (ultrapure *E. coli* K12) and the TLR2 agonist Pam<sub>3</sub>CSK<sub>4</sub>, a synthetic lipopeptide, were tested for their ability to stimulate TNF $\alpha$  production from THP-1 cells (data not shown). TNF $\alpha$  is an important product of the MyD88-dependent innate immune response (Kielian 2006). THP-1 cell supernatants were collected 6 h post-stimulation and secreted TNF $\alpha$  measurements revealed a concentration-dependent response for both compounds. 6-h incubation times were chosen based on separate time-dependent experiments showing maximal TNF $\alpha$  production by LPS and Pam<sub>3</sub>CSK<sub>4</sub> after 6 h of cell exposure (data not shown). Curve fitting of the concentration-dependence data was performed as described in the Materials and methods and produced EC<sub>50</sub> values of 5 ng/mL for ultrapure K12 LPS and 1 ng/mL for Pam<sub>3</sub>CSK<sub>4</sub>.

Human monocytes produce a significant proinflammatory response to aggregated  $\text{A}\beta$  and our studies supported these findings using the THP-1 monocytic cell line.  $\text{A}\beta(1-42)$  aggregates were prepared by reconstitution in water and quiescent incubation at  $4^{\circ}\text{C}$ . The aggregation was monitored by atomic force microscopy (AFM) (Fig. 1). Freshly reconstituted  $\text{A}\beta(1-42)$  monomer (Fig. 1, left panel) showed a dense field of small punctate species that had little stimulatory effect on the cells. The heights for the vast majority of

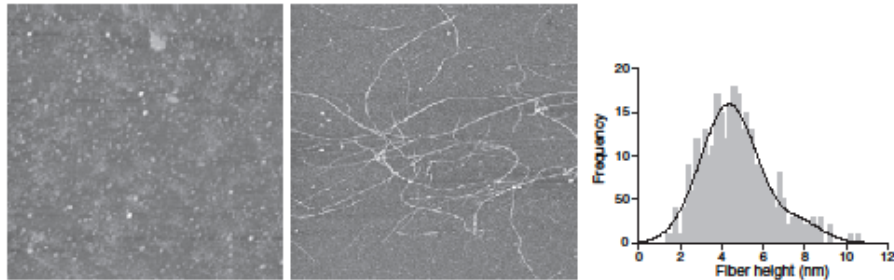


**Fig. 1** Morphology of stimulatory amyloid-beta (A $\beta$ ) (1–42) aggregated species. A $\beta$ (1–42) aggregation solutions (100  $\mu$ mol/L) were prepared and incubated as described in the Materials and methods. Aliquots were removed at 0 h (left panel) and 48 h (middle panel), diluted to 1  $\mu$ mol/L in water and imaged by atomic force microscopy

(AFM). The 5  $\mu$ m  $\times$  5  $\mu$ m images are shown in 'height' mode. The frequency histogram (right panel) was prepared from 300 height measurements of the 48 h image and fitted ( $r^2 = 0.932$ ) to a two-peak Gaussian area curve using PeakFit software v3.0 (Systat Software, Inc., San Jose, CA, USA).

these adsorbed peptide species were < 2 nm. A lesser population of small spherical species was also observed in the freshly reconstituted A $\beta$ (1–42) sample. The heights for these ranged from 2 to 5 nm with an average of  $3.2 \pm 0.8$  nm (SD) for  $n = 115$  measurements suggesting that they may be fibrillar precursors. The few bright spots (heights > 20 nm) in the 0 h image may represent the rapid formation of amorphous aggregates immediately following reconstitution. Continued incubation of the A $\beta$ (1–42) solution produced thin flexible fiber-like structures (Fig. 1, middle panel) which coincided with the ability of the peptide to provoke a marked increase in TNF $\alpha$  production. Using the conditions described in the Materials and methods, an incubation time of typically 48 h was necessary to produce an A $\beta$ (1–42) aggregated species that induced a significant cell response. AFM height measurements of the A $\beta$ (1–42) fibers were plotted as a histogram (Fig. 1, right panel) and fitted for multiple peaks. Peak-fitting analysis subdivided the fibers into two populations. The first, and most populated peak, had a mean height and SE of  $4.4 \pm 0.1$  nm. The second, less populated peak had a mean height of  $7.9 \pm 0.6$  nm (SE). These values were similar to previous AFM-based morphological analyses of types I and II fibrillar A $\beta$  (Harper *et al.* 1997a,b; Stine *et al.* 2003) and agreed with an earlier report by Fassbender *et al.* linking fibrillar A $\beta$ (1–42) with activation of the innate immune response (Liu *et al.* 2005). Our results demonstrated that fibrillar A $\beta$ (1–42) was largely responsible for THP-1 cell activation.

The THP-1 TNF $\alpha$  production versus cell exposure time to 15  $\mu$ mol/L fibrillar A $\beta$ (1–42) was slightly different from that of LPS and Pam $_2$ CSK $_4$  in that it peaked consistently at 10 h (Fig. 2, circles) compared with 6 h. THP-1 cells were not pre-treated with a differentiating agent in these studies although we observed that A $\beta$ (1–42) rapidly and effectively

converted the suspension monocytes into adherent cells. A representative cell adherence time course is shown in Fig. 2 (triangles). Multiple experiments found that fibrillar A $\beta$ (1–42) at 48 h of aggregation typically induced  $74 \pm 4\%$  (SE)

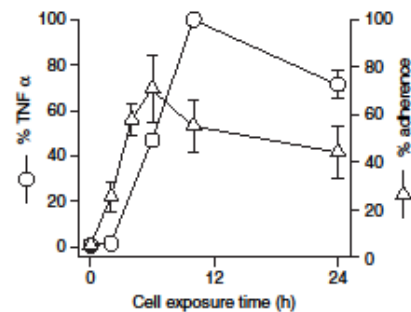


**Fig. 2** Time course of amyloid-beta (A $\beta$ ) (1–42)-induced THP-1 cell adherence and tumor necrosis factor alpha (TNF $\alpha$ ) production. Transformation of THP-1 suspension monocytes into adherent cells (triangles) during exposure to 15  $\mu$ mol/L fibrillar A $\beta$ (1–42) was quantitated by direct counting as described in the Materials and methods and presented as % of adherent cells relative to the total counted cells found in the suspension, wash, and adherent pools. Error bars (SE) were calculated by error propagation from  $n = 5$  sets of counts from each of the pools at each time point. TNF $\alpha$  levels were determined in THP-1 cell supernatants at the above times following treatment with 15  $\mu$ mol/L fibrillar A $\beta$ (1–42). TNF $\alpha$  is represented as % of the maximum response which was 10 h for each experiment. Error bars represent SE for six trials in two experiments for 0, 6, 10, and 24 h and three trials in one experiment for 2 and 48 h. Error bars that are not visible are smaller than the symbol. Actual TNF $\alpha$  levels for the 10 h time point averaged 507 pg/mL.

adherence of the THP-1 cells after 6 h of A $\beta$ (1–42) exposure (five separate experiments, nine trials total, data not shown). The observation that a longer cell exposure time was necessary to reach peak A $\beta$ (1–42)-induced TNF $\alpha$  production suggests that THP-1 cell adherence or differentiation is important for A $\beta$  responsiveness. Subsequent experiments in this report utilized a 6 h cell exposure to fibrillar A $\beta$ (1–42) to limit any long-term proinflammatory effects to the cells. The A $\beta$ (1–42) concentration (15  $\mu$ mol/L) that was used is based on monomeric units and does not reflect the actual fibrillar A $\beta$ (1–42) concentration which is likely much lower. A $\beta$ (1–42) concentrations below 15  $\mu$ mol/L did not effectively induce TNF $\alpha$  production from the THP-1 cells.

To delineate differences in the fibrillar A $\beta$ (1–42) response compared with ultrapure K12 LPS and rule out the presence of small traces of contaminating LPS, the compound PMX-B was tested for its effect on both stimuli. PMX-B neutralizes the endotoxicity of LPS by binding directly with the LPS lipid A moiety and disorganizing the outer bacterial membrane (Vaara 1992; Tsubery *et al.* 2000). The inclusion here of 0.1  $\mu$ g/mL PMX-B with ultrapure K12 LPS and A $\beta$ (1–42) had dramatically different effects on the two proinflammatory molecules (Fig. 3). Greater than 98% of the K12 LPS signal was blocked by PMX-B with little effect on the A $\beta$  signal. PMX-B (0.1  $\mu$ g/mL) also had a small effect on the THP-1 response evoked by 300 pg/mL Pam<sub>3</sub>CSK<sub>4</sub> (data not shown) suggesting that PMX-B may have some non-specific effects or there are subtle structural similarities between the three proinflammatory stimuli used in these studies. A $\beta$ /PMX-B and LPS/PMX-B samples were included in all experiments for continual monitoring of trace contamination. Some experiments showed a greater than  $\pm$ 10% effect of

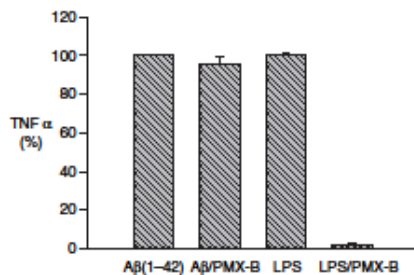


**Fig. 3** Effect of polymyxin B (PMX-B) on the proinflammatory response. THP-1 cells were treated with 15  $\mu$ mol/L amyloid-beta (A $\beta$ )(1–42) and 10 ng/mL ultrapure K12 lipopolysaccharide (LPS) in the absence or presence of 0.1  $\mu$ g/mL PMX-B. Tumor necrosis factor alpha (TNF $\alpha$ ) levels are presented as % of the A $\beta$ (1–42) and ultrapure K12 LPS response in the absence of PMX-B. Actual TNF $\alpha$  levels averaged 328 and 859 pg/mL for A $\beta$ (1–42) and LPS, respectively. Error bars represent SE for 15 trials in five separate experiments.

PMX-B on the A $\beta$  response although XTT cell proliferation measurements indicated there was no detectable presence of bacterial contamination within the A $\beta$  sample. For clarity, these experiments were not included in the TLR antibody neutralization studies described in the ensuing sections.

A TLR antibody neutralization assay was developed to investigate which transmembrane TLRs mediate the A $\beta$ (1–42) proinflammatory response. The assay was initially tested on the TLR agonists LPS and Pam<sub>3</sub>CSK<sub>4</sub> to determine and demonstrate the sensitivity of the antibody neutralization approach. The ultrapure K12 LPS from InvivoGen has been stringently purified by double phenol extraction of a 0.2% triethylamine/0.5% deoxycholate aqueous phase. This procedure has been shown to remove contaminating lipoproteins responsible for TLR2-mediated signaling (Hirschfeld *et al.* 2000). Our TLR antibody neutralization results were consistent with those findings. The ultrapure K12 LPS response was significantly attenuated by CD14 (75% inhibition) and TLR4 (87% inhibition) antibodies (Fig. 4, black bars) with no effect by the TLR2 antibody (12% inhibition) compared with the IgG2 isotype control (10% inhibition). The CD14 isotype control, IgG1, inhibited just 6% of the K12 LPS response. Antibody neutralization of the TLR2 agonist Pam<sub>3</sub>CSK<sub>4</sub> was clear. Only the CD14 and TLR2 antibodies had blocking activity (Fig. 4, gray bars). The TLR2 antibody was extremely effective and blocked 96% of the Pam<sub>3</sub>CSK<sub>4</sub>

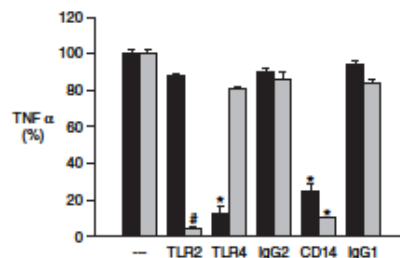


**Fig. 4** Toll-like receptor (TLR) antibody neutralization of lipopolysaccharide (LPS) and tripalmitoyl cysteinyl seryl tetralysine (Pam<sub>3</sub>CSK<sub>4</sub>). THP-1 cells were pre-incubated with 10  $\mu$ g/mL TLR antibodies and mouse antibody isotype controls as described in Materials and Methods prior to addition of 10 ng/mL ultrapure K12 LPS (black bars), or 1 ng/mL Pam<sub>3</sub>CSK<sub>4</sub> (gray bars). Antibodies (eBioscience) with corresponding isotype controls were TLR2 and TLR4 (IgG2) and CD14 (IgG1). Error bars represent SE for six trials, two experiments for the LPS data and three trials, one experiment for the Pam<sub>3</sub>CSK<sub>4</sub> data. Statistically significant differences determined by *t*-test are denoted with symbols (\**p* < 0.001 and \**p* < 0.0025 from respective IgG controls). Actual tumor necrosis factor alpha (TNF $\alpha$ ) levels, which are presented as % of the ultrapure K12 LPS and Pam<sub>3</sub>CSK<sub>4</sub> response pre-treated with phosphate-buffered saline (PBS) vehicle, averaged 216 and 257 pg/mL, respectively.

response while neutralization with the CD14 antibody blocked 90% of the response. Neutralization of LPS and Pam<sub>3</sub>CSK<sub>4</sub> with anti-TLR2 and -TLR4 antibodies respectively was not statistically different from IgG2 control ( $p < 0.25$ ).

The TLR antibody neutralization studies were conducted against the A $\beta$ (1–42) proinflammatory response to elucidate which CD14/TLR receptor combination was mediating A $\beta$ (1–42)-induced TNF $\alpha$  production. Pre-treatment of the THP-1 cells with a CD14 antibody effectively attenuated the A $\beta$ (1–42) response (62% inhibition relative to A $\beta$ /IgG1 control) (Fig. 5) consistent with a previous report (Fassbender *et al.* 2004). Surprisingly, both TLR4 (35% inhibition) and TLR2 (50% inhibition) antibodies were effective at signal attenuation compared with the rat IgG control with TLR2 possessing greater blocking activity. Statistical analysis indicated significant inhibitory differences between the antibodies and their respective IgG controls ( $p < 0.001$ ). These data indicate that multiple TLRs may interact with fibrillar A $\beta$ (1–42). PMX-B had an average attenuation of  $4 \pm 3\%$  SE on the A $\beta$ (1–42) response in these experiments (see Fig. 3). A different set of TLR antibodies and isotype controls were required for the A $\beta$ (1–42) neutralization studies because of significant attenuation of the A $\beta$ (1–42) response by the mouse IgG2 control used in the LPS and Pam<sub>3</sub>CSK<sub>4</sub> studies (Fig. 4). For this reason we utilized TLR2 and 4 antibodies produced in rat (InvivoGen). Furthermore,

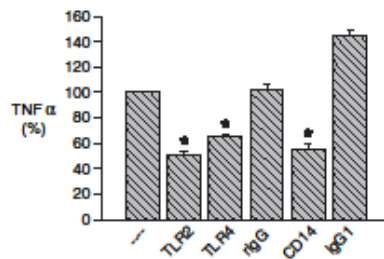


**Fig. 5** Toll-like receptor (TLR) antibody neutralization of the amyloid-beta (A $\beta$ ) (1–42) proinflammatory response. THP-1 cells were pre-incubated with 10  $\mu$ g/mL TLR antibodies and isotype controls prior to the addition of 15  $\mu$ mol/L aggregated A $\beta$ (1–42). Antibodies with corresponding isotype controls were TLR2 and TLR4 (rat IgG) (InvivoGen) and CD14 (mouse IgG1) (eBioscience). Tumor necrosis factor alpha (TNF $\alpha$ ) levels are presented as % of the A $\beta$ (1–42) response treated with phosphate-buffered saline (PBS) vehicle. Error bars represent SE for 12 trials in four separate experiments for TLR2, TLR4, and rat IgG and six trials in two experiments for CD14 and IgG1. Statistically significant differences from respective IgG controls are denoted with an asterisk (\* $p < 0.001$ ). Actual TNF $\alpha$  levels induced by A $\beta$ (1–42) alone averaged 328 pg/mL.

the mouse IgG1 isotype control at 10–20  $\mu$ g/mL showed a consistent 20–30% stimulation of the A $\beta$ (1–42) response (Fig. 5), which may have offset some of the effectiveness of the anti-CD14 neutralization. These issues underscored the importance of including IgG isotype controls in antibody neutralization experiments for proper interpretation. Because of these IgG effects, we were careful not to assign too much importance to differences between TLR2, TLR4, and CD14 antibodies in A $\beta$ (1–42) neutralizing ability. The antibody neutralization results demonstrated that multiple TLRs mediate the A $\beta$ (1–42) innate immune response and that both TLR2 and TLR4 have active roles in the pathway.

Antibody blockade of the A $\beta$ (1–42) innate immune response was dose dependent. In separate experiments TLR2 and TLR4 antibodies concentrations were evaluated at 5 and 20  $\mu$ g/mL compared with 10  $\mu$ g/mL antibody in Fig. 5. Neutralization effectiveness increased with higher concentrations of TLR2 and TLR4 antibodies (Fig. 6). Similar to Fig. 5, the TLR2 antibody again was a slightly more effective blocker of the A $\beta$ (1–42) response than the TLR4 antibody. Overall, the individual TLR antibodies clearly blocked A $\beta$ (1–42) activity but only to a certain extent of around 50–70% inhibition. The results presented here and those of Fassbender *et al.* (2004) suggest that a significant amount of the A $\beta$ -induced proinflammatory response is

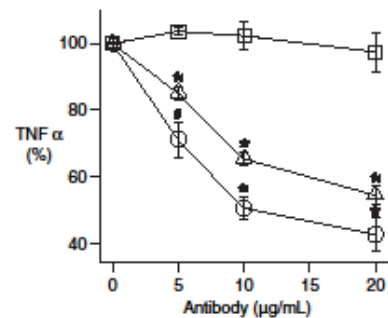


**Fig. 6** Dose-dependence of toll-like receptor (TLR) antibody neutralizing ability against amyloid-beta (A $\beta$ ) (1–42). THP-1 cells were pre-incubated with increasing concentrations of TLR2 (circles) and TLR4 (triangles) antibodies (InvivoGen) or rat IgG isotype control (squares) prior to the addition of 15  $\mu$ mol/L aggregated A $\beta$ (1–42). Tumor necrosis factor alpha (TNF $\alpha$ ) levels are presented as % of the A $\beta$ (1–42) response pre-treated with phosphate-buffered saline (PBS) vehicle. The 10  $\mu$ g/mL TLR2, TLR4, and rat IgG data are reproduced from Fig. 5. Neutralization data are the average  $\pm$  SE for  $n = 3$  trials (5  $\mu$ g/mL) and  $n = 6$  trials (20  $\mu$ g/mL). Statistically significant differences from respective IgG controls are denoted by symbols (\* $p < 0.001$  and \* $p < 0.005$ ). Actual TNF $\alpha$  levels induced by A $\beta$ (1–42) alone were the same as Fig. 5.

controlled by innate immune receptors. One explanation for the remaining unblocked activity may be contributions from other receptors that mediate the A $\beta$  proinflammatory response such as the CD36/ $\alpha_6\beta_1$ -integrin/CD47 multireceptor complex (Bamberger *et al.* 2003).

A second explanation may be that since both TLR2 and TLR4 mediate A $\beta$ -induced TNF $\alpha$  production, one receptor may compensate for the other when either one is inaccessible. To test this idea, a neutralization assay utilizing combinations of TLR2, TLR4, and CD14 antibodies was conducted to assess the effect of blocking multiple TLR pathways mediating the A $\beta$ (1–42) response. All four permutations were examined at 5  $\mu$ g/mL of each antibody. A lower antibody concentration was used to better observe the effect of combination antibody treatment. Furthermore, each cell treatment was supplemented up to 10  $\mu$ g/mL rat IgG and 5  $\mu$ g/mL mouse IgG1 to match the triple-combination TLR2/TLR4/CD14 antibody treatment with isotype control amounts. For this reason, direct comparison of the combination antibody treatments in Fig. 7 with those in

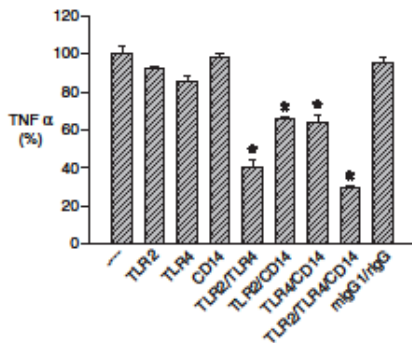


**Fig. 7** Combination antibody neutralization of the amyloid-beta (A $\beta$ ) (1–42) proinflammatory response. THP-1 cells were pre-incubated with 5  $\mu$ g/mL toll-like receptor (TLR) 2, TLR4 (InvivoGen), or CD14 (eBioScience) antibodies or combinations of the three prior to the addition of 15  $\mu$ mol/L aggregated A $\beta$ (1–42). A mixed isotype control sample was also used which contained 5  $\mu$ g/mL mouse IgG1 (CD14) and 10  $\mu$ g/mL rat IgG (TLR2, TLR4). Antibody pre-treatments were supplemented with one or both of the above IgGs so that each antibody treatment contained similar antibody and IgG amounts. Tumor necrosis factor alpha (TNF $\alpha$ ) levels are presented as % of the A $\beta$ (1–42) response pre-treated with phosphate-buffered saline (PBS) vehicle. Error bars represent SE for  $n = 3$  trials. Statistically significant differences from the rat IgG/mouse IgG1 control are denoted with an asterisk ( $p < 0.001$ ). Less significant differences were observed for individual anti-TLR2 ( $p < 0.25$ ), anti-TLR4 ( $p < 0.05$ ), and anti-CD14 ( $p < 0.20$ ) antibody treatments. Actual TNF $\alpha$  level induced by A $\beta$ (1–42) alone was 487 pg/mL.

Figs 5 and 6 is not straightforward. A small reduction of the A $\beta$ (1–42)-induced TNF $\alpha$  response was observed in the presence of 5  $\mu$ g/mL of each antibody (Fig. 7). As noted earlier, the mouse IgG1 isotype control for CD14 augmented the A $\beta$ (1–42) response. Mouse IgG1 (5  $\mu$ g/mL) was included in each sample that did not contain CD14 and may have masked some of the TLR blocking ability. The differences in neutralizing ability of each antibody at 5  $\mu$ g/mL in comparison with the mouse IgG1/rat IgG control were of small or no statistical importance (Fig. 7 legend). TLR antibody double combinations were much more effective, particularly the combination of TLR2/TLR4 which blocked 60% of the response. Interestingly, TLR2/CD14 and TLR4/CD14 antibody combinations also blocked the response better than the individual antibodies suggesting that A $\beta$  interactions may overlap to some extent with both TLRs and CD14. The most effective neutralization occurred after antibody pre-treatment with a TLR2/TLR4/CD14 triple combination which blocked 70% of the A $\beta$ (1–42) response compared with the mixed mouse IgG1/rat IgG isotype control (Fig. 7).

## Discussion

The data presented here demonstrate a role for both TLR2 and TLR4 in mediating the THP-1 monocyte/macrophage proinflammatory response initiated by fibrillar A $\beta$ (1–42). Our results are consistent with a previous report by Fassbender *et al.* (2004) showing CD14 antibody neutralization of A $\beta$ -induced microglial activation. Although CD14 functions as a ligand-binding accessory protein for both TLR4 and TLR2, Fassbender *et al.* proposed that the A $\beta$  cellular activation was likely transmitted by TLR4 based on a positive response obtained in Chinese hamster ovary cells lacking a functional TLR2. However, this result was not confirmed in cells that do express TLR2 such as microglia, peripheral blood monocytes, or THP-1 cells and therefore did not exclude a role for TLR2 when present in the cell. In fact, our data indicates that TLR2 and TLR4 can both transduce the A $\beta$  signal and may compensate for each other when necessary. The convergence of A $\beta$  and the innate immune system suggests that in some manner fibrillar A $\beta$ (1–42) may act like a PAMP-like infectious agent through TLR activation and a proinflammatory cascade.

Several reports suggest that A $\beta$  activation of the innate immune response may have beneficial aspects. Cultured primary microglial cells prepared from CD14-wild type mice were significantly better at internalizing fibrillar A $\beta$ (1–42) compared with cells prepared from CD14-deficient mice (Liu *et al.* 2005). Furthermore, it was shown that stimulation of BV2 mouse microglial cells with TLR4, TLR2, and TLR9 agonists caused significant uptake of A $\beta$ (1–42) (Tahara *et al.* 2006). Moreover, the activation of TLR2 in primary mouse microglial cells with TLR2 agonist peptidoglycan enhanced

formyl peptide receptor-like 2-mediated uptake of A $\beta$ (1–42) (Chen *et al.* 2006). *In vivo* studies support the cellular studies and have shown an increased A $\beta$  load in Mo/Hu APPswe PS1dE9 mice with deficiencies in TLR4 (Tahara *et al.* 2006). The observation of increased CD14 immunostaining in AD brain slices compared with age-matched controls (Liu *et al.* 2005) has added to the growing body of evidence linking innate immunity with neurodegenerative disease (discussed in Nguyen *et al.* 2002).

The sensitivity of innate immune receptors to LPS (TLR4) and lipoproteins (TLR2) demands that careful consideration be given to experimental preparations. Caution has been suggested when interpreting an innate immune response and potential contamination of the preparation with bacterial components must be ruled out (Kielian 2006). Endotoxin measurements of the commercial A $\beta$  lots utilized in these studies found undetectable levels of LPS and the possibility of externally introduced bacterial contamination was routinely monitored using an XTT cell proliferation assay. These tests were substantiated in Fig. 3 where PMX-B had no effect on the A $\beta$ (1–42) response in the same experiments in which TLR antibodies showed neutralizing activity. Furthermore, the innate immune response dependency on A $\beta$ (1–42) aggregation time also argued against the presence of contaminants in the A $\beta$  sample. Low levels of TNF $\alpha$  production were typically observed when the peptide was freshly reconstituted. Continued incubation (48–96 h) of the peptide at 4°C produced maximal stimulatory activity followed by a decline to baseline levels upon further aging of the A $\beta$  sample. This type of time course would not be expected if the sample contained contaminating TLR agonists and degradation of the contaminants after 1 week would not be expected either as A $\beta$ (1–42) aggregation solutions were incubated at 4°C until cell exposure. The decline in stimulatory activity upon continued aggregation of the peptide is of interest and currently under investigation in our laboratory. One explanation may be that midway through the aggregation process the actual concentration of fibrillar A $\beta$  is well below 15  $\mu\text{mol/L}$ , which is based on monomer units. Continued formation of fibers may create toxic effects thereby muting cellular responses. We are currently investigating the structural and biochemical basis for the A $\beta$  aggregation time-dependent response. The cumulative results and analyses indicate that the THP-1 monocyte TNF $\alpha$  signal is caused by A $\beta$  and not contaminants.

The structural features of PAMPs that confer TLR ligand specificity are not completely understood. The lipid A moiety of LPS is the primary region responsible for LPS activity (Chiller *et al.* 1973) and is thought to possess the PAMP motif. Lipid A is composed of a diglucosamine backbone with ester- and amide-linked long-chain fatty acids. The number and length of lipid A acyl chains vary among bacteria and alter LPS potency (Miller *et al.* 2005). Although some TLR2 antagonists have a protein component the

common structural feature among PAMPs appears to be amphiphilicity with significant regions of hydrophobicity. A $\beta$  fibrils can be included in this category based on solid state NMR studies indicating a hydrophobic core running along the fiber axis (Petkova *et al.* 2002). Crystallographic studies of soluble CD14 show a large N-terminal hydrophobic pocket important for LPS binding (Kim *et al.* 2005). The binding pocket overlaps with areas of conserved leucine-rich repeats which are also found on TLR4. A $\beta$  fibrils may possess structural components that have similarities with both TLR2 and TLR4 agonists.

The role of innate immunity in the pathogenesis of AD will need further investigation. Effective TLR-mediated phagocytosis and clearance of A $\beta$  aggregates would theoretically provide beneficial effects although a sustained inflammatory response to aggregated A $\beta$  has been suggested as one of the underlying mechanisms of progressive neurodegeneration in AD (McGeer and McGeer 1998) and may in fact exacerbate A $\beta$  deposition (Golde 2002). A $\beta$  plaque-induced recruitment of peripheral monocytes into the brain parenchyma and their subsequent differentiation into phagocytic microglial cells may help explain the increased CD14 expression in AD brain slices reported by Liu *et al.* (2005). The PAMP-like features necessary to activate the innate immune response may not be present in all A $\beta$  aggregate morphologies thereby allowing certain populations to elude recognition and suggesting that not all can trigger a response. This idea is consistent with the observed diversity in A $\beta$  aggregate morphologies in the AD brain. Some of these deposits are surrounded by inflammatory markers while others lack inflammatory cytopathology (Selkoe 2004). Furthermore, some A $\beta$  aggregate structures that initiate an innate immune response may be resistant to phagocytic degradation. In summary, the interaction between A $\beta$  aggregates, TLRs, and innate immunity may further explain some of the complexities of AD etiology and provide a potential point of therapeutic intervention.

#### Acknowledgements

This work was supported by grants from the Alzheimer's Association (NIRG-06-27267) and the Missouri Alzheimer's and Related Disorders Research Program.

#### References

- Aderem A. and Ulevitch R. J. (2000) Toll-like receptors in the induction of the innate immune response. *Nature* 406, 782–787.
- Bamberger M. E., Harris M. E., McDonald D. R., Husemann J. and Landreth G. E. (2003) A cell surface receptor complex for fibrillar  $\beta$ -amyloid mediates microglial activation. *J. Neurosci.* 23, 2665–2674.
- Boehme K. W. and Compton T. (2004) Innate sensing of viruses by Toll-like receptors. *J. Virol.* 78, 7867–7873.

- Chen K., Inbauren P., Hu J., Chen J., Gong W., Cho E. H., Lockett S., Dunlop N. M. and Wang J. M. (2006) Activation of Toll-like receptor 2 on microglia promotes cell uptake of Alzheimer disease-associated amyloid  $\beta$  peptide. *J. Biol. Chem.* **281**, 3651–3659.
- Chiller J. M., Skidmore B. J., Morrison D. C. and Weigle W. O. (1973) Relationship of the structure of bacterial lipopolysaccharides to its function in mitogenesis and adjuvanticity. *Proc. Natl Acad. Sci. USA* **70**, 2129–2133.
- Combs C. K., Karlo J. C., Kao S. C. and Landreth G. E. (2001)  $\beta$ -amyloid stimulation of microglia and monocytes results in TNF $\alpha$ -dependent expression of inducible nitric oxide synthase and neuronal apoptosis. *J. Neurosci.* **21**, 1179–1188.
- Dahlgen K. N., Manelli A. M., Stine W. B. Jr, Baker L. K., Knfft G. A. and LaDu M. J. (2002) Oligomeric and fibrillar species of amyloid- $\beta$  peptides differentially affect neuronal viability. *J. Biol. Chem.* **277**, 32046–32053.
- Deshpande A., Mina E., Glabe C. and Busciglio J. (2006) Different conformations of amyloid  $\beta$  induce neurotoxicity by distinct mechanisms in human cortical neurons. *J. Neurosci.* **26**, 6011–6018.
- El Khoury J., Hickman S. E., Thomas C. A., Cao L., Silvestrin S. C. and Loike J. D. (1996) Scavenger receptor-mediated adhesion of microglia to  $\beta$ -amyloid fibrils. *Nature* **382**, 716–719.
- Fasbender K., Walter S., Kuhl S. et al. (2004) The LPS receptor (CD14) links innate immunity with Alzheimer's disease. *BISEB J.* **18**, 203–205.
- Gao B. and Tsan M. F. (2003) Endotoxin contamination in recombinant human heat shock protein 70 (Hsp70) preparation is responsible for the induction of tumor necrosis factor  $\alpha$  release by murine macrophages. *J. Biol. Chem.* **278**, 174–179.
- Glenn G. G. and Wong C. W. (1984) Alzheimer's disease and Down's syndrome: sharing of a unique cerebrovascular amyloid fibril protein. *Biochem. Biophys. Res. Commun.* **122**, 1131–1135.
- Gold T. E. (2002) Inflammation takes on Alzheimer disease. *Nat. Med.* **8**, 936–938.
- Haass C. and Selkoe D. J. (2007) Soluble protein oligomers in neurodegeneration: lessons from the Alzheimer's amyloid  $\beta$ -peptide. *Nat. Rev. Mol. Cell Biol.* **8**, 101–112.
- Harper J. D., Lieber C. M. and Lansbury P. T. Jr (1997a) Atomic force microscopic imaging of seeded fibril formation and fibril branching by the Alzheimer's disease amyloid- $\beta$  protein. *Chem. Biol.* **4**, 951–959.
- Harper J. D., Wong S. S., Lieber C. M. and Lansbury P. T. Jr (1997b) Observation of metastable A $\beta$  amyloid protofibrils by atomic force microscopy. *Chem. Biol.* **4**, 119–125.
- Harper J. D., Wong S. S., Lieber C. M. and Lansbury P. T. Jr (1999) Assembly of A $\beta$  amyloid peptides: an *in vitro* model for a possible early event in Alzheimer's disease. *Biochemistry* **38**, 8972–8980.
- Hirschfeld M., Ma Y., Weis J. H., Vogel S. N. and Weis J. J. (2000) Cutting edge: repurification of lipopolysaccharide eliminates signaling through both human and murine Toll-like receptor 2. *J. Immunol.* **165**, 618–622.
- Hoffmann J. A., Kafatos E. C., Janeway C. A. and Ezekowitz R. A. (1999) Phylogenetic perspectives in innate immunity. *Science* **284**, 1313–1318.
- Jarrett J. T., Berger E. P. and Lansbury P. T. Jr (1993) The carboxy terminus of the beta amyloid protein is critical for the seeding of amyloid formation: implications for the pathogenesis of Alzheimer's disease. *Biochemistry* **32**, 4693–4697.
- Kielian T. (2006) Toll-like receptors in central nervous system glial inflammation and homeostasis. *J. Neurosci. Res.* **83**, 711–730.
- Kim J. I., Lee C. J., Jin M. S., Lee C. H., Paik S. G., Lee H. and Lee J. O. (2005) Crystal structure of CD14 and its implications for lipopolysaccharide signaling. *J. Biol. Chem.* **280**, 11347–11351.
- Klegeris A., Walker D. G. and McGeer P. L. (1997) Interaction of Alzheimer  $\beta$ -amyloid peptide with the human monocytic cell line THP-1 results in a protein kinase C-dependent secretion of tumor necrosis factor- $\alpha$ . *Brain Res.* **747**, 114–121.
- Koenigsnecht J. and Landreth G. (2004) Microglial phagocytosis of fibrillar  $\beta$ -amyloid through a  $\beta_1$  integrin-dependent mechanism. *J. Neurosci.* **24**, 9838–9846.
- Lee H. K., Duzendorfer S., Soldau K. and Tobias P. S. (2006) Double-stranded RNA-mediated TLR3 activation is enhanced by CD14. *Immunity* **24**, 153–163.
- Liu Y., Walter S., Stagi M., Cherny D., Letiembre M., Schulz-Schaefer W., Heine H., Penke B., Neumann H. and Fasbender K. (2005) LPS receptor (CD14): a receptor for phagocytosis of Alzheimer's amyloid peptide. *Brain* **128**, 1778–1789.
- McGeer E. G. and McGeer P. L. (1998) The importance of inflammatory mechanisms in Alzheimer disease. *Exp. Gerontol.* **33**, 371–378.
- McGeer P. L., Itagaki S., Tago H. and McGeer E. G. (1987) Reactive microglia in patients with senile dementia of the Alzheimer type are positive for the histocompatibility glycoprotein HLA-DR. *Neurosci. Lett.* **79**, 195–200.
- Miller S. I., Ernst R. K. and Bader M. W. (2005) LPS, TLR4 and infectious disease diversity. *Nat. Rev. Microbiol.* **3**, 36–46.
- Mun-Bryce S., Lukes A., Wallace J., Lukes-Marx M. and Rosenberg G. A. (2002) Stromelysin-1 and gelatinase A are upregulated before TNF- $\alpha$  in LPS-stimulated neuroinflammation. *Brain Res.* **933**, 42–49.
- Nguyen M. D., Julien J. P. and Rivest S. (2002) Innate immunity: the missing link in neuroprotection and neurodegeneration? *Nat. Rev. Neurosci.* **3**, 216–227.
- Parsec D. M., Ghosh R. N. and Maxfield F. R. (1996) Microglial cells internalize aggregates of the Alzheimer's disease amyloid  $\beta$ -protein via a scavenger receptor. *Neuron* **17**, 553–565.
- Petkova A. T., Ishii Y., Balbach J. J., Antzutkin O. N., Leapman R. D., Delaglio F. and Tycko R. (2002) A structural model for Alzheimer's  $\beta$ -amyloid fibrils based on experimental constraints from solid state NMR. *Proc. Natl Acad. Sci. USA* **99**, 16742–16747.
- Sudiero D. A., Shoemaker R. H., Paull K. D., Monks A., Tierney S., Nofziger T. H., Currens M. J., Smiff D. and Boyd M. R. (1988) Evaluation of a soluble tetrazolium/formazan assay for cell growth and drug sensitivity in culture using human and other tumor cell lines. *Cancer Res.* **48**, 4827–4833.
- Selkoe D. J. (2001) Alzheimer's disease: genes, proteins, and therapy. *Physiol. Rev.* **81**, 741–766.
- Selkoe D. J. (2004) Cell biology of protein misfolding: the examples of Alzheimer's and Parkinson's diseases. *Nat. Cell Biol.* **6**, 1054–1061.
- Stine W. B. Jr, Dahlgen K. N., Knfft G. A. and LaDu M. J. (2003) *In vitro* characterization of conditions for amyloid- $\beta$  peptide oligomerization and fibrillogenesis. *J. Biol. Chem.* **278**, 11612–11622.
- Tahan K., Kim H. D., Jin J. J., Maxwell J. A., Li L. and Fukuchi K. I. (2006) Role of Toll-like receptor signalling in A $\beta$  uptake and clearance. *Brain* **129**, 3006–3019.
- Tabery H., Ofek I., Cohen S. and Fridkin M. (2000) The functional association of polymyxin B with bacterial lipopolysaccharide is stereospecific: studies on polymyxin B nonapeptide. *Biochemistry* **39**, 11837–11844.

- Vaan M. (1992) Agents that increase the permeability of the outer membrane. *Microbiol. Rev.* **56**, 395–411.
- Walsh D. M., Hartley D. M., Kusumoto Y., Fezoui Y., Condron M. M., Lomakin A., Benedek G. B., Selkoe D. J. and Teplow D. B. (1999) Amyloid  $\beta$ -protein fibrillogenesis: structure and biological activity of protofibrillar intermediates. *J. Biol. Chem.* **274**, 25945–25952.
- Wegiel J., Inaki H., Wang K. C. and Rubenstein R. (2004) Cells of monocyte/microglial lineage are involved in both microvessel amyloidosis and fibrillar plaque formation in APPsw tg mice. *Brain Res.* **1022**, 19–29.
- Westerman M. A., Cooper-Blacketer D., Mariash A., Kotilinek L., Kawarabayashi T., Younkin L. H., Carlson G. A., Younkin S. G. and Ashe K. H. (2002) The relationship between A $\beta$  and memory in the Tg2576 mouse model of Alzheimer's disease. *J. Neurosci.* **22**, 1858–1867.
- Yan S. D., Chen X., Fu J. *et al.* (1996) RAGE and amyloid- $\beta$  peptide neurotoxicity in Alzheimer's disease. *Nature* **382**, 685–691.
- Yankner B. A. (1996) Mechanisms of neuronal degeneration in Alzheimer's disease. *Neuron* **16**, 921–932.
- Yates S. L., Burgess L. H., Koosis-Angle J., Antal J. M., Dority M. D., Embury P. B., Piotrkowski A. M. and Brunden K. R. (2000) Amyloid beta and amylin fibrils induce increases in proinflammatory cytokine and chemokine production by THP-1 cells and murine microglia. *J. Neurochem.* **74**, 1017–1025.

## 1 INTRODUCTION

### 1.1 Alzheimer's Disease: Comprehending the etiology of the disease

Advances in scientific and medical research have resulted in a dramatic rise in human life expectancy. In the 20<sup>th</sup> century, an increasing number of individuals have reached the age at which short-term memory defects linked with normal aging of the human brain has become one of the major concerns. Although this is a common occurrence among older people, the problem arises when a person starts to have trouble following complex discussions and making decisions, and begins to experience a heightened degree of forgetfulness. These are common symptoms of dementia, an illness that is associated with age, in which parts of the brain begin to malfunction causing disruptions and progressive loss in memory, judgement, reasoning and behavioral stability (St George-Hyslop 2000).

Alzheimer's Disease (AD) is the most common form of neurodegenerative dementia. This illness currently affects about 10% of persons over 65 years of age, and >40% of people over 85 years (Buxbaum and Tagoe 2000). Globally, the disease affects almost 2% of the population in industrialized countries, and it is predicted that the occurrence of AD will increase three-fold within the next fifty years (<http://www.alz.org>). There is no strong correlation between the occurrence of AD and race or sex type. However, it is more prevalent in women mainly due to the fact that women live longer

than men (Irvine, El-Agnaf et al. 2008). To date, there is still no definitive diagnosis of the disease other than postmortem analysis of the brain (Georganopoulou, Chang et al. 2005). However, the effort to decipher the causes and mechanism of AD has gone a long way since its discovery in 1906 by Alois Alzheimer (Selkoe 2001). Studies done for the past decades have identified two proteins that comprise the classical neuropathological lesions that are diagnostic of AD: the neurofibrillary tangles and senile plaques.

### 1.1.1 Neurofibrillary Tangles

In an effort to better understand the pathology of AD, researchers have done post-mortem analysis of the human AD brain. Examination of the degenerating neurons in the diseased brain regions showed the presence of nonmembrane-bound clusters of abnormal cytoplasmic fibers ~20-nm length, which are referred to as neurofibrillary tangles (Kosik, Joachim et al. 1986; Selkoe 1996; Selkoe 2001). Furthermore, rigorous immunocytochemical and biochemical analyses identified the microtubule-associated phosphoprotein tau as the main component of neurofibrillary tangles (Grundke-Iqbal, Iqbal et al. 1986; Kosik, Joachim et al. 1986; Selkoe 1996). In the neurons, tau proteins can be found predominantly in axons. Under normal conditions, tau exists as a highly soluble phosphorylated protein, which functions as a stabilizer and promoter of microtubule polymerization (Hanger, Anderton et al. 2009). Microtubules are important for providing routes where nutrients and other molecules can move through cells (St George-Hyslop 2000). However, excessive tau phosphorylation and overexpression was found to be the main cause of transformation of soluble tau into tangles. Moreover,

numerous studies using antibodies specific for various phosphor-tau epitopes have suggested that the dysregulation of tau phosphorylation is due to the augmented activity of certain kinases, such as glycogen synthase kinase-3 (GSK-3), cyclin-dependent kinase 5 (cdk5), casein kinase 1 (CK1) and cyclic AMP-dependent protein kinase (PKA), as well as inactivation of certain phosphatases (Selkoe 1996; Patrick, Zukerberg et al. 1999; Churcher 2006; Hanger, Byers et al. 2007; Hanger, Anderton et al. 2009). So far, one recent therapeutic strategy focuses on how to subtly regulate the activity of kinases. The activation of phosphatases as a therapeutic target seems unlikely due to still poorly understood mechanism and involvement of phosphatases in tau pathology (Hanger, Anderton et al. 2009).

### 1.1.2. Senile plaques

Another directly observable hallmark of AD is the presence of extracellular senile or amyloid plaques. These clusters of protein accumulate in the spaces between nerve cells and are present extensively in the hippocampus and the cerebral cortex region of the AD brain. Closer analysis showed that these plaques contain extracellular deposition of numerous proteins, the principal of which is amyloid  $\beta$ - protein ( $A\beta$ ) (Selkoe 2001). Numerous studies have associated both the more common 40-amino acids long  $A\beta$  (designated as  $A\beta(1-40)$ ) and the less common but faster aggregating 42-amino acids long  $A\beta(1-42)$  with AD. There are two forms of senile plaques that have been detected in the diseased brain: neuritic plaques and diffuse plaques. Neuritic plaques are compact and contain the fibrillar form of both  $A\beta(1-40)$  and  $A\beta(1-42)$ . Further evidences revealed the

presence of reactive proinflammatory cells called microglia, as well as reactive astrocytes, along with the plaques (El Khoury, Moore et al. 2003). Swollen and deformed neurons in the vicinity of the plaques are also observed. Microscopic analysis of the diseased brain sections showed that the size (diameter) of neuritic plaques vary greatly, from 10 to >120  $\mu\text{m}$  (Selkoe 2001). In contrast, diffuse plaques are composed exclusively of  $\text{A}\beta(1-42)$ . These amorphous plaques are also observed in young individuals afflicted with Down's syndrome before Alzheimer's type-dementia is manifested (Irvine, El-Agnaf et al. 2008). Moreover, immunohistochemical studies of patients with Down's syndrome demonstrated the presence of diffuse plaques at an early age, but neuritic plaques only occur at a later age, along with the presence of abundant neurofibrillary tangles (Lemere, Blusztajn et al. 1996; Selkoe 2001). Due to these findings, scientists considered diffuse plaques to be precursors of the neuritic plaques, and thus called diffuse plaques as "preamyloid deposits".

## 1.2 Probing the molecular mechanism of AD: Focus on amyloid $\beta$ - protein ( $\text{A}\beta$ )

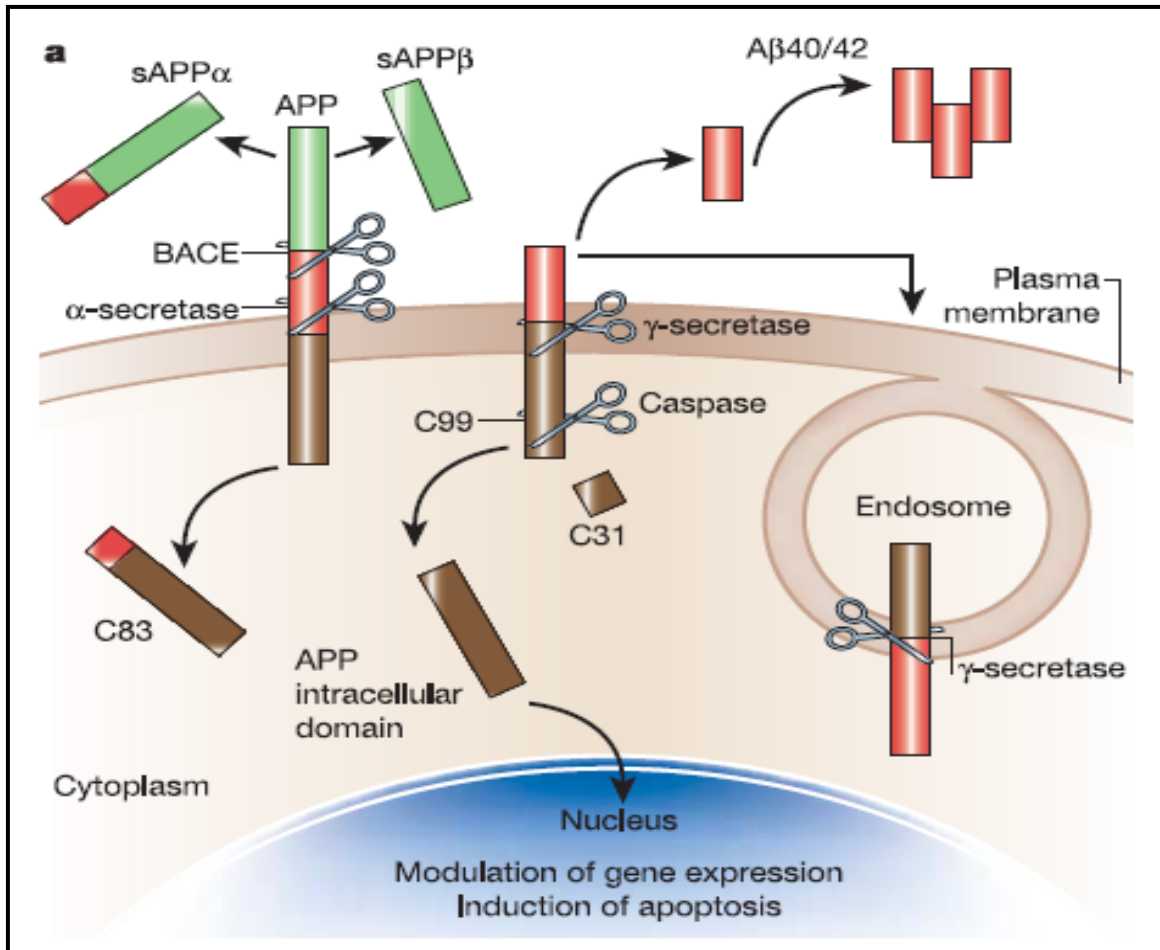
As mentioned previously, AD is characterized by progressive accumulation of  $\text{A}\beta$  protein in the brain sections, mainly in the cerebral cortex, hippocampus and other regions of the brain. To understand the protein's involvement in the disease, it is crucial to fully comprehend the molecular mechanism of  $\text{A}\beta$  production. A major breakthrough in the study of  $\text{A}\beta$  and its connection with AD transpired when scientists effectively isolated plaque amyloid deposits from the diseased brain and successfully sequenced the  $\text{A}\beta$  protein (Selkoe 1996; Mattson 2004). This led to the identification of amyloid

precursor protein (APP) as the major source of A $\beta$  (Selkoe 1998; Castellani, Lee et al. 2008). The subsequent discussions below will focus on the mechanism of A $\beta$  production, A $\beta$  hypothesis, and structural studies of A $\beta$  and how it contributes to AD pathogenesis.

### 1.2.1 Amyloid precursor protein processing and generation of A $\beta$

Extensive reviews have been written about the nature of the human amyloid precursor protein. APP was identified as the main source of A $\beta$  that is implicated in AD. Numerous researchers like Dennis Selkoe of Harvard, Mark Mattson of U. Kentucky and Edward Koo of UC San Diego, among others, have focused on elucidating the nature and function of this type-1 integral membrane glycoprotein. The human amyloid precursor protein (APP), which is located on chromosome 21, is composed of a single membrane spanning domain, a large extracellular domain and a shorter (~47 amino acid) cytoplasmic COOH-terminal region (Selkoe 2001; Thinakaran and Koo 2008). Studies now show that approximately half of A $\beta$ (1-40) or A $\beta$ (1-42) sequence lies on the extracellular part of APP (A $\beta$  amino acids 1-17, from amino acids 597-613 of APP that is 695-amino acid long (APP-695)), while the other half, which contains hydrophobic residues, lies within the phospholipid bilayer (Mattson 1997). Among the numerous isoforms, the largest of the known APP splice forms is comprised of 770 amino acids (Suzuki and Nakaya 2008). This particular APP is expressed throughout the body, as well as in neurons. Increasing evidence suggests that APP is important in neuronal growth and survival, synaptic plasticity and cell adhesion (Buxbaum and Tagoe 2000; Mattson 2004; Thinakaran and Koo 2008).

A model of APP processing is illustrated in Figure 1.1 (Mattson 2004). APP trafficking involves transit from the endoplasmic reticulum to the plasma membrane where it undergoes post-translational modification. After which, APP is rapidly internalized and translocated back to secretory vesicles through endocytic and recycling compartments (Selkoe 1998; Thinakaran and Koo 2008). During this trafficking process, APP molecules can undergo specific proteolytic cleavage through the action of enzymes  $\alpha$ ,  $\beta$  and  $\gamma$  secretases to release the secreted products into the extracellular space. The likely APP cleavage sites by the secretase enzymes that are discussed in this section are based on the sequence of APP-695. The action of  $\alpha$  secretase on APP was the first to be identified. Investigations showed that  $\alpha$  secretase clips 12 amino acids NH<sub>2</sub>-terminal to the single transmembrane domain of APP (between amino acids 612 and 613, amino acids 16 and 17 of A $\beta$ ) (Sisodia, Koo et al. 1990). This cleavage releases the non-amyloidogenic form secreted APP $\alpha$  ectodomain from the cell surface, leaving an 83-residue (APP83) COOH-terminal fragment in the membrane. This residue is further acted upon by  $\gamma$ -secretase (cleavage between amino acids 639 and 640 of APP-695, and at the COOH terminus of A $\beta$ ) to form a shorter 3 kDa peptide p3 into the extracellular space. Aside from the products produced through the action of  $\alpha$ -secretase, alternate APP cleavage occurs 16 amino acids NH<sub>2</sub>-terminal to the  $\alpha$ -cleavage site is mediated by  $\beta$  secretase (amino acid residues 596 and 597 of APP-695 that corresponds to the NH<sub>2</sub> terminus of A $\beta$ ) (Mattson 1997; Selkoe 1998; Selkoe 2001). Consequently, a smaller fragment (s)APP $\beta$  is released into extracellular milieu, retaining a 99-residue (APP99) COOH-terminal fragment that contains intact A $\beta$  in the membrane. This COOH-terminal fragment can be further proteolytically cleaved by  $\gamma$ -secretase to generate an intact A $\beta$



**(b)** A $\beta$  (1-40): ***DAEFRHDSGY EVHHQKLVFF*** AEDVGSNKGA IIGLMVGGVV

A $\beta$  (1-42): ***DAEFRHDSGY EVHHQKLVFF*** AEDVGSNKGA IIGLMVGGVVIA

**Figure 1.1. Processing of Amyloid precursor protein (APP).** (a) Cleavage of APP involves the activities of  $\alpha$ -,  $\beta$ - (BACE1) and  $\gamma$ -secretase.  $\alpha$  secretase cleavage results in the release of soluble non-amyloidogenic APP fragment (sAPP $\alpha$ ) from the cell surface and leaves an 83-amino acid-C-terminal fragment (C83). BACE cleavage leaves a 99-aa residue, which can be further processed by  $\gamma$ -secretase to generate and liberate a 39-42 residue amyloidogenic peptide. The 99-residue fragment can also be internalized and further processed by  $\gamma$ -secretase to produce A $\beta$  (1-40)/(1-42) in endocytic compartments. C99 cleavage by  $\gamma$ -secretase also liberates an APP cytoplasmic domain that can translocate to the nucleus for modulation of gene expression, i.e., induction of apoptotic genes. Processing of APP/C99 residue by caspases results in the production of neurotoxic peptide C31. (b) Amino acid sequence of A $\beta$ (1-40) and A $\beta$ (1-42). The bold italics represent the part of A $\beta$  that lies partly outside the cell membrane and is being liberated upon cleavage of APP by  $\alpha$  secretase (Mattson 1997; Mattson 2004)

peptide 38-42 amino acid residues in length (Mastrangelo, Ahmed et al. 2006; Pearson and Peers 2006). Under normal conditions, APP cleavage by  $\beta$  and  $\gamma$  secretases typically results in the formation of 40-residue A $\beta$  peptide. However, about 10% of the cleavage product is A $\beta$ (1-42) (St George-Hyslop 2000). Because the nature of  $\gamma$  secretase has not been fully understood, further studies are still being done as to the site of cleavage of APP99 and APP83. However, several lines of evidence showed that considerable amount of A $\beta$ (1-40) and A $\beta$ (1-42) are made during internalization and internal processing of the APP COOH fragment (Mattson 1997; Selkoe 2001; Mattson 2004). The formed A $\beta$ (1-40) or A $\beta$ (1-42) is then released from the cell and has likelihood to form fibrils.

The  $\alpha$  secretase-catalyzed APP cleavage is believed to be the predominant processing pathway for APP and the APPs $\alpha$  have distinct extracellular functions. Numerous *in vitro* studies reveal increasing number of roles of sAPP $\alpha$  in neurons including cell survival (Mattson, Cheng et al. 1993; Ohsawa, Hirose et al. 1995), stimulation of neurite outgrowth (Clarris, Nurcombe et al. 1994; Ohsawa, Hirose et al. 1995; Furukawa, Sopher et al. 1996), regulation of cell adhesion, and protection against a range of metabolic, excitotoxic and oxidative insults, among others (Mattson, Cheng et al. 1993; Smith-Swintosky, Pettigrew et al. 1994; Selkoe 1998).

The cleavage by  $\beta$ -secretase also normally occurs to produce and release A $\beta$ . Studies indicate that A $\beta$  is being generated constitutively by normal cells in blood and cerebrospinal fluid (CSF) with normal concentrations in the low nanomolar range (3-8 nM for CSF and under 500 pM in plasma) (Seubert, Vigo-Pelfrey et al. 1992; Motter, Vigo-Pelfrey et al. 1995; Scheuner, Eckman et al. 1996; Dumery, Bourdel et al. 2001; Ramsden, Plant et al. 2001). Thus, unaffected individuals normally produce and clear A $\beta$ .

Additionally, the A $\beta$  protein being normally generated is thought to have a normal physiological role. On the other hand, individuals afflicted with AD generate A $\beta$  that forms ordered aggregates, which are deposited as amyloid plaques.

### 1.2.2 Missense mutations in APP and other mutations cause autosomal dominant AD

Familial AD (FAD) occurs in mid, rather than late, adulthood (Buxbaum and Tagoe 2000). Numerous studies of FAD cases reveal that early-onset AD (EOAD) is caused by mutations in APP and presenilin genes. These mutations affect the metabolism or stability of A $\beta$  and cause autosomal forms of AD (Selkoe 1996; LaFerla, Green et al. 2007).

Several lines of evidence showed that mutations affecting the APP gene (Figure 1.2 adapted from (Selkoe 2001)) are closely associated with AD by increasing local concentration and deposition of A $\beta$  (1-42). Most of the mutations are located within the A $\beta$  sequence or in regions of the  $\beta$ -APP gene that encode amino acids that lie immediately adjacent to the  $\beta$ - or  $\gamma$ -secretase cleavage sites (Chartier-Harlin, Crawford et al. 1991; Goate, Chartier-Harlin et al. 1991; Mullan, Crawford et al. 1992; Dumery, Bourdel et al. 2001). The following discussion enumerates some of the known missense APP mutations that are linked to familial or early-onset AD.

A double mutation (APP $\Delta_{NL}$ ) that alters Lys670Met671 in APP<sub>770</sub> to asparagine and leucine, respectively, also known as Swedish mutation, can be found just adjacent to the site of  $\beta$  secretase cleavage and induces heightened  $\beta$ -secretase cleavage to produce more A $\beta$ (1-40) and A $\beta$ (1-42) (Citron, Oltersdorf et al. 1992; Mullan, Crawford et al.

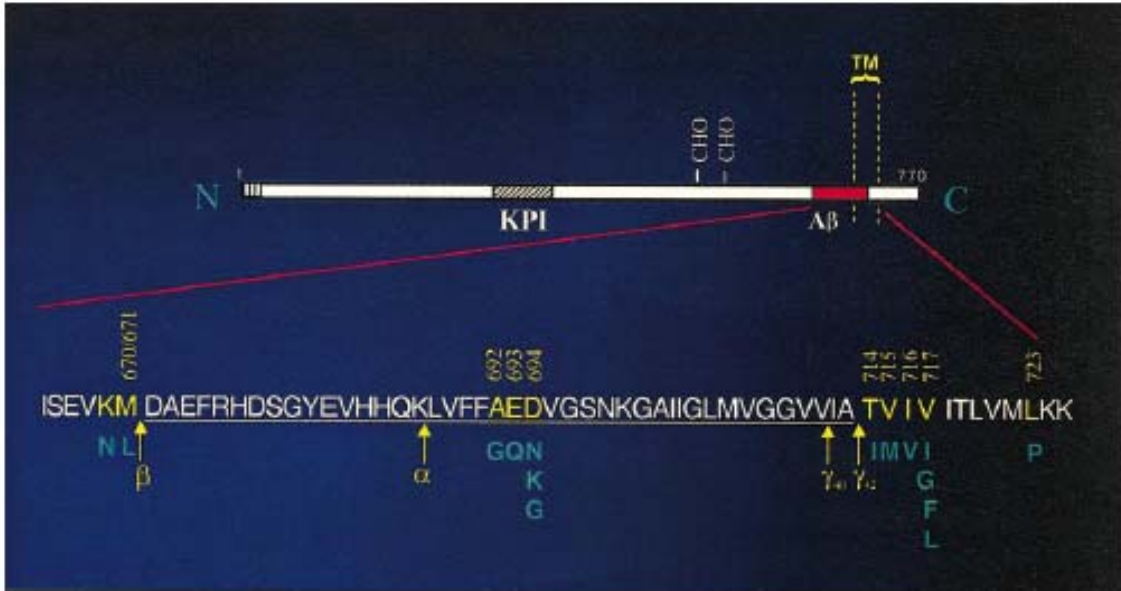


**Figure 1.2. APP mutations genetically linked to familial Alzheimer's disease.** The sequence within APP region that contains the A $\beta$  and transmembrane region is shown in expanded form, with a single-letter amino acid code. The underlined residues represent the A $\beta$  sequence. Arrows represent the cleavage sites for  $\alpha$ ,  $\beta$  and  $\gamma$  secretases. The vertical broken lines indicate the transmembrane region of the APP. Residues in yellow are the known sites for missense mutations, and residues in blue are the amino acids that replace the amino acids in original sequence. These are mutations identified in certain patients with familial Alzheimer's disease. The three-digit numbers represent the residue number according to the APP-770 isoform. (Selkoe 2001)

1992; Selkoe 2001). On the other hand, the five mutation sites that occur just COOH-terminal to the  $\gamma$ -secretase cleavage sites (some of which are London mutation (Val717Ile), Rouen mutation (Val715Met) and Florida mutation (Ile716Val)) seemingly have an enhancing effect on the production of A $\beta$ (1-42) species (Goate, Chartier-Harlin et al. 1991). The mutations within the A $\beta$  sequence enhance the aggregational properties of all A $\beta$  species. For instance, Dutch mutation (Ala692Gly) results in formation of plaques and tangles associated with dementia, and severe hereditary cerebral hemorrhage with  $\beta$ -amyloidosis (Hendriks, van Duijn et al. 1992; Buxbaum and Tagoe 2000; Selkoe 2001). Afflicted individuals show extensive amyloid deposition in vessel walls of cerebral cortex and leptomeninges (Levy, Carman et al. 1990). In general, vast evidences revealed that APP mutation increases A $\beta$ (1-42) concentration by a factor of 1.5 to 1.9, while A $\beta$ (1-40) concentration remains the same (Findeis 2007).

Aside from APP mutations, mutations in presenilin 1 (PS1, found on chromosome 14) and presenilin 2 (PS2, on chromosome 1) have also accounted for 30% to 40% of all cases of EOAD. Presenilins are expressed in brain and concentrated in neurons (Scheuner, Eckman et al. 1996; Uchihara, el Hachimi et al. 1996). More than 30 mutations in PS1 and 2 in PS2 have been reported (Selkoe 1997) and they generally result in increase of A $\beta$ (1-42) production (Scheuner, Eckman et al. 1996; Buxbaum and Tagoe 2000). For instance, immunohistochemical analyses of brains of patients with Glu280Ala PS-1 mutation showed a greatly elevated A $\beta$ (1-42), but not A $\beta$ (1-40), levels in the cerebellum (Lemere, Blusztajn et al. 1996). Evidences also showed that mutations in gene encoding PS lead to a 1.5 to 3-fold increase in the relative abundance of plaques containing A $\beta$ (1-42) peptides in FAD, compared with the levels in sporadic cases of AD

(Lemere, Blusztajn et al. 1996; Mann, Iwatsubo et al. 1996; Selkoe 2001). Moreover, the rate of A $\beta$ (1-42) aggregation was significantly enhanced in the presence of PS mutation, compared to that of A $\beta$ (1-40) peptide (Jarrett, Berger et al. 1993).

Taken together, these genetic studies support the notion that the mutations in APP and PS lead to a significantly increased production of faster-nucleating A $\beta$  variant A $\beta$ (1-42) (Jarrett, Berger et al. 1993), and further underscores the idea that the acceleration of amyloid fibril formation is critical for the study of AD (Selkoe 1997).

As discussed in the previous section (1.1), neurofibrillary tangles that contain hyperphosphorylated tau proteins and A $\beta$ -containing senile plaques are hallmark characteristic features of AD. Over the years, debate has ensued over whether there is a link between A $\beta$  and tau abnormalities, and whether either contribute to the pathogenesis of the disease. Numerous evidences have demonstrated that mutations in both genes encoding APP and tau result in dementing illness. However, further inquiry of the molecular effects and characterizing the clinical signs and symptoms of these mutations clarified the significance of tau and A $\beta$  in AD progression. APP mutations were proven to accelerate A $\beta$  production (as discussed above), and these mutations have been linked to some cases of EOAD (Goate, Chartier-Harlin et al. 1991). EOAD, although rare, reflects the histological profile of plaques and tangles. Furthermore, clinical studies of EOAD showed a characteristic hippocampal-predominant dysfunction as well as dysfunction in other neocortical sites. In comparison, investigations focusing on mutations of gene encoding tau showed that although these mutations promoted tau hyperphosphorylation, they did not lead to AD. Instead, the mutations resulted in the development of fronto-temporal dementia (FTD), which is another type of dementia

different from AD and characterized by frontotemporal atrophy (Hutton, Lendon et al. 1998). Furthermore, the presence of tangles that appear first in extrahippocampal sites and the absence of plaques make FTD histologically distinct from AD (Small and Duff 2008). These genetic findings led to the proposed “amyloid hypothesis” that A $\beta$  is the primary instigator for pathogenicity in AD, and its accumulation and elevation result in the hyperphosphorylation of tau and other clinical features of AD (Small and Duff 2008).

### 1.2.3 Amyloid $\beta$ - peptide

As discussed previously, the heterogeneous cleavage property of  $\beta$  and  $\gamma$  secretase gives rise to a 39 to 42 amino acid long fragment of A $\beta$ , with 40- residue peptide (termed A $\beta$ (1-40)) and 42-residue peptide (A $\beta$ (1-42)) as the most common. The presence of two additional amino acids in A $\beta$ (1-42) has extensive consequence with regards to its tendency to aggregate and form fibrils, with the longer A $\beta$ (1-42) having a faster aggregation rate and being more pathogenic (McLaurin, Yang et al. 2000; Castellani, Lee et al. 2008). In 1985, researchers purified and characterized the peptide from post-mortem brain of AD patients. Using liquid chromatography and western blotting, Beyreuther’s group revealed that the A $\beta$  peptides isolated from diseased patients are 4-5 kDa in size (Masters, Simms et al. 1985).

The presence of A $\beta$  in individuals not afflicted with AD indicates that the protein has a role in the normal physiology of the central nervous system; but the normal function of A $\beta$  is less understood as compared to its cytotoxic effects and its pathological role in AD. Nevertheless, numerous investigations have revealed some of the roles of this

APP fragment in the normal function of neuronal cells. Teng and co-workers suggested that the more predominant form A $\beta$ (1-40) functions as an antioxidant (Teng and Tang 2005). A $\beta$ (1-40) was also shown to counteract the toxic effects of  $\beta$  and  $\gamma$  secretase inhibitors at concentration as low as 10 pM (Plant, Boyle et al. 2003). Further studies have demonstrated that both A $\beta$ (1-40) and A $\beta$ (1-42) were found to moderate potassium channels in neurons (Ramsden, Plant et al. 2001; Findeis 2007).

Despite the normal physiological roles of A $\beta$ , the main focus of investigations is the ability of this protein to form fibrils and its role in neurodegeneration. Increasing interest in structural and functional properties of A $\beta$  led to a better understanding of this protein fragment. Numerous investigators have utilized various methods like circular dichroism (CD), nuclear magnetic resonance (NMR), Fourier Transform Infrared spectroscopy (FTIR) and microscopy techniques, among others, to extensively study the structure of A $\beta$  and its formation of fibrils (Hilbich, Kisters-Woike et al. 1991; Shen and Murphy 1995; Nilsson 2004; Stromer and Serpell 2005).

One challenge that researchers encountered in studying the structure of Alzheimer's A $\beta$  is the insolubility of the amyloid plaque, and as a result, the analysis of A $\beta$  from the diseased brain proved to be extremely difficult (Serpell 2000). This prompted researchers to concentrate on A $\beta$  fibrils that are formed *in vitro*. *In vitro* structural prediction studies revealed that the fibrils were of varying lengths, about 6-8 nm in diameter, and generally possess a parallel  $\beta$ -sheet conformation (as shown in Figure 1.3a and b) in which amino acids 41-42 of one peptide strand interact with amino acids 34-35 of the second peptide monomer (Lansbury, Costa et al. 1995; Mattson 1997;

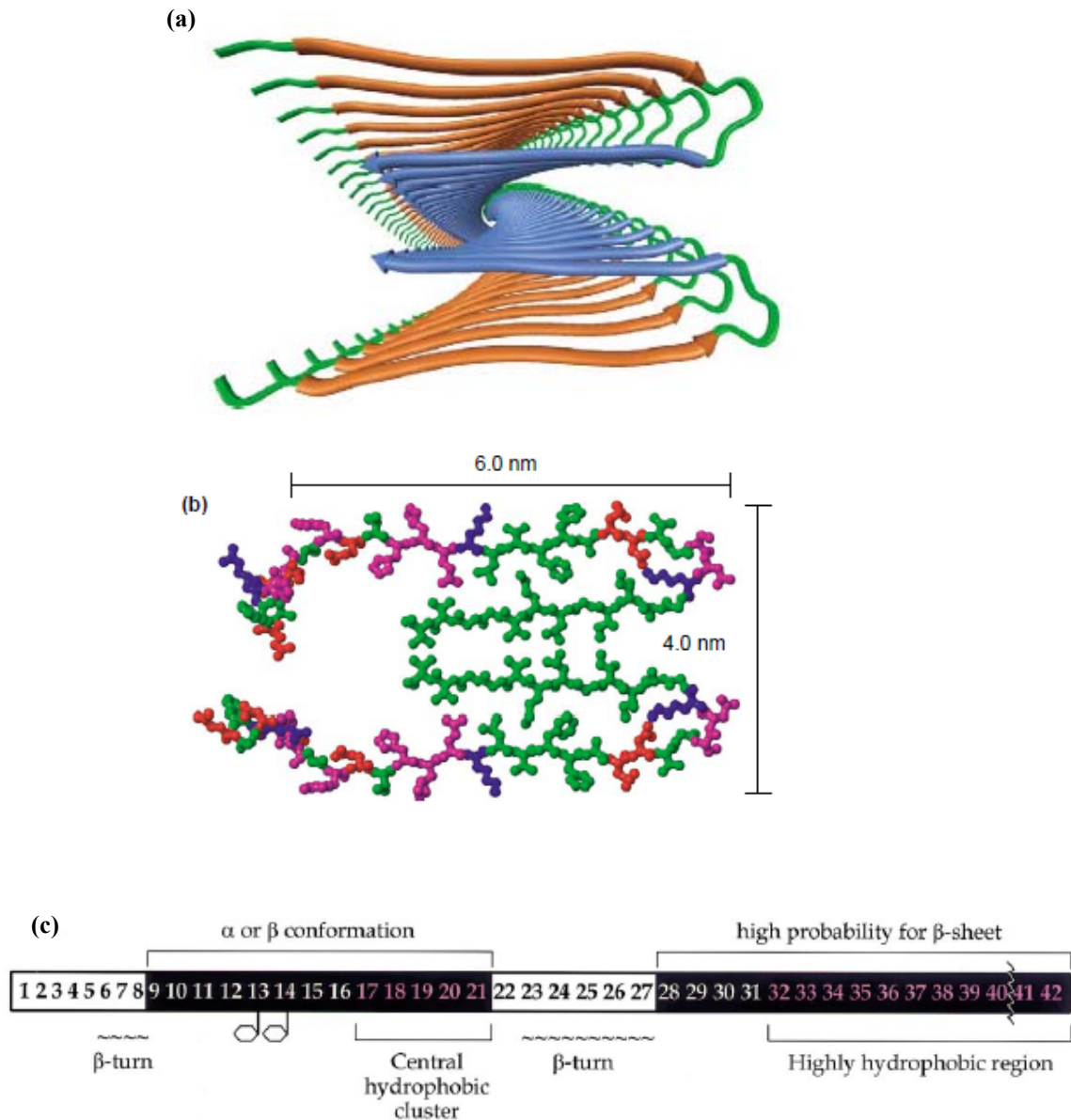


**Figure 1.3. Structural studies of Aβ.** (a) Ribbon diagram of residues 9-40 of Aβ (1-40) showing two β-sheet per molecule. Parallel β-sheets also observed on cross-β motif. (b) Atomic representation of fibers, showing the length (in diameter) of about 6-8 nm. (c) Structure prediction of Aβ (1-42), showing residues with high propensity for β-sheet. Highly hydrophobic regions are also shown. (Serpell 2000; Tycko 2004)

Kowalewski and Holtzman 1999; Tycko 2004). For fibrils of relatively shorter peptides (15 residues or less), an antiparallel  $\beta$ -sheet structure was demonstrated (Lansbury, Costa et al. 1995; Balbach, Ishii et al. 2000; Tycko 2004). Moreover, analysis of soluble A $\beta$  peptide uncovered amino acid characteristics that favor  $\beta$ -sheet conformation and revealed that C-terminal residues 28 to 40/42 have the highest probability for  $\beta$ -sheet formation, while residues 9 to 21 showed a lower probability for  $\beta$ -sheet. Further investigations showed that the propensity of residues 28 to 40/42 to form  $\beta$ -sheet is due to its highly hydrophobic property. Residues 17-21 also exhibit greatest hydrophobicity. Two predicted sites for  $\beta$ -turn in the peptide structure can be found between residues 6 to 8, and 23 to 27 (Figure 1.3c) (Serpell 2000).

Using X-ray diffraction, Kirschner *et al.* revealed the  $\beta$ -sheet conformation of the A $\beta$  fibers, estimating the length to be 80Å long and about 40Å thick (Kirschner, Abraham et al. 1986). These measurements correspond to four pleated sheets, with approximately 16 hydrogen-bonds for each sheet. Halverson *et al.* (1990) correlated peptide insolubility with  $\beta$ -sheet conformation using Fourier Transform Infrared spectroscopy (FTIR) studies. His group reported that residue A $\beta$ (34-42) possessed antiparallel stable  $\beta$ -sheet structure in the solid state (Halverson, Fraser et al. 1990). It was also shown that the residues 10 to 42 may form the  $\beta$ -sheet core of the fibrils, while fragments 1-9 were not required for fibril formation. Furthermore, this N-terminal region may be exposed on the surface of the fibers and may play a role in interaction between fibrils (Hilbich, Kisters-Woike et al. 1991). In addition, using electron microscopy, A $\beta$ (14-23) was found to be the shortest N-terminal fragment capable of fibril formation, and that deletions or substitutions on this fragment completely abolished or impaired

fibril formation (Tjernberg, Callaway et al. 1999). This led to the conclusion that sequence 14 to 23 of A $\beta$  forms the core of A $\beta$  fibrils.

As shown by evidences that are stated previously, A $\beta$  is a normal product in the brain and cerebrospinal fluid of normal individuals. This signifies that A $\beta$  itself does not lead to neurodegeneration. However, studies showed that the key to neuronal injury seems to lie on the aggregation state of A $\beta$ . Moreover, the ability of synthetic A $\beta$  to form fibrils *in vitro* may be influenced by various parameters such as variations in pH, temperature, buffers or solvent composition, presence of metals such as iron, copper and zinc, peptide concentration and peptide sequence (Fraser, Nguyen et al. 1991; Shen and Murphy 1995; Mattson 1997; Lansbury 1999; Serpell 2000; Walsh, Tseng et al. 2000; Nichols, Moss et al. 2005). The following discussion will focus on the study of amyloid  $\beta$  fibril formation *in vitro*.

#### 1.2.4 Amyloid $\beta$ fibrillogenesis

Why is the study of amyloid  $\beta$  fibrillogenesis relevant? It has been about a decade since the amyloid- $\beta$  cascade hypothesis was first proposed. According to this hypothesis, deposition and accumulation of fibrillar A $\beta$  in brain tissues are the key causative agent that drives AD pathogenesis (Hardy and Selkoe 2002; Teng and Tang 2005; Castellani, Lee et al. 2008). This led to an increased interest on understanding A $\beta$  fibril formation and how it can be a key to developing therapeutic strategies. Though numerous studies have focused on the biophysical aspects affecting formation of A $\beta$  fibrils, the kinetics or mechanism of A $\beta$  fibrillogenesis was poorly understood. Numerous

laboratories investigated the mechanism governing A $\beta$  fibrillogenesis by utilizing synthetic peptides. However, investigating the kinetics of A $\beta$  fibril formation proved to be a challenging quest due to limitations on available techniques. FTIR spectroscopy, CD, turbidity, thioflavin-T binding or microscopy could not provide detailed information on fibril size, nor was it appropriate for real time analysis. Moreover, these techniques are of limited use in clarifying the structures of fibrillogenesis intermediates (Kirschner, Abraham et al. 1986; Fraser, Nguyen et al. 1991; Hilbich, Kisters-Woike et al. 1991). The *in vitro* finding that A $\beta$  fibrillogenesis follows a nucleation-dependent polymerization mechanism (as illustrated in Figure 1.4a) was first verified in 1986 when Teplow's group extensively studied the nucleation and growth of A $\beta$ (1-40) fibrils using quasielastic light scattering spectroscopy (QLS) along with size exclusion chromatography (SEC) and electron microscopy (EM) (Lomakin, Chung et al. 1996). QLS is a useful technique in monitoring the sizes of protein polymers in solution. The combination of QLS, SEC, and microscopy allows a direct and rapid estimation of the A $\beta$  oligomerization state (Walsh, Lomakin et al. 1997).

The A $\beta$  kinetic process is dependent on two parameters, namely the nucleation rate and the rapid elongation or growth rate (Figure 1.4b, (Nilsson 2004)). Nucleation is considered to be an initial rate-limiting step characterized by a lag period in which A $\beta$  monomers self-associate to form micelles of A $\beta$  from which fibrils materialize and elongate (Serpell 2000; Carrotta, Barthes et al. 2007). The lag period of initial association of monomers to form a nucleus is an entropically unfavorable process (Nilsson 2004). However, once nucleus is formed, the aggregation proceeds rapidly to form fibrils. The lag phase can be overcome experimentally by several ways such as seeding and other

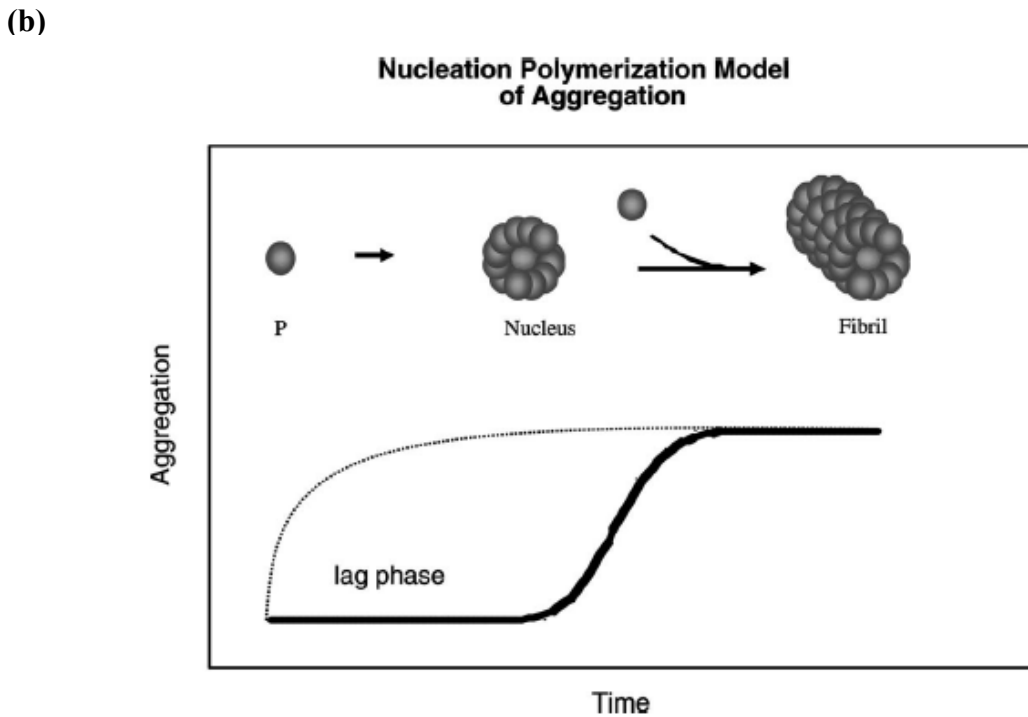
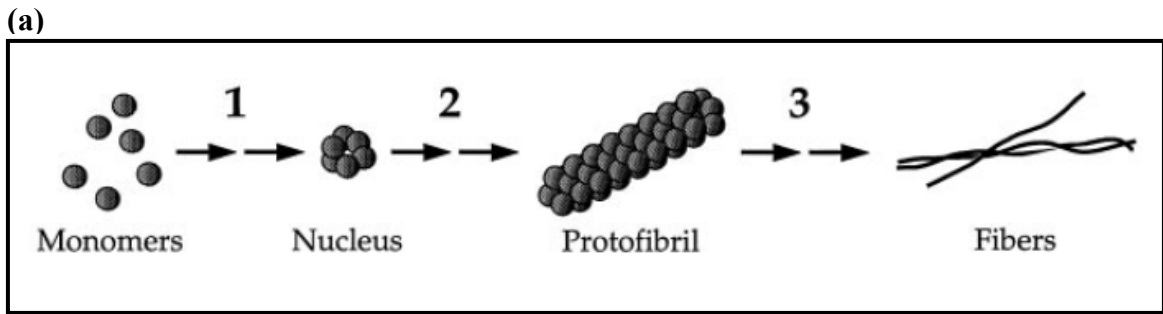


**Figure 1.4. Mechanism of A $\beta$  fibril- formation** (a) Process of A $\beta$  fibril-formation from monomers follows a nucleation-dependent polymerization mechanism (illustration from Walsh, Lomakin et al. 1997). (b) The nucleation polymerization model of aggregation follows two processes: nucleation, which is a slow process, and elongation which is rapid. The lag phase in nucleation process can be eliminated using various parameters such as variations in pH, temperature, solvent or buffer system, peptide concentration, or peptide sequence among others (illustration from Nilsson 2004).

biophysical processes (briefly discussed in section 1.4.3) Several laboratories have shown that A $\beta$  fibril polymerization proceeds with the formation of dimers, tetramers, and finally oligomers (Tjernberg, Callaway et al. 1999). Moreover, further structural and kinetic characterization of A $\beta$  fibrillogenesis utilizing X-ray fiber diffraction, light scattering, SEC and microscopy methods revealed that a time-dependent decrease in dimer levels was paralleled by an increase of transient prefibrillar intermediate in the fibril assembly, termed protofibrils (Harper, Wong et al. 1997; Walsh, Lomakin et al. 1997; Harper, Wong et al. 1999; Walsh, Hartley et al. 1999; Serpell 2000). Protofibrils are small elongated oligomers with beaded appearance observed early on in the A $\beta$  fibril formation process, are about 2.7 to 4.2 nm in diameter, and measure <200 nm in length which disappeared immediately with longer incubation time and were replaced by rigid, amyloid-type full-length fibrils (Harper, Wong et al. 1997; Kowalewski and Holtzman 1999; Walsh, Hartley et al. 1999; Dumery, Bourdel et al. 2001; Kaye, Head et al. 2003). Harper *et al* (1997) investigated A $\beta$ (1-40) protofibril formation by AFM and reported the appearance of small elongated A $\beta$  oligomers with average height of  $4.3 \pm 0.5$  nm and lengths that range from 20-70 nm, characteristic of protofibrils (Harper, Wong et al. 1997). Using QLS, Walsh *et al* reported a hydrodynamic radius  $R_H$  of  $27.8 \pm 1.8$  nm for the initially formed protofibrils, and steadily increased to a maximal value of  $80.6 \pm 14.4$  nm (Walsh, Hartley et al. 1999). Other evidences have demonstrated that protofibril formation was observed at the early stages of both A $\beta$ (1-40) and A $\beta$ (1-42) fibrillogenesis although they have differences in the diameter ( $\sim 4.2$  nm for A $\beta$  (1-42) and  $\sim 2.2$  nm for A $\beta$ (1-40) ) that may be attributed to the extra two residues of A $\beta$ (1-42) (Harper, Wong et al. 1997). Radiochemical and immunological assays revealed that other short-lived

intermediates are being produced prior to protofibril formation, however, it is the dimer and protofibrils that accumulate during fibrillogenesis substantiating the main idea that protofibrils act as centers of growth of mature fibers (Walsh, Lomakin et al. 1997). AFM analysis demonstrated that protofibril height is 40% that of fibrils (Harper, Wong et al. 1997; Harper, Wong et al. 1999). Several evidences also showed that protofibrils were in equilibrium with lower molecular weight (LMW) A $\beta$  in the course of A $\beta$  fibril formation. Further characterizations revealed that protofibrils are not easily sedimented, are too small to produce turbidity, and have significant  $\beta$ -sheet content, as shown by binding to Congo red and thioflavin T, as well as CD data (Harper, Wong et al. 1997; Walsh, Hartley et al. 1999).

Active research on the mechanism of A $\beta$  fibrillogenesis resulted in several proposed models that may further clarify the transition from protofibril to fibril formation. One possible mechanism introduced is end-to-end association of protofibrils. However, this model is unlikely due to kinetic barriers that may be encountered with regards to proper alignment of protofibril ends. Another possible mechanism is “lateral association” in which protofibrils combine laterally followed by addition of smaller A $\beta$  species (ie. monomers and dimers) to the end. Lateral association of protofibrils followed by end-to-end annealing is another possible alternative explanation for A $\beta$  fibril formation (Burdick, Soreghan et al. 1992; Harper, Wong et al. 1997; Walsh, Lomakin et al. 1997; Walsh, Hartley et al. 1999; Nichols, Moss et al. 2002).

The investigation of A $\beta$  fibrillogenesis proved to be a very challenging endeavor. Numerous investigators reported other structures preceding fibril formation including A $\beta$ -derived diffusible ligands (ADDLs), A $\beta$ \*56, “globulomers” and “A $\beta$  oligomers”

(Roychaudhuri, Yang et al. 2009). These fibrillar intermediates differ in morphology and size, but it is still a challenge to distinguish one from the other. AFM analysis showed that ADDLs are small “globules” of diffusible A $\beta$  oligomers that measures 4.8 to 5.7 nm. Further characterization of ADDLs by western blot analysis and SDS revealed a molecular weight that ranges between 17 and 42 kDa, with the predominant species at 27 kDa (Lambert, Barlow et al. 1998). A $\beta$ \*56, which has a molecular weight of 56 kDa characteristic of dodecameric species and morphology of prostate ellipsoid, was isolated and identified from brains of *Tg2576* mice (Lesne, Koh et al. 2006). AFM analysis of the isolated A $\beta$ \*56 measured ~1 nm in height (Cheng, Scarce-Levie et al. 2007). On the other hand, “globulomers”, so called due to the globular oligomeric structure, do not form fibrils despite their ability to form  $\beta$ -sheet structure (Gellermann, Byrnes et al. 2008). A $\beta$  oligomers that were produced *in vitro* were found to be composed of 15 – 20 monomers, with approximate MW of ~90,000 characteristic of an octadodecamer (Kayed, Head et al. 2003). Taken together, these intermediate species were termed “soluble oligomers” (Deshpande, Mina et al. 2006). This general term applies to all forms of A $\beta$  that do not pellet down after high speed centrifugation (typically >100,00g for more than 1h) (Irvine, El-Agnaf et al. 2008).

It is apparent that the extensive efforts of various laboratories to study and elucidate the mechanism of A $\beta$  fibrillogenesis unexpectedly revealed a wide range of fibrillar and oligomeric intermediates that may have a contribution to development of AD. Biochemical and biophysical methods such as size measurement, however, could not sufficiently provide the required sensitivity to distinguish one aggregation state to another. Recent advances in the study of A $\beta$  polymerization have included the use of

conformation-specific antibodies that recognize generic structural features for providing more detailed and sensitive information about the identity of aggregated species (O'Nuallain and Wetzel 2002; Kaye, Head et al. 2003; Glabe 2004). The continuing progress in the research of A $\beta$  polymerization process, and the availability of numerous tools for studying A $\beta$  aggregation, are instrumental for elucidating the pathogenesis of AD and in designing strategies for therapeutic intervention.

### 1.2.5 Correlation between A $\beta$ assembly and AD

According to the A $\beta$  cascade hypothesis, the overproduction of A $\beta$  or the increased proportion of the A $\beta$ 42/A $\beta$ 40 ratio is the basic pathophysiological process that causes early-onset AD. Over the years, numerous *in vitro* and *in vivo* studies have demonstrated that the fibrillar form of A $\beta$  is toxic to the neurons (Table 1.1 (Mattson 1997)). Several investigators, for instance, Yankner *et al* (Lorenzo and Yankner 1994) studied the neurotoxicity of different A $\beta$  species by creating nonamyloidogenic amorphous A $\beta$  aggregates and the amyloidogenic A $\beta$  fibrils and comparing their neurotoxic effects to primary rat hippocampal cultures. The prepared peptides were characterized by microscopy and Congo red staining technique. For this study, 20  $\mu$ M of A $\beta$  was applied to the hippocampal cultures and the biological effects were determined by immunohistochemical process. Their results showed that the fibrillar form caused significant neuronal cell loss and synapse loss while the nonfibrillar form was not toxic. The neurotoxic effects of fibrillar A $\beta$  to neurons were also demonstrated by other laboratories as well (Kowall, Beal et al. 1991; Pike, Burdick et al. 1993; Geula, Wu et al.

**Table 1.1. Cytotoxic actions of amyloid- $\beta$  peptide** (adapted from (Mattson 1997))

<b>Cell Type</b>	<b>Toxic Action</b>
Hippocampal neurons	Cell death, sensitivity to excitotoxicity
Cortical neurons	Cell death, sensitivity to excitotoxicity, sensitivity to energy depletion, impaired muscarinic signaling
Neocortical neurons	Cell death
Neuroblastoma cells	Cell death
PC12 cells	Impaired mitochondrial function
Synaptosomes	Impaired glutamate transport, impaired mitochondrial function
Astrocytes	Reactive phenotype, glutamate transport impairment
Microglia	Cell activation/injury
Smooth muscle	Damage and death
Vascular endothelial	Impaired glucose transport, loss of barrier function, apoptosis influx

1998). However, upon analyzing the post-mortem brains of the diseased patients, there is insubstantial correlation between dementia and the density of fibrillar amyloid (Walsh, Klyubin et al. 2002b; Walsh and Selkoe 2007; Irvine, El-Agnaf et al. 2008). This observation eventually became a flaw of the amyloid- $\beta$  cascade hypothesis.

In contrast, for the past decade, evidences of the significant connection between soluble A $\beta$  levels and the extent of synaptic loss and cognitive impairment have continuously emerged (Lambert, Barlow et al. 1998; Lansbury 1999; Lue, Kuo et al. 1999; Walsh and Selkoe 2007). The use of synthetic A $\beta$  peptides, cell systems with over-expressed APP, APP transgenic mouse models and human CSF and postmortem brain contributed to the conclusion that soluble A $\beta$  induces neurotoxicity rather than fibrillar A $\beta$  (Kirkitadze, Bitan et al. 2002; Irvine, El-Agnaf et al. 2008). Krafft and coworkers (Roher, Chaney et al. 1996) isolated A $\beta$  from the post-mortem brain of AD patients, characterized the peptides using SEC, mass spectrometry (MS), and microscopy techniques, and applied the peptides to cultures of rat hippocampal neuron glia cells. Their study shows that dimers caused neuronal killing in the presence of microglia.

Similarly, Teplow's group demonstrated using MTT (3-(4,5-dimethylthiazol-2-yl)-2,5-diphenyltetrazolium bromide) assay that protofibrils perturb the normal metabolism of cultured rat cortical neurons, which may be an early indicator of neuronal dysfunction and cell death (Walsh, Hartley et al. 1999).

Utilizing *Tg(APP<sup>Swe</sup>)2576Kahs* mice (Tg2576), a well-characterized APP transgenic mouse model that expresses APP mutation that is linked to AD, Lesne and colleagues investigated the cause of memory decline in the absence of neurodegeneration (Lesne, Koh et al. 2006). Using the performance on the Morris-water maze as a measure

of spatial memory, they showed that mice started to develop memory deficits during the middle age (6-14 months). When they analyzed the A $\beta$  species in the forebrain extracts of these mice, they found that the nonameric and dodecameric A $\beta$  species correlated with the impairment of spatial memory.

Despite the emerging evidences implying the toxicity of soluble oligomers and their ability to cause neuronal injury, it must be emphasized that the large insoluble A $\beta$  fibrils have been observed in the vicinity of the plaques and are also likely to be intimately surrounded by a number of soluble oligomers. Taken together, the conclusion that the large insoluble deposits, or the small oligomeric structures are the sole neurotoxic entity is not yet established. Rather, it may be possible that there is a continuous exchange between the two forms and both species are detrimental.

### 1.3 AD and inflammation

Closer analysis of the senile plaques observed in AD revealed the presence of several cells that include astrocytes and activated microglia (El Khoury, Moore et al. 2003). Astrocytes are the largest population of cells in the central nervous system (CNS). These cells function as major contributors to the structure and preservation of the blood-brain barrier (BBB). They also help in maintaining homeostasis of the extracellular environment (Moore and O'Banion 2002). In the presence of inflammatory stimulus, astrocytes respond by expressing class I and II major histocompatibility molecules (MHC-I and MHC-II, respectively). However, astrocytes are deficient in costimulatory molecules. This deficiency inhibits them from presenting the antigen to naïve T-cells

although they can present antigens to primed memory T cells (Halliday, Robinson et al. 2000).

Microglial cells are the resident immune cells of the CNS with properties and staining characteristics similar to macrophages (Ulvestad, Williams et al. 1994; Halliday, Robinson et al. 2000). The morphology of the microglial cells was first described in 1932 by Rio-Hortega in silver carbonate-stained brain preparations at the light microscope level (Rio-Hortega 1932; Lee, Nagai et al. 2002). Under normal physiological conditions and in the normal adult brain, the microglia are found as “resting” microglia, and adopt a morphology characterized by a small cell body with fine and ramified processes and low expression of surface antigens (Garden and Moller 2006). The role of “resting” microglia is for immune surveillance and host defense (Liu and Hong 2003). Microglial cells are considered the first line of host defense against pathogens. However, when there is an injury or infection in the CNS, the “resting” microglia becomes activated, bringing about a change in morphology from ramified morphology to a more spherical cell morphology and more elongated or extended processes (Fischer and Reichmann 2001). Moreover, similar to activated astrocytes, activated microglia up-regulate a variety of cell-surface receptors, including MHC-II, proinflammatory cytokines and chemokines which include tumor necrosis factor alpha (TNF $\alpha$ ), free radicals (NO), reactive oxygen species (ROS) and complement proteins (Moore and O'Banion 2002; Liu and Hong 2003).

Numerous studies of AD have demonstrated that microglia often cluster at sites of extracellular deposits of A $\beta$  (Masumura, Hata et al. 2000). The first animal model evidence linking A $\beta$  plaque formation with microglial activation was reported in 1998 when Cole and co-workers utilized hybrid Tg2576(HuAPPsw) mice (Tg2576 with

Swedish familial K670N/M671L double mutation) in probing microglial response to A $\beta$  formation (Frautschy, Yang et al. 1998). This transgenic mouse model progressively develops A $\beta$  deposits that test positive in Congo red staining between 26 and 32 weeks of age. Swedish mutation also increases the total cerebral burden of A $\beta$  than with the mutant APP (Buxbaum and Tagoe 2000). In the study, Cole *et al.* used *Griffonia simplicifolia* (GS) lectin labeling and phosphotyrosine staining to identify microglia. These methods were chosen due to the fact that GS lectin specifically labels microglia in the rodent brain (Kato, Kogure et al. 1995) and plaque-associated microglia express high levels of phosphotyrosine (Akiyama, Barger et al. 2000). The investigators' results demonstrate that an increased density of enlarged microglia gathered in and around plaques that are present predominantly in the hippocampus and cerebral cortex of 10- to 16-month HuAPP<sup>sw</sup> mice. This finding is very similar to the microglial activation related to A $\beta$  formation in the AD brain.

Similar transgenic mouse (Tg2576APP<sup>sw</sup>) model studies showed activation of the microglial cells in and around the fibrillary A $\beta$  plaque perimeter (Apelt and Schliebs 2001; Wegiel, Wang et al. 2001). Moreover, several studies have demonstrated the microglia's capacity to phagocytose and internally degrade A $\beta$  (Frautschy, Cole et al. 1992; Moore and O'Banion 2002). This phagocytic activity of microglia is considered to be an antigen-presenting ability of the microglial cells and this may be substantial in activation of the immune response.

Evidences have also emerged as to the contribution of A $\beta$  in neurotoxicity and AD pathogenesis. Both *in vivo* and *in vitro* studies have shown that A $\beta$ (1-42) induce neuronal apoptosis (Kowall, Beal et al. 1991; Loo, Copani et al. 1993; Pike, Burdick et

al. 1993; LaFerla, Tinkle et al. 1995; Masumura, Hata et al. 2000; Combs, Karlo et al. 2001; Morishima, Gotoh et al. 2001) as manifested by changes in morphology and biochemistry of the neurons, such as membrane blebbing, compaction of nuclear chromatin and intranucleosomal DNA fragmentation (Loo, Copani et al. 1993; LaFerla, Tinkle et al. 1995).

Perhaps the most studied effect of A $\beta$  in neuroinflammatory process is as an inflammatory stimulus. It has been well documented that AD is characterized by a wide array of pro- and anti-inflammatory mediators. Analysis of microglia associated with senile plaques showed the presence of or a significant upregulation of inflammatory activity, such as production of cytokines and chemokines including interleukin (IL) -1 $\beta$ , IL-6, TNF- $\alpha$ , IL-8, transforming growth factor- $\beta$  (TGF- $\beta$ ), and macrophage inflammatory protein-1 $\alpha$  (MIP-1 $\alpha$ ), as compared to the age-matched, non-demented controls (Table 1.2) (Akiyama, Barger et al. 2000; Halliday, Robinson et al. 2000; Dumery, Bourdel et al. 2001; Perry, Newman et al. 2003). Likewise, several *in vitro* immunohistochemical studies have demonstrated the same findings of A $\beta$ -induced microglial upregulation of cytokines and chemokines (Meda, Cassatella et al. 1995; Yates, Burgess et al. 2000; Apelt and Schliebs 2001; Floden and Combs 2006). Using an *in vitro* cellular model of human monocytes/macrophages, Klegeris *et al.* showed that A $\beta$  peptide induced TNF $\alpha$  secretion on THP-1 cells (Klegeris, Walker et al. 1997). These accumulated data of an increased level of the proinflammatory products in the vicinity of senile plaques suggests that a chronic inflammatory process contributes to the progression of AD. Despite the numerous studies showing that several of these bioactive species promote neurodegenerative mechanisms, others exert beneficial neurotrophic effects (Halliday,

Robinson et al. 2000).

The role of TNF $\alpha$  in AD, for instance, is surprisingly controversial since it has both pro-apoptotic and anti-apoptotic effects. This proinflammatory cytokine, which is a powerful inflammatory mediator, is reported to kill human cortical neurons (Good, Werner et al. 1996; Venters, Tang et al. 1999) and was found to be accountable for the neurotoxic activity of microglia such as an increased expression of inducible nitric oxide synthase (Combs, Karlo et al. 2001). Along with interferon gamma (IFN $\gamma$ ), TNF $\alpha$  is a potent paracrine stimulator of other proinflammatory cytokines (Perry, Collins et al. 2001). On the other hand, TNF $\alpha$  production has also been reported to have a neuroprotective role in neurons by inducing the expression of protective molecules including manganese superoxide dismutase (Akiyama, Barger et al. 2000).

There is strong evidence of increased levels of TNF $\alpha$  in the brain microvessels and cerebrospinal fluid of clinically diagnosed AD patients (Bruunsgaard, Andersen-Ranberg et al. 1999; Tarkowski, Blennow et al. 1999; Tarkowski, Andreasen et al. 2003). For example, Blasko *et al* showed that TNF $\alpha$ , in combination of interferon (IFN)- $\gamma$ , increases the production of A $\beta$  and inhibits the production of soluble APP in human neuronal and nonneuronal cells (Blasko, Marx et al. 1999). These demonstrate the participation of proinflammatory factors in the exacerbation of AD pathology.

Thus, vast data now have convincingly demonstrated that extracellular deposition of A $\beta$  in the AD brains triggers inflammation. How A $\beta$  stimulates microglia at a molecular level is still unclear. Several studies have shown that A $\beta$  induces glial activation through nuclear factor- $\kappa$ B (NF- $\kappa$ B) (Akama, Albanese et al. 1998; Bales, Du et al. 2000; Combs, Karlo et al. 2001). Moreover, several laboratories suggested the

**Table 1.2. Microglial antigens and inflammatory mediators elevated in Alzheimer's disease** (reproduced from (Perry, Newman et al. 2003))

Surface/membrane receptors	MHC class I, MHC class II Leukocyte common antigen, CD11a Complement receptor 3 Complement receptor 4 Vitronecting receptor Fc- $\gamma$ receptor CSF1 receptor Macrosialin (CD68)
Complement and related proteins	C1q, C3, C5, C6, C7, C8, C9 C3b, C4b and C5b opsonins C5b9 membrane attack complex C4 binding proteins Clusterin (apolipoprotein J)
Cytokines and Chemokines (and receptors)	IL1 $\beta$ IL6 (IL6R, gp130) TNF $\alpha$ TGF $\beta$ 1, 2 (TGF $\beta$ R1, TGF $\beta$ R2) IL8 (CXCR2) MIP1 $\alpha$ (CCR3, CCR5) MIP1 $\beta$ (CCR3, CCR5) MCP1 (CCR3, CCR5)
Effector enzymes	Cyclooxygenase 2 Inducible nitric oxide synthase
Acute phase proteins	Plasminogen activator inhibitor-1 $\alpha$ 1-Antichymotrypsin Tissue plasminogen activator Urokinase plasminogen activator Protease nexin-1 $\alpha$ 2- Macroglobulin Serum amyloid protein C-reactive protein Thrombin Apolipoprotein E $\alpha$ 2-Antiplasmin

CD, cluster differentiation; CSF, colony stimulating factor; IL, interleukin, MCP, monocyte chemoattractant; MHC, major histocompatibility complex; MIP, macrophage inflammatory protein; TGF, transforming growth factor; TNF, tumor necrosis factor

involvement of receptors in A $\beta$ -induced microglial activation. For instance, El-Khoury *et al.* (El Khoury, Hickman *et al.* 1996) reported that the scavenger receptor on the surface of microglia binds to A $\beta$  fibrils leading to cell adhesion and activation. Furthermore, other investigators suggested that A $\beta$ -induced microglial activation is due to A $\beta$  binding to the receptor for advanced glycation end products (RAGE) (Yan, Chen *et al.* 1996; Walsh, Lomakin *et al.* 1997). Using myeloid cells (e.g., THP-1 monocytes) and microglia, Bamberger *et al.* reported the involvement of a receptor complex (B-class scavenger receptor CD36, integrin associated protein/CD47 and the  $\alpha_6\beta_1$ -integrin) for microglial activation and proinflammatory response by fibrillar A $\beta$  (Bamberger, Harris *et al.* 2003). Recently, Fassbender's group showed that fibrillar A $\beta$ (1-42) interacts with LPS accessory receptor CD14 and triggers the release of proinflammatory products in primary murine microglial cells and human peripheral blood mononuclear (PBM) cells (Fassbender, Walter *et al.* 2004). This involvement of CD14 in A $\beta$ -induced microglial activation now presents a possible connection between innate immunity and AD pathology.

#### 1.4 Toll-like Receptors and Innate Immunity

“Immunity” refers to the ability of the host to protect itself from microbes that would otherwise destroy it (Hoebe, Janssen *et al.* 2004). Immunity can be broadly classified into two inducible systems: the innate immunity (‘natural immunity’) and adaptive immunity (‘acquired immunity’) (Kielian 2006). During infection, these two systems are activated sequentially to fight off and eliminate the microbe. Innate immunity

is the first line of host defense towards these invading microbes while adaptive immunity is activated later, usually about 4-7 days after infection (Albiger, Dahlberg et al. 2007). The adaptive immune response is mediated by clonally distributed B and T lymphocytes and is characterized by specificity and memory (Akira, Uematsu et al. 2006). Microbial recognition involves the production of random and highly diverse antigen T- and B- cell receptors, followed by clonal selection and amplification of these receptors with relevant specificities. This mechanism requires augmentation and differentiation of the specific clones into effector cells before they can contribute to host defense. The whole process takes, as mentioned above, about 4-7 days thus making adaptive immune response a delayed response (Akira, Takeda et al. 2001; Janssens and Beyaert 2003).

Innate immune response, on the other hand, is responsible for early detection of invading pathogens. It is largely mediated by white blood cells (neutrophils and macrophages), natural killer cells, dendritic cells, as well as perivascular macrophages and microglia in CNS (Aderem and Ulevitch 2000; Kielian 2006). Originally thought of as nonspecific, later investigations showed that innate immune response can discriminate self and a variety of potential pathogens. Cells of the innate immunity effectively recognize the antigens by predetermined sets of germline-encoded pattern recognition receptors (PRRs) (Janssens and Beyaert 2003; Lee and Kim 2007). These PRRs are involved in opsonization, activation of complement and coagulation cascades as well as of proinflammatory signaling cascades, phagocytosis and apoptosis (Medzhitov 2001).

Because of limited receptor expression, the cells of the innate immune system recognize the antigen by virtue of highly conserved structures that are expressed on these invading microorganisms. These specific, highly conserved motifs are termed pathogen-

associated molecular patterns (PAMPs) (Aderem and Ulevitch 2000; Kielian 2006; Lee and Kim 2007). PAMPs are produced only by microbes and not by host cells and do not vary between microorganisms of the same class. Moreover, they are vital for microbial survival. These features make them the perfect target for innate immune recognition (Medzhitov 2001). PAMPs recognition by PRRs results in activation of both extracellular (such as complement pathways) and intracellular signaling cascades that eventually culminate in the production of inflammatory response (Lee and Kim 2007).

The innate immune system uses PRRs that are located in three different compartments: those that are secreted into the blood stream and tissue fluids, expressed on the cell surface, or those that are expressed in intracellular compartments (Janssens and Beyaert 2003). PRRs in body fluids functions include PAMPs opsonization, activation of complement pathways and transfer of PAMPs to other PRRs. PRRs on the cell surface presents PAMPs to other PRRs, promotes phagocytosis, and initiates major signaling pathways. The cytoplasmic PRRs, on the other hand, are involved in antibacterial immune response and antiviral defense (Lee and Kim 2007). One of the most important and best characterized pattern recognition receptor families on the cell surface are the Toll-like receptors.

#### 1.4.1 Toll-like receptors (TLR)

Toll like receptors (TLRs) are products of evolutionary process. Analogous receptors are found in plants, insects, worms (*Caenorhabditis elegans*) and vertebrates (Albiger, Dahlberg et al. 2007). The founding member of the Toll family, termed Toll,

was identified in 1996 in the fruit fly *Drosophila melanogaster* (Parker, Prince et al. 2007). *Drosophila Toll* was initially reported to be responsible for controlling dorsoventral patterning during the fruitfly development (Medzhitov 2001; Kielian 2006; Glezer, Simard et al. 2007). Later, Lemaitre *et al.* (Lemaitre, Nicolas et al. 1996) reported that *Drosophila Toll* was also involved in antifungal immunity in adult fruit flies. In this study, they utilized Toll-mutant *Drosophila* and found that these species rapidly succumb to fungal infection due to failure to induce Drosomycin, an antifungal peptide. When the *Drosophila Toll* was sequenced, Gay and Keith (Gay and Keith 1991) realized that their intracellular domains showed striking similarity with the intracellular signaling domain of the mammalian interleukin-1 (IL-1) receptor. This discovery prompted investigators to search and identify mammalian Toll-like homologues.

TLRs are type I transmembrane proteins that are composed of a highly variable ectodomain of leucine-rich repeats (LRRs) and a highly conserved intracellular or cytoplasmic domain that is homologous to the interleukin-1 receptor (IL-1R) thus called Toll/IL-1 receptor (TIR) domain (Miggin and O'Neill 2006; Trinchieri and Sher 2007). LRR domains consist of 19-25 tandem repeats, each repeat contains 24-29 amino acids and is involved directly or through accessory molecules in ligand binding (Albiger, Dahlberg et al. 2007; Trinchieri and Sher 2007). TIR domain, on the other hand, interacts with TIR-domain-containing adaptor molecules for signal transduction (Janssens and Beyaert 2003). To date, 13 mammalian TLRs have been identified (10 human (TLR1-10) and 12 murine (TLR1-9 and TLR11-13)) (Kielian 2006; Konat, Kielian et al. 2006; Albiger, Dahlberg et al. 2007; Parker, Prince et al. 2007), and at least one agonist has been identified for each TLR, with the exception of TLR10 (Kopp and Medzhitov 2003;

Konat, Kielian et al. 2006). The agonists that are being recognized by TLRs, some of which are listed in Table 1.3, include microbial components in bacteria, fungi, parasites and viruses, including lipid-based cell wall components, microbial protein components and nucleic acids.

TLRs are expressed in several immune cells including human monocytes and macrophages, microglia, astrocytes, oligodendrocytes, dendritic cells (DC), B-cell, specific types of T-cells, as well as nonimmune cells such as fibroblasts and epithelial cells (Andreakos, Foxwell et al. 2004; Akira, Uematsu et al. 2006; Konat, Kielian et al. 2006). Furthermore, expression of TLRs may be extracellular or intracellular. TLRs 1, 2, 4, 5 and 6 are expressed on the cell surface while TLR 3, 7, 8 and 9 are almost exclusively found in intracellular compartments such as endosomes. TLRs that are intracellularly expressed have ligands that are mainly nucleic acids, and these ligands need to be internalized to the endosome before signaling is possible (Kielian 2006; Parker, Prince et al. 2007).

Figure 1.5 ( adapted from (Konat, Kielian et al. 2006)) illustrates the general signaling pathway by TLRs. Upon PAMPs recognition, TLR activation results in initiation of the downstream signaling pathway through recruitment and activation of a TIR-domain containing adaptor molecule, myeloid differentiation factor 88 (MyD88). Activation of MyD88 leads to further activation of other adaptor molecules such as serine/threonine kinase IL-1R-associated kinase (IRAK), which is associated with MyD88, as well as TNF-receptor associated factor 6 (TRAF6). This downstream activation cascade eventually leads to the activation of nuclear factor (NF)- $\kappa$ B family of

**Table 1.3 Human TLRs and ligands** (adapted from (Akashi-Takamura and Miyake 2006; Albiger, Dahlberg et al. 2007))

TLR	Major Ligands	Major Ligands and species
TLR1/TLR2	Triacyl lipopeptides	Bacteria and mycobacteria
TLR2	LTA	Gram-positive bacteria, i.e. <i>Staphylococcus aureus</i> , <i>Streptococcus pneumoniae</i> , etc.
	Atypical LPS	Gram-negative bacteria, i.e. <i>Porphyromonas gingivalis</i>
	Porins	Gram-negative bacteria, i.e. <i>Neisseria sp.</i> , <i>Shigella sp.</i> , <i>Haemophilus influenzae</i>
	Lipoarabinomannan	Mycobacteria
	Lipopeptides (Pam <sub>3</sub> CSK <sub>4</sub> , MALP2)	
	Peptidoglycan	Gram-positive bacteria
TLR3	dsRNA	Virus
TLR4	LPS	Gram-negative bacteria
	Fusion protein	RSV
	EDA domain fibronectin	(endogenous)
	HSP60	(endogenous)
TLR5	Flagellin	Flagellated Gram-positive and Gram-negative bacteria
TLR6/TLR2	Diacylated lipopeptides	Mycoplasma
	Zymosan	Yeast
	LTA	Group B streptococci
TLR7	ssRNA	Virus
TLR8	ssRNA	Virus
TLR9	Unmethylated CpGDNA	Bacteria
	Herpes virus DNA	Virus
TLR10	Not determined	
TLR11	Unknown	Uropathogenic <i>E. coli</i>

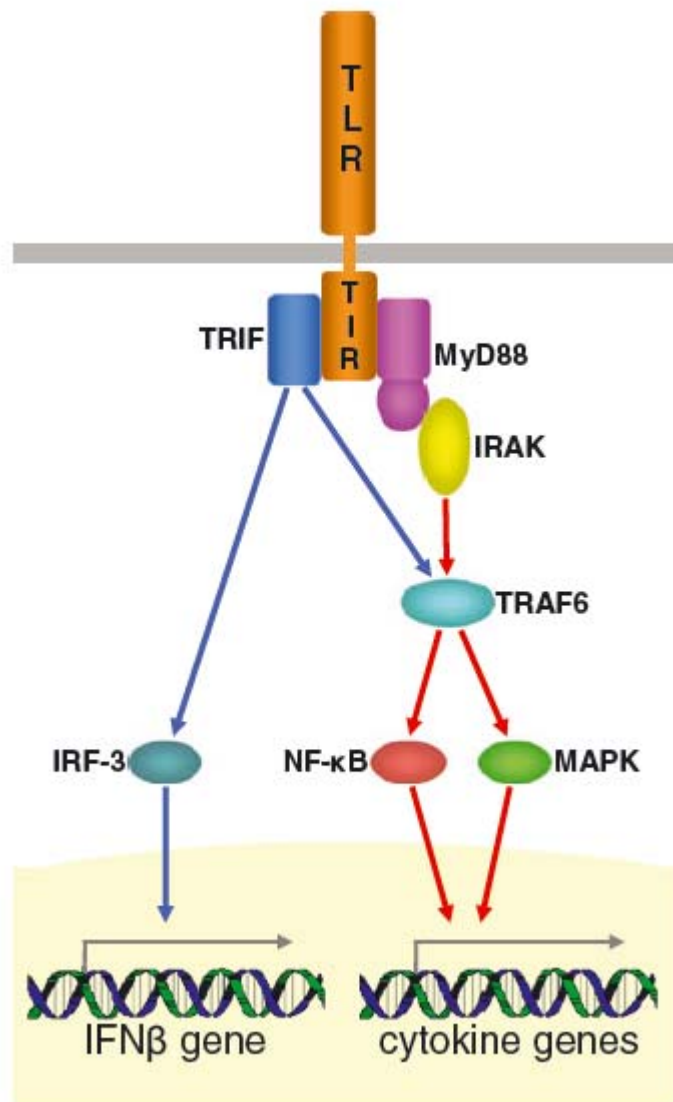


**Figure 1.5. The Toll-like receptor signaling pathway.** TLR activation by PAMPs recognition results in the activation of the downstream signaling pathway that culminates in the production of proinflammatory cytokines and chemokines, as well as IFN $\beta$ . The initiation of downstream signaling begins by activation and recruitment of adaptor molecules such as MyD88 (as shown). TLR signaling pathway also utilizes a MyD88-independent pathway, wherein TIRAP, TRIF and TRAM adaptor molecules are recruited and activated (not shown). (illustration from Konat, Kielian et al. 2006)

transcription factors, as well as initiation of distinct parallel signaling pathways leading to mitogen-activated protein (MAP) kinase. Initiation of these pathways subsequently result in transcription of a myriad of pro- and anti-inflammatory cytokines, chemokines and costimulatory molecules, such as TNF- $\alpha$ , IL-6, IL-1 $\beta$  and IL-12 (Kielian 2006; Konat, Kielian et al. 2006; Albiger, Dahlberg et al. 2007; Guo and Schluesener 2007; Parker, Prince et al. 2007).

TLR also utilizes other adaptor proteins for downstream signaling through a MyD88- independent pathway. This pathway starts with the TLR recruitment of adaptor proteins such as Toll-IR-1 receptor (TIR)-associated protein (TIRAP, also known as MAL), Toll-associated activator of IFN (TRIF) and Toll receptor-associated molecule (TRAM), which are crucial for the expression of interferon (IFN)-inducible genes (Akira, Uematsu et al. 2006; Kielian 2006; Konat, Kielian et al. 2006; Miggin and O'Neill 2006).

The study of human TLRs has progressed in the last 5 years (Kielian 2006), and investigations on TLR expression are rapidly expanding. The following discussion will focus on the most common and well defined TLRs, TLR2 and TLR4, as well as TLR accessory proteins.

#### 1.4.1.1 TLR4

TLR4 is perhaps the most extensively studied PRR. Furthermore, human TLR4 was the first characterized mammalian Toll (Medzhitov, Preston-Hurlburt et al. 1997). Like other TLRs, TLR4 is expressed in various cell types, predominantly in immune cells such as macrophages and DCs (Medzhitov 2001). It recognizes a variety of ligands, like

mannan (yeast) and host heat shock proteins and fibrinogen (virus) (Albiger, Dahlberg et al. 2007); however, TLR4 is mostly known to recognize gram negative bacterial cell wall component lipopolysaccharide (LPS) (Hoshino, Takeuchi et al. 1999). Hoshino *et al* and several other investigators demonstrated that TLR4 mediates responses to LPS using several mouse models that are TLR4-gene deficient, or LPS hyporesponsive mouse strains (Poltorak, He et al. 1998; Hoshino, Takeuchi et al. 1999; Qureshi, Lariviere et al. 1999). LPS, a major constituent of the outer membrane of the Gram-negative bacteria, consists of three regions (Figure 1.6 (Miller, Ernst et al. 2005)): the O-polysaccharide chain, the core saccharide and the lipid A (Huber, Kalis et al. 2006). The O-specific chain consists of a polymer of oligosaccharides with a repeating unit of one to eight glycosyl residues. Core saccharide (or core region), on the other hand, is made up of heterooligosaccharide that is subdivided into inner and outer core (Rietschel, Kirikae et al. 1994). Lipid A is composed of a diglucosamine backbone containing ester-linked and amide-linked long-chain fatty acids (Aderem and Ulevitch 2000) and functions as a hydrophobic anchor of LPS on the major gram-negative outer membranes (Dixon and Darveau 2005). It was already postulated since the 1950s that the lipid A is the toxic component of LPS. But it was not until the late 1980s when the chemical structure of lipid A was elucidated and chemically synthesized, and the biological activity of synthetic lipid A was compared with bacterial lipid A and LPS that lipid A was shown to be, in fact, the bioactive component of LPS (Loppnow, Brade et al. 1989; Rietschel, Kirikae et al. 1994)

LPS is an amphiphilic molecule and it forms aggregates in solution (Jerala 2007). Numerous evidences have established LPS as a powerful proinflammatory activator of

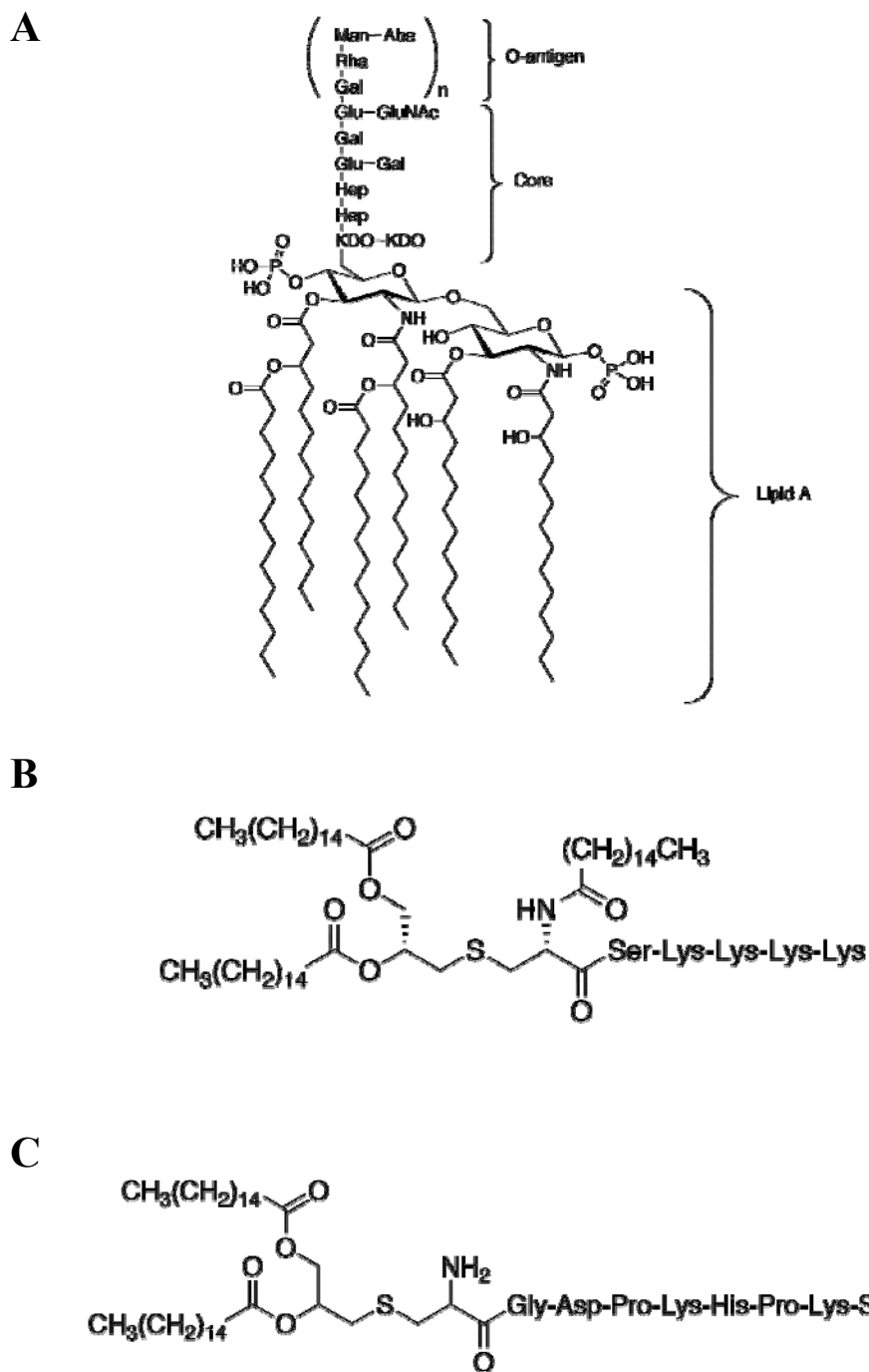


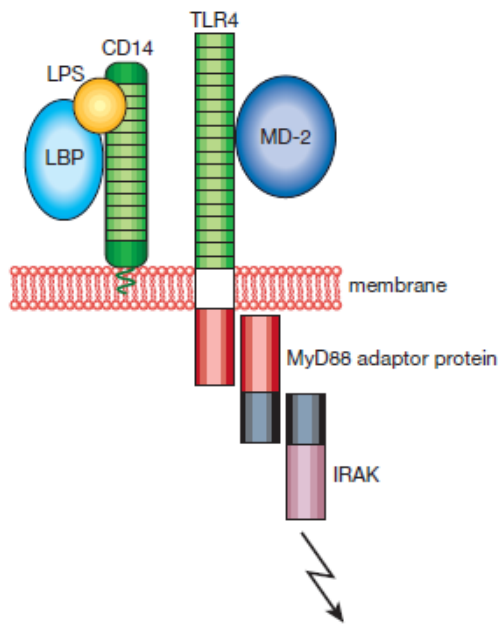
**Figure 1.6 Chemical structure of known TLR agonists.** (A) Bacterial lipopolysaccharide (LPS). (B) synthetic triacylated bacterial lipoprotein tripalmitoyl cysteinyl seryl tetralysine (Pam<sub>3</sub>CSK<sub>4</sub>). (C) synthetic diacylated bacterial lipoprotein FSL-1.

mononuclear cells, and TLR4- dependent activation of macrophages and microglia by nanogram quantities of LPS results in the production of myriad cytokines such as TNF- $\alpha$ , IL-1, -6, -8, as well as nitric oxide (NO), and superoxide which are capable of inducing apoptotic cell death (Poltorak, He et al. 1998; Moore, Andersson et al. 2000).

The molecular pathway of TLR4 activation by LPS has been extensively studied and is depicted in Figure 1.7a and 1.7b (Aderem and Ulevitch 2000; Akashi-Takamura and Miyake 2006; Kielian 2006). LPS recognition by TLR4 starts with the lipid A moiety binding to a 58-60 kDa serum protein, human lipopolysaccharide-binding protein (LBP). LBP is a serum glycoprotein belonging to a family of lipid-binding proteins that includes bactericidal/permeability-increasing protein (BPI), phospholipid ester transfer protein and cholesterol ester transfer protein (Gutsmann, Muller et al. 2001). In normal serum, LBP is present at concentrations of  $\approx 5$  to 15  $\mu\text{g/ml}$  (Kitchens, Wolfbauer et al. 1999). Investigations have shown that the function of LBP in LPS signaling is to convert oligomeric micelles of LPS to monomers, and to shuttle the monomeric LPS to CD14 (Jerala 2007). Disaggregating the LPS increases the transfer and binding of LPS to CD14 (Hailman, Lichenstein et al. 1994; Miller, Ernst et al. 2005).

CD14, a 55-kDa high-affinity LPS receptor, can either be secreted in the serum (soluble or sCD14) or expressed as a glycosphosphoinositol (GPI)-anchored protein (membrane or mCD14) on the surface of macrophages. Pugin *et al* reported the sCD14 level in normal serum to be 2 to 3  $\mu\text{g/ml}$  (Pugin, Schurer-Maly et al. 1993). Several biochemical and genetic evidences showed that CD14 binds to LPS with dissociation constant ( $K_D$ ) between 30 and 74 nM (Miyake 2004) and facilitates its signaling, but it does not appear to be essential in direct LPS response (da Silva Correia, Soldau et al.

(a)



(b)

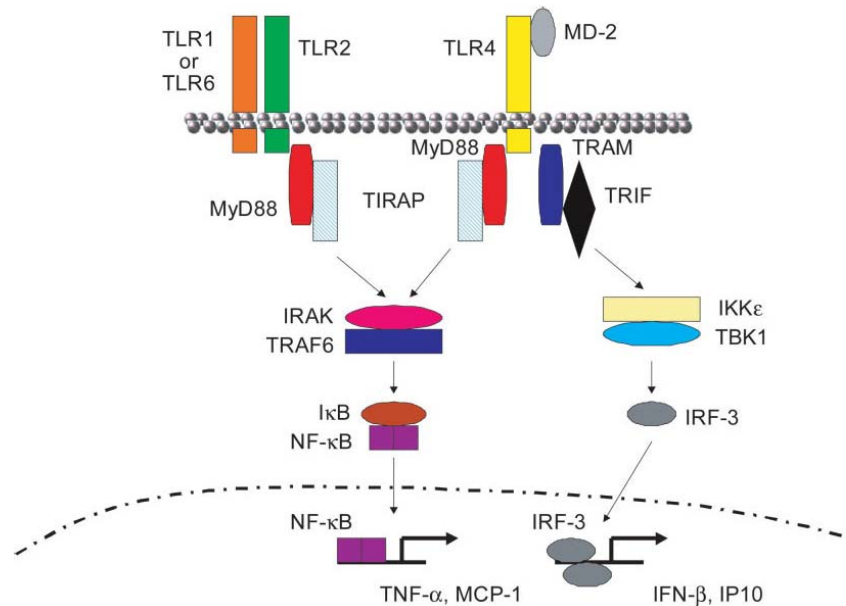


**Figure 1.7. TLR2 and TLR4 signaling pathway.** (a) TLR4 signaling starts with the binding of LPS, the most common TLR4 ligand, to LBP. LBP then transfers monomeric LPS to CD14. CD14 then presents LPS to TLR4:MD2. The trimeric complex LPS:TLR4:MD2 activates downstream TLR signaling leading to formation of proinflammatory products (Aderem and Ulevitch 2000). (b) Both TLR2 and TLR4 utilize the adaptor molecule MyD88 for downstream signaling pathway. TLR2 forms a complex with either TLR1 or TLR6 for recognition of triacylated or diacylated lipopeptide, respectively (illustration from Kielian 2006).

2001). Although CD14-knockout mouse studies have shown that LPS responses are detectable without CD14, this TLR accessory protein is essential for the initiation of the TRAM-TRIF pathway by TLR4/MD2 (Jiang, Georgel et al. 2005). Moreover, the significance of CD14 in LPS signaling was evidenced *in vivo* by an impaired TNF $\alpha$  response when CD14-deficient mice were challenged with LPS (Haziot, Ferrero et al. 1996).

*In vitro* studies showed the LPS/CD14 complex utilizes another host-derived soluble adaptor molecule for the activation of downstream TLR signaling. This co-receptor, termed MD-2, is a 25-30 kDa protein, lacks the transmembrane and intracellular region and is expressed on the cell surface in association with the ectodomain of TLR4 (Akira, Takeda et al. 2001; Medzhitov 2001; Akashi-Takamura and Miyake 2006; Kielian 2006). LPS bound to CD14 is transferred to MD-2, which associates with the ectodomain of TLR4. Together, the MD-2/TLR4 oligomer binds LPS with nanomolar affinity and the trimeric complex LPS:MD-2:TLR4 induces LPS signaling, translocation of nuclear proteins and transcriptional activation of genes associated with the inflammatory processes (Viriyakosol, Tobias et al. 2001; Akira, Uematsu et al. 2006; Glezer, Simard et al. 2007).

TLR4 interaction with MD-2 is crucial for efficient responses to LPS. This was supported by experiments that demonstrated unresponsive phenotype of mice carrying knockout mutations in either TLR4 or MD-2 genes (Hoshino, Takeuchi et al. 1999; Shimazu, Akashi et al. 1999; Nagai, Akashi et al. 2002). Recent efforts to elucidate the MD-2:TLR4 binding to LPS showed that the TLR4 region Glu<sup>24</sup>-Lys<sup>47</sup> is the site for MD-2 binding. Moreover, Cys<sup>29</sup> and Cys<sup>40</sup> within this region are critical for interaction with

MD-2 and LPS signaling (Nishitani, Mitsuzawa et al. 2006). Furthermore, a model for LPS-induced TLR4:MD-2 dimer was constructed based on mutational analysis wherein the structure formed resembles the 'm' shaped dimers (Jin and Lee 2008). Crystal structures of human MD-2 and its complex with LPS lipid A suggested that MD-2 plays a principal role in endotoxin recognition (Ohto, Fukase et al. 2007). Several lines of evidence also showed that TLR4 and MD-2 are important in ligand-recognition specificity (Shimazu, Akashi et al. 1999; Miyake 2004; Prohinar, Re et al. 2007), thus, it is plausible that TLR4 and MD-2 work together for ligand recognition and signal transduction.

#### 1.4.1.2 TLR2, TLR1, TLR6

Among all the TLRs that have been identified, TLR2 is considered the one with the broadest specificity when it pertains to PAMPs recognition. TLR2 has been shown to recognize a broad range of microbial products including peptidoglycan (PGN) from Gram-positive bacteria, bacterial lipoproteins (LP), mycobacterial cell-wall lipoarabinomannan, lipoteichoic acid (LTA), tripalmitoyl-S-glycerol-cysteine (Pam<sub>3</sub>Cys), glycosylphosphatidylinositol lipid from *Trypanosoma Cruzi*, a phenol-soluble modulin produced by *Staphylococcus epidermidis*, zymoan from fungi and glycolipids from *Treponema maltophilum* (Janeway and Medzhitov 1999; Medzhitov 2001; Kielian 2006). Moreover, studies have also shown that TLR2 recognize atypical LPS, which is structurally different from bacterial LPS by virtue of the number of acyl chains in the lipid A component (Takeda, Kaisho et al. 2003), from *Leptospira interrogans* (Medzhitov

2001) and *Porphyromonas gingivitis* (Hirschfeld, Weis et al. 2001). The wide spectrum of microbial components that TLR2 can recognize may be due, in part, to the ability of TLR2 to cooperate or complex with at least two other TLRs: TLR1 and TLR6. Therefore, TLR2 dimer formation with TLR1 or TLR6 may dictate specificity of ligand recognition (Ozinsky, Underhill et al. 2000; Takeuchi, Kawai et al. 2001; Akira, Uematsu et al. 2006). For instance, TLR2/TLR1 heterodimers preferentially act as a receptor for triacylated lipopeptides whereas TLR2/TLR6 heterodimers are the receptors for diacylated lipopeptides (Figure 1.6) (Ozinsky, Underhill et al. 2000; Takeuchi, Kawai et al. 2001; Takeuchi, Sato et al. 2002; Dziarski 2003; Omueti, Beyer et al. 2005).

TLR2 is expressed on monocytes, macrophages, microglia, dendritic cells, B cells and, to a lesser extent, on neutrophils and few other cells, whereas it has been shown that both TLR1 and TLR6 are expressed by microglia (Dziarski 2003; Kielian 2006). As presented in Figure 1.7b, TLR2 downstream signaling pathway begins with TLR2 complex formation with either TLR1 or TLR6, after which, the complex utilizes both the intracellular adaptor proteins MyD88 and TIRAP for subsequent induction of target genes such as TNF $\alpha$  and other cytokines and chemokines (Kielian 2006).

Evidences also demonstrate the role of CD14 on TLR2 recognition of gram-positive PAMPs, such as PGN and LTA. Schröder *et al.* used human embryonic kidney (HEK) cells and chinese hamster ovary (CHO) cells transfected with both TLR2 and CD14 to show that LTA of *Streptococcus pneumoniae* and *Staphylococcus aureus* utilize CD14 and TLR2 to activate immune cells (Schroder, Morath et al. 2003). Moreover, using a CD14 mutant with deletion of the part of possible N-terminal ligand binding pocket, and an anti-CD14 monoclonal antibody, Nakata's group demonstrated that CD14

binds to triacylated lipopeptides and facilitates its recognition by TLR2/TLR1 complex (Nakata, Yasuda et al. 2006). Other investigations utilizing knockout mice and transfected cell lines also demonstrated the necessity of CD14 for TLR2/TLR1 or TLR2/TLR6 heterodimer recognition of PAMPs (Gupta, Kirkland et al. 1996; Henneke, Takeuchi et al. 2001; Dziarski 2003; Esen and Kielian 2005; Manukyan, Triantafilou et al. 2005).

Earlier studies implicated TLR2, along with TLR4, as a receptor for LPS signaling (Kirschning, Wesche et al. 1998; Yang, Mark et al. 1998; Yang, Mark et al. 1999). However, a closer examination revealed that the original discrepancy on the involvement of TLR2 in LPS activation was due to the contaminating lipoproteins, which are TLR2 ligands, in commercially available LPS preparations (Kielian 2006). In fact, when LPS was repurified and the contaminating lipoproteins were removed, the LPS was unable to signal via TLR2 (Hirschfeld, Ma et al. 2000). Thus, investigations of PAMPs recognition by TLRs require careful scrutiny to ascertain that the TLR agonists are not contaminated with other biologically active PAMPs.

#### 1.4.2 TLRs and A $\beta$ : What is the connection?

In 2003, Fassbender's group published results demonstrating the role of CD14 in linking A $\beta$  with the innate immunity (Fassbender, Walter et al. 2004). By surface plasmon resonance spectroscopy (SPR), immunoprecipitation and western blotting, they showed that CD14 binds fibrillar A $\beta$  (1-42) with a dissociation constant ( $K_D$ ) of  $1.1 \pm 0.1 \times 10^{-7}$  M. Moreover, CD14 binding to fibrillar A $\beta$ 42 was 20-fold stronger as compared to

CD14 and nonfibrillar A $\beta$  (1-42) ( $K_D$  [M] =  $2.2 \pm 0.7 \times 10^{-6}$ ). The huge difference in the  $K_D$  values suggests that CD14 recognizes the  $\beta$ -sheet structure of the fibrillar A $\beta$ (1-42). The group also tested the role of CD14 in fibrillar A $\beta$ (1-42) – induced microglial activation using primary murine microglia from wildtype (WT) and CD14-deficient mice, treated the cells with fibrillar A $\beta$ (1-42) and interferon (IFN)- $\gamma$ , and analyzed the proinflammatory marker IL-6. Results showed that CD14-deficient microglia released significantly lower amounts of IL-6 in response to A $\beta$  as compared to WT microglia. A significant reduction of proinflammatory products was also observed when human peripheral blood monocytes (PBM) induced with fibrillar A $\beta$  was treated with anti-human CD14 monoclonal antibody, 3C10. These data further strengthens the interaction between CD14 and fibrillar A $\beta$ (1-42) in induction of proinflammatory products. The authors also showed overexpression of CD14 in APP transgenic mice, which signifies that CD14 significantly contributes to the inflammatory responses in AD.

However, CD14 does not contain a cytoplasmic domain (Haziot, Chen et al. 1988; Muta and Takeshige 2001; Viriyakosol, Tobias et al. 2001; Kim, Lee et al. 2005) that could activate the downstream signaling that induces production of proinflammatory products (see Figure 4). As explained earlier, CD14 functions as a co-receptor for LPS (Wright, Ramos et al. 1990; da Silva Correia, Soldau et al. 2001; Medzhitov 2001), as well as for Gram-positive cell walls and their PGN component (Pugin, Schurer-Maly et al. 1993; Gupta, Kirkland et al. 1996; Henneke, Takeuchi et al. 2001; Muta and Takeshige 2001; Nakata, Yasuda et al. 2006). These PAMPs utilize TLR4 and TLR2 for intracellular signal transduction. Fassbender *et al* (Fassbender, Walter et al. 2004) proposed that the observed A $\beta$  cellular activation may likely be transmitted by TLR4

based on the positive inflammatory response obtained from CHO cells which lack a functional TLR2.

In this regard, the purpose of this research is to investigate the possible involvement of TLR(s) in A $\beta$ (1-42) induction of the innate immune response. Specifically, this research aims to identify the TLR that functionally interacts with A $\beta$ (1-42). We also aim to investigate the possible involvement of other TLR accessory proteins and TLR complexes in A $\beta$ (1-42) innate immune activation. The field of TLR research is still in its infancy; thus, the information that will be obtained from this research may contribute to increased understanding of how A $\beta$  assemblies interact with TLR family members. Additionally, this investigation will contribute to further understanding the role of A $\beta$  in AD-associated neurodegeneration, and possibly, open a therapeutically relevant perspective for TLRs and their recognition abilities for host-derived pathogens.

## 1.5 Bibliography

- Aderem, A. and R. J. Ulevitch (2000). "Toll-like receptors in the induction of the innate immune response." Nature **406**(6797): 782-7.
- Akama, K. T., C. Albanese, et al. (1998). "Amyloid beta-peptide stimulates nitric oxide production in astrocytes through an NFkappaB-dependent mechanism." Proc Natl Acad Sci U S A **95**(10): 5795-800.
- Akashi-Takamura, S. and K. Miyake (2006). "Toll-like receptors (TLRs) and immune disorders." J Infect Chemother **12**(5): 233-40.
- Akira, S., K. Takeda, et al. (2001). "Toll-like receptors: critical proteins linking innate and acquired immunity." Nat Immunol **2**(8): 675-80.
- Akira, S., S. Uematsu, et al. (2006). "Pathogen recognition and innate immunity." Cell **124**(4): 783-801.
- Akiyama, H., S. Barger, et al. (2000). "Inflammation and Alzheimer's disease." Neurobiol Aging **21**(3): 383-421.
- Albiger, B., S. Dahlberg, et al. (2007). "Role of the innate immune system in host defence against bacterial infections: focus on the Toll-like receptors." J Intern Med **261**(6): 511-28.
- Andreaskos, E., B. Foxwell, et al. (2004). "Is targeting Toll-like receptors and their signaling pathway a useful therapeutic approach to modulating cytokine-driven inflammation?" Immunol Rev **202**: 250-65.
- Apelt, J. and R. Schliebs (2001). "Beta-amyloid-induced glial expression of both pro- and anti-inflammatory cytokines in cerebral cortex of aged transgenic Tg2576 mice with Alzheimer plaque pathology." Brain Res **894**(1): 21-30.
- Balbach, J. J., Y. Ishii, et al. (2000). "Amyloid fibril formation by A beta 16-22, a seven-residue fragment of the Alzheimer's beta-amyloid peptide, and structural characterization by solid state NMR." Biochemistry **39**(45): 13748-59.
- Bales, K. R., Y. Du, et al. (2000). "Neuroinflammation and Alzheimer's disease: critical roles for cytokine/Abeta-induced glial activation, NF-kappaB, and apolipoprotein

- E." Neurobiol Aging **21**(3): 427-32; discussion 451-3.
- Bamberger, M. E., M. E. Harris, et al. (2003). "A cell surface receptor complex for fibrillar beta-amyloid mediates microglial activation." J Neurosci **23**(7): 2665-74.
- Blasko, I., F. Marx, et al. (1999). "TNFalpha plus IFNgamma induce the production of Alzheimer beta-amyloid peptides and decrease the secretion of APPs." Faseb J **13**(1): 63-8.
- Brunnsgaard, H., K. Andersen-Ranberg, et al. (1999). "A high plasma concentration of TNF-alpha is associated with dementia in centenarians." J Gerontol A Biol Sci Med Sci **54**(7): M357-64.
- Burdick, D., B. Soreghan, et al. (1992). "Assembly and aggregation properties of synthetic Alzheimer's A4/beta amyloid peptide analogs." J Biol Chem **267**(1): 546-54.
- Buxbaum, J. N. and C. E. Tagoe (2000). "The genetics of the amyloidoses." Annu Rev Med **51**: 543-69.
- Carrotta, R., J. Barthes, et al. (2007). "Large size fibrillar bundles of the Alzheimer amyloid beta-protein." Eur Biophys J.
- Castellani, R. J., H. G. Lee, et al. (2008). "Alzheimer disease pathology as a host response." J Neuropathol Exp Neurol **67**(6): 523-31.
- Chartier-Harlin, M. C., F. Crawford, et al. (1991). "Early-onset Alzheimer's disease caused by mutations at codon 717 of the beta-amyloid precursor protein gene." Nature **353**(6347): 844-6.
- Cheng, I. H., K. Scearce-Levie, et al. (2007). "Accelerating amyloid-beta fibrillization reduces oligomer levels and functional deficits in Alzheimer disease mouse models." J Biol Chem **282**(33): 23818-28.
- Churcher, I. (2006). "Tau therapeutic strategies for the treatment of Alzheimer's disease." Curr Top Med Chem **6**(6): 579-95.
- Citron, M., T. Oltersdorf, et al. (1992). "Mutation of the beta-amyloid precursor protein in familial Alzheimer's disease increases beta-protein production." Nature **360**(6405): 672-4.
- Clarris, H. J., V. Nurcombe, et al. (1994). "Secretion of nerve growth factor from septum stimulates neurite outgrowth and release of the amyloid protein precursor of Alzheimer's disease from hippocampal explants." J Neurosci Res **38**(3): 248-58.
- Combs, C. K., J. C. Karlo, et al. (2001). "beta-Amyloid stimulation of microglia and

- monocytes results in TNFalpha-dependent expression of inducible nitric oxide synthase and neuronal apoptosis." J Neurosci **21**(4): 1179-88.
- da Silva Correia, J., K. Soldau, et al. (2001). "Lipopolysaccharide is in close proximity to each of the proteins in its membrane receptor complex. transfer from CD14 to TLR4 and MD-2." J Biol Chem **276**(24): 21129-35.
- Deshpande, A., E. Mina, et al. (2006). "Different conformations of amyloid beta induce neurotoxicity by distinct mechanisms in human cortical neurons." J Neurosci **26**(22): 6011-8.
- Dixon, D. R. and R. P. Darveau (2005). "Lipopolysaccharide heterogeneity: innate host responses to bacterial modification of lipid a structure." J Dent Res **84**(7): 584-95.
- Dumery, L., F. Bourdel, et al. (2001). "beta-Amyloid protein aggregation: its implication in the physiopathology of Alzheimer's disease." Pathol Biol (Paris) **49**(1): 72-85.
- Dziarski, R. (2003). "Recognition of bacterial peptidoglycan by the innate immune system." Cell Mol Life Sci **60**(9): 1793-804.
- El Khoury, J., S. E. Hickman, et al. (1996). "Scavenger receptor-mediated adhesion of microglia to beta-amyloid fibrils." Nature **382**(6593): 716-9.
- El Khoury, J. B., K. J. Moore, et al. (2003). "CD36 mediates the innate host response to beta-amyloid." J Exp Med **197**(12): 1657-66.
- Esen, N. and T. Kielian (2005). "Recognition of Staphylococcus aureus-derived peptidoglycan (PGN) but not intact bacteria is mediated by CD14 in microglia." J Neuroimmunol **170**(1-2): 93-104.
- Fassbender, K., S. Walter, et al. (2004). "The LPS receptor (CD14) links innate immunity with Alzheimer's disease." Faseb J **18**(1): 203-5.
- Findeis, M. A. (2007). "The role of amyloid beta peptide 42 in Alzheimer's disease." Pharmacol Ther **116**(2): 266-86.
- Fischer, H. G. and G. Reichmann (2001). "Brain dendritic cells and macrophages/microglia in central nervous system inflammation." J Immunol **166**(4): 2717-26.
- Floden, A. M. and C. K. Combs (2006). "Beta-amyloid stimulates murine postnatal and adult microglia cultures in a unique manner." J Neurosci **26**(17): 4644-8.
- Fraser, P. E., J. T. Nguyen, et al. (1991). "pH-dependent structural transitions of Alzheimer amyloid peptides." Biophys J **60**(5): 1190-201.

- Frautschy, S. A., G. M. Cole, et al. (1992). "Phagocytosis and deposition of vascular beta-amyloid in rat brains injected with Alzheimer beta-amyloid." Am J Pathol **140**(6): 1389-99.
- Frautschy, S. A., F. Yang, et al. (1998). "Microglial response to amyloid plaques in APPsw transgenic mice." Am J Pathol **152**(1): 307-17.
- Furukawa, K., B. L. Sopher, et al. (1996). "Increased activity-regulating and neuroprotective efficacy of alpha-secretase-derived secreted amyloid precursor protein conferred by a C-terminal heparin-binding domain." J Neurochem **67**(5): 1882-96.
- Garden, G. A. and T. Moller (2006). "Microglia biology in health and disease." J Neuroimmune Pharmacol **1**(2): 127-37.
- Gay, N. J. and F. J. Keith (1991). "Drosophila Toll and IL-1 receptor." Nature **351**(6325): 355-6.
- Gellermann, G. P., H. Byrnes, et al. (2008). "Abeta-globulomers are formed independently of the fibril pathway." Neurobiol Dis **30**(2): 212-20.
- Georganopoulou, D. G., L. Chang, et al. (2005). "Nanoparticle-based detection in cerebral spinal fluid of a soluble pathogenic biomarker for Alzheimer's disease." Proc Natl Acad Sci U S A **102**(7): 2273-6.
- Geula, C., C. K. Wu, et al. (1998). "Aging renders the brain vulnerable to amyloid beta-protein neurotoxicity." Nat Med **4**(7): 827-31.
- Glabe, C. G. (2004). "Conformation-dependent antibodies target diseases of protein misfolding." Trends Biochem Sci **29**(10): 542-7.
- Glezer, I., A. R. Simard, et al. (2007). "Neuroprotective role of the innate immune system by microglia." Neuroscience **147**(4): 867-83.
- Goate, A., M. C. Chartier-Harlin, et al. (1991). "Segregation of a missense mutation in the amyloid precursor protein gene with familial Alzheimer's disease." Nature **349**(6311): 704-6.
- Good, P. F., P. Werner, et al. (1996). "Evidence of neuronal oxidative damage in Alzheimer's disease." Am J Pathol **149**(1): 21-8.
- Grundke-Iqbal, I., K. Iqbal, et al. (1986). "Abnormal phosphorylation of the microtubule-associated protein tau (tau) in Alzheimer cytoskeletal pathology." Proc Natl Acad Sci U S A **83**(13): 4913-7.
- Guo, L. H. and H. J. Schluesener (2007). "The innate immunity of the central nervous

- system in chronic pain: the role of Toll-like receptors." Cell Mol Life Sci **64**(9): 1128-36.
- Gupta, D., T. N. Kirkland, et al. (1996). "CD14 is a cell-activating receptor for bacterial peptidoglycan." J Biol Chem **271**(38): 23310-6.
- Gutsmann, T., M. Muller, et al. (2001). "Dual role of lipopolysaccharide (LPS)-binding protein in neutralization of LPS and enhancement of LPS-induced activation of mononuclear cells." Infect Immun **69**(11): 6942-50.
- Hailman, E., H. S. Lichenstein, et al. (1994). "Lipopolysaccharide (LPS)-binding protein accelerates the binding of LPS to CD14." J Exp Med **179**(1): 269-77.
- Halliday, G., S. R. Robinson, et al. (2000). "Alzheimer's disease and inflammation: a review of cellular and therapeutic mechanisms." Clin Exp Pharmacol Physiol **27**(1-2): 1-8.
- Halverson, K., P. E. Fraser, et al. (1990). "Molecular determinants of amyloid deposition in Alzheimer's disease: conformational studies of synthetic beta-protein fragments." Biochemistry **29**(11): 2639-44.
- Hanger, D. P., B. H. Anderton, et al. (2009). "Tau phosphorylation: the therapeutic challenge for neurodegenerative disease." Trends Mol Med **15**(3): 112-9.
- Hanger, D. P., H. L. Byers, et al. (2007). "Novel phosphorylation sites in tau from Alzheimer brain support a role for casein kinase 1 in disease pathogenesis." J Biol Chem **282**(32): 23645-54.
- Hardy, J. and D. J. Selkoe (2002). "The amyloid hypothesis of Alzheimer's disease: progress and problems on the road to therapeutics." Science **297**(5580): 353-6.
- Harper, J. D., S. S. Wong, et al. (1997). "Observation of metastable Abeta amyloid protofibrils by atomic force microscopy." Chem Biol **4**(2): 119-25.
- Harper, J. D., S. S. Wong, et al. (1999). "Assembly of A beta amyloid protofibrils: an in vitro model for a possible early event in Alzheimer's disease." Biochemistry **38**(28): 8972-80.
- Haziot, A., S. Chen, et al. (1988). "The monocyte differentiation antigen, CD14, is anchored to the cell membrane by a phosphatidylinositol linkage." J Immunol **141**(2): 547-52.
- Haziot, A., E. Ferrero, et al. (1996). "Resistance to endotoxin shock and reduced dissemination of gram-negative bacteria in CD14-deficient mice." Immunity **4**(4): 407-14.

- Hendriks, L., C. M. van Duijn, et al. (1992). "Presenile dementia and cerebral haemorrhage linked to a mutation at codon 692 of the beta-amyloid precursor protein gene." Nat Genet **1**(3): 218-21.
- Henneke, P., O. Takeuchi, et al. (2001). "Novel engagement of CD14 and multiple toll-like receptors by group B streptococci." J Immunol **167**(12): 7069-76.
- Hilbich, C., B. Kisters-Woike, et al. (1991). "Aggregation and secondary structure of synthetic amyloid beta A4 peptides of Alzheimer's disease." J Mol Biol **218**(1): 149-63.
- Hirschfeld, M., Y. Ma, et al. (2000). "Cutting edge: repurification of lipopolysaccharide eliminates signaling through both human and murine toll-like receptor 2." J Immunol **165**(2): 618-22.
- Hirschfeld, M., J. J. Weis, et al. (2001). "Signaling by toll-like receptor 2 and 4 agonists results in differential gene expression in murine macrophages." Infect Immun **69**(3): 1477-82.
- Hoebe, K., E. Janssen, et al. (2004). "The interface between innate and adaptive immunity." Nat Immunol **5**(10): 971-4.
- Hoshino, K., O. Takeuchi, et al. (1999). "Cutting edge: Toll-like receptor 4 (TLR4)-deficient mice are hyporesponsive to lipopolysaccharide: evidence for TLR4 as the Lps gene product." J Immunol **162**(7): 3749-52.
- Huber, M., C. Kalis, et al. (2006). "R-form LPS, the master key to the activation of TLR4/MD-2-positive cells." Eur J Immunol **36**(3): 701-11.
- Hutton, M., C. L. Lendon, et al. (1998). "Association of missense and 5'-splice-site mutations in tau with the inherited dementia FTDP-17." Nature **393**(6686): 702-5.
- Irvine, G. B., O. M. El-Agnaf, et al. (2008). "Protein aggregation in the brain: the molecular basis for Alzheimer's and Parkinson's diseases." Mol Med **14**(7-8): 451-64.
- Janeway, C. A., Jr. and R. Medzhitov (1999). "Lipoproteins take their toll on the host." Curr Biol **9**(23): R879-82.
- Janssens, S. and R. Beyaert (2003). "Role of Toll-like receptors in pathogen recognition." Clin Microbiol Rev **16**(4): 637-46.
- Jarrett, J. T., E. P. Berger, et al. (1993). "The carboxy terminus of the beta amyloid protein is critical for the seeding of amyloid formation: implications for the pathogenesis of Alzheimer's disease." Biochemistry **32**(18): 4693-7.

- Jerala, R. (2007). "Structural biology of the LPS recognition." Int J Med Microbiol **297**(5): 353-63.
- Jiang, Z., P. Georgel, et al. (2005). "CD14 is required for MyD88-independent LPS signaling." Nat Immunol **6**(6): 565-70.
- Jin, M. S. and J. O. Lee (2008). "Structures of TLR-ligand complexes." Curr Opin Immunol **20**(4): 414-9.
- Kato, H., K. Kogure, et al. (1995). "Graded expression of immunomolecules on activated microglia in the hippocampus following ischemia in a rat model of ischemic tolerance." Brain Res **694**(1-2): 85-93.
- Kayed, R., E. Head, et al. (2003). "Common structure of soluble amyloid oligomers implies common mechanism of pathogenesis." Science **300**(5618): 486-9.
- Kielian, T. (2006). "Toll-like receptors in central nervous system glial inflammation and homeostasis." J Neurosci Res **83**(5): 711-30.
- Kim, J. I., C. J. Lee, et al. (2005). "Crystal structure of CD14 and its implications for lipopolysaccharide signaling." J Biol Chem **280**(12): 11347-51.
- Kirkitadze, M. D., G. Bitan, et al. (2002). "Paradigm shifts in Alzheimer's disease and other neurodegenerative disorders: the emerging role of oligomeric assemblies." J Neurosci Res **69**(5): 567-77.
- Kirschner, D. A., C. Abraham, et al. (1986). "X-ray diffraction from intraneuronal paired helical filaments and extraneuronal amyloid fibers in Alzheimer disease indicates cross-beta conformation." Proc Natl Acad Sci U S A **83**(2): 503-7.
- Kirschning, C. J., H. Wesche, et al. (1998). "Human toll-like receptor 2 confers responsiveness to bacterial lipopolysaccharide." J Exp Med **188**(11): 2091-7.
- Kitchens, R. L., G. Wolfbauer, et al. (1999). "Plasma lipoproteins promote the release of bacterial lipopolysaccharide from the monocyte cell surface." J Biol Chem **274**(48): 34116-22.
- Klegeris, A., D. G. Walker, et al. (1997). "Interaction of Alzheimer beta-amyloid peptide with the human monocytic cell line THP-1 results in a protein kinase C-dependent secretion of tumor necrosis factor-alpha." Brain Res **747**(1): 114-21.
- Konat, G. W., T. Kielian, et al. (2006). "The role of Toll-like receptors in CNS response to microbial challenge." J Neurochem **99**(1): 1-12.
- Kopp, E. and R. Medzhitov (2003). "Recognition of microbial infection by Toll-like receptors." Curr Opin Immunol **15**(4): 396-401.

- Kosik, K. S., C. L. Joachim, et al. (1986). "Microtubule-associated protein tau (tau) is a major antigenic component of paired helical filaments in Alzheimer disease." Proc Natl Acad Sci U S A **83**(11): 4044-8.
- Kowalewski, T. and D. M. Holtzman (1999). "In situ atomic force microscopy study of Alzheimer's beta-amyloid peptide on different substrates: new insights into mechanism of beta-sheet formation." Proc Natl Acad Sci U S A **96**(7): 3688-93.
- Kowall, N. W., M. F. Beal, et al. (1991). "An in vivo model for the neurodegenerative effects of beta amyloid and protection by substance P." Proc Natl Acad Sci U S A **88**(16): 7247-51.
- LaFerla, F. M., K. N. Green, et al. (2007). "Intracellular amyloid-beta in Alzheimer's disease." Nat Rev Neurosci **8**(7): 499-509.
- LaFerla, F. M., B. T. Tinkle, et al. (1995). "The Alzheimer's A beta peptide induces neurodegeneration and apoptotic cell death in transgenic mice." Nat Genet **9**(1): 21-30.
- Lambert, M. P., A. K. Barlow, et al. (1998). "Diffusible, nonfibrillar ligands derived from Abeta1-42 are potent central nervous system neurotoxins." Proc Natl Acad Sci U S A **95**(11): 6448-53.
- Lansbury, P. T., Jr. (1999). "Evolution of amyloid: what normal protein folding may tell us about fibrillogenesis and disease." Proc Natl Acad Sci U S A **96**(7): 3342-4.
- Lansbury, P. T., Jr., P. R. Costa, et al. (1995). "Structural model for the beta-amyloid fibril based on interstrand alignment of an antiparallel-sheet comprising a C-terminal peptide." Nat Struct Biol **2**(11): 990-8.
- Lee, M. S. and Y. J. Kim (2007). "Pattern-recognition receptor signaling initiated from extracellular, membrane, and cytoplasmic space." Mol Cells **23**(1): 1-10.
- Lee, M. S. and Y. J. Kim (2007). "Signaling pathways downstream of pattern-recognition receptors and their cross talk." Annu Rev Biochem **76**: 447-80.
- Lee, Y. B., A. Nagai, et al. (2002). "Cytokines, chemokines, and cytokine receptors in human microglia." J Neurosci Res **69**(1): 94-103.
- Lemaitre, B., E. Nicolas, et al. (1996). "The dorsoventral regulatory gene cassette spatzle/Toll/cactus controls the potent antifungal response in Drosophila adults." Cell **86**(6): 973-83.
- Lemere, C. A., J. K. Blusztajn, et al. (1996). "Sequence of deposition of heterogeneous amyloid beta-peptides and APO E in Down syndrome: implications for initial events in amyloid plaque formation." Neurobiol Dis **3**(1): 16-32.

- Lesne, S., M. T. Koh, et al. (2006). "A specific amyloid-beta protein assembly in the brain impairs memory." Nature **440**(7082): 352-7.
- Levy, E., M. D. Carman, et al. (1990). "Mutation of the Alzheimer's disease amyloid gene in hereditary cerebral hemorrhage, Dutch type." Science **248**(4959): 1124-6.
- Liu, B. and J. S. Hong (2003). "Role of microglia in inflammation-mediated neurodegenerative diseases: mechanisms and strategies for therapeutic intervention." J Pharmacol Exp Ther **304**(1): 1-7.
- Lomakin, A., D. S. Chung, et al. (1996). "On the nucleation and growth of amyloid beta-protein fibrils: detection of nuclei and quantitation of rate constants." Proc Natl Acad Sci U S A **93**(3): 1125-9.
- Loo, D. T., A. Copani, et al. (1993). "Apoptosis is induced by beta-amyloid in cultured central nervous system neurons." Proc Natl Acad Sci U S A **90**(17): 7951-5.
- Loppnow, H., H. Brade, et al. (1989). "IL-1 induction-capacity of defined lipopolysaccharide partial structures." J Immunol **142**(9): 3229-38.
- Lorenzo, A. and B. A. Yankner (1994). "Beta-amyloid neurotoxicity requires fibril formation and is inhibited by congo red." Proc Natl Acad Sci U S A **91**(25): 12243-7.
- Lue, L. F., Y. M. Kuo, et al. (1999). "Soluble amyloid beta peptide concentration as a predictor of synaptic change in Alzheimer's disease." Am J Pathol **155**(3): 853-62.
- Mann, D. M., T. Iwatsubo, et al. (1996). "Amyloid beta protein (A $\beta$ ) deposition in chromosome 14-linked Alzheimer's disease: predominance of A $\beta$ <sub>42</sub>(43)." Ann Neurol **40**(2): 149-56.
- Manukyan, M., K. Triantafilou, et al. (2005). "Binding of lipopeptide to CD14 induces physical proximity of CD14, TLR2 and TLR1." Eur J Immunol **35**(3): 911-21.
- Masters, C. L., G. Simms, et al. (1985). "Amyloid plaque core protein in Alzheimer disease and Down syndrome." Proc Natl Acad Sci U S A **82**(12): 4245-9.
- Mastrangelo, I. A., M. Ahmed, et al. (2006). "High-resolution atomic force microscopy of soluble A $\beta$ <sub>42</sub> oligomers." J Mol Biol **358**(1): 106-19.
- Masumura, M., R. Hata, et al. (2000). "Caspase-3 activation and inflammatory responses in rat hippocampus inoculated with a recombinant adenovirus expressing the Alzheimer amyloid precursor protein." Brain Res Mol Brain Res **80**(2): 219-27.
- Mattson, M. P. (1997). "Cellular actions of beta-amyloid precursor protein and its soluble and fibrillogenic derivatives." Physiol Rev **77**(4): 1081-132.

- Mattson, M. P. (2004). "Pathways towards and away from Alzheimer's disease." Nature **430**(7000): 631-9.
- Mattson, M. P., B. Cheng, et al. (1993). "Evidence for excitoprotective and intraneuronal calcium-regulating roles for secreted forms of the beta-amyloid precursor protein." Neuron **10**(2): 243-54.
- McLaurin, J., D. Yang, et al. (2000). "Review: modulating factors in amyloid-beta fibril formation." J Struct Biol **130**(2-3): 259-70.
- Meda, L., M. A. Cassatella, et al. (1995). "Activation of microglial cells by beta-amyloid protein and interferon-gamma." Nature **374**(6523): 647-50.
- Medzhitov, R. (2001). "Toll-like receptors and innate immunity." Nat Rev Immunol **1**(2): 135-45.
- Medzhitov, R., P. Preston-Hurlburt, et al. (1997). "A human homologue of the Drosophila Toll protein signals activation of adaptive immunity." Nature **388**(6640): 394-7.
- Miggin, S. M. and L. A. O'Neill (2006). "New insights into the regulation of TLR signaling." J Leukoc Biol **80**(2): 220-6.
- Miller, S. I., R. K. Ernst, et al. (2005). "LPS, TLR4 and infectious disease diversity." Nat Rev Microbiol **3**(1): 36-46.
- Miyake, K. (2004). "Innate recognition of lipopolysaccharide by Toll-like receptor 4-MD-2." Trends Microbiol **12**(4): 186-92.
- Moore, A. H. and M. K. O'Banion (2002). "Neuroinflammation and anti-inflammatory therapy for Alzheimer's disease." Adv Drug Deliv Rev **54**(12): 1627-56.
- Moore, K. J., L. P. Andersson, et al. (2000). "Divergent response to LPS and bacteria in CD14-deficient murine macrophages." J Immunol **165**(8): 4272-80.
- Morishima, Y., Y. Gotoh, et al. (2001). "Beta-amyloid induces neuronal apoptosis via a mechanism that involves the c-Jun N-terminal kinase pathway and the induction of Fas ligand." J Neurosci **21**(19): 7551-60.
- Motter, R., C. Vigo-Pelfrey, et al. (1995). "Reduction of beta-amyloid peptide42 in the cerebrospinal fluid of patients with Alzheimer's disease." Ann Neurol **38**(4): 643-8.
- Mullan, M., F. Crawford, et al. (1992). "A pathogenic mutation for probable Alzheimer's disease in the APP gene at the N-terminus of beta-amyloid." Nat Genet **1**(5): 345-7.

- Muta, T. and K. Takeshige (2001). "Essential roles of CD14 and lipopolysaccharide-binding protein for activation of toll-like receptor (TLR)2 as well as TLR4 Reconstitution of TLR2- and TLR4-activation by distinguishable ligands in LPS preparations." Eur J Biochem **268**(16): 4580-9.
- Nagai, Y., S. Akashi, et al. (2002). "Essential role of MD-2 in LPS responsiveness and TLR4 distribution." Nat Immunol **3**(7): 667-72.
- Nakata, T., M. Yasuda, et al. (2006). "CD14 directly binds to triacylated lipopeptides and facilitates recognition of the lipopeptides by the receptor complex of Toll-like receptors 2 and 1 without binding to the complex." Cell Microbiol **8**(12): 1899-909.
- Nichols, M. R., M. A. Moss, et al. (2005). "Rapid assembly of amyloid-beta peptide at a liquid/liquid interface produces unstable beta-sheet fibers." Biochemistry **44**(1): 165-73.
- Nichols, M. R., M. A. Moss, et al. (2002). "Growth of beta-amyloid(1-40) protofibrils by monomer elongation and lateral association. Characterization of distinct products by light scattering and atomic force microscopy." Biochemistry **41**(19): 6115-27.
- Nilsson, M. R. (2004). "Techniques to study amyloid fibril formation in vitro." Methods **34**(1): 151-60.
- Nishitani, C., H. Mitsuzawa, et al. (2006). "Toll-like receptor 4 region Glu24-Lys47 is a site for MD-2 binding: importance of CYS29 and CYS40." J Biol Chem **281**(50): 38322-9.
- O'Nuallain, B. and R. Wetzel (2002). "Conformational Abs recognizing a generic amyloid fibril epitope." Proc Natl Acad Sci U S A **99**(3): 1485-90.
- Ohsawa, I., Y. Hirose, et al. (1995). "Expression, purification, and neurotrophic activity of amyloid precursor protein-secreted forms produced by yeast." Biochem Biophys Res Commun **213**(1): 52-8.
- Ohto, U., K. Fukase, et al. (2007). "Crystal structures of human MD-2 and its complex with antiendotoxic lipid IVa." Science **316**(5831): 1632-4.
- Omueti, K. O., J. M. Beyer, et al. (2005). "Domain exchange between human toll-like receptors 1 and 6 reveals a region required for lipopeptide discrimination." J Biol Chem **280**(44): 36616-25.
- Ozinsky, A., D. M. Underhill, et al. (2000). "The repertoire for pattern recognition of pathogens by the innate immune system is defined by cooperation between toll-like receptors." Proc Natl Acad Sci U S A **97**(25): 13766-71.

- Parker, L. C., L. R. Prince, et al. (2007). "Translational mini-review series on Toll-like receptors: networks regulated by Toll-like receptors mediate innate and adaptive immunity." Clin Exp Immunol **147**(2): 199-207.
- Patrick, G. N., L. Zukerberg, et al. (1999). "Conversion of p35 to p25 deregulates Cdk5 activity and promotes neurodegeneration." Nature **402**(6762): 615-22.
- Pearson, H. A. and C. Peers (2006). "Physiological roles for amyloid beta peptides." J Physiol **575**(Pt 1): 5-10.
- Perry, R. T., J. S. Collins, et al. (2001). "The role of TNF and its receptors in Alzheimer's disease." Neurobiol Aging **22**(6): 873-83.
- Perry, V. H., T. A. Newman, et al. (2003). "The impact of systemic infection on the progression of neurodegenerative disease." Nat Rev Neurosci **4**(2): 103-12.
- Pike, C. J., D. Burdick, et al. (1993). "Neurodegeneration induced by beta-amyloid peptides in vitro: the role of peptide assembly state." J Neurosci **13**(4): 1676-87.
- Plant, L. D., J. P. Boyle, et al. (2003). "The production of amyloid beta peptide is a critical requirement for the viability of central neurons." J Neurosci **23**(13): 5531-5.
- Poltorak, A., X. He, et al. (1998). "Defective LPS signaling in C3H/HeJ and C57BL/10ScCr mice: mutations in Tlr4 gene." Science **282**(5396): 2085-8.
- Prohinar, P., F. Re, et al. (2007). "Specific high affinity interactions of monomeric endotoxin-protein complexes with Toll-like receptor 4 ectodomain." J Biol Chem **282**(2): 1010-7.
- Pugin, J., C. C. Schurer-Maly, et al. (1993). "Lipopolysaccharide activation of human endothelial and epithelial cells is mediated by lipopolysaccharide-binding protein and soluble CD14." Proc Natl Acad Sci U S A **90**(7): 2744-8.
- Qureshi, S. T., L. Lariviere, et al. (1999). "Endotoxin-tolerant mice have mutations in Toll-like receptor 4 (Tlr4)." J Exp Med **189**(4): 615-25.
- Ramsden, M., L. D. Plant, et al. (2001). "Differential effects of unaggregated and aggregated amyloid beta protein (1-40) on K(+) channel currents in primary cultures of rat cerebellar granule and cortical neurones." J Neurochem **79**(3): 699-712.
- Rietschel, E. T., T. Kirikae, et al. (1994). "Bacterial endotoxin: molecular relationships of structure to activity and function." Faseb J **8**(2): 217-25.
- Rio-Hortega (1932). Microglia. Cytology and cellular pathology of nervous system. P.

- W. New York, PB Hoeber. **2**: 481-534.
- Roher, A. E., M. O. Chaney, et al. (1996). "Morphology and toxicity of Abeta-(1-42) dimer derived from neuritic and vascular amyloid deposits of Alzheimer's disease." J Biol Chem **271**(34): 20631-5.
- Roychaudhuri, R., M. Yang, et al. (2009). "Amyloid {beta}-Protein Assembly and Alzheimer Disease." J Biol Chem **284**(8): 4749-4753.
- Scheuner, D., C. Eckman, et al. (1996). "Secreted amyloid beta-protein similar to that in the senile plaques of Alzheimer's disease is increased in vivo by the presenilin 1 and 2 and APP mutations linked to familial Alzheimer's disease." Nat Med **2**(8): 864-70.
- Schroder, N. W., S. Morath, et al. (2003). "Lipoteichoic acid (LTA) of Streptococcus pneumoniae and Staphylococcus aureus activates immune cells via Toll-like receptor (TLR)-2, lipopolysaccharide-binding protein (LBP), and CD14, whereas TLR-4 and MD-2 are not involved." J Biol Chem **278**(18): 15587-94.
- Selkoe, D. J. (1996). "Amyloid beta-protein and the genetics of Alzheimer's disease." J Biol Chem **271**(31): 18295-8.
- Selkoe, D. J. (1997). "Alzheimer's disease: genotypes, phenotypes, and treatments." Science **275**(5300): 630-1.
- Selkoe, D. J. (1998). "The cell biology of beta-amyloid precursor protein and presenilin in Alzheimer's disease." Trends Cell Biol **8**(11): 447-53.
- Selkoe, D. J. (2001). "Alzheimer's disease: genes, proteins, and therapy." Physiol Rev **81**(2): 741-66.
- Serpell, L. C. (2000). "Alzheimer's amyloid fibrils: structure and assembly." Biochim Biophys Acta **1502**(1): 16-30.
- Seubert, P., C. Vigo-Pelfrey, et al. (1992). "Isolation and quantification of soluble Alzheimer's beta-peptide from biological fluids." Nature **359**(6393): 325-7.
- Shen, C. L. and R. M. Murphy (1995). "Solvent effects on self-assembly of beta-amyloid peptide." Biophys J **69**(2): 640-51.
- Shimazu, R., S. Akashi, et al. (1999). "MD-2, a molecule that confers lipopolysaccharide responsiveness on Toll-like receptor 4." J Exp Med **189**(11): 1777-82.
- Sisodia, S. S., E. H. Koo, et al. (1990). "Evidence that beta-amyloid protein in Alzheimer's disease is not derived by normal processing." Science **248**(4954): 492-5.

- Small, S. A. and K. Duff (2008). "Linking Abeta and tau in late-onset Alzheimer's disease: a dual pathway hypothesis." Neuron **60**(4): 534-42.
- Smith-Swintosky, V. L., L. C. Pettigrew, et al. (1994). "Secreted forms of beta-amyloid precursor protein protect against ischemic brain injury." J Neurochem **63**(2): 781-4.
- St George-Hyslop, P. H. (2000). "Piecing together Alzheimer's." Sci Am **283**(6): 76-83.
- Stromer, T. and L. C. Serpell (2005). "Structure and morphology of the Alzheimer's amyloid fibril." Microsc Res Tech **67**(3-4): 210-7.
- Suzuki, T. and T. Nakaya (2008). "Regulation of amyloid beta-protein precursor by phosphorylation and protein interactions." J Biol Chem **283**(44): 29633-7.
- Takeda, K., T. Kaisho, et al. (2003). "Toll-like receptors." Annu Rev Immunol **21**: 335-76.
- Takeuchi, O., T. Kawai, et al. (2001). "Discrimination of bacterial lipoproteins by Toll-like receptor 6." Int Immunol **13**(7): 933-40.
- Takeuchi, O., S. Sato, et al. (2002). "Cutting edge: role of Toll-like receptor 1 in mediating immune response to microbial lipoproteins." J Immunol **169**(1): 10-4.
- Tarkowski, E., N. Andreasen, et al. (2003). "Intrathecal inflammation precedes development of Alzheimer's disease." J Neurol Neurosurg Psychiatry **74**(9): 1200-5.
- Tarkowski, E., K. Blennow, et al. (1999). "Intracerebral production of tumor necrosis factor-alpha, a local neuroprotective agent, in Alzheimer disease and vascular dementia." J Clin Immunol **19**(4): 223-30.
- Teng, F. Y. and B. L. Tang (2005). "Widespread gamma-secretase activity in the cell, but do we need it at the mitochondria?" Biochem Biophys Res Commun **328**(1): 1-5.
- Thinakaran, G. and E. H. Koo (2008). "Amyloid precursor protein trafficking, processing, and function." J Biol Chem **283**(44): 29615-9.
- Tjernberg, L. O., D. J. Callaway, et al. (1999). "A molecular model of Alzheimer amyloid beta-peptide fibril formation." J Biol Chem **274**(18): 12619-25.
- Trinchieri, G. and A. Sher (2007). "Cooperation of Toll-like receptor signals in innate immune defence." Nat Rev Immunol **7**(3): 179-90.
- Tycko, R. (2004). "Progress towards a molecular-level structural understanding of amyloid fibrils." Curr Opin Struct Biol **14**(1): 96-103.

- Uchihara, T., H. K. el Hachimi, et al. (1996). "Widespread immunoreactivity of presenilin in neurons of normal and Alzheimer's disease brains: double-labeling immunohistochemical study." Acta Neuropathol **92**(4): 325-30.
- Ulvestad, E., K. Williams, et al. (1994). "Human microglial cells have phenotypic and functional characteristics in common with both macrophages and dendritic antigen-presenting cells." J Leukoc Biol **56**(6): 732-40.
- Venters, H. D., Q. Tang, et al. (1999). "A new mechanism of neurodegeneration: a proinflammatory cytokine inhibits receptor signaling by a survival peptide." Proc Natl Acad Sci U S A **96**(17): 9879-84.
- Viriyakosol, S., P. S. Tobias, et al. (2001). "MD-2 binds to bacterial lipopolysaccharide." J Biol Chem **276**(41): 38044-51.
- Walsh, D. M., D. M. Hartley, et al. (1999). "Amyloid beta-protein fibrillogenesis. Structure and biological activity of protofibrillar intermediates." J Biol Chem **274**(36): 25945-52.
- Walsh, D. M., I. Klyubin, et al. (2002b). "Amyloid-beta oligomers: their production, toxicity and therapeutic inhibition." Biochem Soc Trans **30**(4): 552-7.
- Walsh, D. M., A. Lomakin, et al. (1997). "Amyloid beta-protein fibrillogenesis. Detection of a protofibrillar intermediate." J Biol Chem **272**(35): 22364-72.
- Walsh, D. M. and D. J. Selkoe (2007). "A beta oligomers - a decade of discovery." J Neurochem **101**(5): 1172-84.
- Walsh, D. M., B. P. Tseng, et al. (2000). "The oligomerization of amyloid beta-protein begins intracellularly in cells derived from human brain." Biochemistry **39**(35): 10831-9.
- Wegiel, J., K. C. Wang, et al. (2001). "The role of microglial cells and astrocytes in fibrillar plaque evolution in transgenic APP(SW) mice." Neurobiol Aging **22**(1): 49-61.
- Wright, S. D., R. A. Ramos, et al. (1990). "CD14, a receptor for complexes of lipopolysaccharide (LPS) and LPS binding protein." Science **249**(4975): 1431-3.
- Yan, S. D., X. Chen, et al. (1996). "RAGE and amyloid-beta peptide neurotoxicity in Alzheimer's disease." Nature **382**(6593): 685-91.
- Yang, R. B., M. R. Mark, et al. (1998). "Toll-like receptor-2 mediates lipopolysaccharide-induced cellular signalling." Nature **395**(6699): 284-8.
- Yang, R. B., M. R. Mark, et al. (1999). "Signaling events induced by lipopolysaccharide-

activated toll-like receptor 2." J Immunol **163**(2): 639-43.

Yates, S. L., L. H. Burgess, et al. (2000). "Amyloid beta and amylin fibrils induce increases in proinflammatory cytokine and chemokine production by THP-1 cells and murine microglia." J Neurochem **74**(3): 1017-25.

## 2 GENERAL METHODS

### 2.1 Cell Culture

#### 2.1.1 THP-1 monocytes

##### 2.1.1.1 THP-1 storage, growth and culture

The cultured human peripheral blood THP-1 monocytes were obtained from ATCC (Manassas, VA, USA) and maintained in RPMI-1640 culture medium (HyClone, Logan, UT, USA) that contains 2 mmol/L L-glutamine, 25 mmol/L HEPES, 1.5 g/L sodium bicarbonate, 10% fetal bovine serum (FBS) (HyClone), 50 U/ml penicillin, 50 µg/ml streptomycin (HyClone), and 50 µmol/L β-mercaptoethanol (Fisher, Pittsburg, PA) at 37°C in 5% CO<sub>2</sub>. For growth and maintenance, THP-1 monocytes were diluted three times a week, with a dilution of 1:1 twice during the week, and 3:10 dilution at the end of the week. For 1:1 dilution, half of the cells were removed from the flask and replaced with the same volume of fresh growth medium for propagation, ensuring that the cell concentration in the flask was maintained at 1 x10<sup>6</sup> cells/ml. For 3:10 dilution, 3 ml of THP-1 cells were removed from the culture flask and spun at 500 xg for 10 minutes. After centrifugation, supernatant was removed and cells were resuspended in 10 ml of growth medium. Cells were transferred to a new cell culture flask for propagation. Cells

were continuously subcultured for 3 weeks prior to experimentation.

For maintaining a continuous supply of THP-1, THP-1 monocytes were cryopreserved. As soon as a small surplus of THP-1 cells becomes available for subculture, several ampules of cells were frozen. Cells were removed from the flask, centrifuged at 500 xg for 10 minutes and supernatant was removed without disturbing the pellet. The pellet was then resuspended to a final concentration of  $5 \times 10^6$  cells/ml in freezing medium (fresh growth medium containing 0.5% sterile dimethyl sulfoxide (DMSO)). The cell suspensions were dispensed into pre-labeled ampules (1 ml cell suspension per ampule) and ampules were transferred to an ampule cooler (Nalge Nunc) containing isopropyl alcohol. The specific heat of the coolant in the base of the cooler insulates the container and gives a cooling rate of  $\sim 1^\circ\text{C}/\text{min}$  in the ampules (Freshney, 2000). The cooler was placed in a  $-70^\circ\text{C}$  freezer overnight prior to transfer of ampules in liquid nitrogen. After overnight freezing at  $-70^\circ\text{C}$ , ampules were rapidly transferred to a cryo-container and THP-1 cells were stored immersed in liquid nitrogen.

Thawing THP-1 ampules needs to be rapid. THP-1 cells were thawed by immersing the lower half of the ampule in  $37^\circ\text{C}$  waterbath for 2-3 minutes (but not exceeding 3 minutes). The ampule containing thawed cells was then immersed in 70% ethanol before opening the container. Cells were pipetted out from the ampule and suspended in 9 ml of fresh THP-1 growth medium. Cell suspension was centrifuged, and reseeded in a new cell culture flask, as described previously.

We have previously observed that the proinflammatory response of our THP-1 monocytes to TLR agonists started to deteriorate when THP-1 cells have been subcultured continuously for greater than 2 months. To avoid this problem, we have

staggered our culture of THP-1 monocytes. We constantly maintained two culture flasks of THP-1 monocytes, in which one flask was cultured a month after the initial culture of the first THP-1 flask. Cells were constantly monitored for viability by stimulation with TLR agonists (section 2.3) and measuring TNF $\alpha$  production (section 2.7).

#### 2.1.1.2 THP-1 preparation for experimentation

For cellular assays, THP-1 monocytes were removed from the culture flask and centrifuged at 500 x g for 10 minutes. After centrifugation, supernatant was removed without disturbing the pellet. The pellet was washed with THP-1 assay culture medium (THP-1 growth but with 2% FBS), and centrifuged as described above. After which, supernatant was removed and pellet was resuspended in assay medium. Cell concentration was determined by direct counting of the cells using a hemocytometer. THP-1 cells (with concentration maintained at  $1 \times 10^6$  cells/ml) were added to individual wells of a 48-well sterile plate to a final volume of 0.3 ml, or 96-well cell culture plate to a final volume of 0.08 ml.

THP-1 monocytes are derived from the blood of a patient with monocytic leukemia (Tsuchiya et al., 1980). The cells grow in suspension, have round morphology, and do not adhere to the plastic surfaces of the culture plates (Takashiba et al., 1999; Zhou et al., 2005). THP-1 can serve as a model of primary human microglia since they acquire a microglia-like morphology when treated with LPS (Yates et al., 2000).

### 2.1.2 Human Embryonic Kidney (HEK293) cells

Null HEK293 (stably transfected with the pUNO-mcs vector), 293-hTLR2 cells (isolated clone of HEK293 cells stably transfected with human TLR2 gene), and 293-hTLR2/CD14 (isolated clone of HEK293 cells stably transfected with human TLR2 and CD14 genes) were obtained from InvivoGen (San Diego, CA, USA). Null HEK293 and HEK 293-hTLR2 cells were maintained in Dubelcco's Modified Eagle's Medium (DMEM) growth medium (HyClone) containing 4 mmol/L L-glutamine, 4.5 g/l glucose, 10% FBS and supplemented with 10 µg/ml Blasticidin (InvivoGen) at 37°C in 5% CO<sub>2</sub>. HEK 293-hTLR2/CD14 cells were maintained in the same growth medium supplemented with 10 µg/ml Blasticidin and 50 µg/ml hygromycin (HygroGold™) (InvivoGen). Cells were subcultured in a T-75 cell culture flask every 4 days. The number of times the cells were subcultured is denoted by passage number. Subculture of HEK 293 cells is illustrated in Figure 2.1 and was done using the following procedure. Briefly, the growth medium in the flask was removed, and the cells were gently washed with sterile phosphate buffered saline (PBS) (Hyclone). After washing, the cells were treated with 2 ml of 0.25% trypsin-EDTA for 5 minutes at 37°C followed by addition of 8 ml of corresponding growth medium. Cells were dispersed by repeated gentle pipetting over the surface bearing the monolayer. Cells were collected, placed in a 15 ml conical tube, centrifuged at 500 xg for 10 minutes, resuspended in appropriate fresh growth medium, diluted to the appropriate seeding concentration, and reseeded in a fresh flask (Freshney, 2000). A surplus of HEK 293 cells were also cryopreserved in a similar manner as in

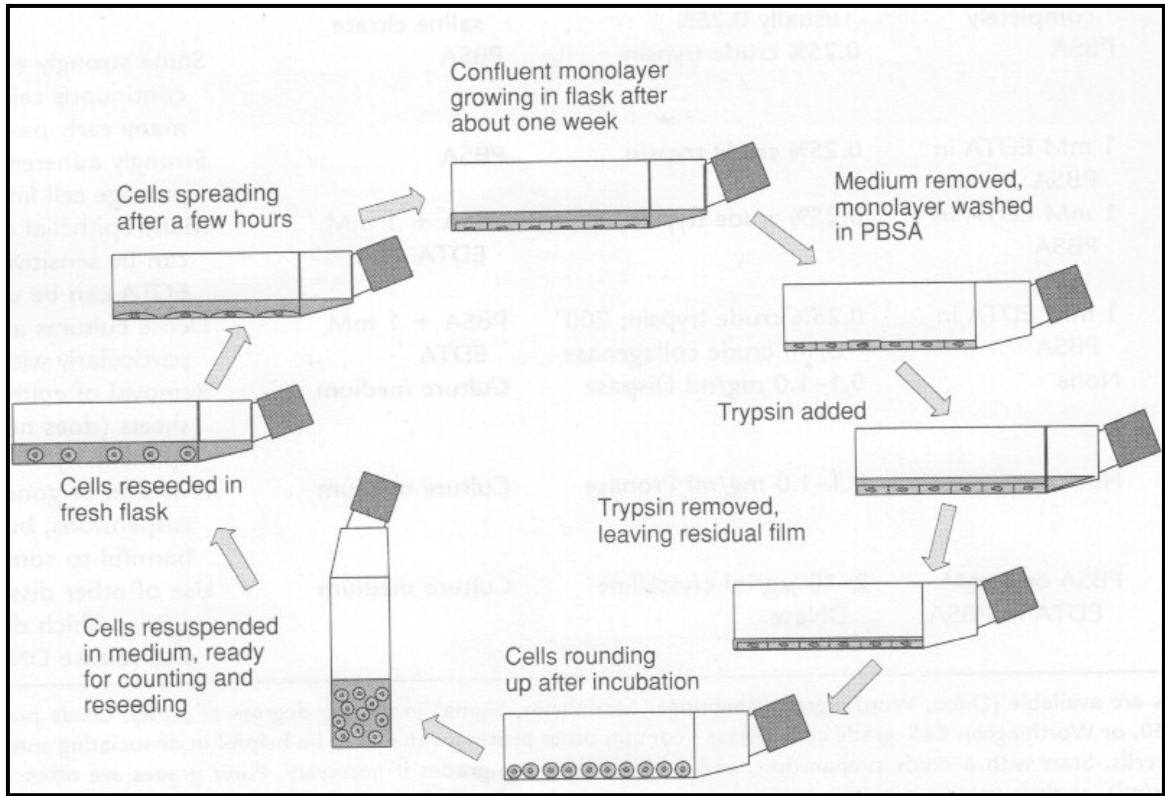


**Figure 2.1 Schematic diagram of the subculture of HEK293 cells.** Stages in the subculture and growth cycle of HEK293 cells following trypsinization (Freshney, 2000)

THP-1 monocytes (section 2.1.1.1), in which 1.0 ml aliquots of cells were kept in liquid nitrogen until needed for growth and culture.

For cellular assays, Null HEK293, 293-hTLR2 and 293-hTLR2/CD14 cells were trypsinized, as described above, to dislodge the cells. Cell supernatant was centrifuged at 500 xg for 10 minutes, and cells were resuspended in fresh growth medium. 0.3 ml or 0.2 ml of cells was plated to individual wells of a 48-well or 96-well sterile culture plate, respectively. The cell concentration for a 48-well plate was maintained at  $3.0 \times 10^5$  cells/ml, and  $2.0 \times 10^5$  for a 96-well culture plate. HEK293 cells were incubated and allowed to adhere for 4h at 37°C, 5% CO<sub>2</sub>. After incubation, growth medium was removed and HEK293 cells were resuspended in their respective assay medium (growth medium with reduced (2%) FBS) prior to treatment with effectors.

We have optimized the conditions of HEK 293 growth to achieve the maximal IL-8 concentration. We varied the length of adhesion of our HEK 293 cells to the cell culture plate prior to stimulation with effectors (section 2.3) and measured the IL-8 secretion after incubation (section 2.7). Results in Figure 2.2 showed the highest IL-8 production was achieved when HEK 293hTLR2 was allowed to adhere to the cell culture plate for 4 hours prior to treatment with effectors. Thus, for all experiments with Null HEK 293, HEK 293hTLR2 and HEK293hTLR2/CD14 cells, cells were incubated for 4 hours prior to stimulation with effectors. Similarly, we tested if proinflammatory production by HEK293 cells is affected by the number of times the cells have been subcultured. Figure 2.3 shows that the ability of HEK 293hTLR2 to produce IL-8 upon stimulation with fibrillar A $\beta$ (1-42) aggregated for 216 hours at 4°C significantly decreased as the cells

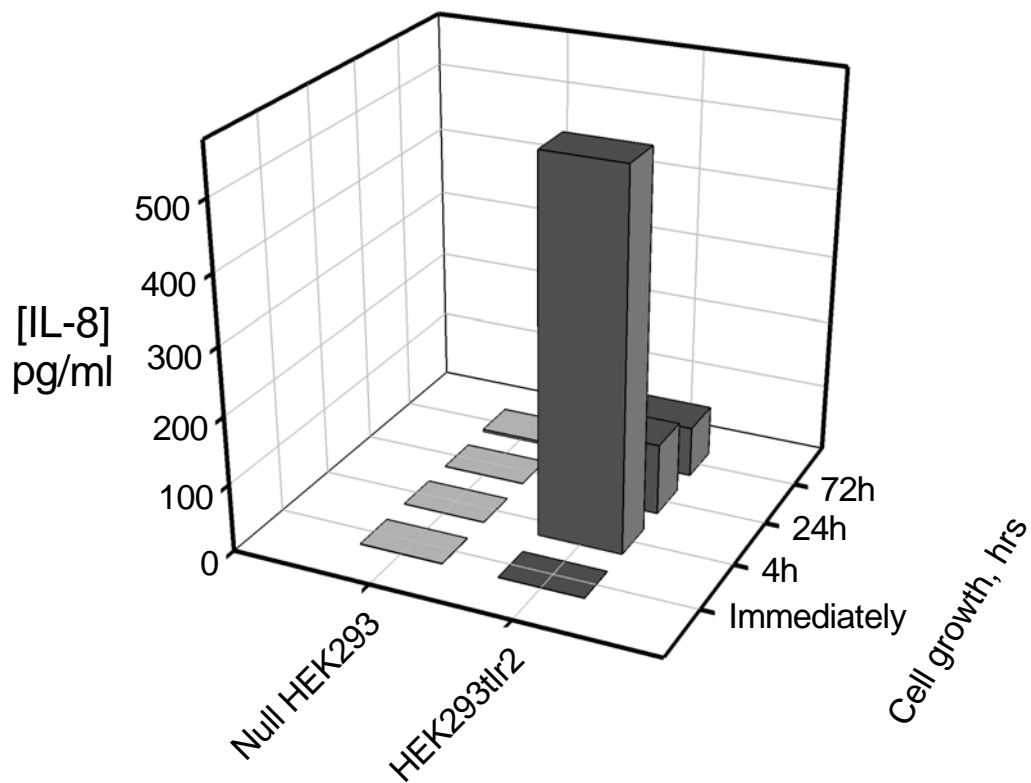


**Figure 2.2. Optimization of HEK 293 adhesion time prior to stimulation with Pam<sub>3</sub>CSK<sub>4</sub>.** Null HEK293 (light gray bars) or HEK 293hTLR2 (dark gray bars) was prepared for experiment, as described. After resuspension in growth medium, cells were plated in a cell culture plate and allowed to adhere at 37°C, 5%CO<sub>2</sub> for 0, 4, 24 or 72 hours prior to stimulation for IL-8 production (in pg/ml). After the given times, growth medium was removed, resuspended in assay medium and cells treated with 1 ng/ml Pam<sub>3</sub>CSK<sub>4</sub>. After 24-hour post-stimulation, IL-8 was measured. HEK 293hTLR2/CD14 cells were also tested and gave a trend similar to that of HEK 293hTLR2 (data not shown).

aged. Therefore, for all experiments employing HEK293 cells, we used cells from either passage 15 or 16 to achieve maximal secretion of IL-8.

## 2.2. Preparation of A $\beta$ peptides

Lyophilized powder of A $\beta$ (1-42) and A $\beta$ (1-40) peptides were purchased from rPeptide (Bogarth, GA, USA). The powder was dissolved in 100% hexafluoroisopropanol (HFIP) (Sigma, St. Louis, MO), and incubated at room temperature for 1 hour. This step is crucial to ensure disaggregation of any pre-formed aggregates. HFIP treatment also allows “normalization” of the properties of different commercial preparations of A $\beta$  (Wood et al., 1996; Zagorski et al., 1999). After incubation, the peptides were aliquotted into sterile microcentrifuge tubes, dried in a vacuum centrifuge, and dried samples stored at -20°C. Before cell treatment, the lyophilized samples were resuspended to 100  $\mu$ mol/L or 1 mmol/L in sterile water and incubated at 4°C. For studying the effect of temperature in A $\beta$ (1-42) aggregation, prepared A $\beta$  peptides were also stored at 25°C and 37°C. For cell treatment, cells were exposed to a final concentration of 15  $\mu$ mol/L of A $\beta$ (1-42) or A $\beta$ (1-40).

## 2.3 Activation of cell model systems

THP-1 monocytes or HEK 293 cells were prepared for experiment as described above, and plated on a sterile 48-well or 96-well cell culture plate. To the wells, pure bacterial LPS (*Escherichia coli* 026.B6, Sigma), ultrapure bacterial LPS (*Escherichia coli*

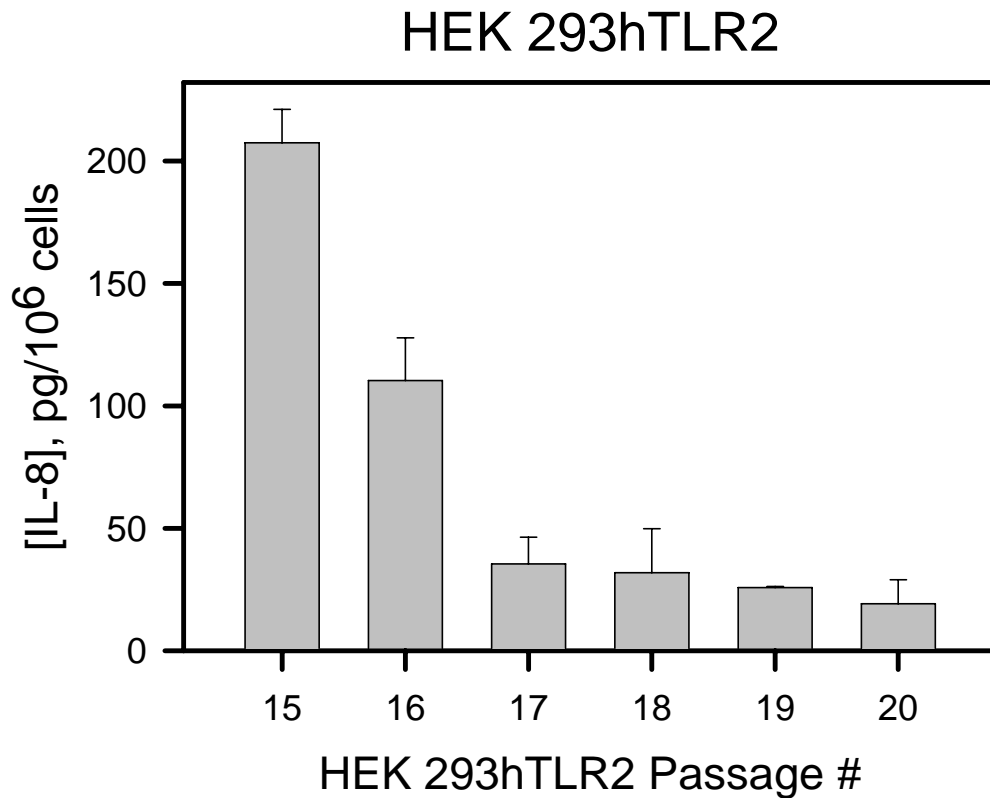


**Figure 2.3. Effect of HEK293 passage number on fibrillar A $\beta$ (1-42) response.** HEK293 hTLR2 cells were subcultured, as described. The number of times the cells have been subcultured is denoted by passage number. For each subculture, cells are prepared for experiment and stimulated with 15  $\mu$ M of fibrillar A $\beta$ (1-42) for 24 hours. After post-stimulation, secreted IL-8 was determined. This result represents 1 representative experiment of 3. Error bars represent n= 3 trials (1 experiment). The same experiment was done in Null HEK293 cells and treatment with A $\beta$  failed to stimulate Null HEK293 cells for IL-8 production (data not shown)

K12, InvivoGen), synthetic bacterial lipoprotein tripalmitoyl cysteinyl seryl tetralysine (Pam<sub>3</sub>CSK<sub>4</sub>, InvivoGen), synthetic Pam<sub>2</sub>CGDPKHPKSF (FSL-1, InvivoGen) (Figure 1.6) or 15 µmol/L Aβ(1-42) or Aβ(1-40) were applied. For HEK 293 experiments, Aβ(1-42) that was allowed to aggregate for 216 hours at 4°C was used. Cells were incubated at 37°C, 5%CO<sub>2</sub> at concentrations and incubation times stated in the experiments. After the indicated incubation time, cell supernatants were removed and centrifuged at 2500 xg for 10 minutes (Microcentrifuge® 18 Centrifuge, Beckman-Coulter) to remove cells, and supernatants were collected and stored at -20°C prior to analysis of proinflammatory products (TNFα or IL-8). For concentration dependence experiment, the EC<sub>50</sub> values were determined by fitting the concentration-dependence data for the agonists to a sigmoidal three-parameter equation ( $y = a / [1 + e^{-([x-x_0]/b)}]$ ) using SigmaPlot graphing program.

#### 2.4 Conversion of non-adherent THP-1 monocytes to adhering cells

THP-1 cell adhesion was described previously (Crouse et al., 2009). Briefly, THP-1 cells were treated with 10 ng/ml phorbol 12-myristate 13-acetate (PMA, Sigma) for 24 hours, and cells incubated at 37°C, 5% CO<sub>2</sub>. Vehicle control was 0.0005% DMSO. After incubation, non-adherent cells in the supernatant were removed and adherent cells were washed with assay medium prior to 6-hour stimulation of cells with known TLR agonists or 15 µM Aβ(1-42).

To verify the extent of adhesion, a separate well containing THP-1 cells was induced with PMA, as described above. After incubation, non-adherent cells were

removed, and adherent cells were washed with PBS. The adherent cells were removed from the bottom surface of the cell-culture plate with 0.25% trypsin-EDTA (HyClone), and counted under a microscope using a hemocytometer. Percent adhesion was calculated by the number of adherent cells divided by the plated cell number. Adherent cells with % adhesion range of 75% and above were used for proinflammatory response experiments.

### 2.5 LPS contamination assay

To test the A $\beta$  preparations for the presence of contaminating bacterial lipopolysaccharide, A $\beta$ (1-42) was routinely tested using Polymyxin B-sulfate (PMX-B) (Sigma). THP-1 monocytes were prepared as described, and plated on a 48-well cell culture plate. Cells were pretreated with 0.1  $\mu$ g/ml of PMX-B and incubated for 30 minutes at 37°C, 5%CO<sub>2</sub>. After incubation, cells were treated with either 10 ng/ml of ultrapure LPS or 100  $\mu$ mol/L of A $\beta$ (1-42) and incubated further for 6 hours at 37°C. Following incubation, cell supernatants were collected, centrifuged as described above, and supernatants stored at -20°C prior to TNF $\alpha$  measurement.

### 2.6 TLR antibody neutralization assay

THP-1 monocytes or HEK293 cells were seeded in 48-well or 96-well cell culture plate, and pre-treated with 5-20  $\mu$ g/ml of TLR antibodies, IgG isotype control or PBS for 1 hour at 37°C, 5% CO<sub>2</sub>. TLR antibodies and IgG isotype controls that were utilized in this experiment were functional grade anti-human TLR2 (clone T2.5), TLR4 (clone

HTA125), CD14 (clone 61D3) antibodies, mouse IgG2, $\kappa$  and IgG1, $\kappa$  isotype controls from eBioscience (San Diego, CA), polyclonal anti-TLR2, TLR4, TLR1 or TLR6 antibodies from InvivoGen, or rat IgG isotype control from Sigma. Following incubation, cells were treated with either 10 ng/ml ultrapure LPS, 1 ng/ml Pam<sub>3</sub>CSK<sub>4</sub>, 3 ng/ml (for THP-1 monocytes) or 1 ng/ml (for HEK293 cells) FSL-1, or 15  $\mu$ mol/L of A $\beta$ (1-42) and further incubated for 6 or 24 hours in the same conditions. After incubation, cell supernatants were collected as described above for TNF $\alpha$  or IL-8 determination.

### 2.7 Measurement of proinflammatory products

Secreted TNF $\alpha$  or CXC chemokine IL-8 in the supernatants were determined using Enzyme-linked immunosorbent assay (ELISA). ELISA has become a standard biochemical technique for determination of cytokine concentration, as well as levels of other proteins of interest, in body fluids and culture medium. An advantage of this method is its high specificity when monoclonal antibodies are used. Moreover, it is quick and easy to perform for large number of samples (Turner et al., 2004).

100  $\mu$ l of 2  $\mu$ g/ml monoclonal anti-human TNF $\alpha$ /TNFSF1A primary antibody (for TNF $\alpha$ ) or monoclonal anti-human CXCL8/IL-8 antibody (for IL-8) (R&D Systems, Minneapolis, MN, USA) was added to 96-well plates for overnight incubation at 24°C. Following incubation, wells were washed with PBS containing 0.05% Tween-20 and blocked with 300 $\mu$ L PBS containing 1% bovine serum albumin (BSA), 5% sucrose, and 0.05% NaN<sub>3</sub> for 1 hour at 24°C. After washing, 50 $\mu$ L of standards or cellular supernatant samples were added and the plate further incubated for 2 hours. After successive washing

and additions of 100 $\mu$ L of 0.1  $\mu$ g/ml biotinylated anti-human TNF- $\alpha$ /TNFSF1A detection antibody (TNF $\alpha$ ) or biotinylated anti-human CXCL8/IL-8 antibody (IL-8) (R&D Systems) in 20mmol/L Tris with 150mmol/L NaCl and 0.1% BSA for 2 hours, 100 $\mu$ L of streptavidin-horseradish peroxidase (R&D Systems) diluted 200 times with PBS containing 1% BSA for 20 minutes, and 100 $\mu$ L of equal volumes of 3,3',5,5'-tetramethylbenzidine and hydrogen peroxide (KPL, Gaithersburg, MD, USA) for 30 minutes, the reaction was stopped by the addition of 1 mol/L H<sub>2</sub>SO<sub>4</sub> solution. The optical density of each sample was analyzed at 450 nm with a reference reading at 630 nm using a SpectraMax 340 absorbance plate reader (Molecular Devices, Union City, CA, USA). A TNF $\alpha$  or IL-8 standard curve, with a range of 15 pg/ml to 2000 pg/ml is used to calculate the actual TNF $\alpha$  or IL-8 in the experimental samples. We made certain that the optical density of each sample falls within the standard curve. Samples whose optical density is outside the standard curve were diluted.

## 2.8 Cell viability assay

Powdered XTT (2,3-bis(2-methoxy-4-nitro-5-sulfophenyl)-2H-tetrazolium-5-carboxanilide) (Sigma) was dissolved in RPMI 1640 medium without phenol red (HyClone) supplemented with 2 mmol/L L-glutamine to make a stock solution of 1 mg/ml. The stock solution was kept at -20 $^{\circ}$ C prior to use.

For assessing the viability of THP-1 monocytes, the cells were plated in a 96-well cell culture plate and treated with effectors as described in section 2.3. After incubation,  $\approx$ 60ml of cell supernatants were treated with 30 ml of thawed 1 mg/ml XTT stock

solution containing 24.9  $\mu\text{mol/L}$  of phenazine methosulfate (PMS) (Fisher Scientific) and cells further incubated for 3 hours at 37°C, 5% CO<sub>2</sub>.

For HEK293 cells, cells were plated in a 96-well cell culture plate and treated with effectors as described. Following the desired incubation time, cell supernatants were removed and adherent cells were washed with corresponding assay medium. After removal of the medium, adherent cells were resuspended in 100  $\mu\text{l}$  of HEK293 assay medium containing 0.33 mg/ml XTT and 8.3  $\mu\text{mol/L}$  PMS. Cells were incubated further for 3 hours at 37°C, 5% CO<sub>2</sub>.

For both cases, cell supernatants were removed from individual wells after incubation, centrifuged at 2500  $\times g$  for 10 minutes to remove cells, and supernatants transferred to a new 96-well plate. XTT reduction was analyzed by reading the absorbance of the solution at 467 nm.

Tetrazolium salts, such as XTT, are commonly used as a measure of the redox potential of cells as a measure of their viability (Braeckman et al., 2002). It is based on the reduction of the colorless XTT tetrazolium salt within active mitochondria of living cells by succinate dehydrogenase to form an orange-colored water-soluble formazan (Figure 2.4) (Braeckman et al., 2002; Brady et al., 2007). The formation of a water-soluble formazan allows direct monitoring of its appearance, and thus, is one of the advantages of XTT over other previous tetrazolium salts like MTT (3-(4,5-dimethylthiazol-2-yl)-2,5-diphenyltetrazolium bromide), which produces insoluble salt when reduced (Scudiero et al., 1988; Kuhn et al., 2003).

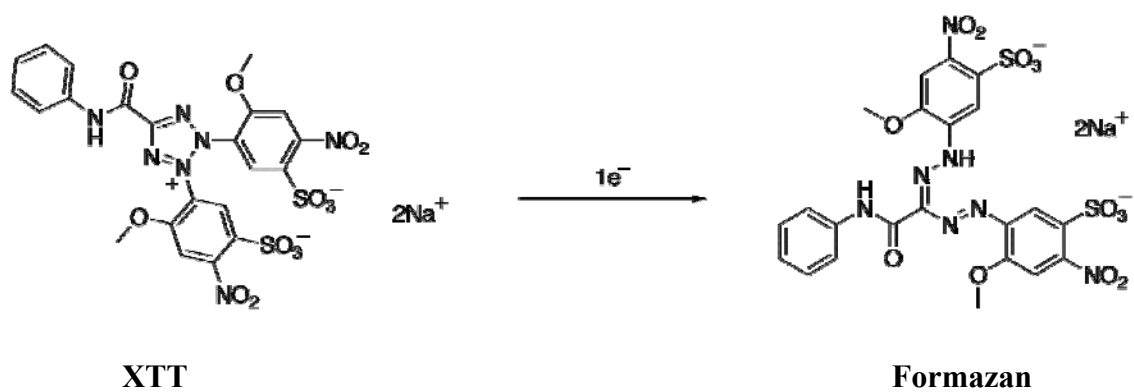


**Figure 2.4. Conversion of XTT to a water-soluble formazan salt by viable cells.** Metabolically active cells cleave the yellow tetrazolium salt XTT to form an orange formazan dye. XTT reduction is measured by reading the optical density at 467 nm.

## 2.9 Atomic Force Microscopy

At different aggregation states of the peptide, samples of A $\beta$ (1-42) or A $\beta$ (1-40) (100  $\mu$ mol/L and 1 mmol/L) solutions were obtained and diluted to 1  $\mu$ mol/L in water. Grade V1 mica (Ted Pella, Inc., Redding, CA, USA) was cut into 11 mm circles and affixed to 12 mm metal discs. 50  $\mu$ L of resulting A $\beta$  aliquots were applied to freshly cleaved mica, allowed to adsorb for 15 minutes, washed twice with water, air dried, and stored in a container with desiccant. Images were obtained with a Nanoscope III multimode atomic force microscope (Digital Instruments, Santa Barbara, CA, USA) in TappingMode<sup>TM</sup>. Height analysis was performed using Nanoscope III software on flattened height mode images.

## 2.10 Statistical Analysis

Data are expressed as mean  $\pm$  SD. Statistical comparisons were made using Student's *t* test (SAS system) (Harris, 2003). Differences between mean were considered significant at  $p < 0.05$ .

## 2.11 Bibliography

- Brady, A. J., P. Kearney, et al. 2007. Comparative evaluation of 2,3-bis [2-methoxy-4-nitro-5-sulfophenyl]-2H-tetrazolium-5-carboxanilide (XTT) and 2-(2-methoxy-4-nitrophenyl)-3-(4-nitrophenyl)-5-(2, 4-disulfophenyl)-2H-tetrazolium, monosodium salt (WST-8) rapid colorimetric assays for antimicrobial susceptibility testing of staphylococci and ESBL-producing clinical isolates. *J Microbiol Methods*. 71:305-311.
- Braeckman, B. P., K. Houthoofd, et al. 2002. Assaying metabolic activity in ageing *Caenorhabditis elegans*. *Mech Ageing Dev*. 123:105-119.
- Crouse, N. R., D. Ajit, et al. 2009. Oligomeric amyloid-beta(1-42) induces THP-1 human monocyte adhesion and maturation. *Brain Res*. 1254:109-119.
- Freshney, R. I. (2000) *Culture of Animal Cells: A Manual of Basic Technique*, 4th Edition. NY: Wiley-Liss, Inc.
- Harris, D. C. (2003) *Quantitative Chemical Analysis*, 6th Edition. New York: W.H. Freeman and Company.
- Kuhn, D. M., M. Balkis, et al. 2003. Uses and limitations of the XTT assay in studies of *Candida* growth and metabolism. *J Clin Microbiol*. 41:506-508.
- Scudiero, D. A., R. H. Shoemaker, et al. 1988. Evaluation of a soluble tetrazolium/formazan assay for cell growth and drug sensitivity in culture using human and other tumor cell lines. *Cancer Res*. 48:4827-4833.
- Takashiba, S., T. E. Van Dyke, et al. 1999. Differentiation of monocytes to macrophages primes cells for lipopolysaccharide stimulation via accumulation of cytoplasmic nuclear factor kappaB. *Infect Immun*. 67:5573-5578.
- Tsuchiya, S., M. Yamabe, et al. 1980. Establishment and characterization of a human acute monocytic leukemia cell line (THP-1). *Int J Cancer*. 26:171-176.
- Turner, C. K., T. M. Blieden, et al. 2004. A novel ELISpot method for adherent cells. *J Immunol Methods*. 291:63-70.
- Wood, S. J., B. Maleeff, et al. 1996. Physical, morphological and functional differences between pH 5.8 and 7.4 aggregates of the Alzheimer's amyloid peptide A $\beta$ . *J*

Mol Biol. 256:870-877.

Yates, S. L., L. H. Burgess, et al. 2000. Amyloid beta and amylin fibrils induce increases in proinflammatory cytokine and chemokine production by THP-1 cells and murine microglia. *J Neurochem.* 74:1017-1025.

Zagorski, M. G., J. Yang, et al. 1999. Methodological and chemical factors affecting amyloid beta peptide amyloidogenicity. *Methods Enzymol.* 309:189-204.

Zhou, J., P. Zhu, et al. 2005. Involvement of CD147 in overexpression of MMP-2 and MMP-9 and enhancement of invasive potential of PMA-differentiated THP-1. *BMC Cell Biol.* 6:25.

### 3 MODULATION OF AMYLOID BETA AGGREGATION MORPHOLOGY AND ITS EFFECT ON PROINFLAMMATORY RESPONSE OF THP-1 MONOCYTES

#### 3.1 Introduction

The brains of individuals with AD are characterized by the presence of two lesions: extracellular deposits of A $\beta$  peptides, so-called neuritic or senile plaques, and intracellular neurofibrillary tangles (NFT) of hyperphosphorylated tau (Selkoe, 2001). Numerous studies have now shown that A $\beta$  plays a very important role in the AD pathogenesis (Walsh et al., 2002a; Walsh et al., 2002b). Although the exact mechanism of neurodegeneration is still uncertain, substantial evidences associate A $\beta$  as fundamental for neurodegeneration in AD (Ramsden et al., 2001). Particularly, several studies with synthetic A $\beta$  pinpoint the fibrillar form similar to those present in amyloid-bearing plaques in AD as neurotoxic both *in vitro* and *in vivo* and causes neuronal dysfunction and loss in AD (Kowall et al., 1991; Pike et al., 1991; Lorenzo and Yankner, 1994; Iversen et al., 1995). However, recent reports suggest that it is the soluble, rather than the insoluble A $\beta$  that is responsible for early dendritic and synaptic injury, and eventually neuronal dysfunction and degeneration (Lambert et al., 1998; Lue et al., 1999; Walsh et al., 2002a; Chromy et al., 2003; Bucciantini et al., 2004).

Besides being known to have direct neurotoxic effect, considerable evidences also favor an indirect effect of A $\beta$  to neurodegeneration based on ability of A $\beta$  to initiate and release inflammatory mediators and neurotoxic factors in microglia, such as secretion of proinflammatory cytokines, respiratory burst activity and increased phagocytosis and chemotaxis (Murphy et al., 1998; Lue et al., 2001a; Lue et al., 2001b; Lee et al., 2002; Floden and Combs, 2006). Consistent with this, reactive microglia has been observed to be in and around A $\beta$  – consisting plaques in AD (Frautschy et al., 1998; Stalder et al., 1999). Thus, these studies suggest that the extracellular deposition of A $\beta$  triggers inflammation in AD brain.

However, despite numerous evidences connecting A $\beta$  to neuronal injury and death, limited information is still available as to the exact mechanism by which A $\beta$  causes neurodegeneration. Similarly, a more complicated question that is a focus of active study and debate is the question of, what A $\beta$  assembly state correlates with the biological activity and contributes most critically to neurological decline in AD. It is thus important to have a clearer understanding of the A $\beta$  structure-function relationship for the reason that determining the trigger of activation will result in a better understanding of the contribution of inflammation in AD, and subsequently, will have important implications to the development of therapeutic strategies.

In this study we investigate the ability of synthetic A $\beta$  peptides to invoke a proinflammatory response in a human monocytic cell line. Moreover, we seek to determine the active A $\beta$  species that induces TNF $\alpha$  production in our THP-1 monocytes. We modulated A $\beta$  aggregation by varying several factors including peptide concentration, peptide length and temperature to examine the A $\beta$  assembly state that

correlates with biological activity. We propose that an A $\beta$  (1-42) fibrillar precursor was largely responsible for THP-1 cell activation. The data presented in this chapter is part of a collaborative study with Deepa Ajit of Department of Chemistry and Biochemistry, University of Missouri-Saint Louis. Additional data, analysis and conclusions will be presented and included in Ms. Ajit's dissertation.

## 3.2 Results

### 3.2.1 A $\beta$ aggregation and proinflammatory response

To study the proinflammatory response of different A $\beta$  aggregation species, we have utilized a well-studied mammalian cell system, THP-1 monocytes. Numerous investigators have utilized THP-1 cells as a model system for the study of proinflammatory production by LPS and A $\beta$ , and have shown that THP-1 cells are morphologically similar to microglia when stimulated with LPS and A $\beta$ , making them a very good model of primary human microglia and for investigating A $\beta$  induced inflammatory activity (Klegeris et al., 1997; Yates et al., 2000; Combs et al., 2001). We prepared the THP-1 monocytes as described in the methods, maintaining a cell concentration of  $1 \times 10^6$  cells/ml. The lyophilized A $\beta$  were resuspended in water to a final concentration of 100  $\mu\text{mol/L}$  and kept at 4°C prior to cellular stimulation. The A $\beta$  was allowed to aggregate at 4°C from 0h (freshly prepared) to 216h. In between these aggregation times, A $\beta$  solution was removed and was used to stimulate the THP-1 monocytes to a final A $\beta$  concentration of 15  $\mu\text{mol/L}$ . Cells were incubated for 6h at 37°C,

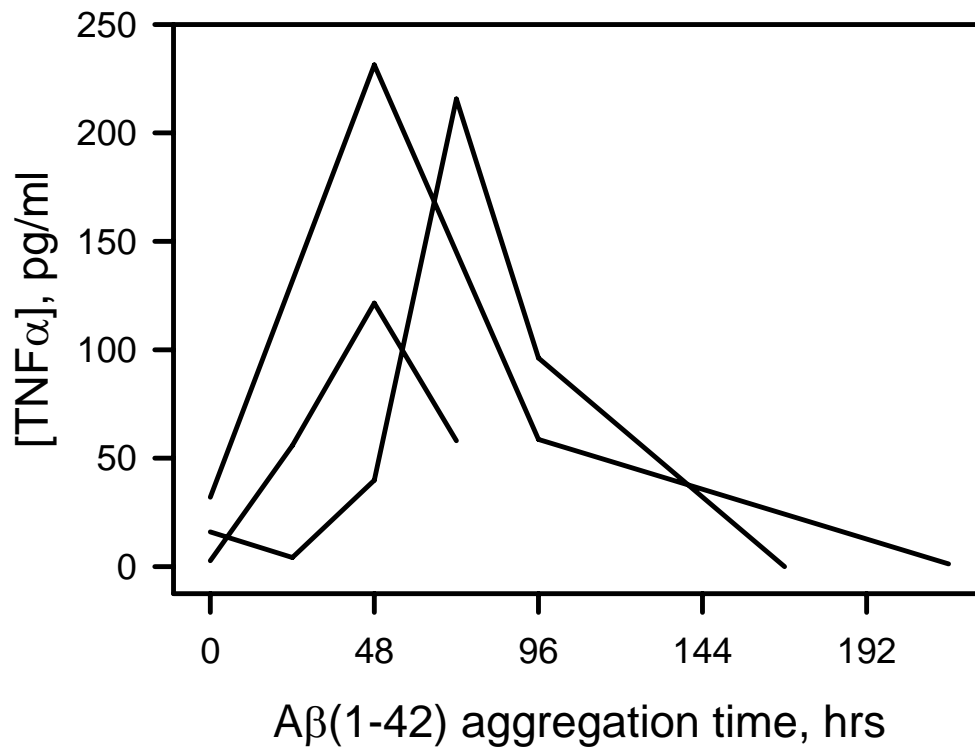


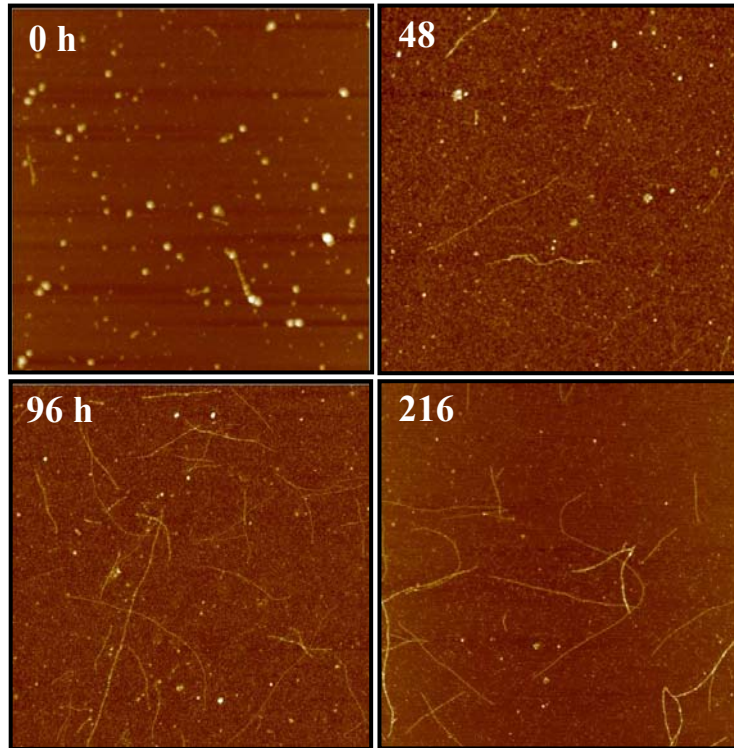
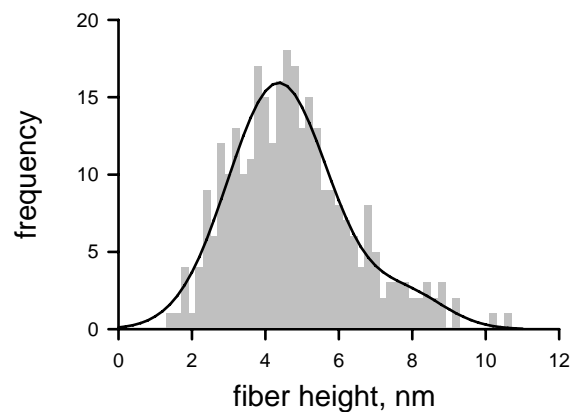
**Figure 3.1 Proinflammatory activity of synthetic Aβ(1-42) at different aggregation.** Aβ(1-42) was prepared in water and stored at 4°C, as described in the Methods. THP-1 monocytes were incubated with 100 μmol/L of Aβ(1-42) at different aggregation age to a final Aβ concentration of 15 μmol/L, and cells incubated for 6h at 37°C, 5% CO<sub>2</sub>. After post-incubation, supernatants were collected and TNFα production was measured using ELISA. Shown are three representative experiments from different Aβ(1-42) lots.

supplemented with 5% CO<sub>2</sub>. After incubation, supernatants were collected and assayed for TNF $\alpha$  production by ELISA. Figure 3.1 illustrates the proinflammatory activity of different aggregates of 100  $\mu$ mol/L A $\beta$ . Minimal TNF $\alpha$  levels were produced when THP-1 cells were treated with freshly reconstituted (0 hours) A $\beta$ (1-42). However, a steady and significant increase in TNF $\alpha$  production was observed when A $\beta$ (1-42) solution was allowed to aggregate further, with the peak TNF $\alpha$  level observed between 48h and 96h of A $\beta$  aggregation. Interestingly, there was a noticeable decline in stimulatory activity when A $\beta$  sample was incubated for a longer aggregation time. Different representative aggregation age profiles of 100  $\mu$ mol/L of A $\beta$  were included in the figure to illustrate that there is a lot-to-lot variation in stimulatory activity by synthetic A $\beta$  (May et al., 1992; Zambrzycka et al., 2000). The toxicity of different A $\beta$  aggregates were also monitored using XTT and results showed that 15  $\mu$ mol/L A $\beta$  aggregates were not toxic to THP-1 cells (data not shown).

We monitored the morphology of the A $\beta$  aggregate species using AFM (Figure 3.2a). The appearance of numerous punctuate species was observed for freshly reconstituted A $\beta$  monomers, with height measurement of <2 nm for majority of the adsorbed species. There was also a noticeable presence of small spherical species in A $\beta$ (1-42) at 0h of aggregation. Height analysis of these species ranged from 2 to 5 nm, with an average of  $3.2 \pm 0.8$  nm (SD) for n = 115 measurements. This suggests that the said spherical species might be fibrillar precursors. Also, a number of bright spots, with height > 20nm, can be detected which may represent the formation of amorphous aggregates immediately following reconstitution of the peptide. Consequently, these spherical species were not able to stimulate THP-1 cells for TNF $\alpha$  production (Figure

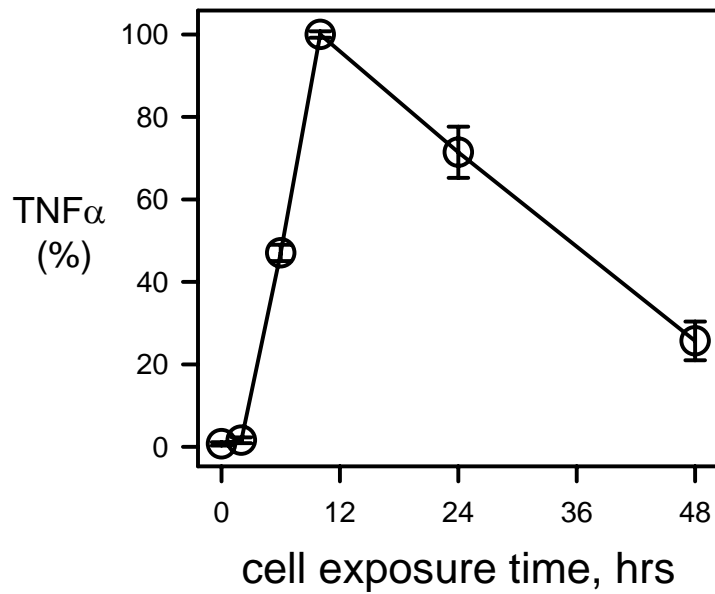
3.1). The appearance of thin flexible fiber-like structures was observed at 48 hours of A $\beta$  aggregation. Continuous incubation of A $\beta$  increased the appearance of fibrillar structures. When applied to THP-1 cells, these A $\beta$  species invoked TNF $\alpha$  production. Height measurements of the 48h aggregated A $\beta$  fibrillar structure were performed and plotted as a histogram (Figure 3.2b) and fitted for multiple peaks. Using peak fitting analysis, we observed two populations: the first with a peak height and SE of  $4.4 \pm 0.1$  nm, and the second having a mean height and SE of  $7.9 \pm 0.6$  nm (Udan et al., 2008). Our height measurements for the fibers formed at 48h were in agreement with previous AFM measurements describing type I and type II fibrillar A $\beta$  (Harper et al., 1997; Stine et al., 2003). Further incubation of the A $\beta$  samples (216 hours) resulted in the formation of longer fibrillar structures. Interestingly, a marked decrease in the presence of spherical species was observed at this incubation time. The longer, more mature fibril structures present at 216 hours surprisingly were not able to stimulate the THP-1 cells in producing TNF $\alpha$ .

We also varied the length of cell exposure to further analyze A $\beta$ -induced proinflammatory production. We found that maximum TNF $\alpha$  production was achieved when THP-1 cells were exposed to 15  $\mu$ mol/L of A $\beta$ (1-42) for 10 hours (Figure 3.3a). This trend was slightly different from that of LPS - and Pam<sub>3</sub>CSK<sub>4</sub> - treated THP-1 cells in that the maximal TNF $\alpha$  response was consistently observed after 6 hours of post-stimulation (Figure 3.3b). Because continual exposure of the cells to proinflammatory products may have a toxic effect on the cells, we have utilized a 6-hour cell exposure despite the observed maximal A $\beta$  TNF $\alpha$  response at 10 hour post stimulation.

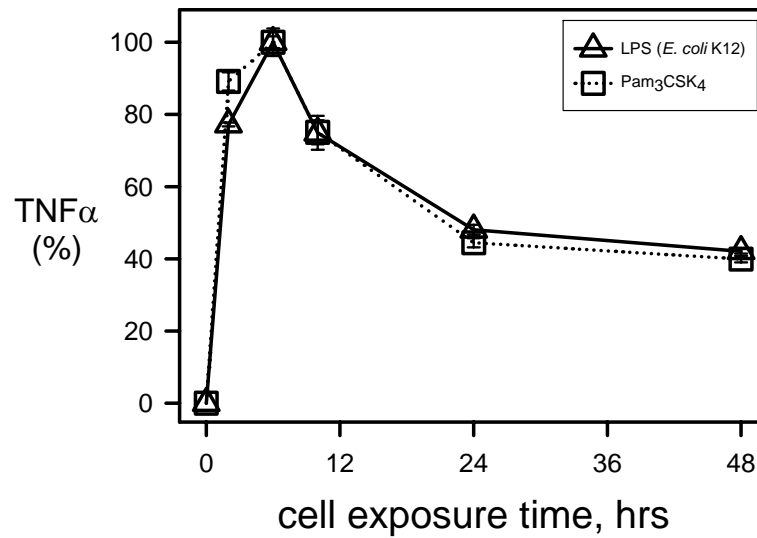
**A****B**

**Figure 3.2. Morphological studies of Aβ(1-42) aggregated species.** (A) Aβ aggregation solutions (100 μmol/L) in water were prepared as described in Methods, and allowed to aggregate at 4°C. Aliquots were removed at 0, 48, 96 and 216h, diluted to 1 μmol/L with water and imaged by AFM. Representative Aβ solutions were also used to treat THP-1 monocytes for TNFα production. AFM images are 5μm x 5μm and are shown in 'height' mode. (B) Representative frequency histogram from 300 height measurements of Aβ(1-42) aggregated at 48h. Graph was fitted ( $r^2 = 0.932$ ) to a two-peak Gaussian area curve using PeakFit software v3.0 (Systat Software, Inc., San Jose, CA, USA). AFM images courtesy of Ms. Deepa Ajit, Univ. of Missouri-St. Louis. Frequency histogram analysis courtesy of Dr. Michael R. Nichols, University of Missouri-St. Louis.

A



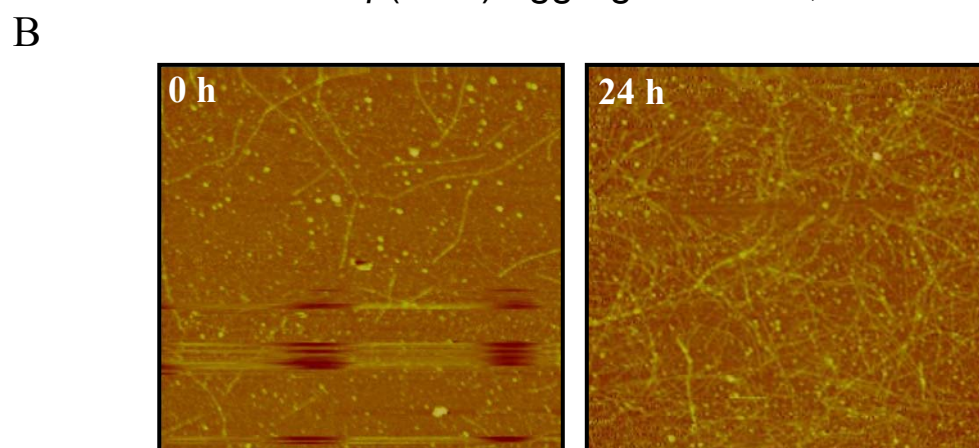
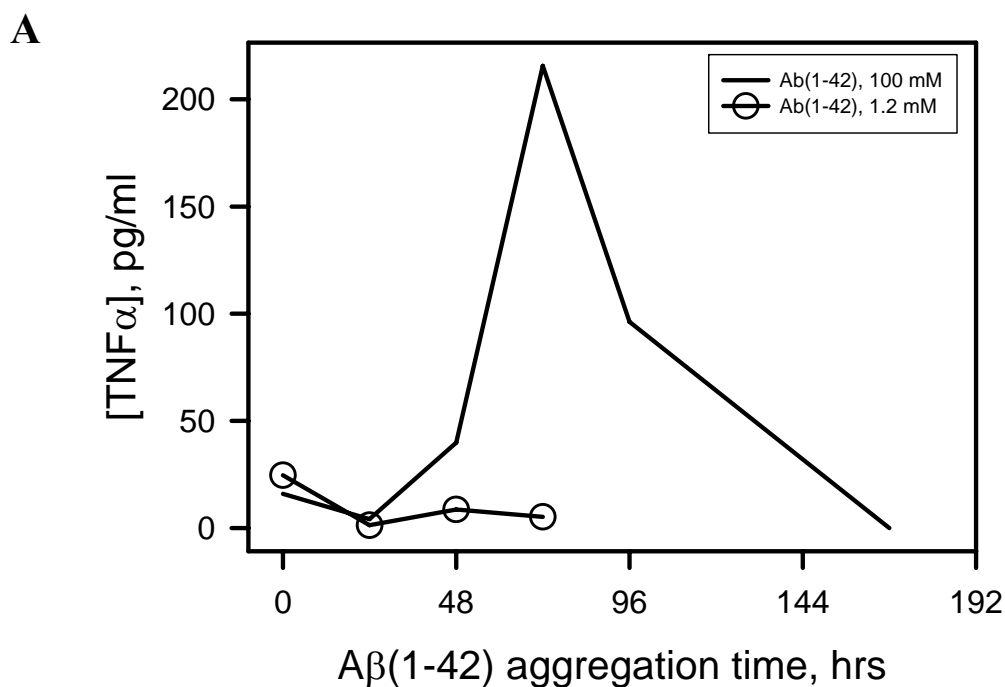
B



**Figure 3.3. Effect of exposure time on Aβ(1-42)-, LPS- and Pam<sub>3</sub>CSK<sub>4</sub>-induced TNFα response in THP-1 cells.** (A) THP-1 cells were exposed to 15 μM Aβ(1-42) at given times. After post-incubation, TNFα production was analyzed by ELISA. (B) THP-1 cells were exposed to 10 ng/ml ultrapure *E. coli* K12 LPS or 1 ng/ml Pam<sub>3</sub>CSK<sub>4</sub> at given times. Supernatants were collected after stimulation and assayed for TNFα. For both figures, TNFα was expressed as % of the maximum response, which was at 10 hours for Aβ(1-42), and 6 hours for LPS and Pam<sub>3</sub>CSK<sub>4</sub>. Error bars for Aβ are standard error for n = 6 trials for 0, 6, 10 and 24h and n = 3 for 48h; and n = 3 for both LPS and Pam<sub>3</sub>CSK<sub>4</sub>. Actual maximum averaged TNFα levels are 507 pg/ml for Aβ, 674 pg/ml for ultrapure LPS and 214 pg/ml for Pam<sub>3</sub>CSK<sub>4</sub>.

### 3.2.2. Modulation of A $\beta$ aggregation

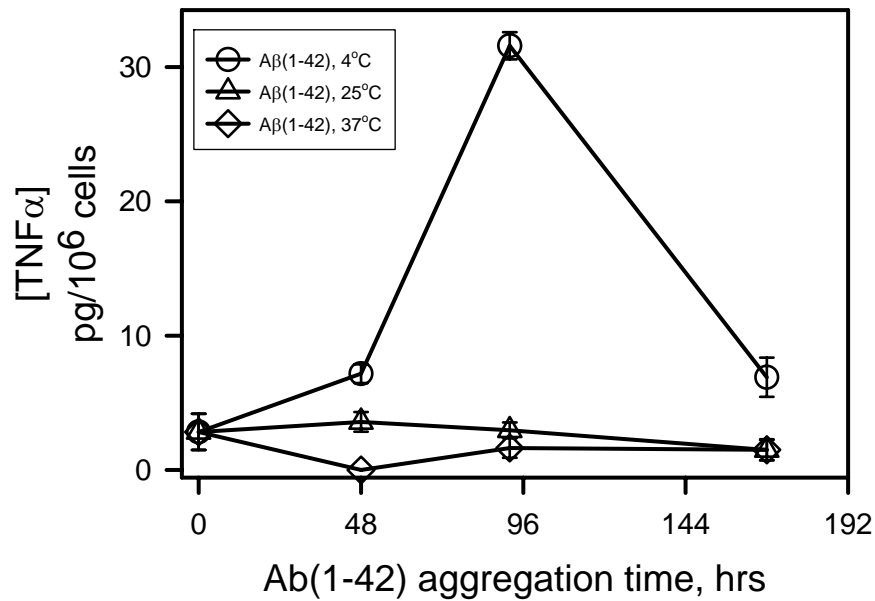
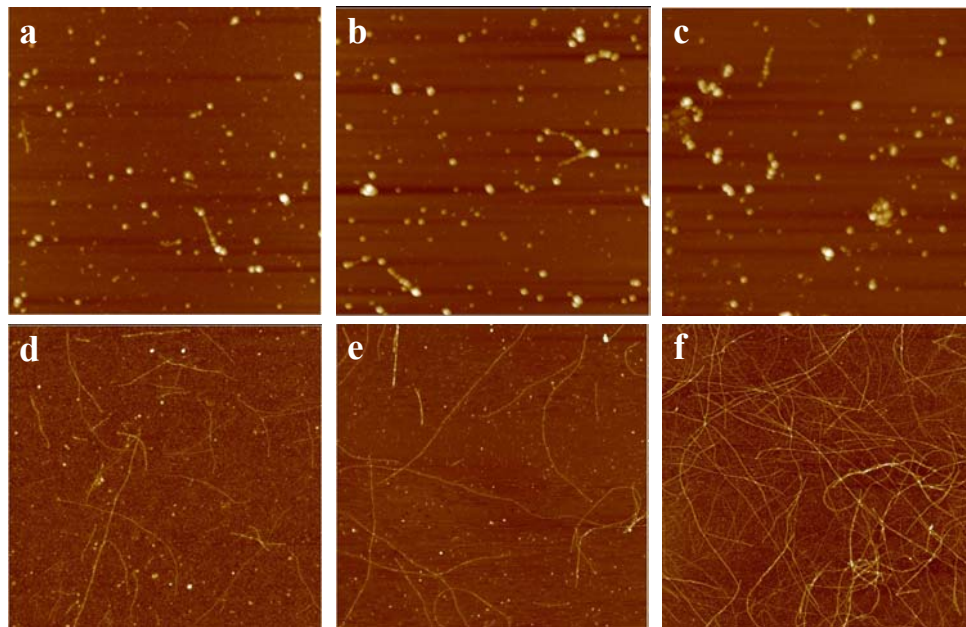
Our data suggests that an intermediate A $\beta$ (1-42) species is stimulating our THP-1 monocytes in producing TNF $\alpha$ . However, as the A $\beta$  aged, the species that were produced failed to invoke TNF $\alpha$  production. To further understand the inability of the later aggregated species to induce proinflammatory response in our THP-1 monocytes, we regulated the aggregation kinetics. Several factors can modulate *in vitro* A $\beta$  fibril formation. One of the factors that affects A $\beta$  fibrillogenesis is the peptide concentration (McLaurin et al., 2000; Taylor et al., 2003). Increasing the peptide concentration considerably enhances the rate of aggregation (Harper et al., 1999; Nilsson, 2004; Chen and Glabe, 2006). For this study, we increased the concentration of A $\beta$ (1-42) stock solution from 100  $\mu$ mol/L to 1.2 mmol/L, and followed the ability of the A $\beta$  aggregation species to invoke TNF $\alpha$  production in THP-1 monocytes. To compare the effect of concentration, the THP-1 cells were treated with both the concentrated A $\beta$  sample and 100  $\mu$ mol/L A $\beta$  preparation, to a final concentration of 15  $\mu$ mol/L. As shown in Figure 3.4a, 1.2 mmol/L A $\beta$  sample invoked TNF $\alpha$  production (24 pg/ml) when it was freshly reconstituted; however, further aging of the concentrated A $\beta$  samples eradicated induction of TNF $\alpha$  response. This response was significantly different from that of 100  $\mu$ mol/L of A $\beta$ , wherein the peak response was observed at 96h of A $\beta$  aggregation. AFM analysis of the 1.2 mmol/L A $\beta$  solutions revealed that aside from the globular species, the freshly reconstituted peptide solution (Figure 3.4b) already formed numerous long fibrillar structures. A longer, intertwined dense population of fibrils was observed as



**Figure 3.4. Proinflammatory activity and morphological studies of concentrated A $\beta$  (1-42) sample.** (A) Unlike 100  $\mu$ M of A $\beta$  (black line), a more concentrated 1.2 mM A $\beta$ (1-42) (circles) failed to induce TNF $\alpha$  response in THP-1 monocytes. A $\beta$  was reconstituted in water to a final concentration 1.2 mM, as described in Methods. THP-1 cells were treated with A $\beta$  solution at different aggregation times, and cells incubated for 6h at 37°C. After incubation, cell supernatants were analyzed for TNF $\alpha$  using ELISA. A representative graph for 100  $\mu$ M A $\beta$  from Figure 3.1 was included for comparison. (B) AFM of freshly reconstituted and 24h aggregated 1.2 mM A $\beta$  showed a population of fibrillar species. AFM was done as described in methods. AFM images courtesy of Deepa Ajit, University of Missouri-St. Louis.

early as 24 hours of A $\beta$  aggregation, however, these species were not able to invoke TNF $\alpha$  response. It was not possible to do height analysis on fibrils at 24 hours of aggregation due to overabundance of intertwined fibrils. Nevertheless, the presented data suggest that a 12-fold increase in A $\beta$  concentration rapidly diminishes the lag phase for fibril formation, and also attenuates the ability to induce TNF $\alpha$  response.

We next studied the effect of A $\beta$  incubation temperature in fibril formation and analyzed the biological activity of the A $\beta$  species that are formed. We resuspended A $\beta$ (1-42) in water, as described in Methods, to a final concentration of 100  $\mu$ mol/L and let the solution aggregate at 4°C, 25°C and 37°C. At different times, solutions were removed and used for THP-1 treatment. As shown in Figure 3.5a, only the A $\beta$  species formed at 4°C, and not at 25°C and 37°C, induced TNF $\alpha$  production in THP-1 monocytes. There was a slight increase in the signal of A $\beta$  at 25°C aggregated for 48 hours, but the increase was not significant. AFM analysis of freshly prepared A $\beta$  solutions contained spherical species (Figure 3.5b), which were still present at 48 hours of aggregation for A $\beta$  stored at 4°C, along with a few fibrillar structures. A $\beta$  solution incubated at 25°C and 37°C quickly formed longer fibrillar structures (data not shown). At 96 hours of aggregation, A $\beta$  incubated at 4°C contained long flexible fibrils (Figure 3.5b) with a mean height of  $5.5 \pm 1.6$  nm (SD), as well as numerous globular structures, which correspondingly elicited an increased TNF $\alpha$  production in THP-1 cells. A $\beta$  samples incubated at 25°C showed longer fibrils, with mean height of  $6.9 \pm 2.1$  nm (SD). Interestingly, a decrease in the presence of globular structures was also noticeable. A $\beta$  samples at 37°C aggregated much faster, as shown by an abundance of fibrils formed at 96 hours of aggregation. These data further suggest that an intermediate fibrillar A $\beta$  species induced TNF $\alpha$  response in THP-1 cells.

**A****B**

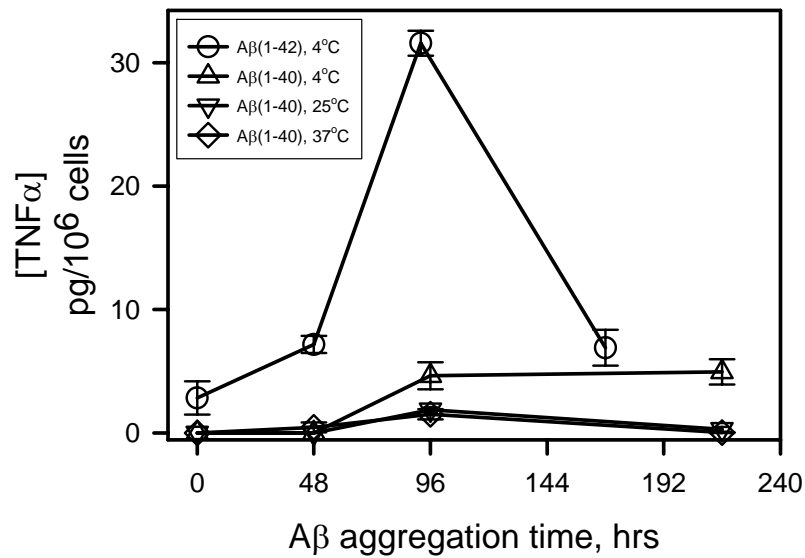
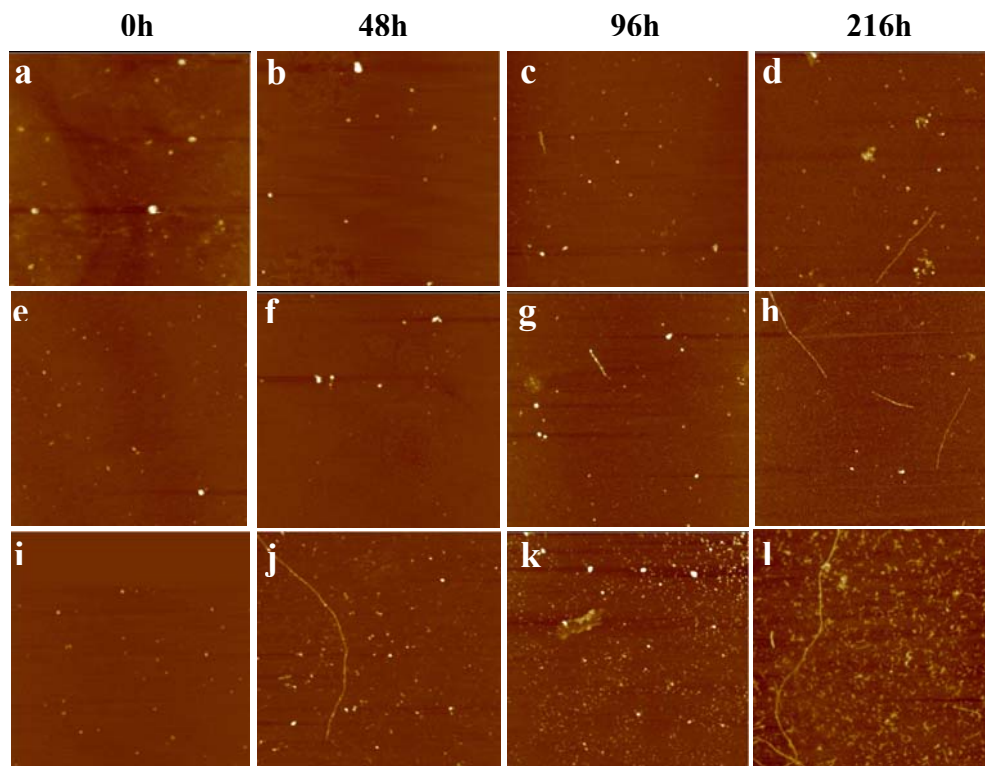
**Figure 3.5. Accelerated aggregation of A $\beta$ (1-42) by increasing the incubation temperature failed to invoke TNF $\alpha$  response in THP-1 monocytes.** (A) 100  $\mu$ M A $\beta$ (1-42) was prepared in water and incubated at 0°C (circles), 25°C (triangles) or 37°C (diamonds). THP-1 cells were incubated with A $\beta$  solutions to a final concentration of 15  $\mu$ M for 6 hours, as described in Methods. After incubation, TNF $\alpha$  was assessed by ELISA. (B) Representative AFM images of freshly prepared (a-c) or 96-hour aggregated (d-f) A $\beta$ (1-42) solutions incubated at 4°C (a,d), 25°C (b,e) or 37°C (c,f) were analyzed as described. Only the A $\beta$  sample incubated at 4°C elicited TNF $\alpha$  response in THP-1 monocytes. AFM images courtesy of Deepa Ajit, University of Missouri-St. Louis.

Increased fibril formation diminished the TNF $\alpha$  response, and prolonged and accelerated aggregation failed to induce TNF $\alpha$  production in THP-1 cells.

A $\beta$ (1-42) and A $\beta$ (1-40) are the most predominant variants of A $\beta$  that are present in amyloid plaques (Taylor et al., 2003). The data that we have shown so far indicate that the active species of A $\beta$ (1-42) was effective in inducing TNF $\alpha$  production in THP-1 monocytes. We wanted to know if the species formed during A $\beta$ (1-40) aggregation will also instigate TNF $\alpha$  response similar to that of A $\beta$ (1-42). For this, we prepared 100  $\mu$ mol/L of A $\beta$ (1-40) in water and treated the THP-1 cells the same way as A $\beta$ (1-42). After 6 hours of post-incubation, supernatants were analyzed for TNF $\alpha$ . Our results showed that A $\beta$ (1-40) samples at 4°C were not effective in inducing TNF $\alpha$  response (Figure 3.6a). Moreover, AFM imaging of the A $\beta$ (1-40) aggregation at 4°C indicated a slower rate of fibril formation (Figure 6b, panels a-d). To hasten A $\beta$  aggregation, samples of A $\beta$ (1-40) were likewise incubated at 25°C or 37°C. AFM analysis showed that although at a much slower rate than A $\beta$ (1-42), A $\beta$ (1-40) also formed fibrils at elevated temperatures (Figure 3.6b, panels e-h, i-l) and longer A $\beta$  incubation (Figure 6b, panels h and l). However, these species were ineffective in inducing TNF $\alpha$  release in THP-1 monocytes (Figure 3.6a).

### 3.3. Discussion

Inflammation plays an essential role in the brain's response to injury and pathology (Moore et al., 2002). Growing evidences have linked inflammation with the development of AD. Microglial cells, the resident immune cells of the CNS, play an

**A****B**

**Figure 3.6. A $\beta$ (1-40) failed to induce proinflammatory activity on THP-1 cells.** (A) 100  $\mu$ M A $\beta$ (1-40) was prepared in water, and incubated at 4°C (triangle) , 25°C (inverted triangle) and 37°C (diamond), as described in Methods. Different aggregation solutions were used to treat the THP-1 monocytes for 6 hours, and TNF $\alpha$  was analyzed after post-stimulation. (B) Representative AFM images of A $\beta$ (1-40) samples at 4°C (a-d), 25°C (e-f) and 37°C (i-l) at different times. AFM images are 5  $\mu$ m x 5  $\mu$ m. AFM images courtesy of Deepa Ajit, University of Missouri-St. Louis.

integral role in inflammation. Moreover, activated microglial cells have been found to be closely associated with and the most prominent component of senile plaques (Combs et al., 2000; Masumura et al., 2000; Selkoe, 2001; Mattson, 2004). Numerous cellular studies using microglia and human macrophage/monocytes cell line have demonstrated that A $\beta$  peptides are able to induce these cells to produce significant amounts of proinflammatory cytokines and chemokines (Meda et al., 1995; Yan et al., 1996).

In studying the correlation between different A $\beta$  aggregation species and proinflammatory production, we have utilized THP-1 monocytes for the main reason that THP-1 cells have expansive properties that are analogous to microglia and mature phagocytes when treated with LPS and A $\beta$  (Klegeris et al., 1997; Combs et al., 1999; Combs et al., 2000). Moreover, THP-1 cells express numerous surface markers such as CD11a, CD11b, CD11c, CD18, CD36, CD44 and Fc immunoglobulin receptors that are pronounced on macrophages and microglia (Klegeris et al., 1997). These metabolic and morphological similarities between human monocytic cell line THP-1 and microglia made the THP-1 an appropriate model for the study of A $\beta$ -induced proinflammatory response in primary human microglia.

We have shown that 100  $\mu$ mol/L of A $\beta$ (1-42) at 4°C was capable of invoking TNF $\alpha$  production in THP-1 monocytes. Although the observed maximum TNF $\alpha$  response varies from lot-to-lot preparation of A $\beta$ , it was still apparent that an intermediate A $\beta$  species activate the THP-1 monocytes and prolonged aggregation (216 hours) of the A $\beta$  was ineffective in stimulating proinflammatory response. Furthermore, enhancing the rate of aggregation and fibril formation by manipulating several factors such as increasing the concentration (Fig. 3.4) or A $\beta$  incubation temperature (Fig. 3.5) produced A $\beta$  species that

were not able to induce proinflammatory response in our THP-1 monocytes. These data suggest that an intermediate A $\beta$  structure, and not the more mature rigid fibrils, act as a proinflammatory stimulus.

Atomic force microscopy (AFM) is an ideal tool to follow the early morphological changes in A $\beta$  fibril formation (Stine et al., 1996). Several investigators have used this technique to understand the process of A $\beta$  fibrillogenesis (Harper et al., 1997; Kowalewski and Holtzman, 1999; Nybo et al., 1999; Mastrangelo et al., 2006). Since we are investigating the A $\beta$  aggregation species that invokes proinflammatory response in our model THP-1 monocytes, it is imperative that we consistently produce an unaggregated starting material. We accomplished this by treating the A $\beta$  with hexafluoroisopropanol (HFIP). HFIP is known to disrupt peptide-peptide interaction thereby disaggregating the pre-formed aggregates (Klein et al., 2004; Findeis, 2007). AFM analysis of our freshly reconstituted A $\beta$ (1-42) samples at 4°C, 25°C and 37°C showed punctate structures that had height measurements of < 2nm, which correspond to monomers (Klein et al., 2004). Moreover, small spherical structures with heights of 2-5 nm were also observed along with the punctuate species. These species were thought to be prefibrillar precursors. These measurements correspond with the findings of Nybo *et al.* (1999) in their investigation of the early stages of A $\beta$ (1-42) fibrillogenesis. They reported the earliest recognizable ultrastructure of A $\beta$  as globular structures with mean height of 4-5 nm. Moreover, these structures appear to fuse and align in a row, which later becomes fibrils (Nybo et al., 1999). Our results showed that further incubation of A $\beta$ (1-42) at 4°C resulted in formation of two populations of fibrils with mean heights of  $4.4 \pm 0.1$  nm (SE) and  $7.9 \pm 0.6$  (SE). These measurements were consistent with that of

Harper and colleagues (1997) when they analyzed the early steps of A $\beta$  formation *in vitro* by AFM. They reported height measurements of  $7.3 \pm 0.53$  nm and  $3.8 \pm 0.43$  nm for their A $\beta$ (1-42) species, which correspond to type-1 and type-2 fibrils, respectively (Harper et al., 1997). Interestingly, these fibrils consistently stimulated our THP-1 cells in producing proinflammatory TNF $\alpha$ . More importantly, the more mature fibrils that we have generated in later A $\beta$  aggregation were ineffective in stimulating a response. This further infers that the intermediate fibrillar aggregation structures of A $\beta$ (1-42) promote TNF $\alpha$  secretion, and not the more mature fibrils.

Unlike A $\beta$ (1-42), our A $\beta$ (1-40) preparations were ineffective in activating our THP-1 cells for TNF $\alpha$  response (Figure 3.6). Morphological analysis of these samples showed a very slow progression of fibril formation. A $\beta$ (1-40) and A $\beta$ (1-42) bear different biochemical properties. Numerous biochemical studies have demonstrated that A $\beta$ (1-42) aggregates much more quickly than A $\beta$ (1-40) (Burdick et al., 1992; Jarrett et al., 1993). Moreover, although there is more A $\beta$ (1-40) that is being secreted, A $\beta$ (1-42) is the major component of senile plaques (Miller et al., 1993), as substantiated by recent findings which showed that high levels of A $\beta$ (1-40) alone do not result in observable amyloid pathology, while low levels of A $\beta$ (1-42) result in a wide range of amyloid pathology (McGowan et al., 2005). These findings, together with our observation, suggest that A $\beta$ (1-42) is a major causative agent in pathogenesis of AD due to its enhanced aggregation properties (Chen and Glabe, 2006).

Although instrumental in surveying the morphology of the species formed during fibril formation, AFM analysis must be combined with other *in vitro* techniques that can further substantiate our finding that intermediate soluble fibrillar structures of A $\beta$  induce

production of proinflammatory products. We have further characterized our A $\beta$  preparation by centrifuging the A $\beta$  samples that were aggregated for 72 or 96 hours at a speed of >100,000g for 1 hour. At this speed, all the rigid fibrillar structures would pellet down and only the soluble oligomers will remain in the solution (Walsh et al., 2002b; Klein et al., 2004; Irvine et al., 2008). After centrifuging the prepared A $\beta$  solution, the supernatant was collected and tested for its ability to invoke proinflammatory response in THP-1 cells. Using AFM, we found that some fibrillar structures were still present in the supernatant after the A $\beta$  samples were spun. Yet, supernatant still invoked a TNF $\alpha$  response (data not shown). Furthermore, the aggregation species in the supernatant was recognized by OC antibody (data not shown). This antibody recognizes fibrils and fibrillar oligomeric species, which are described as small soluble aggregates that are arranged in a similar conformation as in fibrils (Kayed et al., 2007). Taken together, these additional results further confirm that a soluble fibrillar precursor species is the proinflammatory form of A $\beta$ . This project was done in collaboration with Deepa Ajit. Several other biophysical methods were utilized for characterization of our bioactive A $\beta$  species and these additional data are presented in her dissertation.

Although numerous investigations have suggested that large fibrillar forms of A $\beta$  can kill neurons (Kowall et al., 1991; Pike et al., 1993; Lorenzo and Yankner, 1994; Geula et al., 1998), accumulating evidence *in vitro* now demonstrate that the soluble assembly forms of A $\beta$  are the key neurotoxic effectors in AD (Lambert et al., 1998; Walsh et al., 1999; Klein et al., 2004). The presence of soluble oligomeric A $\beta$  assemblies have also been observed from the supernates of AD brain and extracts of amyloid plaques (Roher et al., 1996; Enya et al., 1999; McLean et al., 1999), which suggest that soluble

A $\beta$  could be the earliest mediators of neuronal dysfunction. A $\beta$  is capable of upregulating cytokine and chemokine expression by microglia and monocytes/macrophages (Meda et al., 1995; Yan et al., 1996; Klegeris et al., 1997); however, there are still conflicting discussions and debates as to whether it is the oligomers or fibrils that are more potent neurotoxins. Recent report by Sondag and colleagues (Sondag et al., 2009) showed that proinflammatory cytokine IL-6 production was significantly higher when microglial cells were stimulated with A $\beta$  oligomers than with fibrils. However, their results also showed that A $\beta$  fibrils are more potent in inducing expression of proinflammatory chemokine keratinocyte chemoattractant (KC, a mouse homologue of chemokine IL-8) than the soluble aggregates. These findings demonstrate the ability of A $\beta$  to act as a proinflammatory stimulus in microglia, but more importantly, these results suggest that the expression and release of proinflammatory products may depend on the specific conformation of A $\beta$ . Our present data reveal that cells of the monocytic origin respond to an intermediate soluble yet fibrillar form of A $\beta$ , and not the later more mature fibrils, by secreting the proinflammatory cytokine, TNF $\alpha$ . Taken together, these evidences further accentuate the intricacy involved in studying the association of A $\beta$  aggregation with the proinflammatory response in AD brain.

### 3.4. Bibliography

- Bucciantini M., G. Calloni, F. Chiti, L. Formigli, D. Nosi, C. M. Dobson, M. Stefani. 2004. Prefibrillar amyloid protein aggregates share common features of cytotoxicity. *J Biol Chem.* 279:31374-31382.
- Burdick D., B. Soreghan, M. Kwon, J. Kosmoski, M. Knauer, A. Henschen, J. Yates, C. Cotman, C. Glabe. 1992. Assembly and aggregation properties of synthetic Alzheimer's A4/beta amyloid peptide analogs. *J Biol Chem.* 267:546-554.
- Chen Y. R., C. G. Glabe. 2006. Distinct early folding and aggregation properties of Alzheimer amyloid-beta peptides Abeta40 and Abeta42: stable trimer or tetramer formation by Abeta42. *J Biol Chem.* 281:24414-24422.
- Chromy B. A., R. J. Nowak, M. P. Lambert, K. L. Viola, L. Chang, P. T. Velasco, B. W. Jones, S. J. Fernandez, P. N. Lacor, P. Horowitz, C. E. Finch, G. A. Krafft, W. L. Klein. 2003. Self-assembly of Abeta(1-42) into globular neurotoxins. *Biochemistry.* 42:12749-12760.
- Combs C. K., J. C. Karlo, S. C. Kao, G. E. Landreth. 2001. beta-Amyloid stimulation of microglia and monocytes results in TNFalpha-dependent expression of inducible nitric oxide synthase and neuronal apoptosis. *J Neurosci.* 21:1179-1188.
- Combs C. K., D. E. Johnson, S. B. Cannady, T. M. Lehman, G. E. Landreth. 1999. Identification of microglial signal transduction pathways mediating a neurotoxic response to amyloidogenic fragments of beta-amyloid and prion proteins. *J Neurosci.* 19:928-939.
- Combs C. K., D. E. Johnson, J. C. Karlo, S. B. Cannady, G. E. Landreth. 2000. Inflammatory mechanisms in Alzheimer's disease: inhibition of beta-amyloid-stimulated proinflammatory responses and neurotoxicity by PPARgamma agonists. *J Neurosci.* 20:558-567.
- Enya M., M. Morishima-Kawashima, M. Yoshimura, Y. Shinkai, K. Kusui, K. Khan, D. Games, D. Schenk, S. Sugihara, H. Yamaguchi, Y. Ihara. 1999. Appearance of sodium dodecyl sulfate-stable amyloid beta-protein (Abeta) dimer in the cortex during aging. *Am J Pathol.* 154:271-279.
- Findeis M. A. 2007. The role of amyloid beta peptide 42 in Alzheimer's disease.

Pharmacol Ther. 116:266-286.

- Floden A. M., C. K. Combs. 2006. Beta-amyloid stimulates murine postnatal and adult microglia cultures in a unique manner. *J Neurosci.* 26:4644-4648.
- Frautschy S. A., F. Yang, M. Irrizarry, B. Hyman, T. C. Saido, K. Hsiao, G. M. Cole. 1998. Microglial response to amyloid plaques in APPsw transgenic mice. *Am J Pathol.* 152:307-317.
- Geula C., C. K. Wu, D. Saroff, A. Lorenzo, M. Yuan, B. A. Yankner. 1998. Aging renders the brain vulnerable to amyloid beta-protein neurotoxicity. *Nat Med.* 4:827-831.
- Harper J. D., S. S. Wong, C. M. Lieber, P. T. Lansbury. 1997. Observation of metastable Abeta amyloid protofibrils by atomic force microscopy. *Chem Biol.* 4:119-125.
- Harper J. D., S. S. Wong, C. M. Lieber, P. T. Lansbury, Jr. 1999. Assembly of A beta amyloid protofibrils: an in vitro model for a possible early event in Alzheimer's disease. *Biochemistry.* 38:8972-8980.
- Irvine G. B., O. M. El-Agnaf, G. M. Shankar, D. M. Walsh. 2008. Protein aggregation in the brain: the molecular basis for Alzheimer's and Parkinson's diseases. *Mol Med.* 14:451-464.
- Iversen L. L., R. J. Mortishire-Smith, S. J. Pollack, M. S. Shearman. 1995. The toxicity in vitro of beta-amyloid protein. *Biochem J.* 311 (Pt 1):1-16.
- Jarrett J. T., E. P. Berger, P. T. Lansbury, Jr. 1993. The carboxy terminus of the beta amyloid protein is critical for the seeding of amyloid formation: implications for the pathogenesis of Alzheimer's disease. *Biochemistry.* 32:4693-4697.
- Kayed R., E. Head, F. Sarsoza, T. Saing, C. W. Cotman, M. Nacula, L. Margol, J. Wu, L. Breydo, J. L. Thompson, S. Rasool, T. Gurlo, P. Butler, C. G. Glabe. 2007. Fibril specific, conformation dependent antibodies recognize a generic epitope common to amyloid fibrils and fibrillar oligomers that is absent in prefibrillar oligomers. *Mol Neurodegener.* 2:18.
- Klegeris A., D. G. Walker, P. L. McGeer. 1997. Interaction of Alzheimer beta-amyloid peptide with the human monocytic cell line THP-1 results in a protein kinase C-dependent secretion of tumor necrosis factor-alpha. *Brain Res.* 747:114-121.
- Klein W. L., W. B. Stine, Jr., D. B. Teplow. 2004. Small assemblies of unmodified amyloid beta-protein are the proximate neurotoxin in Alzheimer's disease. *Neurobiol Aging.* 25:569-580.
- Kowalewski T., D. M. Holtzman. 1999. In situ atomic force microscopy study of Alzheimer's beta-amyloid peptide on different substrates: new insights into

- mechanism of beta-sheet formation. *Proc Natl Acad Sci U S A.* 96:3688-3693.
- Kowall N. W., M. F. Beal, J. Busciglio, L. K. Duffy, B. A. Yankner. 1991. An in vivo model for the neurodegenerative effects of beta amyloid and protection by substance P. *Proc Natl Acad Sci U S A.* 88:7247-7251.
- Lambert M. P., A. K. Barlow, B. A. Chromy, C. Edwards, R. Freed, M. Liosatos, T. E. Morgan, I. Rozovsky, B. Trommer, K. L. Viola, P. Wals, C. Zhang, C. E. Finch, G. A. Krafft, W. L. Klein. 1998. Diffusible, nonfibrillar ligands derived from Abeta1-42 are potent central nervous system neurotoxins. *Proc Natl Acad Sci U S A.* 95:6448-6453.
- Lee Y. B., A. Nagai, S. U. Kim. 2002. Cytokines, chemokines, and cytokine receptors in human microglia. *J Neurosci Res.* 69:94-103.
- Lorenzo A., B. A. Yankner. 1994. Beta-amyloid neurotoxicity requires fibril formation and is inhibited by congo red. *Proc Natl Acad Sci U S A.* 91:12243-12247.
- Lue L. F., D. G. Walker, J. Rogers. 2001b. Modeling microglial activation in Alzheimer's disease with human postmortem microglial cultures. *Neurobiol Aging.* 22:945-956.
- Lue L. F., Y. M. Kuo, A. E. Roher, L. Brachova, Y. Shen, L. Sue, T. Beach, J. H. Kurth, R. E. Rydel, J. Rogers. 1999. Soluble amyloid beta peptide concentration as a predictor of synaptic change in Alzheimer's disease. *Am J Pathol.* 155:853-862.
- Lue L. F., R. Rydel, E. F. Brigham, L. B. Yang, H. Hampel, G. M. Murphy, Jr., L. Brachova, S. D. Yan, D. G. Walker, Y. Shen, J. Rogers. 2001a. Inflammatory repertoire of Alzheimer's disease and nondemented elderly microglia in vitro. *Glia.* 35:72-79.
- Mastrangelo I. A., M. Ahmed, T. Sato, W. Liu, C. Wang, P. Hough, S. O. Smith. 2006. High-resolution atomic force microscopy of soluble Abeta42 oligomers. *J Mol Biol.* 358:106-119.
- Masumura M., R. Hata, I. Nishimura, T. Uetsuki, T. Sawada, K. Yoshikawa. 2000. Caspase-3 activation and inflammatory responses in rat hippocampus inoculated with a recombinant adenovirus expressing the Alzheimer amyloid precursor protein. *Brain Res Mol Brain Res.* 80:219-227.
- Mattson M. P. 2004. Pathways towards and away from Alzheimer's disease. *Nature.* 430:631-639.
- May P. C., B. D. Gitter, D. C. Waters, L. K. Simmons, G. W. Becker, J. S. Small, P. M. Robison. 1992. beta-Amyloid peptide in vitro toxicity: lot-to-lot variability. *Neurobiol Aging.* 13:605-607.

- McGowan E., F. Pickford, J. Kim, L. Onstead, J. Eriksen, C. Yu, L. Skipper, M. P. Murphy, J. Beard, P. Das, K. Jansen, M. Delucia, W. L. Lin, G. Dolios, R. Wang, C. B. Eckman, D. W. Dickson, M. Hutton, J. Hardy, T. Golde. 2005. Abeta42 is essential for parenchymal and vascular amyloid deposition in mice. *Neuron*. 47:191-199.
- McLaurin J., D. Yang, C. M. Yip, P. E. Fraser. 2000. Review: modulating factors in amyloid-beta fibril formation. *J Struct Biol*. 130:259-270.
- McLean C. A., R. A. Cherny, F. W. Fraser, S. J. Fuller, M. J. Smith, K. Beyreuther, A. I. Bush, C. L. Masters. 1999. Soluble pool of Abeta amyloid as a determinant of severity of neurodegeneration in Alzheimer's disease. *Ann Neurol*. 46:860-866.
- Meda L., M. A. Cassatella, G. I. Szendrei, L. Otvos, Jr., P. Baron, M. Villalba, D. Ferrari, F. Rossi. 1995. Activation of microglial cells by beta-amyloid protein and interferon-gamma. *Nature*. 374:647-650.
- Miller D. L., I. A. Papayannopoulos, J. Styles, S. A. Bobin, Y. Y. Lin, K. Biemann, K. Iqbal. 1993. Peptide compositions of the cerebrovascular and senile plaque core amyloid deposits of Alzheimer's disease. *Arch Biochem Biophys*. 301:41-52.
- Moore K. J., J. El Khoury, L. A. Medeiros, K. Terada, C. Geula, A. D. Luster, M. W. Freeman. 2002. A CD36-initiated signaling cascade mediates inflammatory effects of beta-amyloid. *J Biol Chem*. 277:47373-47379.
- Murphy G. M., Jr., L. Yang, B. Cordell. 1998. Macrophage colony-stimulating factor augments beta-amyloid-induced interleukin-1, interleukin-6, and nitric oxide production by microglial cells. *J Biol Chem*. 273:20967-20971.
- Nilsson M. R. 2004. Techniques to study amyloid fibril formation in vitro. *Methods*. 34:151-160.
- Nybo M., S. E. Svehag, E. Holm Nielsen. 1999. An ultrastructural study of amyloid intermediates in A beta1-42 fibrillogenesis. *Scand J Immunol*. 49:219-223.
- Pike C. J., A. J. Walencewicz, C. G. Glabe, C. W. Cotman. 1991. In vitro aging of beta-amyloid protein causes peptide aggregation and neurotoxicity. *Brain Res*. 563:311-314.
- Pike C. J., D. Burdick, A. J. Walencewicz, C. G. Glabe, C. W. Cotman. 1993. Neurodegeneration induced by beta-amyloid peptides in vitro: the role of peptide assembly state. *J Neurosci*. 13:1676-1687.
- Ramsden M., L. D. Plant, N. J. Webster, P. F. Vaughan, Z. Henderson, H. A. Pearson. 2001. Differential effects of unaggregated and aggregated amyloid beta protein (1-40) on K(+) channel currents in primary cultures of rat cerebellar granule and cortical neurones. *J Neurochem*. 79:699-712.

- Roher A. E., M. O. Chaney, Y. M. Kuo, S. D. Webster, W. B. Stine, L. J. Haverkamp, A. S. Woods, R. J. Cotter, J. M. Tuohy, G. A. Krafft, B. S. Bonnell, M. R. Emmerling. 1996. Morphology and toxicity of Abeta-(1-42) dimer derived from neuritic and vascular amyloid deposits of Alzheimer's disease. *J Biol Chem.* 271:20631-20635.
- Selkoe D. J. 2001. Alzheimer's disease: genes, proteins, and therapy. *Physiol Rev.* 81:741-766.
- Sondag C. M., G. Dhawan, C. K. Combs. 2009. Beta amyloid oligomers and fibrils stimulate differential activation of primary microglia. *J Neuroinflammation.* 6:1.
- Stalder M., A. Phinney, A. Probst, B. Sommer, M. Staufenbiel, M. Jucker. 1999. Association of microglia with amyloid plaques in brains of APP23 transgenic mice. *Am J Pathol.* 154:1673-1684.
- Stine W. B., Jr., K. N. Dahlgren, G. A. Krafft, M. J. LaDu. 2003. In vitro characterization of conditions for amyloid-beta peptide oligomerization and fibrillogenesis. *J Biol Chem.* 278:11612-11622.
- Stine W. B., Jr., S. W. Snyder, U. S. Lador, W. S. Wade, M. F. Miller, T. J. Perun, T. F. Holzman, G. A. Krafft. 1996. The nanometer-scale structure of amyloid-beta visualized by atomic force microscopy. *J Protein Chem.* 15:193-203.
- Taylor B. M., R. W. Sarver, G. Fici, R. A. Poorman, B. S. Lutzke, A. Molinari, T. Kawabe, K. Kappenman, A. E. Buhl, D. E. Epps. 2003. Spontaneous aggregation and cytotoxicity of the beta-amyloid Abeta1-40: a kinetic model. *J Protein Chem.* 22:31-40.
- Udan M. L., D. Ajit, N. R. Crouse, M. R. Nichols. 2008. Toll-like receptors 2 and 4 mediate Abeta(1-42) activation of the innate immune response in a human monocytic cell line. *J Neurochem.* 104:524-533.
- Walsh D. M., I. Klyubin, J. V. Fadeeva, M. J. Rowan, D. J. Selkoe. 2002b. Amyloid-beta oligomers: their production, toxicity and therapeutic inhibition. *Biochem Soc Trans.* 30:552-557.
- Walsh D. M., I. Klyubin, J. V. Fadeeva, W. K. Cullen, R. Anwyl, M. S. Wolfe, M. J. Rowan, D. J. Selkoe. 2002a. Naturally secreted oligomers of amyloid beta protein potently inhibit hippocampal long-term potentiation in vivo. *Nature.* 416:535-539.
- Walsh D. M., D. M. Hartley, Y. Kusumoto, Y. Fezoui, M. M. Condron, A. Lomakin, G. B. Benedek, D. J. Selkoe, D. B. Teplow. 1999. Amyloid beta-protein fibrillogenesis. Structure and biological activity of protofibrillar intermediates. *J Biol Chem.* 274:25945-25952.

- Yan S. D., X. Chen, J. Fu, M. Chen, H. Zhu, A. Roher, T. Slattery, L. Zhao, M. Nagashima, J. Morser, A. Migheli, P. Nawroth, D. Stern, A. M. Schmidt. 1996. RAGE and amyloid-beta peptide neurotoxicity in Alzheimer's disease. *Nature*. 382:685-691.
- Yates S. L., L. H. Burgess, J. Kocsis-Angle, J. M. Antal, M. D. Dority, P. B. Embury, A. M. Piotrkowski, K. R. Brunden. 2000. Amyloid beta and amylin fibrils induce increases in proinflammatory cytokine and chemokine production by THP-1 cells and murine microglia. *J Neurochem*. 74:1017-1025.
- Zambrzycka A., R. P. Strosznajder, J. B. Strosznajder. 2000. Aggregated beta amyloid peptide 1-40 decreases Ca<sup>2+</sup>- and cholinergic receptor-mediated phosphoinositide degradation by alteration of membrane and cytosolic phospholipase C in brain cortex. *Neurochem Res*. 25:189-196.

## 4 THE ROLE OF TOLL-LIKE RECEPTORS IN AMYLOID BETA(1-42) ACTIVATION OF THE INNATE IMMUNE RESPONSE

### 4.1 Introduction

The brains of individuals with Alzheimer's disease contain reactive microglia and these immune cells cluster at sites of A $\beta$  deposition (Akiyama et al., 2000; Perry et al., 2003). Microglial activation is always associated with production of inflammatory products and mediators, which include complement proteins, cytokines and chemokines (Das and Potter, 1995; Yates et al., 2000). Extensive and compelling evidence shows that these activated microglia surround A $\beta$  plaques (Miyazono et al., 1991; Frautschy et al., 1998; Apelt and Schliebs, 2001; Wegiel et al., 2001) and *in vitro* activation of microglia by A $\beta$  results in the production and secretion of proinflammatory molecules such as reactive oxygen species, cytokines and neurotoxins (Griffin et al., 1989; Venters et al., 1999; Akiyama et al., 2000; Yates et al., 2000; Combs et al., 2001). However, it was difficult to ascertain whether A $\beta$ -induced inflammation contributes to or causes AD. Several investigators have reported that the use of anti-inflammatory agents or non-steroidal anti-inflammatory drugs (NSAIDs) significantly reduced the risk for AD (McGeer et al., 1996; Stewart et al., 1997; Rogers, 2008). These evidences strongly support the concept that chronic inflammatory process contributes to AD progression.

Inflammation is considered to be a double-edged sword: it may be useful when

controlled, but deadly when it is not (Akiyama et al., 2000; Lai et al., 2006). Over the years, investigators have tried to answer the mechanism by which A $\beta$  causes heightened expression of proinflammatory products in microglia. Some groups reported several inflammation-related receptors present in the microglia as key players in A $\beta$ -induced microglial activation and inflammatory response. These include receptors for advanced glycosylated end-products (RAGE) (Yan et al., 1996), scavenger receptor class A (El Khoury et al., 1996; Paresce et al., 1996), B-class scavenger receptor CD36, integrin associated protein/CD47 and  $\alpha_6\beta_1$ -integrin receptor complex (Bamberger et al., 2003), as well as calcium-, protein kinase C-, and tyrosine kinase- dependent second messenger pathways (Klegeris et al., 1997; Combs et al., 1999; Yates et al., 2000). Recent studies by Fassbender and colleagues demonstrated that fibrillar A $\beta$  interacts and binds with the bacterial lipopolysaccharide (LPS) receptor, CD14 (Fassbender et al., 2004). Moreover, Bate *et al* reported that the subsequent killing of A $\beta$ -damaged neurons by microglia is a CD14 dependent process (Bate et al., 2004; Heneka and O'Banion, 2007). Furthermore, Liu *et al* demonstrated a direct role of CD14 in fibrillar A $\beta$ (1-42) phagocytosis, and an observed elevation of CD14 immunostaining in AD brains compared with controls (Liu et al., 2005). These evidences connecting CD14 with A $\beta$  strongly suggest that innate immunity is related to AD pathology.

A wealth of data now indicates that CD14 interacts with TLR4 and TLR2 (Chapter 1 review). In this study, we aspired to investigate and identify the transmembrane TLR(s) that may be involved in the induction of innate immune response by A $\beta$ (1-42). For this investigation, we utilized cell systems including THP-1 monocytes as a model of primary microglia (Chapter 3 review), as well as human embryonic kidney

(HEK293) cells. We propose that TLR4 and TLR2 are highly involved in A $\beta$ (1-42)-induced proinflammatory cytokine production in these mammalian cell model systems.

## 4.2 Results

### 4.2.1 Mammalian cell model system: THP-1 monocytes

#### 4.2.1.1 Toll-like receptor ligands activate the proinflammatory response in THP-1 monocytes

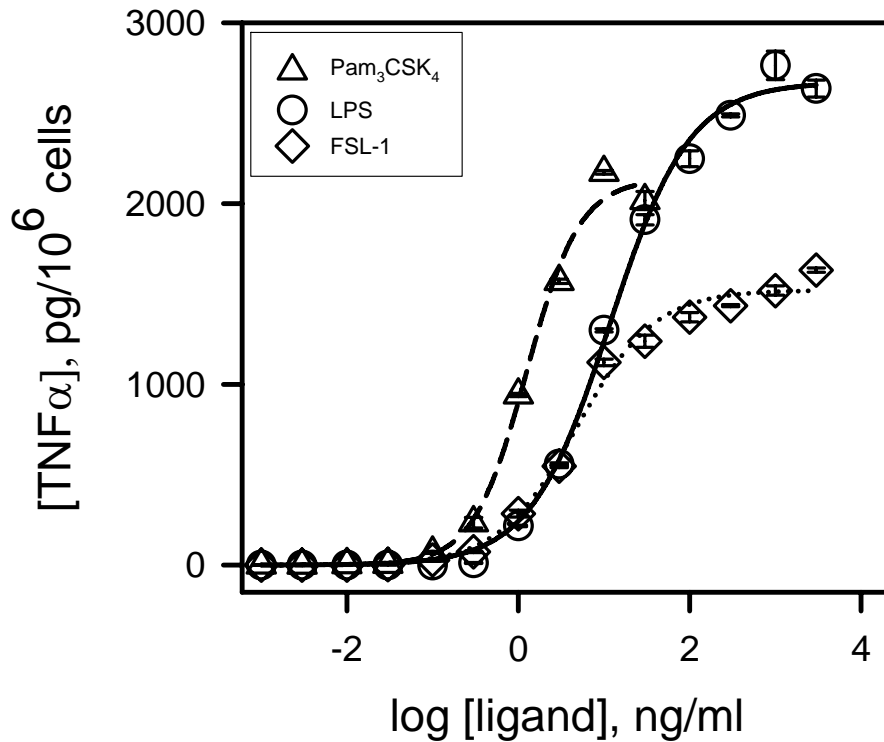
The interaction of LPS with TLR4 is the best studied model of innate immunity (Aderem and Ulevitch, 2000). Several groups have extensively analyzed LPS-mediated TLR4 downstream signaling for induction of proinflammatory response (Poltorak et al., 1998; Hoshino et al., 1999; Qureshi et al., 1999). Aside from TLR4, numerous studies also focused on TLR2 due to its capability to recognize a broad range of ligands (Chapter 1 review; (Albiger et al., 2007)). We started our investigation by first testing whether THP-1 monocytes produce TNF $\alpha$  upon induction with known TLR agonists LPS (TLR4), synthetic tripalmytoyl cysteinyl seryl tetralysine Pam<sub>3</sub>CSK<sub>4</sub> (TLR2/1) and synthetic diacylated lipopeptide FSL (TLR2/6). THP-1 monocytes were treated with increasing concentration of the agonists, and incubated for 6 hours, as discussed in Methods. Supernatants were collected after incubation, and secreted TNF $\alpha$  was measured by ELISA. TNF $\alpha$  measurements revealed a concentration-dependent response for all TLR agonists (Figure 4.1). Fitting the data to a sigmoidal three-parameter equation produced

EC<sub>50</sub> values of 5 ng/ml for ultrapure K12 LPS, 1 ng/ml for Pam<sub>3</sub>CSK<sub>4</sub> and 7 ng/ml FSL-1. For succeeding experiments, we decided to utilize the following concentrations: 10 ng/ml LPS, 1 ng/ml Pam<sub>3</sub>CSK<sub>4</sub> and 1 or 3 ng/ml FSL-1. We further extended our investigation by determining the best condition for maximal TNF $\alpha$  production by our TLR agonists. We found highest TNF $\alpha$  response for LPS, Pam<sub>3</sub>CSK<sub>4</sub> and FSL-1 when cells were exposed to these agonists for 6 hours (Figure 3.3, FSL data not shown). These data confirmed the responsiveness of THP-1 monocytes to known TLR ligands, and is particularly useful in our investigation of A $\beta$ -TLR interaction since these agonists can be used in later experiments as positive controls.

#### 4.2.1.2 Amyloid beta(1-42) is devoid of any contamination

We have previously shown that soluble fibrillar A $\beta$ (1-42) activates THP-1 monocytes for proinflammatory response (Chapter 3). In the previous report, we have demonstrated that the maximal TNF $\alpha$  response was achieved when 100  $\mu$ mol/L A $\beta$ (1-42) was allowed to aggregate at 4°C between 48 and 96 hours. Because of this result, the same conditions were utilized for the A $\beta$  samples in this study. For every analysis, corresponding AFM images and height analyses were performed. Height measurements were in accord with the soluble fibrillar A $\beta$ (1-42), discussed in chapter 3.

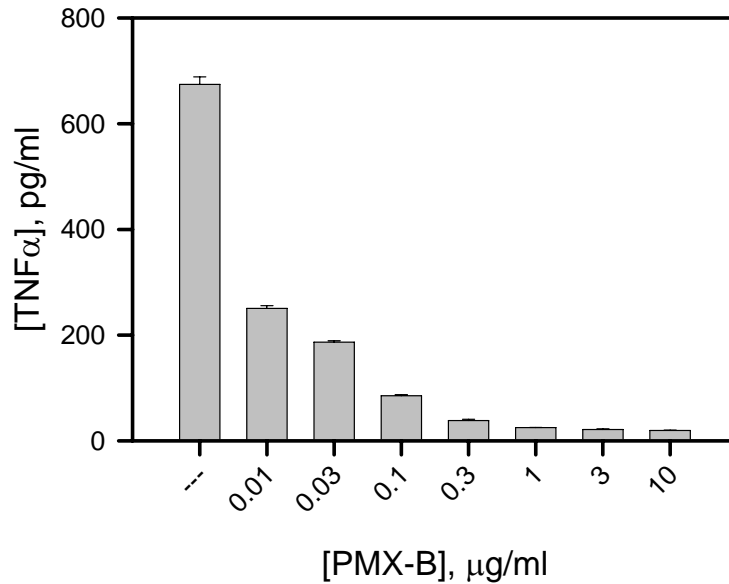
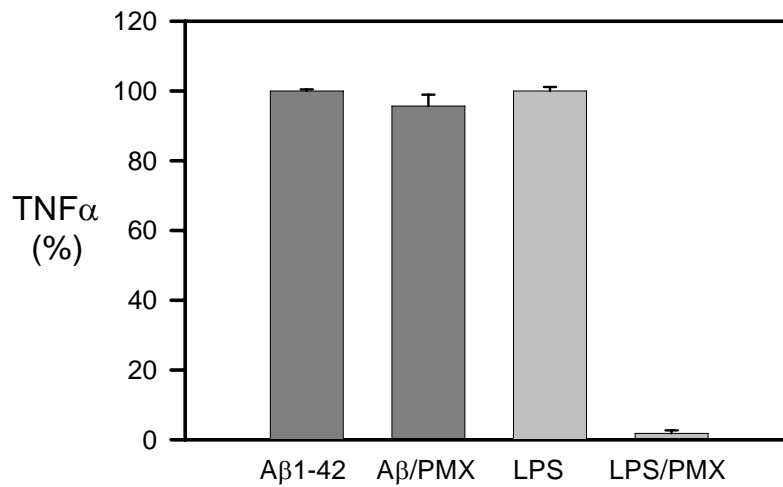
Bacterial LPS utilizes TLR4 for activation of TLR downstream signaling that culminates in production of proinflammatory cytokines and chemokines such as TNF $\alpha$ . Because our main objective is to identify the TLR that plays a functional role in A $\beta$ -



**Figure 4.1. Known TLR agonists induce TNF $\alpha$  production in a dose-dependent manner.** THP-1 monocytes were stimulated with increasing concentration of ultrapure K12 LPS (circles), synthetic Pam<sub>3</sub>CSK<sub>4</sub> (triangles) or synthetic FSL-1 (diamonds) for 6 hours, as described in Methods. The same volume of water was added to the cells as a control in the absence of agonist. After stimulation, secreted TNF $\alpha$  in the supernatants was analyzed by ELISA. Error bars represent standard error for three measurements. Data was fit to sigmoidal three-parameter equation using SigmaPlot graphing program.

induced inflammatory response, we have to ensure that our A $\beta$ (1-42) is devoid of any contaminating bacterial lipopolysaccharide that might interfere with the proper interpretation of our results. We also wanted to confirm that the secreted TNF $\alpha$  observed in THP-1 monocytes was due to A $\beta$  as a proinflammatory stimulus, and not due to traces of contaminating bacterial LPS. To rule out the presence of traces of LPS in our A $\beta$ (1-42) samples, we tested our A $\beta$  preparation using the compound Polymyxin-B sulfate (PMX-B). PMX-B is a cationic decapeptide that binds to lipid A moiety of LPS and neutralizes its pathogenicity and prevents LPS-induced cytokine production (Pristovsek and Kidric, 1999). To determine if PMX-B can neutralize TNF $\alpha$  secretion by 10 ng/ml of ultrapure K12 LPS, THP-1 monocytes were pretreated with medium alone, or with increasing concentration of PMX-B for 30 minutes. After preincubation, cells were stimulated with 10 ng/ml LPS for 6 hours prior to TNF $\alpha$  measurement. PMX-B effectively neutralized the proinflammatory effect of LPS in a dose-dependent manner, with a 2-fold reduction of LPS signal for as low as 10 ng/ml of PMX-B (Figure 4.2a). This data implies that PMX-B is an effective tool in neutralizing LPS response and thus, can be used to test for LPS contamination in our A $\beta$  samples. Using XTT proliferation assay, it was found that PMX-B alone did not have any toxic effect on our THP-1 monocytes (data not shown).

Next, we pretreated the THP-1 cells with 0.1  $\mu$ g/ml of PMX-B for 30 minutes, as described previously, prior to THP-1 stimulation with 15  $\mu$ mol/L of A $\beta$ (1-42). Figure 4.2b shows different profiles for PMX-pretreated A $\beta$  and PMX-pretreated LPS (Udan et al., 2008). PMX-B almost completely abrogated the K12 LPS signal (LPS/PMX % response of  $1.85 \pm 0.84$ , as compared to  $100 \pm 1.1$  % response by LPS alone), but with little or no effect on A $\beta$  signal (A $\beta$ /PMX % response of  $95.7 \pm 3.25$  compared to  $100 \pm$

**A****B**

**Figure 4.2. PMX-B is a powerful tool for ruling out the presence of small traces of contaminating bacterial LPS.** (A) The LPS proinflammatory response was neutralized by PMX-B in a dose-dependent manner. THP-1 were preincubated with increasing concentrations of PMX-B prior to stimulation with 10 ng/ml LPS, as described in Methods. Error bars represent standard error for three experiments. (B) PMX-B does not have an effect on Aβ(1-42) proinflammatory response. THP-1 cells were treated with 15 μM Aβ or 10 ng/ml LPS in the presence or absence of 0.1 μg/ml of PMX-B. Results are presented as % TNFα of the Aβ or K12 LPS without PMX-B. Error bars represent standard errors for 15 trials in five separate experiments. Actual TNFα levels averaged 328 pg/ml for Aβ and 859 pg/ml for K12 LPS.

0.43 % response by A $\beta$  without PMX-B). This signifies that our A $\beta$  preparations are devoid of contaminating LPS. Moreover, the results imply that TNF $\alpha$  production in THP-1 is mainly due to A $\beta$  as a proinflammatory stimulus, and not because of possible traces of LPS in the A $\beta$  preparation. For subsequent experiments involving A $\beta$ , A $\beta$ /PMX-B and LPS/PMX-B samples were included for continual monitoring of trace contamination. Some results showed greater than 10% reduction in A $\beta$ - induced TNF $\alpha$  response when pretreated with PMX-B, although XTT cell proliferation experiments indicated that our A $\beta$  samples are devoid of any bacterial contamination (data not shown). For accurate interpretation of results, those experiments were not included in the study of A $\beta$ -TLR interaction.

#### 4.2.1.3 Toll-like receptor antibody neutralization assay was effective in blocking the activity of known TLR agonists bacterial LPS and synthetic Pam<sub>3</sub>CSK<sub>4</sub>

We have developed a TLR antibody neutralization assay to aid us in investigating which transmembrane TLR mediates A $\beta$ -induced immune response. We initially tested the effectiveness of this assay on our known TLR ligands, bacterial LPS (TLR4) and synthetic Pam<sub>3</sub>CSK<sub>4</sub> (TLR2). THP-1 cells were preincubated with 10  $\mu$ g/ml TLR antibodies prior to addition of either 10 ng/ml *E. coli* 026.B6 LPS or 1 ng/ml Pam<sub>3</sub>CSK<sub>4</sub>. TLR4 neutralization lowered the *E. coli* 026.B6 LPS response by almost 79% (% response of  $29.3 \pm 1.56$  compared to  $100 \pm 2.9$  of LPS alone) (Figure 4.3, gray bars). Surprisingly, TLR2 also had a significant effect on our LPS response. Antibody blockade of TLR2 considerably decreased the % LPS response to  $33.2 \pm 0.25$ . This result implies

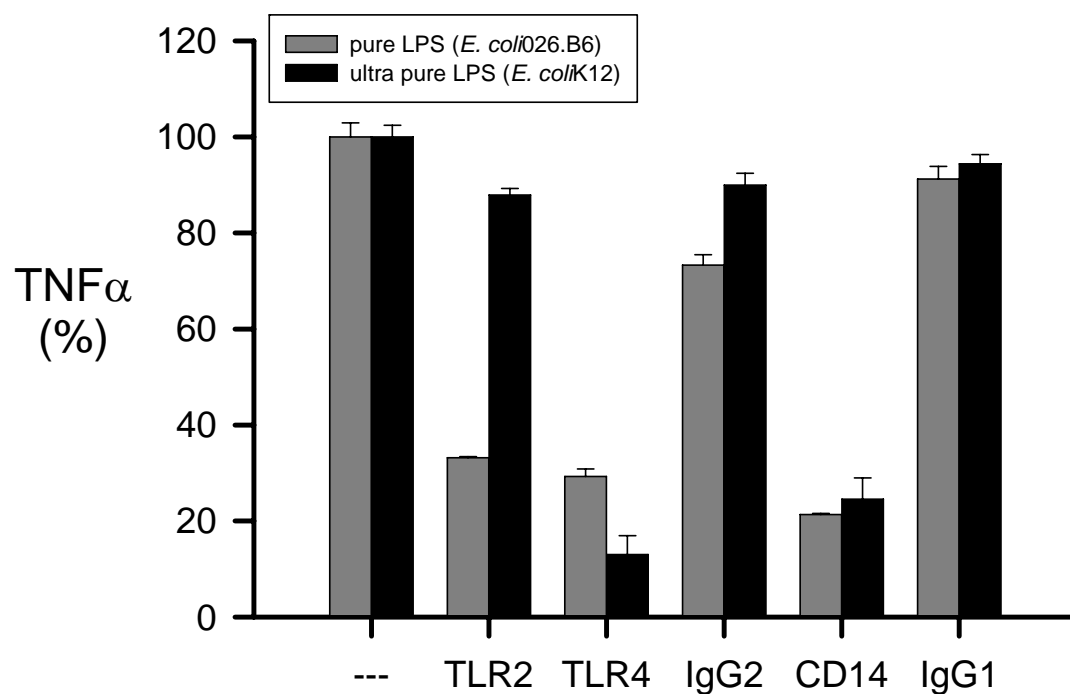


**Figure 4.3. Toll-like receptor (TLR) neutralization of bacterial lipopolysaccharide.** THP-1 cells were pre-incubated with 10  $\mu$ g/ml of TLR antibodies (eBioscience) or mouse isotype controls (IgG2 isotype control for TLR2 and TLR4 antibodies, IgG1 isotype control for CD14) for 1 hour prior to addition of 10 ng/ml LPS, as described in methods. Experiments done several times, and representative graph is shown. Pure LPS (*E. coli* 026.B6) (gray bars) utilized both TLR4 and TLR2 in secretion of TNF $\alpha$ . TLR2 conferred sensitivity to LPS may be due to contaminating bacterial lipoproteins. Repurified LPS preparation (*E. coli* K12) abolished the effect of TLR2 on LPS-induced TNF $\alpha$  response. Error bars are SE of three measurements.

that TLR2 lowered the TNF $\alpha$  response by almost 70%, similar to the effect of TLR4 neutralization. Because substantial evidences show that LPS utilizes TLR4 for downstream activation of innate immunity, this finding was unexpected. Several investigators reported that TLR2-conferred sensitivity to LPS may be due to contaminating lipoproteins (TLR2 agonists) in commercially available LPS preparations (Kielian, 2006), and repurifying the LPS preparations and removal of trace amounts of TLR2 agonists abated the effect of TLR2 in LPS activation (Hirschfeld et al., 2000). Because of this possibility, we repeated the TLR neutralization using a commercially available repurified, ultrapure K12 LPS. This LPS preparation has undergone stringent repurification by double phenol extraction of a 0.2% triethylamine/0.5% deoxycholate aqueous phase which ensures removal of contaminating lipoproteins that signal through TLR2 ((Hirschfeld et al., 2000), InvivoGen.com). Our result (Figure 4.3, black bars) demonstrated a TLR4-, but not TLR2-, dependent LPS-induced TNF $\alpha$  production (% TNF $\alpha$  response of  $13.0 \pm 3.4$  for TLR4,  $87.9 \pm 1.4$  for TLR2). The TLR2 and TLR4 isotype control IgG2 had 10% inhibitory effect (% response of  $90.0 \pm 2.4$ ) on LPS response; this denotes that the 10% inhibitory effect observed on K12 LPS response when TLR2 was neutralized was not statistically significant.

Pam<sub>3</sub>CSK<sub>4</sub> utilizes TLR2 in activation of the innate immune response. This was clearly demonstrated by an almost complete eradication of Pam<sub>3</sub>CSK<sub>4</sub>- induced secreted TNF $\alpha$  when TLR2 was blocked by 10  $\mu$ g/ml of the TLR2 antibody (Figure 4.4, gray bar; % response of  $4.2 \pm 0.76$ ) (Udan et al., 2008). As expected, TLR4 is not being utilized by Pam<sub>3</sub>CSK<sub>4</sub> for TNF $\alpha$  secretion ( $80.9 \pm 1.4$  % TNF $\alpha$  response). Although there is a 20% inhibitory effect of TLR4 neutralization in Pam<sub>3</sub>CSK<sub>4</sub> response, the value was not

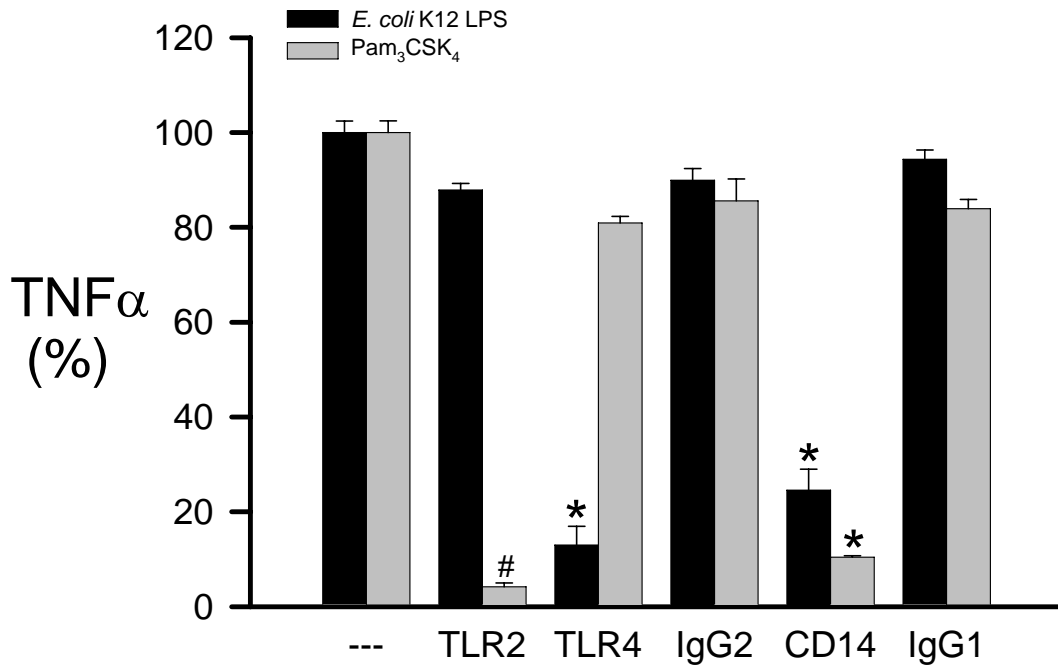


**Figure 4.4 TLR antibody neutralization of bacterial lipopolysaccharide and Pam<sub>3</sub>CSK<sub>4</sub>.** THP-1 monocytes were pre-incubated with 10  $\mu$ g/ml of TLR antibodies (eBioscience) or isotype controls (IgG2 for TLR2 and TLR4 antibodies; IgG1 for CD14) as described in Methods, prior to treatment with either 10 ng/ml of ultrapure *E. coli*K12 LPS (black bars) or 1 ng/ml Pam<sub>3</sub>CSK<sub>4</sub> (gray bars). Secreted TNF $\alpha$  was measured by ELISA. Results are presented as % TNF $\alpha$  of LPS or Pam<sub>3</sub>CSK<sub>4</sub> pre-incubated with phosphate-buffered saline (PBS) medium. Actual TNF $\alpha$  levels were 216 pg/ml for LPS and 257 pg/ml for Pam<sub>3</sub>CSK<sub>4</sub>. Error bars for LPS data correspond to SE for six trials (2 experiments), and three trials, one experiment for Pam<sub>3</sub>CSK<sub>4</sub> data. A Student's t-test was used to calculate the significance between individual TLR and their respective isotype IgG controls ( \*p < 0.001 and # p < 0.0025)

statistically different ( $p < 0.25$ ) from the TLR2 IgG2 isotype control (% response of  $85.6 \pm 4.6$ ).

This experiment also demonstrated the necessity of the accessory protein CD14 for ultrapure LPS- and Pam<sub>3</sub>CSK<sub>4</sub>- induced activation of downstream TLR signaling. K12 LPS response was significantly attenuated by CD14 antibody, as shown by 75% inhibition. This result was significantly different from the CD14 isotype control IgG1 which inhibited only 6% of the K12 LPS response. Likewise, neutralization with the CD14 antibody blocked 90% of Pam<sub>3</sub>CSK<sub>4</sub> signal. The data presented here indicates that the developed TLR neutralization assay is sensitive in specific recognition of TLR agonists and may be a tool for investigating A $\beta$ -TLR interaction.

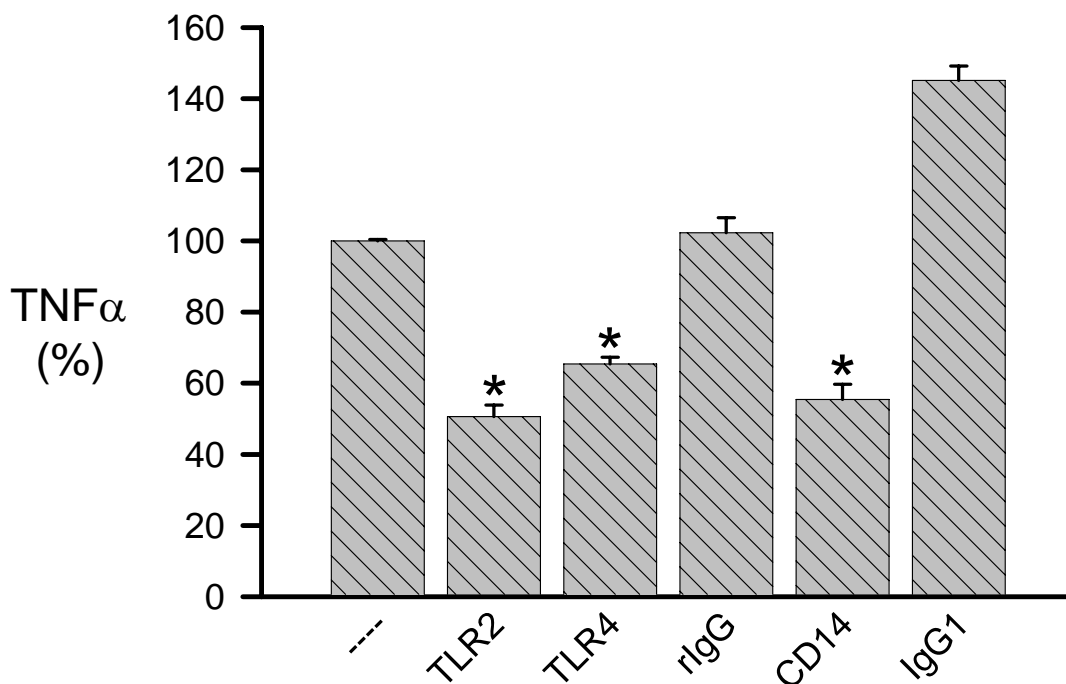
#### 4.2.1.4 TLR2 and TLR4 play a role in fibrillar A $\beta$ (1-42)-induced TNF $\alpha$ response in THP-1 monocytes

TLR neutralization was performed to clarify which TLR is being utilized by fibrillar A $\beta$  for TNF $\alpha$  production. As described in methods, THP-1 cells were incubated with 10  $\mu$ g/ml of TLR antibodies or isotype control for 1 hour prior to stimulation with 15  $\mu$ mol/L of A $\beta$ (1-42). Our results demonstrated the importance of TLRs and TLR accessory protein CD14 for A $\beta$ -induced activation of innate immune response. As shown in Figure 4.5, CD14 neutralization significantly reduced A $\beta$  response by 62%, relative to its isotype control IgG1 (Udan et al., 2008). This result suggests that A $\beta$  utilizes CD14 for TNF $\alpha$  production, which was in accord with the previous report (Fassbender et al., 2004). Surprisingly, both TLR2 and TLR4 neutralization also diminished A $\beta$ - induced

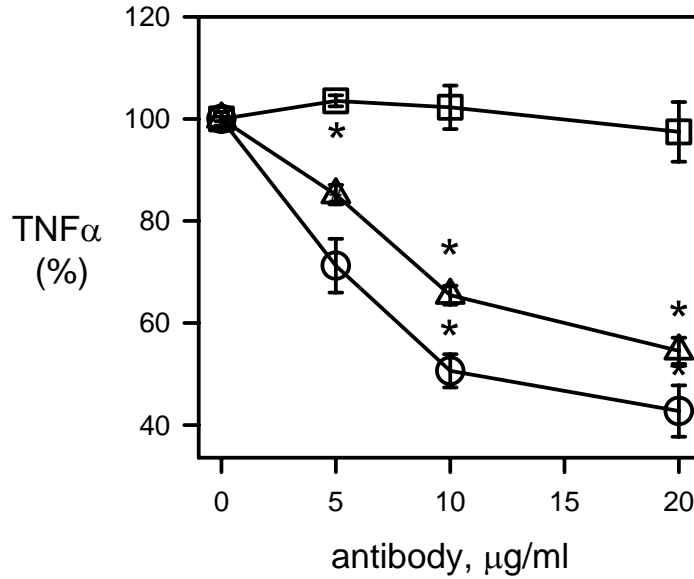
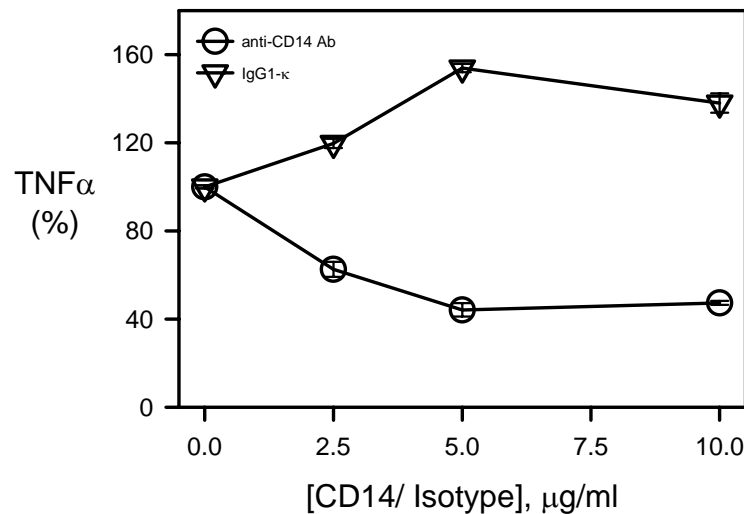
TNF $\alpha$  response. TLR4 blockade decreased the TNF $\alpha$  response by 35% (% response of  $65.45 \pm 1.87$ ). More surprisingly, TLR2 antibody was more effective in neutralizing the A $\beta$  response, as evidenced by 50% attenuation of TNF $\alpha$  signal (% response of  $50.62 \pm 3.26$ ). Using Student's t-test, these results were significantly different from IgG control ( $p < 0.001$ ).

The TLR2 and TLR4 antibodies (InvivoGen) that were used in this experiment were different from the ones used for TLR neutralization of LPS and Pam<sub>3</sub>CSK<sub>4</sub>. This is due to a consistent significant attenuation of A $\beta$  response by IgG2 control used in LPS and Pam<sub>3</sub>CSK<sub>4</sub> studies. Nevertheless, this different set of TLR antibodies was still effective in blocking TLR. Moreover, a consistent 20 – 30% increase in A $\beta$  response was observed when THP-1 monocytes were pre-treated with 10 to 20  $\mu\text{g/ml}$  of CD14 isotype control, IgG1 (Figure 4.5 and 4.6b). This consistent stimulation may have cancelled out some of the effectiveness of anti-CD14 neutralization. Because of the IgG effect, it was not possible to compare the differences between TLR2, TLR4 and CD14 antibody neutralizing ability of A $\beta$  response.

The A $\beta$ -induced TNF $\alpha$  response was neutralized by TLR antibodies in a dose-dependent manner (Figure 4.6 a and b) (Udan et al., 2008). The effectiveness of TLR antibodies in neutralizing A $\beta$  response was clearly demonstrated when THP-1 cells were pre-treated with as low as 5  $\mu\text{g/ml}$  TLR antibodies. About 29% reduction of TNF $\alpha$  response was observed when THP-1 cells were treated with 2.5  $\mu\text{g/ml}$  of TLR2 antibody, and 15% reduction of TNF $\alpha$  response for TLR neutralization. Increasing the concentration of the TLR antibodies augmented the effectiveness of neutralization, as depicted by a more dramatic decrease in TNF $\alpha$  response. A boost of TLR2 or TLR4



**Figure 4.5. TLR2, TLR4 and CD14 play an active role in A $\beta$ -induced innate immune response activation.** THP-1 monocytes were pre-incubated with 10  $\mu$ g/ml of TLR2, TLR4 (InvivoGen), CD14 (eBioscience) antibodies, or IgG isotype controls, as described in Methods. Isotype controls were rat IgG (Sigma) for TLR2 and TLR4, and mouse IgG1 (eBioscience) for CD14. After incubation, THP-1 cells were stimulated with 15  $\mu$ M of A $\beta$ (1-42) for 6 hours. TNF $\alpha$  was measured using ELISA. Results are expressed as % TNF $\alpha$  of A $\beta$  response treated with phosphate buffered saline (PBS) medium. 20-30% stimulation of A $\beta$  response was consistently observed for IgG1. Actual TNF $\alpha$  levels induced by A $\beta$  alone averaged 328 pg/ml. Error bars correspond to SE for 12 trials (four separate experiments) for TLR2, TLR4 and rat IgG, and six trials (2 experiments) for CD14 and mouse IgG1. A Student's t-test was used to calculate the significance between individual TLR and their respective isotype IgG controls (\*p < 0.0001). rIgG; rat IgG

**A****B**

**Figure 4.6. Dose-dependent neutralizing ability of TLR antibodies against A $\beta$ (1-42).** THP-1 cells were pre-incubated for 1 hour with increasing concentrations of TLR antibodies or their isotype controls, as described in the Methods, prior to stimulation with 15  $\mu$ M of A $\beta$ (1-42). After 6 hours post-stimulation, TNF $\alpha$  was measured using ELISA. Results are expressed as % TNF $\alpha$  of A $\beta$  response treated with phosphate buffered saline (PBS) medium. (A) TLR2 (circles) and TLR4 (triangles) antibodies (InvivoGen) blocked A $\beta$  response in a dose-dependent manner. Rat IgG (rIgG, squares) is the isotype control for TLR2 and TLR4. The 10  $\mu$ g/ml TLR and IgG result are reproduced from Figure 4.5. Standard errors are SE for n = 3 trials (5  $\mu$ g/ml) and n = 6 trials (20  $\mu$ g/ml). A Student's t-test was used to calculate the significance between individual TLR and their respective isotype rat IgG (\*p < 0.0001). Actual TNF $\alpha$  was the same as Figure 4.5 (B) CD14 (circles) antibody (eBioscience) also efficiently blocked A $\beta$  response in a dose-dependent manner. Error bars are SE of three trials. Actual TNF $\alpha$  of A $\beta$  alone averaged 170 pg/ml

concentration from 10  $\mu\text{g/ml}$  to 20  $\mu\text{g/ml}$  further lowered the  $\text{TNF}\alpha$  response by 10%. On the other hand, the neutralizing effect of CD14 antibody on  $\text{A}\beta$  appeared to plateau at  $\sim 45 \pm 3.0\%$  starting at 5  $\mu\text{g/ml}$ . The TLR2 and TLR4 isotype control rat IgG did not have an effect on  $\text{A}\beta$  response. However, a consistent stimulation of the response was observed for CD14 isotype control mouse IgG1. Moreover, similar with the results for neutralization using 10  $\mu\text{g/ml}$  TLR antibodies, TLR2 antibody was more effective in blocking  $\text{A}\beta$  response than TLR4. Nevertheless, the results presented here suggest that  $\text{A}\beta$  is utilizing multiple toll receptors for the activation of innate immune response. More importantly, TLR2 and TLR4 play an active role in  $\text{A}\beta$ -induced production of proinflammatory products. Noticeably, a complete abrogation of the  $\text{A}\beta$ -induced immune response was not observed when higher concentrations of TLR antibodies were used. Individual TLR neutralization using 20  $\mu\text{g/ml}$  antibodies caused only 50-70% inhibition. A number of reasons may explain this result. First, previous reports suggested that  $\text{A}\beta$  fibrils also interact with other receptors for cellular activation and neurotoxicity like scavenger receptors, RAGE, CD11b/CD18receptor, CD36/ $\alpha_6\beta_1$ -integrin/CD47 multireceptor complex or complement factor C1 (Bamberger et al., 2003; Fassbender et al., 2004). Thus, to explain the remaining unblocked activity, it is possible that  $\text{A}\beta$  utilized these other receptors when TLRs were made unavailable.

A second possibility may be that since TLR2 and TLR4 play a role in  $\text{A}\beta$  response, one receptor may compensate for the other when one is inaccessible. We tested this hypothesis by using a combination of TLR2, TLR4 and CD14 antibodies to investigate whether neutralizing multiple receptors will further enhance the reduction of  $\text{TNF}\alpha$  response as compared to individual receptor blockade. For this study, we lowered

our TLR antibody concentration to 5  $\mu\text{g/ml}$  to better observe the effect of combination antibody treatment. Moreover, we also supplemented each cell treatment with up to 10  $\mu\text{g/ml}$  of rat IgG or 5  $\mu\text{g/ml}$  of mouse IgG1 to match the triple combination TLR2/TLR4/CD14 neutralization with isotype control amounts. Since we have used a lower antibody concentration, and individual TLR neutralization was supplemented with IgG isotype controls, it is not possible to directly compare the results that we obtained in this experiment with that in Figure 4.5 and Figure 4.6. This experiment was performed numerous times and the results are shown in Figure 4.7 (Udan et al., 2008). As shown, the A $\beta$ -induced TNF $\alpha$  response was only slightly reduced when individual TLRs were blocked with 5  $\mu\text{g/ml}$  of the antibody (% response of  $92.6 \pm 0.72$ ,  $85.2 \pm 3.73$  and  $98.52 \pm 1.57$  for TLR2, TLR4 and CD14, respectively). These individual TLR neutralization results were not statistically different from that of the mouse IgG1/rat IgG control (% response of  $95.2 \pm 2.7$ ). As discussed earlier (Figures 4.5 and 4.6), a consistent enhancement of A $\beta$  response was observed when cells were treated with mouse IgG1 control. Since the individual TLR2 and TLR4 (and all other samples that do not contain CD14) were supplemented with mouse IgG1 to match the concentration of the triple combination TLR2/TLR4/CD14, this may have masked some of the TLR blocking activity. A double combination of TLR2/CD14 and TLR4/CD14 antibody neutralization was better in lowering the A $\beta$  response compared to the individual TLR blockade (34.4% and 35.5% reduction, respectively). The neutralizing activity of TLR2/CD14 and TLR4/CD14 compared to that of mouse IgG1/ rat IgG control was significantly different ( $p < 0.001$ ). These comparable results of TLR2/CD14 or TLR4/CD14 blockade suggest that an overlap to some extent of A $\beta$  interaction with both TLRs and CD14 may be

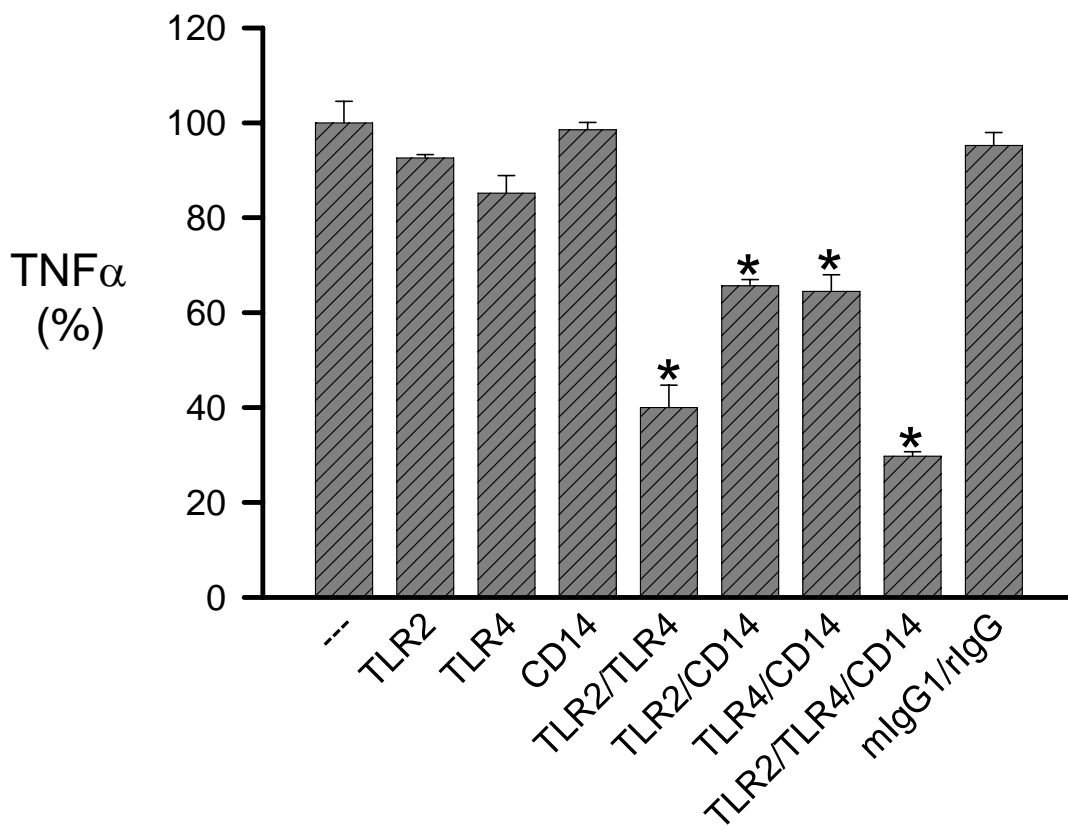


**Figure 4.7. Combination TLR antibody neutralization of A $\beta$ (1-42)-induced TNF  $\alpha$  response.** THP-1 monocytes were pre-incubated with 5  $\mu$ g/ml of TLR2, TLR4 (InvivoGen), CD14 (eBioscience) antibodies, or a combination of 5  $\mu$ g/ml mouse IgG1 and 10  $\mu$ g/ml rat IgG isotype control, as described in Methods. Individual cell treatments were also supplemented with one or both of the mentioned IgGs to match the concentration of the IgG controls. After pre-treatment, THP-1 cells were stimulated with 15  $\mu$ M of A $\beta$ (1-42) for 6 hours. TNF $\alpha$  was measured using ELISA. Results are presented as % TNF $\alpha$  of A $\beta$  response treated with phosphate buffered saline (PBS) medium. Actual TNF $\alpha$  levels induced by A $\beta$  alone averaged 487 pg/ml. Error bars correspond to SE for n = 3 trials. A Student's t-test was used to calculate the significance between individual TLR and the mouse IgG1/rat IgG isotype control (\*p < 0.001). Less significant differences were observed for individual anti-TLR2 (p < 0.25), anti-TLR4 (p < 0.05) and anti-CD14 (p < 0.20) antibody treatments. rIgG; rat IgG, mIgG1; mouse IgG1

occurring. Blocking both TLR2 and TLR4 simultaneously (TLR2/TLR4) was much more effective in neutralizing the response (60% reduction). The most effective reduction of A $\beta$  response was observed when all TLR2, TLR4 and CD14 (TLR2/TLR4/CD14 triple combination) were neutralized (71.3% reduction, compared with the mouse IgG1/rat IgG isotype control).

#### 4.2.1.5 TLR1 and TLR6 may also be involved in fibrillar A $\beta$ (1-42)-induced activation of the innate immune response

We have so far demonstrated that TLR2 plays an active role in A $\beta$ -induced initiation of innate immune response. TLR2 forms a TLR2/TLR6 or TLR2/TLR1 heterodimer to recognize diacylated and triacylated lipopeptides (LPT), respectively (Nakata et al., 2006). To assess if TLR2 also requires complex formation with either TLR1 or TLR6 for recognition of fibrillar A $\beta$ , we have included TLR1 and TLR6 antibodies in our TLR neutralization analysis.

To test the effectivity of the added antibodies, we performed neutralization assay using the known TLR2 agonists, Pam<sub>3</sub>CSK<sub>4</sub> (for TLR2/1) or FSL-1 (for TLR2/6) (Figure 4.8). Unlike the previous neutralization experiment for TLR ligands (Figure 4.3 and 4.4), we lowered our TLR antibody concentration to 1  $\mu$ g/ml in this study to better assess the effect of the antibody neutralization, since using 10  $\mu$ g/ml of the TLR1 or TLR6 antibody completely eradicated the agonist signals (data not shown). As described in Methods, THP-1 cells were pre-incubated with TLR antibodies or isotype control for 1 hour prior to 6-hour cellular stimulation with A $\beta$ (1-42). Results clearly showed that triacylated

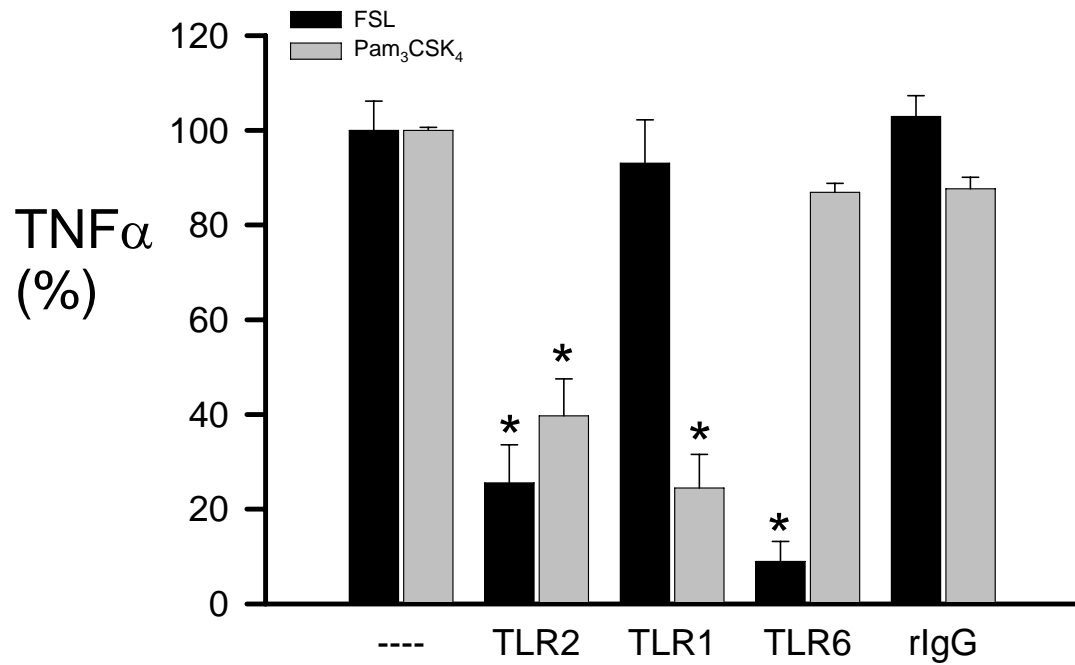


**Figure 4.8. TLR2 complex antibody neutralization of known TLR2 agonists, synthetic diacylated or triacylated lipopeptides.** THP-1 monocytes were pre-incubated with 1  $\mu$ g/ml of TLR antibodies (InvivoGen) or its isotype control rat IgG (Sigma) for 1 hour, prior to 6-hour cellular stimulation with either 10 ng/ml of FSL-1 (black bars) or 1 ng/ml of Pam<sub>3</sub>CSK<sub>4</sub> (gray bars). Secreted TNF $\alpha$  was measured by ELISA. Results are presented as % TNF $\alpha$  of FSL-1 or Pam<sub>3</sub>CSK<sub>4</sub> pre-incubated with phosphate-buffered saline (PBS) medium. Error bars represent SE for nine trials. A Student's t-test was used to calculate the significance between individual TLR and their respective isotype IgG controls (\*p < 0.001)

synthetic Pam<sub>3</sub>CSK<sub>4</sub> activates downstream immune signaling via TLR2/TLR1 heterodimers. A significant 60% and 75% reduction in TNF $\alpha$  response were observed when TLR2 and TLR1 were neutralized, respectively ( $p < 0.001$ ). Antibody blockade of TLR6 lowered the Pam<sub>3</sub>CSK<sub>4</sub>- induced secretion of TNF $\alpha$  by 13% (% response of  $86.9 \pm 1.9$ ); however, this result was not significantly different from that of its isotype control rat IgG (% response of  $87.65 \pm 2.4$ ). Likewise, diacylated synthetic FSL-1 utilizes TLR2/TLR6 complex for activation of downstream signaling, as depicted by 71% and 91% reduction in TNF $\alpha$  response when TLR2 and TLR6 were blocked with 1  $\mu$ g of the antibody, respectively.

Next, the TLR antibody neutralization experiment was utilized to answer the question: is TLR2/TLR1 or TLR2/TLR6 complex formation required for A $\beta$ -induced activation of the innate immune response, or does A $\beta$  interact with TLR2 alone? For this study, we have reverted back to using 10  $\mu$ g/ml of the TLR antibodies. For the purpose of investigating the importance of TLR2 complex formation, we have included combination neutralization of TLR2/TLR1 and TLR2/TLR6 in our neutralization experiment. The cell treatments with individually blocked TLRs were supplemented with 10  $\mu$ g/ml of the isotype rat IgG control to match the concentration of double combination TLR2/TLR1 or TLR2/TLR6 with isotype control amounts. Our preliminary results suggest that TLR1 and/or TLR6 may also have an active role in A $\beta$  response (Figure 4.9). Neutralizing TLR2 with 10  $\mu$ g/ml of the antibody decreased the A $\beta$ -induced %TNF $\alpha$  response to  $39.9 \pm 2.6$  (70% reduction). Surprisingly, blocking either TLR1 or TLR6 also significantly lowered the TNF $\alpha$  response, compared to the isotype rate IgG ( $p < 0.001$ ). TLR1 was much more effective in neutralizing the A $\beta$  signal than TLR6, as shown by 57%

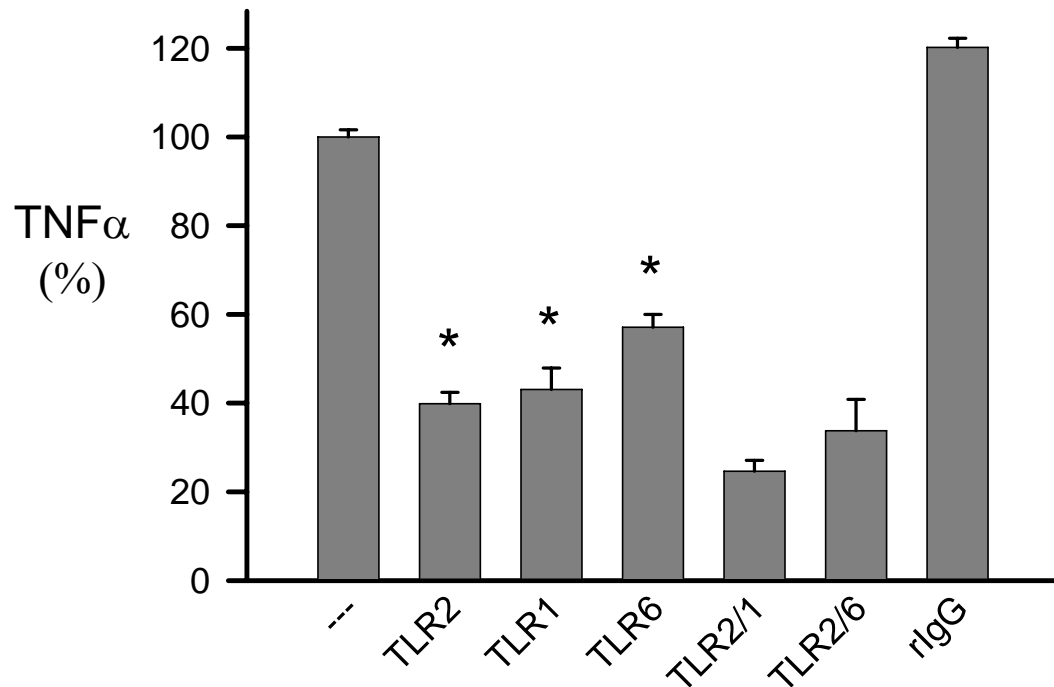


**Figure 4.9. Combination TLR2 complex antibody neutralization of A $\beta$ (1-42)-induced TNF  $\alpha$  response.** THP-1 monocytes were pre-incubated with 10  $\mu$ g/ml of TLR2, TLR1, TLR6 (InvivoGen) antibodies, or 20  $\mu$ g/ml rat IgG isotype control for 1 hour, as described in Methods. Individual cell treatments were also supplemented with 10  $\mu$ g/ml of rat IgG to match the concentration of the 20  $\mu$ g/ml rat IgG control. After pre-treatment, THP-1 cells were stimulated with 15  $\mu$ M of A $\beta$ (1-42) for 6 hours. TNF $\alpha$  was measured using ELISA. Results are presented as % TNF $\alpha$  of A $\beta$  response treated with phosphate buffered saline (PBS) medium. Error bars represent SE for n= 18 trials (6 separate experiments) for TLR2, TLR1, TLR6, and n = 6 trials (2 separate experiments) for TLR2/TLR1 and TLR2/TLR6. A Student's t-test was used to calculate the significance between individual TLR and the rat IgG isotype control (\*p < 0.001). rIgG; rat IgG

reduction for TLR1 neutralization compared to 43% for TLR6 blockade. The A $\beta$  signal was further decreased when the combination of TLR2/TLR1 or TLR2/TLR6 were blocked. Neutralization of TLR2/TLR1 complex decreased the % response to  $24.7 \pm 2.43$ , while TLR2/TLR6 complex blockade lowered the % response to  $33.77 \pm 2.04$ . A slight enhancement of A $\beta$  response was observed for cells pre-incubated with 20  $\mu\text{g/ml}$  of TLR isotype rat IgG control. Overall, the presented results demonstrated that TLR2 and TLR4 have an active role in A $\beta$ -induced activation of the innate immune response. Additionally, our recent data also suggests a possible involvement of TLR1 and TLR6 as well for A $\beta$  activation of downstream TLR signaling.

#### 4.2.2. Mammalian Cell System: Human Embryonic Kidney (HEK) cells

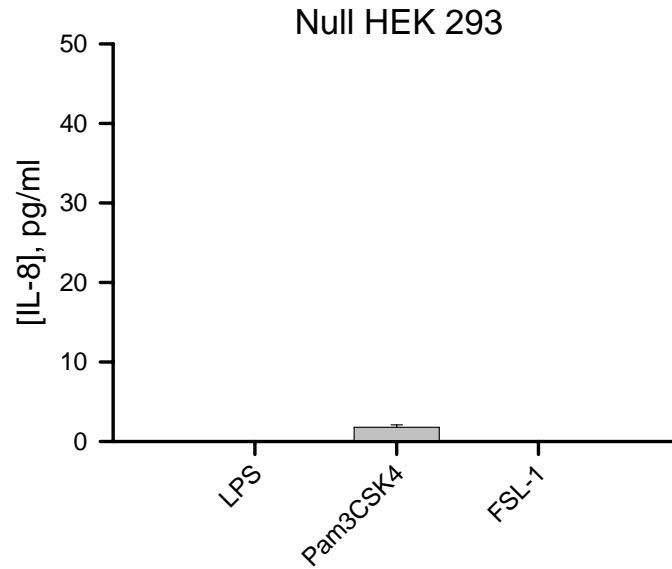
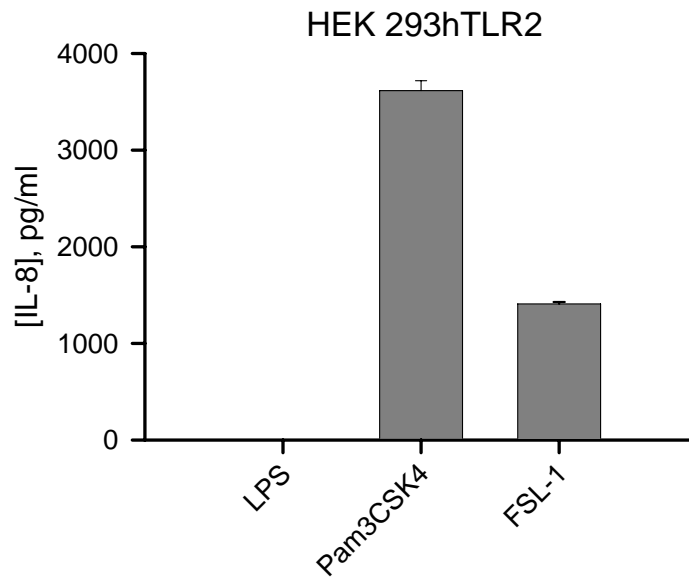
##### 4.2.2.1 Induction of proinflammatory IL-8 production in transfected HEK 293 cells with known TLR agonists

The main purpose of the study is to determine which TLR is responsible for A $\beta$ -dependent inflammatory response. Using THP-1 monocytes, we have identified TLR2 and TLR4 to have a role in A $\beta$  activation of the innate immune response. Numerous investigators whose focus is to study the mechanisms involved in TLR recognition and signaling utilize model cell lines such as Human embryonic kidney (HEK) cells (Bauer; Chen et al., 2006; Walter et al., 2007; Goodridge and Underhill, 2008). We have started utilizing HEK293 cells to further investigate the role of TLR2 and its complex (TLR2/1 or TLR2/6) in A $\beta$  proinflammatory response. This mammalian cell line does not express

TLR2 and other TLRs (Razonable et al., 2006), although recent studies have shown that HEK293 cells express low amounts of TLR1 and TLR6 (InvivoGen, 2006). We have acquired human HEK293 cells transfected with TLR2 (herein referred to as HEK 293hTLR2) to substantiate the role of TLR2 in A $\beta$  response. For proper interpretation of results, we have also acquired non-transfected HEK293 cells (herein referred to as null HEK293).

We began our investigation by first testing the ability of our known TLR agonists to induce IL-8 production in our HEK293 cell lines (Figure 4.10). HEK 293hTLR2 cells were strongly stimulated to produce IL-8 in the presence of 1 ng/ml of Pam<sub>3</sub>CSK<sub>4</sub> (TLR2/1 ligand) or 1 ng/ml of FSL-1 (TLR2/6 ligand) (Figure 4.10b). Expectedly, our ultrapure LPS (TLR4 ligand) failed to stimulate our TLR2 transfected cells in producing IL-8. Null HEK293 cells, on the other hand, were not stimulated by same concentration of the known TLR agonists (Figure 4.10a). The data presented here signify that the acquired TLR2-transfected HEK 293 cells are devoid of any traces of TLR4, and our Null HEK293 cells may be used for succeeding experiments as control cells.

We wanted to know if our TLR neutralization assay can also be applied to our HEK 293hTLR2. HEK 293TLR2 cells were grown, as described in Methods. Cells were pre-treated with 10  $\mu$ g/ml of the TLR antibodies or isotype rat IgG control for 1 hour prior to 24-hour stimulation with either 1 ng/ml of Pam<sub>3</sub>CSK<sub>4</sub> or 1 ng/ml of FSL-1. After post-stimulation, IL-8 levels were measured by ELISA. Our results confirmed the effectiveness of the TLR neutralization assay on this cell line. Antibody blockade of TLR2 or TLR1 decreased the Pam<sub>3</sub>CSK<sub>4</sub>-induced IL-8 response to  $30.9 \pm 0.84$  and  $20.9 \pm 1.34$ , respectively (Figure 4.11). These signify a 48% reduction for TLR2, and 58%

**A****B**

**Figure 4.10. PAMP activity on HEK 293 cells.** (A) Activity of PAMPs on Null HEK293 cells. Cells were grown, as described in Methods, prior to 24-hour stimulation with known TLR PAMPs. Concentration of the agonists are *E. coli* K12 LPS (10 ng/ml), Pam<sub>3</sub>CSK<sub>4</sub> (1 ng/ml), and FSL-1 (1 ng/ml). (B) Stimulation of TLR2-transfected HEK 293 cells (HEK 293hTLR2) with known TLR agonists. Concentration of agonists is the same as in A. For both instances, secreted IL-8 was measured by ELISA. These results represent 1 representative experiment of 4. Error bars represent SE of n= 3 trials (1 experiment)

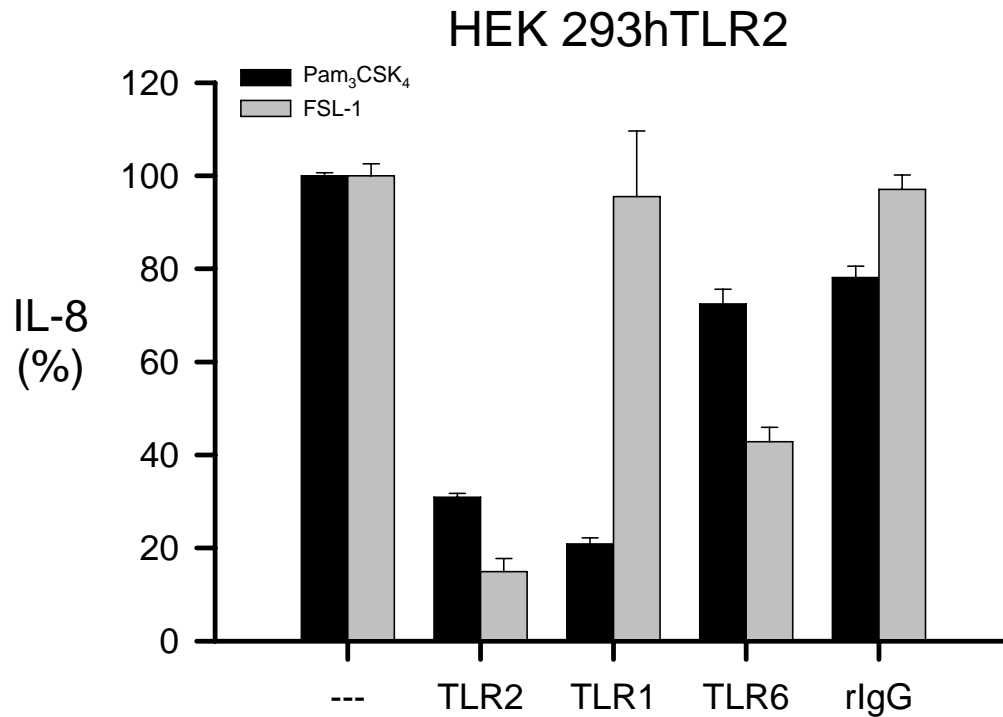


**Figure 4.11. TLR2 complex antibody neutralization of TLR2 ligands.** HEK 293hTLR2 cells were pre-incubated with 10  $\mu\text{g/ml}$  of TLR2, TLR1, TLR6 (InvivoGen) antibodies, or 20  $\mu\text{g/ml}$  rat IgG isotype control for 1 hour, as described in Methods. After pre-treatment, HEK 293hTLR2 cells were stimulated with 1 ng/ml of either Pam<sub>3</sub>CSK<sub>4</sub> or FSL-1 for 24 hours. IL-8 was measured using ELISA. Results are presented as % IL-8 of Pam<sub>3</sub>CSK<sub>4</sub> or FSL response treated with phosphate buffered saline (PBS) medium. Error bars represent SE for n= 6 trials (2 separate experiments) for Pam<sub>3</sub>CSK<sub>4</sub> and n = 3 trials (1 experiment) for FSL-1. rIgG; rat IgG

reduction for TLR1, compared to the rat IgG isotype control. TLR6 blockade evoked a 28% attenuation of Pam<sub>3</sub>CSK<sub>4</sub> response. However, this attenuation was comparable to that of the rat IgG isotype control (22% reduction). Antibody neutralization of the TLR2/TLR6 agonist FSL-1 was clear. TLR2 neutralization almost completely abrogated FSL-1- induced IL-8 response (85% reduction) while TLR6 blockade lowered the FSL-1 response by 57% (% response of  $42.8 \pm 3.13$ ). TLR1 neutralization did not have an effect on the FSL-1 response. For all neutralization experiments, we have included stimulation of null HEK293 cells with the TLR agonists. Similar to Figure 4.10, 1 ng/ml of Pam<sub>3</sub>CSK<sub>4</sub> or FSL-1 did not induce IL-8 production in null HEK 293 cells.

#### 4.2.2.2 Induction of proinflammatory IL-8 production in transfected HEK 293 cells with fibrillar A $\beta$ (1-42)

To understand the contribution of TLR2 in A $\beta$ -induced immune response, and to assess the responsiveness of the HEK cells to A $\beta$ , we next stimulated our HEK 293 cells with 15  $\mu$ mol/L of A $\beta$ (1-42). Null HEK 293 cells and HEK 293hTLR2 cells were grown, as described in Methods. After 4 hours of allowing the cells to adhere in the cell culture plate, cells were stimulated with 15  $\mu$ mol/L of A $\beta$ (1-42) for 24 hours. The IL-8 level was measured post-stimulation by ELISA. As seen in Figure 4.12, TLR2-transfected HEK cells produced a significant amount of IL-8 (81 pg/ml/10<sup>6</sup> cells  $\pm$  1.8), while null HEK cells failed to produce IL-8 upon A $\beta$  stimulation. This result further substantiates our finding that TLR2 plays a role for A $\beta$ -induced proinflammatory production.

We carried out the TLR antibody neutralization to further verify the role of TLR2,

as well as TLR2 complex, in A $\beta$  response. We pre-treated our Null HEK cells and HEK 293hTLR2 cells with 10  $\mu$ g/ml of TLR antibodies (InvivoGen) or rat IgG isotype control (Sigma) for 1 hour prior to 24-hour cell stimulation with 15  $\mu$ mol/L of A $\beta$ (1-42). As expected, A $\beta$  treatment did not stimulate our null HEK cells in producing IL-8. Our initial results with the HEK 293TLR2 cells (data not shown) revealed a big reduction in A $\beta$ -IL-8 response when TLR1 was neutralized (70% reduction). A 30% reduction was also observed when TLR2 and TLR6 were blocked. However, there was a substantial attenuation of A $\beta$  response when cells were pre-treated with the isotype IgG control. This issue of reduced A $\beta$  response with IgG control made it impossible to interpret our TLR neutralization results properly. The TLR neutralization of A $\beta$ -induced IL-8 response in HEK 293TLR2 is an ongoing investigation in our lab and the effect of isotype IgG control needs further analysis.

### 4.3. Discussion

The data that we have presented in this study emphasize the role of toll-like receptors in A $\beta$ -induced activation of the innate immune response. By utilizing THP-1 monocytes which naturally express TLRs ((Faure et al., 2000), we have identified TLR4 and TLR2 to be involved in proinflammatory response initiated by fibrillar A $\beta$ (1-42). These results were consistent with that of Fassbender and colleagues (Fassbender et al., 2004). Using an antibody neutralization assay, they reported a CD14-dependent microglial activation by fibrillar A $\beta$ . Moreover, they presented A $\beta$  activation by nuclear

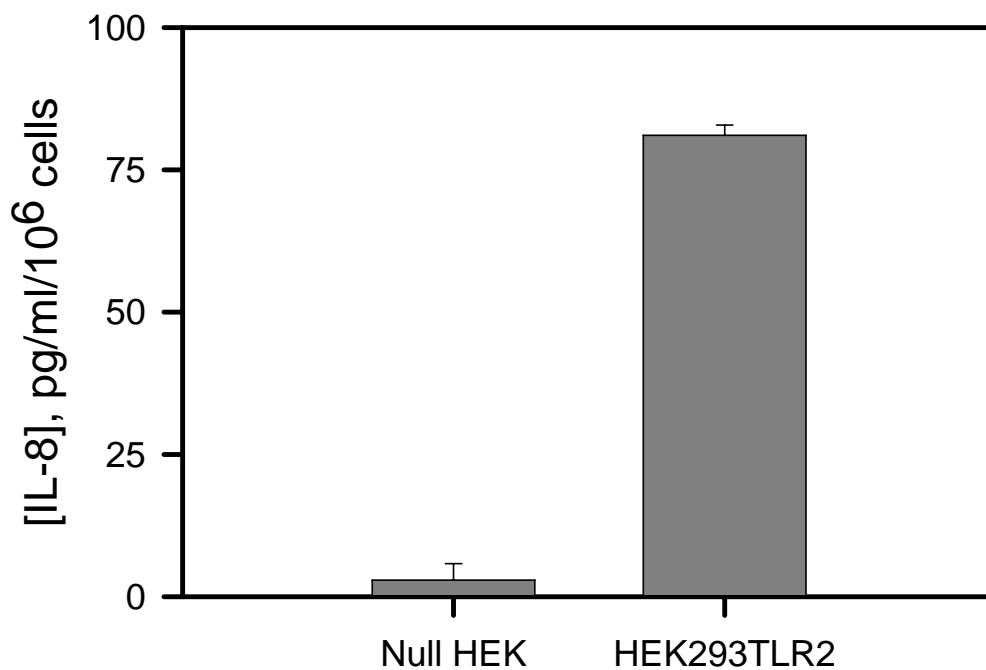


**Figure 4.12. Fibrillar A $\beta$ (1-42) activity on HEK 293 cells.** Null HEK293 cells and TLR-2 transfected HEK293 cells (HEK 293hTLR2) were grown, as described in Methods, prior to 24-hour stimulation with 15  $\mu$ M of A $\beta$  aggregated at 216 hours. Secreted IL-8 was measured by ELISA. This result represent 1 representative experiment of 3. Error bars represent SE of n= 3 trials (1 experiment)

translocation of NF $\kappa$ B in CD14-transfected Chinese hamster ovary (CHO-K1) cells. Since the CHO cells lack a functional TLR2, they suggested that TLR4 may be responsible for A $\beta$  signal transduction.

Our TLR antibody neutralization in THP-1 monocytes clearly demonstrated the importance of TLR4 in A $\beta$ -induced immune response (Figure 4.5, 4.6b, 4.7). A consistent 50-60% reduction of the A $\beta$ -induced TNF $\alpha$  response was observed when cells were pre-incubated with TLR4 antibody. Additionally, we identified TLR2 to be equally responsible for fibrillar A $\beta$  response. In fact, our results showed a more significant reduction of A $\beta$  response from TLR2 antibodies than from TLR4 antibodies (Figure 4.5, 4.6b). We have further substantiated our finding that TLR2 is involved in fibrillar A $\beta$ -induced immune response by using a TLR2-transfected cell line. HEK cells do not express TLR2 (Razonable et al., 2006), thus it is a model system in further clarifying the importance of TLR in agonist signaling. Stimulation of HEK 293hTLR2 with 15  $\mu$ mol/L of A $\beta$  resulted in the production of proinflammatory IL-8, while the same concentration of A $\beta$  failed to stimulate the Null HEK293 cells for IL-8 production (Figure 4.12). This result implies that the transfected TLR2 gene was responsible for A $\beta$ -induced IL-8 response.

Our results have also indicated that TLR2 and TLR4 may compensate for each other for transduction of A $\beta$  signal when necessary (Figure 4.7). Moreover, we have further demonstrated the importance of CD14 on the A $\beta$ -induced activation of downstream signaling (Figure 4.5, 4.6a, 4.7). One difficulty that we encountered using TLR neutralization of A $\beta$  response is a consistent stimulation of TNF $\alpha$  response for CD14 isotype control, IgG1 (Figure 4.5, 4.6a). This 20-30% increase in signal may have

offset the effectiveness of our anti-CD14 neutralization. These issues emphasize the importance of including the isotype controls in the experiment for proper and accurate interpretation of results.

Several groups have started to focus on Toll-like receptors and its accessory proteins to better understand the mechanism of A $\beta$  inflammatory response or clearance. Using cultured CD14-positive microglia and microglia derived from CD14-deficient mice, Liu *et al* emphasized the importance of CD14 in A $\beta$ (1-42) phagocytosis by microglia (Liu et al., 2005). *In vivo* studies using Mo/Hu APP<sup>swe</sup> PS1<sup>DE9</sup> mice deficient in TLR4 showed a decreased clearance of diffuse and fibrillar A $\beta$  deposits, demonstrating the significance of TLR4 signaling pathway in A $\beta$  load and clearance in AD brain (Tahara et al., 2006). Furthermore, using immunohistochemical staining, Liu *et al.* reported a strong expression of CD14 on brain sections of AD patients as compared to that of control subjects (Liu et al., 2005). Recently, Fassbender's group also released their findings that TLR4-deficient mice C3H/HeJ strongly inhibited monocytic and microglial activation by aggregated A $\beta$ (1-42) as demonstrated by a significant decrease in the secretion of IL-6, TNF $\alpha$  and nitric oxide compared to the wildtype C3H/HeN (expressing TLR4) mice (Walter et al., 2007). This result further supported our findings of TLR4-mediated A $\beta$  proinflammatory response. Similarly, findings by Jin, *et al.* showed that TLR4 was also implicated in the upregulation of proinflammatory (TNF $\alpha$ , IL-1 $\beta$ , IL-10, IL-17) products in the brains of TLR4 wildtype AD mice as compared to TLR4 wildtype non-transgenic mice (Jin et al., 2008). Recently, Rivest and colleagues have also published reports implicating TLR2 an endogenous receptor that is involved in clearance of A $\beta$ (1-42) (Richard et al., 2008). Overall, our findings, together with these other

studies, contributed to growing evidences linking neurodegenerative diseases with innate immune response.

Investigating the ligand-TLR interaction means that utmost care should be taken to ensure that the agonists are free of contamination that might falsely activate certain TLRs (Kielian, 2006). Over the years, the purity of TLR agonists has been an ongoing issue in investigating agonist-TLR interaction (Hirschfeld et al., 2000; Gao et al., 2001; Lee et al., 2002). We have carefully prepared our A $\beta$ (1-42) samples and made sure that our preparations are free of contaminating traces of LPS. Although the commercial A $\beta$  lots were already endotoxin-tested prior to shipment (0.35 EU/mg, which corresponds into an effective LPS concentration of 8 pg/ml) (Gao and Tsan, 2003), we still have continuously monitored our A $\beta$  preparations using PMX-B. PMX-B is often used in cell culture systems to test for LPS contamination (Weaver et al., 2007). Our A $\beta$  preparations were devoid of any traces of bacterial LPS contamination, as depicted by Figure 4.2b. XTT proliferation assay was also done routinely to verify the purity of our A $\beta$  preparations. Moreover, the possibility of contamination in our A $\beta$  preparation was invalidated by our A $\beta$  aggregation data (Figure 3.1) which demonstrated a steady increase of TNF $\alpha$  production when A $\beta$  was aggregated at 4°C for up to 96 hours, followed by a decline of the TNF $\alpha$  signal to baseline level when A $\beta$  was incubated for longer period of time (216 hours). This trend would not be observed if traces of contaminating TLR ligands are present in our A $\beta$  preparation. Degradation of the contaminants is also not expected, thus, if there is a presence of any traces of bacterial contaminants, the A $\beta$ -induced TNF $\alpha$  signal should remain at 216 hours.

Our preliminary results with THP-1 monocytes (Figure 4.9) also suggest a

possible role for TLR1 and TLR6 in A $\beta$  activation of the innate immune response. Our laboratory, and others, have demonstrated the importance of TLR2 in A $\beta$ -induced immune response (Jana et al., 2008; Richard et al., 2008; Udan et al., 2008). TLR2 is known to form a heterodimeric complex with either TLR1 or TLR6 for recognition of a wide spectrum of ligands (Schroder et al., 2004; Manukyan et al., 2005; Kielian, 2006). Our TLR neutralization revealed a significantly decreased TNF $\alpha$  response for A $\beta$  when TLR1 and TLR6 were blocked. Interestingly, TLR1 seems to have more effect in A $\beta$  response than TLR6, as demonstrated by greater inhibition with 10  $\mu$ g/ml of TLR1 antibody as compared to TLR6. We wanted to further investigate the possibility of TLR2-complex formation for recognition of A $\beta$  by doing antibody neutralization on TLR2-transfected HEK293 cell line. We are on our preliminary stage of investigation using HEK 293 cells, however, rat IgG effects on the A $\beta$  response have been encountered and are being carefully assessed. Nevertheless, understanding the role of TLR1 and TLR6 in A $\beta$  interaction with TLR2 will give us further insight on A $\beta$ -TLR2 recognition.

Numerous investigations about structures of TLR-ligand complexes have continuously emerged over the years to better understand their activation mechanisms. Previous report about the crystal structure of TLR1-TLR2-Pam<sub>3</sub>CSK<sub>4</sub> emphasizes the importance of the lipid chains of Pam<sub>3</sub>CSK<sub>4</sub> in its interaction with the TLR2/TLR1 heterodimers (Jin et al., 2007). The crystal structure showed the interaction of two of the three lipid chains of Pam<sub>3</sub>CSK<sub>4</sub> with TLR2 pocket, and the last lipid chain is inserted into a hydrophobic channel of TLR1. Likewise, structure studies of LPS-TLR4-MD2 binding were done using LPS antagonist Eritoran. LPS is an amphipathic macromolecule composed of hydrophobic lipid A, composed of four to seven acyl chains and

phosphorylated di-glucosamine, core and O-antigen (Chapter 1, Figure 1.5). Eritoran, on the other hand, is a structural mimic of lipid A of LPS, with four acyl chains and a phosphorylated glucosamine backbone (Mullarkey et al., 2003; Rossignol and Lynn, 2005). Structural studies of Eritoran-MD2-TLR4 shows binding of Eritoran to the hydrophobic pocket of MD-2 via its acyl chains (Kim et al., 2007). Moreover, a crystal structure of mouse CD14 shows a large hydrophobic pocket on the N-terminal which was identified to be the main component of the LPS-binding site (Kim et al., 2005). A structural model of A $\beta$  fibrils by NMR spectroscopy revealed a double-layered  $\beta$  sheet structure with a hydrophobic core and a hydrophobic face. It is thus possible that hydrophobicity plays a big role in ligand-TLR recognition, and the hydrophobicity possessed by A $\beta$  may also be responsible for its recognition by CD14, TLR4 and TLR2.

The association of A $\beta$  with inflammation is ongoing research in the field of AD. It remains to be determined whether inflammatory response is advantageous or detrimental to neuron survival. The identification of several receptors on microglia and monocytes that recognize fibrillar A $\beta$  has opened new venues for understanding the mechanism of A $\beta$  and inflammatory response. The inclusion of TLRs in the list of receptors that recognize A $\beta$  contributes to the role of innate immunity in the pathogenesis of AD, and therefore may be a powerful tool for identification of therapeutic targets that slow the progression of AD.

#### 4.4. Bibliography

- Aderem, A., R. J. Ulevitch. 2000. Toll-like receptors in the induction of the innate immune response. *Nature*. 406:782-787.
- Akiyama, H., S. Barger, et al. 2000. Inflammation and Alzheimer's disease. *Neurobiol Aging*. 21:383-421.
- Albiger, B., S. Dahlberg, et al. 2007. Role of the innate immune system in host defence against bacterial infections: focus on the Toll-like receptors. *J Intern Med*. 261:511-528.
- Apelt, J., R. Schliebs. 2001. Beta-amyloid-induced glial expression of both pro- and anti-inflammatory cytokines in cerebral cortex of aged transgenic Tg2576 mice with Alzheimer plaque pathology. *Brain Res*. 894:21-30.
- Bamberger, M. E., M. E. Harris, et al. 2003. A cell surface receptor complex for fibrillar beta-amyloid mediates microglial activation. *J Neurosci*. 23:2665-2674.
- Bate, C., R. Veerhuis, et al. 2004. Microglia kill amyloid-beta1-42 damaged neurons by a CD14-dependent process. *Neuroreport*. 15:1427-1430.
- Bauer, S., S. Akira, Gunther Hartmann *Toll-like Receptors (TLRs) and Innate Immunity*: Springer.
- Chen, K., P. Iribarren, et al. 2006. Activation of Toll-like receptor 2 on microglia promotes cell uptake of Alzheimer disease-associated amyloid beta peptide. *J Biol Chem*. 281:3651-3659.
- Combs, C. K., J. C. Karlo, et al. 2001. beta-Amyloid stimulation of microglia and monocytes results in TNFalpha-dependent expression of inducible nitric oxide synthase and neuronal apoptosis. *J Neurosci*. 21:1179-1188.
- Combs, C. K., D. E. Johnson, et al. 1999. Identification of microglial signal transduction pathways mediating a neurotoxic response to amyloidogenic fragments of beta-amyloid and prion proteins. *J Neurosci*. 19:928-939.
- Das, S., H. Potter. 1995. Expression of the Alzheimer amyloid-promoting factor antichymotrypsin is induced in human astrocytes by IL-1. *Neuron*. 14:447-456.
- El Khoury, J., S. E. Hickman, et al. 1996. Scavenger receptor-mediated adhesion of

microglia to beta-amyloid fibrils. *Nature*. 382:716-719.

- Fassbender, K., S. Walter, et al. 2004. The LPS receptor (CD14) links innate immunity with Alzheimer's disease. *Faseb J*. 18:203-205.
- Faure, E., O. Equils, et al. 2000. Bacterial lipopolysaccharide activates NF-kappaB through toll-like receptor 4 (TLR-4) in cultured human dermal endothelial cells. Differential expression of TLR-4 and TLR-2 in endothelial cells. *J Biol Chem*. 275:11058-11063.
- Frautschy, S. A., F. Yang, et al. 1998. Microglial response to amyloid plaques in APPsw transgenic mice. *Am J Pathol*. 152:307-317.
- Gao, B., M. F. Tsan. 2003. Endotoxin contamination in recombinant human heat shock protein 70 (Hsp70) preparation is responsible for the induction of tumor necrosis factor alpha release by murine macrophages. *J Biol Chem*. 278:174-179.
- Gao, J. J., Q. Xue, et al. 2001. Commercial preparations of lipoteichoic acid contain endotoxin that contributes to activation of mouse macrophages in vitro. *Infect Immun*. 69:751-757.
- Goodridge, H. S., D. M. Underhill. 2008. Fungal Recognition by TLR2 and Dectin-1. *Handb Exp Pharmacol*. 87-109.
- Griffin, W. S., L. C. Stanley, et al. 1989. Brain interleukin 1 and S-100 immunoreactivity are elevated in Down syndrome and Alzheimer disease. *Proc Natl Acad Sci U S A*. 86:7611-7615.
- Heneka, M. T., M. K. O'Banion. 2007. Inflammatory processes in Alzheimer's disease. *J Neuroimmunol*. 184:69-91.
- Hirschfeld, M., Y. Ma, et al. 2000. Cutting edge: repurification of lipopolysaccharide eliminates signaling through both human and murine toll-like receptor 2. *J Immunol*. 165:618-622.
- Hoshino, K., O. Takeuchi, et al. 1999. Cutting edge: Toll-like receptor 4 (TLR4)-deficient mice are hyporesponsive to lipopolysaccharide: evidence for TLR4 as the Lps gene product. *J Immunol*. 162:3749-3752.
- InvivoGen (2006) Neutralization with Pab-hTLRs. In: *InvivoGen Insight*, p 3.
- Jana, M., C. A. Palencia, et al. 2008. Fibrillar amyloid-beta peptides activate microglia via TLR2: implications for Alzheimer's disease. *J Immunol*. 181:7254-7262.
- Jin, J. J., H. D. Kim, et al. 2008. Toll-like receptor 4-dependent upregulation of cytokines in a transgenic mouse model of Alzheimer's disease. *J Neuroinflammation*. 5:23.
- Jin, M. S., S. E. Kim, et al. 2007. Crystal structure of the TLR1-TLR2 heterodimer

- induced by binding of a tri-acylated lipopeptide. *Cell*. 130:1071-1082.
- Kielian, T. 2006. Toll-like receptors in central nervous system glial inflammation and homeostasis. *J Neurosci Res*. 83:711-730.
- Kim, H. M., B. S. Park, et al. 2007. Crystal structure of the TLR4-MD-2 complex with bound endotoxin antagonist Eritoran. *Cell*. 130:906-917.
- Kim, J. I., C. J. Lee, et al. 2005. Crystal structure of CD14 and its implications for lipopolysaccharide signaling. *J Biol Chem*. 280:11347-11351.
- Klegeris, A., D. G. Walker, et al. 1997. Interaction of Alzheimer beta-amyloid peptide with the human monocytic cell line THP-1 results in a protein kinase C-dependent secretion of tumor necrosis factor-alpha. *Brain Res*. 747:114-121.
- Lai, J. P., W. Z. Ho, et al. 2006. Full-length and truncated neurokinin-1 receptor expression and function during monocyte/macrophage differentiation. *Proc Natl Acad Sci U S A*. 103:7771-7776.
- Lee, H. K., J. Lee, et al. 2002. Two lipoproteins extracted from *Escherichia coli* K-12 LCD25 lipopolysaccharide are the major components responsible for Toll-like receptor 2-mediated signaling. *J Immunol*. 168:4012-4017.
- Liu, Y., S. Walter, et al. 2005. LPS receptor (CD14): a receptor for phagocytosis of Alzheimer's amyloid peptide. *Brain*. 128:1778-1789.
- Manukyan, M., K. Triantafilou, et al. 2005. Binding of lipopeptide to CD14 induces physical proximity of CD14, TLR2 and TLR1. *Eur J Immunol*. 35:911-921.
- McGeer, P. L., M. Schulzer, et al. 1996. Arthritis and anti-inflammatory agents as possible protective factors for Alzheimer's disease: a review of 17 epidemiologic studies. *Neurology*. 47:425-432.
- Miyazono, M., T. Iwaki, et al. 1991. A comparative immunohistochemical study of Kuru and senile plaques with a special reference to glial reactions at various stages of amyloid plaque formation. *Am J Pathol*. 139:589-598.
- Mullarkey, M., J. R. Rose, et al. 2003. Inhibition of endotoxin response by e5564, a novel Toll-like receptor 4-directed endotoxin antagonist. *J Pharmacol Exp Ther*. 304:1093-1102.
- Nakata, T., M. Yasuda, et al. 2006. CD14 directly binds to triacylated lipopeptides and facilitates recognition of the lipopeptides by the receptor complex of Toll-like receptors 2 and 1 without binding to the complex. *Cell Microbiol*. 8:1899-1909.
- Paresce, D. M., R. N. Ghosh, et al. 1996. Microglial cells internalize aggregates of the Alzheimer's disease amyloid beta-protein via a scavenger receptor. *Neuron*.

17:553-565.

- Perry, V. H., T. A. Newman, et al. 2003. The impact of systemic infection on the progression of neurodegenerative disease. *Nat Rev Neurosci.* 4:103-112.
- Poltorak, A., X. He, et al. 1998. Defective LPS signaling in C3H/HeJ and C57BL/10ScCr mice: mutations in Tlr4 gene. *Science.* 282:2085-2088.
- Pristovsek, P., J. Kidric. 1999. Solution structure of polymyxins B and E and effect of binding to lipopolysaccharide: an NMR and molecular modeling study. *J Med Chem.* 42:4604-4613.
- Qureshi, S. T., L. Lariviere, et al. 1999. Endotoxin-tolerant mice have mutations in Toll-like receptor 4 (Tlr4). *J Exp Med.* 189:615-625.
- Razonable, R. R., M. Henault, et al. 2006. Stimulation of toll-like receptor 2 with bleomycin results in cellular activation and secretion of pro-inflammatory cytokines and chemokines. *Toxicol Appl Pharmacol.* 210:181-189.
- Richard, K. L., M. Filali, et al. 2008. Toll-like receptor 2 acts as a natural innate immune receptor to clear amyloid beta 1-42 and delay the cognitive decline in a mouse model of Alzheimer's disease. *J Neurosci.* 28:5784-5793.
- Rogers, J. 2008. The inflammatory response in Alzheimer's disease. *J Periodontol.* 79:1535-1543.
- Rossignol, D. P., M. Lynn. 2005. TLR4 antagonists for endotoxemia and beyond. *Curr Opin Investig Drugs.* 6:496-502.
- Schroder, N. W., H. Heine, et al. 2004. Lipopolysaccharide binding protein binds to triacylated and diacylated lipopeptides and mediates innate immune responses. *J Immunol.* 173:2683-2691.
- Stewart, W. F., C. Kawas, et al. 1997. Risk of Alzheimer's disease and duration of NSAID use. *Neurology.* 48:626-632.
- Tahara, K., H. D. Kim, et al. 2006. Role of toll-like receptor signalling in Abeta uptake and clearance. *Brain.* 129:3006-3019.
- Udan, M. L., D. Ajit, et al. 2008. Toll-like receptors 2 and 4 mediate Abeta(1-42) activation of the innate immune response in a human monocytic cell line. *J Neurochem.* 104:524-533.
- Venters, H. D., Q. Tang, et al. 1999. A new mechanism of neurodegeneration: a proinflammatory cytokine inhibits receptor signaling by a survival peptide. *Proc Natl Acad Sci U S A.* 96:9879-9884.

- Walter, S., M. Letiembre, et al. 2007. Role of the toll-like receptor 4 in neuroinflammation in Alzheimer's disease. *Cell Physiol Biochem.* 20:947-956.
- Weaver, L. K., P. A. Pioli, et al. 2007. Up-regulation of human monocyte CD163 upon activation of cell-surface Toll-like receptors. *J Leukoc Biol.* 81:663-671.
- Wegiel, J., K. C. Wang, et al. 2001. The role of microglial cells and astrocytes in fibrillar plaque evolution in transgenic APP(SW) mice. *Neurobiol Aging.* 22:49-61.
- Yan, S. D., X. Chen, et al. 1996. RAGE and amyloid-beta peptide neurotoxicity in Alzheimer's disease. *Nature.* 382:685-691.
- Yates, S. L., L. H. Burgess, et al. 2000. Amyloid beta and amylin fibrils induce increases in proinflammatory cytokine and chemokine production by THP-1 cells and murine microglia. *J Neurochem.* 74:1017-1025.

## 5 THE ROLE OF MONOCYTE MATURATION AND ITS RELATIONSHIP TO AMYLOID BETA AND INFLAMMATION

### 5.1 Introduction

The presence of activated microglia surrounding neuritic plaques in the AD brain strongly suggests a specific interaction between A $\beta$  and microglia. Moreover, numerous evidence now shows that microglia may be activated by A $\beta$ , leading to initiation of inflammation (Frautschy et al., 1992; Barger and Harmon, 1997; Akama et al., 1998; Hu and Van Eldik, 1999). A plethora of inflammatory products in the brain upon microglial activation may encourage the transmigration of monocytes from the circulation across the blood-brain barrier. Thus, the peripheral monocytes, which differentiate into macrophages during the infective process, may also be present as infiltrated phagocytes along with the resident microglia surrounding the senile plaques (Fiala et al., 1998). Previous reports have shown that A $\beta$  modulates monocyte adhesion (Yan et al., 1996) and differentiation to macrophages (Fiala et al., 1998). Our recent finding demonstrating oligomeric A $\beta$ (1-42)- induced THP-1 monocyte maturation and adhesion was consistent with these previous reports (Crouse et al., 2009). Furthermore, additional studies have documented monocyte/macrophage infiltration to sites of brain A $\beta$  accumulation (Simard et al., 2006; El Khoury et al., 2007). Macrophages play an important role in inflammation through production of proinflammatory cytokines and chemokines, cell adhesion molecules and nitric oxide (NO), among others (Kim et al.,

2006). Thus, the presence of macrophages in the brain may also contribute to the exacerbation of inflammation induced by A $\beta$ .

To study the contribution of macrophages in A $\beta$ -induced immune response, we have modeled the macrophages present in the brain by differentiating our THP-1 monocytes using phorbol myristate acetate (PMA) (Tsuchiya et al., 1982). We have chosen TNF $\alpha$  production as the outcome variable for studying effect of macrophages in A $\beta$ -induced proinflammatory production. In this investigation, we report that differentiation of THP-1 monocytes to macrophages significantly enhanced TNF $\alpha$  production by fibrillar A $\beta$ (1-42), and may further contribute to inflammation in the diseased brain.

## 5.2. Results

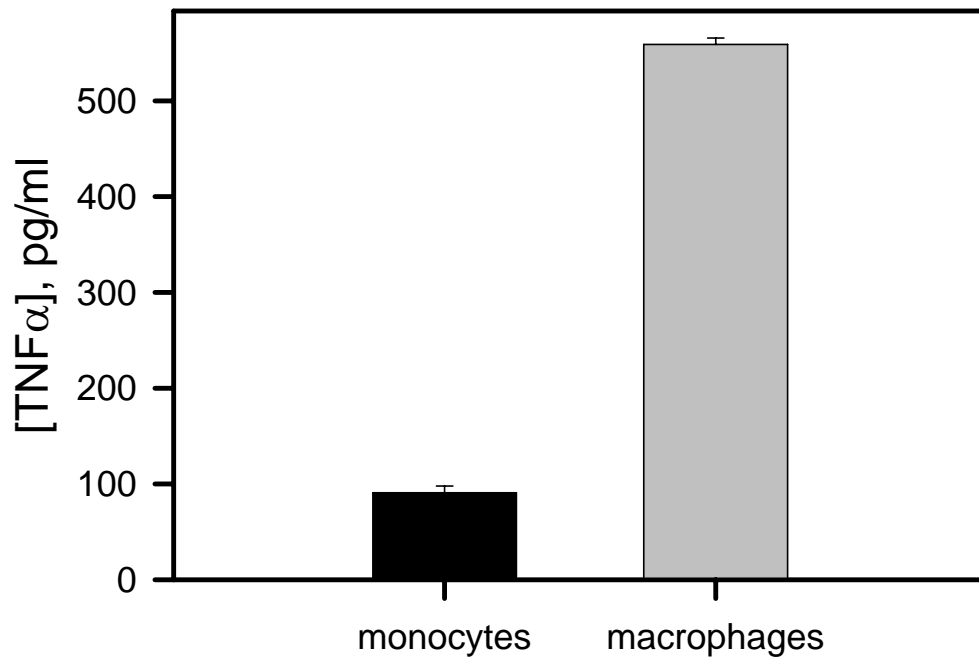
### 5.2.1 TNF $\alpha$ production induced by known TLR agonists in differentiated and undifferentiated THP-1 cells

For our initial investigation, we examined the proinflammatory response of PMA-differentiated THP-1 macrophages to known TLR agonists. THP-1 monocytes grow in suspension and they do not adhere to the surfaces of the cell culture plates. For the induction of differentiation to macrophage-like cells, THP-1 monocytes were treated with 10 ng/ml of PMA for 24 hours, as described in Methods. After incubation with PMA, THP-1 cells became adherent and developed morphological changes characteristics of differentiation to macrophages. The extent of cell adherence was

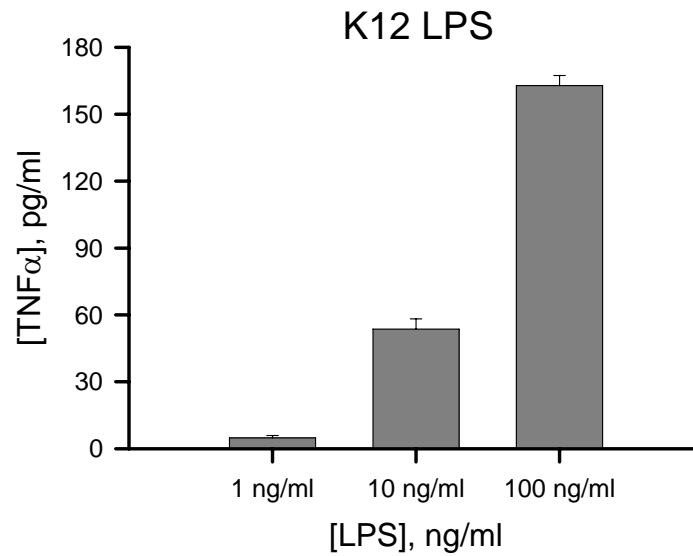
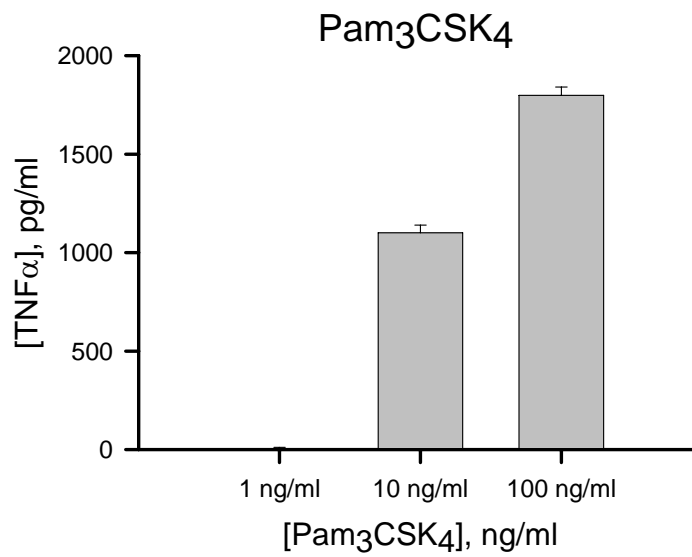
measured by direct counting of the adherent cells and dividing it by the total number of plated cells. Cells that were used for subsequent experiments have % adherence values of 75% and above. Cells that were poorly adherent were not used. Once the % adherence was measured, cells were treated with either ultrapure K12 LPS (TLR4 agonist) or Pam<sub>3</sub>CSK<sub>4</sub> for 6 hours. Figure 5.1 shows the comparison of TNF $\alpha$  secretion for THP-1 monocytes or PMA-induced macrophages that were stimulated with 10 ng/ml of ultrapure K12 LPS. Although undifferentiated THP-1 cells produced TNF $\alpha$  upon stimulation with ultrapure LPS, differentiation of monocytes to macrophages substantially elevated the LPS-induced TNF $\alpha$  response five-fold. Moreover, PMA-differentiated THP-1 macrophages responded to LPS and Pam<sub>3</sub>CSK<sub>4</sub> (TLR2 agonist) stimulation in a dose-dependent manner (Figure 5.2). Our data is consistent with that of Takashiba (Takashiba et al., 1999). The extent of TNF $\alpha$  secretion varies from one experiment to another. This explains the different levels of TNF $\alpha$  when PMA-differentiated THP-1 monocytes were stimulated with 10 ng/ml LPS (Figure 5.1 and 5.2).

#### 5.2.2 A $\beta$ -induced TNF $\alpha$ production is augmented in PMA-derived THP-1 macrophages

We next compared the proinflammatory response of A $\beta$ (1-42) in PMA-differentiated THP-1 cells to that of undifferentiated THP-1 cells. We incubated our THP-1 monocytes and PMA-differentiated THP-1 cells with 15  $\mu$ mol/L of A $\beta$ (1-42) aggregated at 4°C for 48 hours. At various incubation times, secreted TNF $\alpha$  was



**Figure 5.1. LPS-induced TNF $\alpha$  production from differentiated and undifferentiated THP-1 cells.** THP-1 monocytes were differentiated for 24 hours using phorbol-myristate acetate (PMA), as described in the Methods. After incubation, undifferentiated cells (THP-1 monocytes, black bars) and PMA-differentiated cells (macrophages, gray bars) were stimulated with 10 ng/ml of LPS for 6 hours. TNF $\alpha$  was measured in the supernatant after stimulation by ELISA. This result is a represent 1 representative experiment of 3. Error bars denote n = 3 trials (1 experiment)

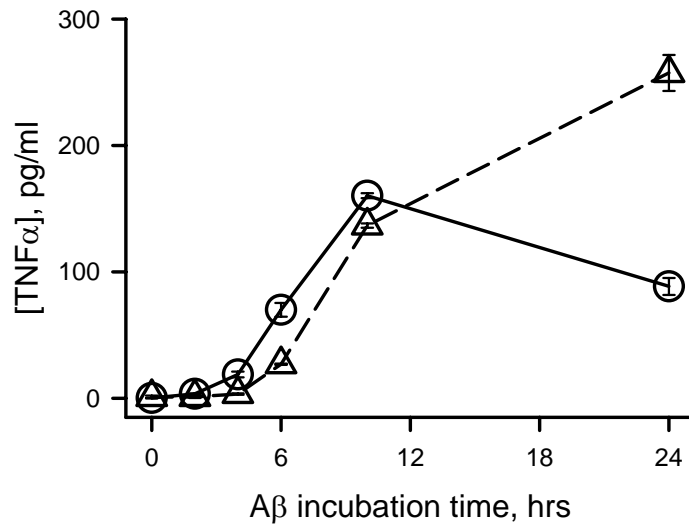
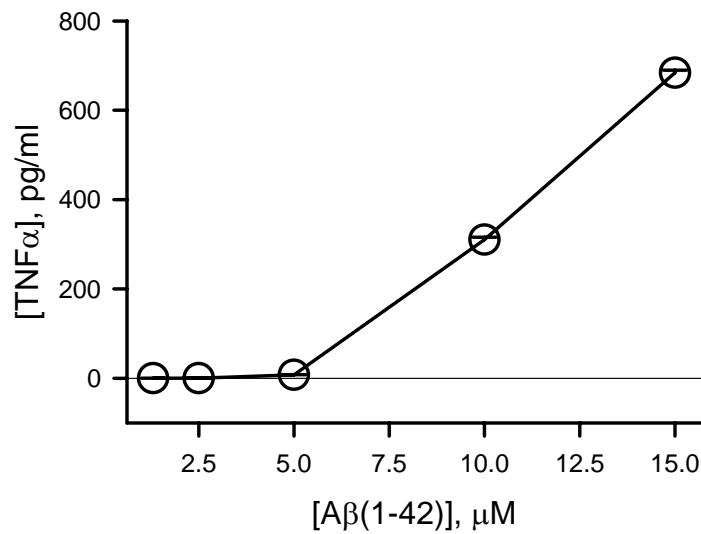
**A****B**

**Figure 5.2. Dose response of TNF $\alpha$  production by known TLR agonists.** THP-1 monocytes were differentiated using 10 ng/ml PMA, as described in Methods. After differentiation, PMA-differentiated cells were treated with increasing concentration of (A)K12 LPS (TLR4 agonist) or (B) Pam<sub>3</sub>CSK<sub>4</sub> (TLR2 agonist) for 6 hours. TNF $\alpha$  was measured using ELISA. This result represent 1 representative experiment of 2. Error bars represent n = 3 trial (1 experiment).

measured. Figure 5.3a demonstrates that A $\beta$ (1-42) stimulated THP-1 monocytes (circle) for TNF $\alpha$  production as early as 4 hours incubation ( $18.9 \pm 2.9$  pg/ml), with maximal response observed at 10 hours (also shown in Figure 3.3a). In comparison, PMA-differentiated THP-1 (triangles) cells began producing considerable TNF $\alpha$  at 6 hours of incubation ( $27 \pm 0.53$  pg/ml) and the TNF $\alpha$  continued to rise even at 24 hours post-stimulation. At this time (24 hours), A $\beta$ -induced TNF $\alpha$  production is three-fold higher in PMA-differentiated cells than undifferentiated cells. Like the response of differentiated THP-1 cells to known TLR agonists, PMA-differentiated THP-1 cells were also stimulated by A $\beta$ (1-42) in a dose-dependent manner (Figure 5.3b). These results demonstrate a more enhanced production of proinflammatory products when macrophages are stimulated by fibrillar A $\beta$ (1-42).

### 5.3 Discussion

Differentiation of THP-1 monocytes to macrophages with phorbol esters have been well-characterized (Tsuchiya et al., 1982; Auwerx, 1991; Takashiba et al., 1999; Traore et al., 2005). One of the most widely-used differentiating agent is 4 $\alpha$ -phorbol-12-myristate-13- acetate (PMA) (Chong et al., 2003; Lai et al., 2006). In this study we have analyzed the contribution of macrophages in A $\beta$ -induced proinflammatory production. We have shown in this preliminary investigation that TNF $\alpha$  production is considerably increased when PMA-derived THP-1 cells were stimulated with known TLR agonists LPS(TLR4) and Pam<sub>3</sub>CSK<sub>4</sub> (TLR2) as compared to undifferentiated cells. Similar results were observed when PMA-differentiated cells were stimulated with 15 $\mu$ M of A $\beta$ (1-42).

**A****B**

**Figure 5.3. Fibrillar A $\beta$ (1-42)-induced TNF $\alpha$  secretion from differentiated and undifferentiated THP-1 cells.** (A) THP-1 monocytes (circles) or PMA-differentiated THP-1 macrophages (triangles) were stimulated for 0, 2, 4, 6, 10 and 24 hours with 15  $\mu$ M A $\beta$ (1-42). After post-stimulation, TNF $\alpha$  was measured using ELISA. (B) Dose response of TNF $\alpha$  secretion. THP-1 monocytes were differentiated with 10 ng/ml PMA, as described in Methods. PMA-derived THP-1 macrophages were stimulated with increasing concentration of A $\beta$ (1-42) for 24 hours. TNF $\alpha$  level was measured by ELISA. For both experiments, error bars represent n = 3 trials (1 experiment)

Takashiba *et al* investigated the relationship between THP-1 cell maturation and mechanism of LPS stimulation. They revealed the novel role for NF- $\kappa$ B in the maturation process. They found that differentiation of THP-1 monocytes to macrophages results in accumulation of NF- $\kappa$ B in the cytoplasm, which is mainly responsible for the enhanced ability of the cell to respond to LPS stimulation (Takashiba *et al.*, 1999). This suggests that accumulation of NF- $\kappa$ B in the cytoplasm upon maturation of monocytes to macrophages primes the cells for increased responsiveness to LPS and in turn, leads to rapid secretion of inflammatory mediators.

Recent reports showed that cytokine gene transcription by A $\beta$  requires stimulation of NF- $\kappa$ B pathway (Combs *et al.*, 2001). The accumulation of NF- $\kappa$ B in the cytoplasm during the differentiation process may thus be correlated to enhanced production of TNF $\alpha$  upon A $\beta$  stimulation. Another possibility for elevated TNF $\alpha$  production in macrophages is the constitutive expression of TLRs. Although the level of TLR2 in macrophages that were derived *in vitro* is similar to that of monocytes, TLR4 expression was significantly increased by about 300% in macrophages when compared to monocytes (O'Mahony *et al.*, 2008). We have previously demonstrated the role of TLR2 and TLR4 in A $\beta$ -induced inflammatory production (Udan *et al.*, 2008) (Chapter 4). A combination of elevated TLR and NF- $\kappa$ B expression in macrophages may be responsible for enhanced proinflammatory production by A $\beta$ .

Several studies have shown a correlation between A $\beta$  accumulation and infiltration of peripheral blood monocytes/macrophages in senile plaques (Fiala *et al.*, 1998; Simard *et al.*, 2006; El Khoury *et al.*, 2007). Oligomeric A $\beta$ (1-42) has likewise been reported to have chemotactic activity (Giri *et al.*, 2000; Le *et al.*, 2001). Moreover,

our lab has reported that oligomeric A $\beta$ (1-42) aggregates induce THP-1 monocyte differentiation to macrophages (Crouse et al., 2009). These evidences suggest that oligomeric A $\beta$ (1-42) may also induce recruitment of blood-derived macrophages to the site of inflammation.

The correlation between A $\beta$  and inflammation in AD brain is an active focus of investigation. Our preliminary data suggests that A $\beta$ -induced heightened inflammation may be mediated by TLRs from resident activated microglia as well as infiltrating macrophages that may also be present surrounding the senile plaque. Further investigations need to be performed to further clarify the mechanism of A $\beta$ -induced immune response and to better understand the contribution of immune cells in AD pathogenesis.

#### 5.4 Bibliography

- Akama K. T., C. Albanese, R. G. Pestell, L. J. Van Eldik. 1998. Amyloid beta-peptide stimulates nitric oxide production in astrocytes through an NFkappaB-dependent mechanism. *Proc Natl Acad Sci U S A.* 95:5795-5800.
- Auwerx J. 1991. The human leukemia cell line, THP-1: a multifaceted model for the study of monocyte-macrophage differentiation. *Experientia.* 47:22-31.
- Barger S. W., A. D. Harmon. 1997. Microglial activation by Alzheimer amyloid precursor protein and modulation by apolipoprotein E. *Nature.* 388:878-881.
- Chong Y. H., Y. J. Shin, Y. H. Suh. 2003. Cyclic AMP inhibition of tumor necrosis factor alpha production induced by amyloidogenic C-terminal peptide of Alzheimer's amyloid precursor protein in macrophages: involvement of multiple intracellular pathways and cyclic AMP response element binding protein. *Mol Pharmacol.* 63:690-698.
- Combs C. K., J. C. Karlo, S. C. Kao, G. E. Landreth. 2001. beta-Amyloid stimulation of microglia and monocytes results in TNFalpha-dependent expression of inducible nitric oxide synthase and neuronal apoptosis. *J Neurosci.* 21:1179-1188.
- Crouse N. R., D. Ajit, M. L. Udan, M. R. Nichols. 2009. Oligomeric amyloid-beta(1-42) induces THP-1 human monocyte adhesion and maturation. *Brain Res.* 1254:109-119.
- El Khoury J., M. Toft, S. E. Hickman, T. K. Means, K. Terada, C. Geula, A. D. Luster. 2007. Ccr2 deficiency impairs microglial accumulation and accelerates progression of Alzheimer-like disease. *Nat Med.* 13:432-438.
- Fiala M., L. Zhang, X. Gan, B. Sherry, D. Taub, M. C. Graves, S. Hama, D. Way, M. Weinand, M. Witte, D. Lorton, Y. M. Kuo, A. E. Roher. 1998. Amyloid-beta induces chemokine secretion and monocyte migration across a human blood-brain barrier model. *Mol Med.* 4:480-489.
- Frautschy S. A., G. M. Cole, A. Baird. 1992. Phagocytosis and deposition of vascular beta-amyloid in rat brains injected with Alzheimer beta-amyloid. *Am J Pathol.* 140:1389-1399.
- Giri R., Y. Shen, M. Stins, S. Du Yan, A. M. Schmidt, D. Stern, K. S. Kim, B. Zlokovic,

- V. K. Kalra. 2000. beta-amyloid-induced migration of monocytes across human brain endothelial cells involves RAGE and PECAM-1. *Am J Physiol Cell Physiol.* 279:C1772-1781.
- Hu J., L. J. Van Eldik. 1999. Glial-derived proteins activate cultured astrocytes and enhance beta amyloid-induced glial activation. *Brain Res.* 842:46-54.
- Kim J. H., J. H. Jeong, S. T. Jeon, H. Kim, J. Ock, K. Suk, S. I. Kim, K. S. Song, W. H. Lee. 2006. Decursin inhibits induction of inflammatory mediators by blocking nuclear factor-kappaB activation in macrophages. *Mol Pharmacol.* 69:1783-1790.
- Lai J. P., W. Z. Ho, L. E. Kilpatrick, X. Wang, F. Tuluc, H. M. Korchak, S. D. Douglas. 2006. Full-length and truncated neurokinin-1 receptor expression and function during monocyte/macrophage differentiation. *Proc Natl Acad Sci U S A.* 103:7771-7776.
- Le Y., W. Gong, H. L. Tiffany, A. Tumanov, S. Nedospasov, W. Shen, N. M. Dunlop, J. L. Gao, P. M. Murphy, J. J. Oppenheim, J. M. Wang. 2001. Amyloid (beta)42 activates a G-protein-coupled chemoattractant receptor, FPR-like-1. *J Neurosci.* 21:RC123.
- O'Mahony D. S., U. Pham, R. Iyer, T. R. Hawn, W. C. Liles. 2008. Differential constitutive and cytokine-modulated expression of human Toll-like receptors in primary neutrophils, monocytes, and macrophages. *Int J Med Sci.* 5:1-8.
- Simard A. R., D. Soulet, G. Gowing, J. P. Julien, S. Rivest. 2006. Bone marrow-derived microglia play a critical role in restricting senile plaque formation in Alzheimer's disease. *Neuron.* 49:489-502.
- Takashiba S., T. E. Van Dyke, S. Amar, Y. Murayama, A. W. Soskolne, L. Shapira. 1999. Differentiation of monocytes to macrophages primes cells for lipopolysaccharide stimulation via accumulation of cytoplasmic nuclear factor kappaB. *Infect Immun.* 67:5573-5578.
- Traore K., M. A. Trush, M. George, Jr., E. W. Spannhake, W. Anderson, A. Asseffa. 2005. Signal transduction of phorbol 12-myristate 13-acetate (PMA)-induced growth inhibition of human monocytic leukemia THP-1 cells is reactive oxygen dependent. *Leuk Res.* 29:863-879.
- Tsuchiya S., Y. Kobayashi, Y. Goto, H. Okumura, S. Nakae, T. Konno, K. Tada. 1982. Induction of maturation in cultured human monocytic leukemia cells by a phorbol diester. *Cancer Res.* 42:1530-1536.
- Udan M. L., D. Ajit, N. R. Crouse, M. R. Nichols. 2008. Toll-like receptors 2 and 4 mediate Abeta(1-42) activation of the innate immune response in a human monocytic cell line. *J Neurochem.* 104:524-533.

Yan S. D., X. Chen, J. Fu, M. Chen, H. Zhu, A. Roher, T. Slattery, L. Zhao, M. Nagashima, J. Morser, A. Migheli, P. Nawroth, D. Stern, A. M. Schmidt. 1996. RAGE and amyloid-beta peptide neurotoxicity in Alzheimer's disease. *Nature*. 382:685-691.

## 6 CONCLUSION

In these studies, we successfully demonstrated that A $\beta$ (1-42) invoked proinflammatory response in human THP-1 monocytes/ macrophages, a mammalian cell model system for human microglia. Moreover, the data presented suggest that the ability of A $\beta$  to induce TNF $\alpha$  production is dependent on its aggregation conformation. Using a combination of AFM and cellular studies, along with high speed centrifugation of A $\beta$  samples and employing conformation-specific antibodies, we reported that the soluble yet fibrillar A $\beta$  species are the bioactive A $\beta$ . These A $\beta$  species exist prior to formation of longer, more mature fibrils, and are thus called fibrillar precursors.

Studying A $\beta$  fibrillogenesis is a very challenging task. Although microscopy (AFM and EM) are valuable tools in studying the morphology of the formed A $\beta$  species, this technique alone could not provide detailed information of the fibril size for different aggregation species nor is appropriate for real time analysis. In order to have a better understanding of the bioactive A $\beta$ (1-42) species, the use of other biophysical techniques that will further provide vital information such as molecular weight and conformation, along with the microscopy studies, may aid in elucidating the A $\beta$ (1-42) species that can activate our THP-1 cells.

We also showed the correlation between A $\beta$  and the innate immune response by identifying the involvement of toll-like receptors, particularly TLR4 and TLR2, in A $\beta$ -induced response. Our findings further suggest that TLR4 and TLR2 may compensate for

one another for A $\beta$ -induced activation of TLR downstream signaling. Moreover, the possibility of A $\beta$  utilizing TLR2/TLR1 or TLR2/TLR6 complex was also suggested based on a significant neutralizing effect of the TLR1 and TLR6 antibodies on A $\beta$  response. The possible involvement of the TLR2/1 or TLR2/6 in A $\beta$ -induced immune response is a good area to follow up on for the information that can be obtained will give us further insight on A $\beta$ -TLR2 recognition. Aside from the TLR neutralization assay, the role of TLRs in A $\beta$ -induced inflammatory response may be confirmed by other methods such as using cell lines transfected with TLR as well as utilizing TLR knockout mice. These are valuable tools for studying the ligand-TLR interaction.

Our results also showed that A $\beta$ -induced TNF $\alpha$  production for PMA-induced THP-1 macrophages is undoubtedly much higher compared to that of THP-1 monocytes. This suggests that infiltrating macrophages that may be present surrounding the senile plaque may also contribute to heightened inflammation that is observed in the AD brain.

Overall, we presented evidences suggesting that inflammation in the AD brain is induced by soluble yet fibrillar species of A $\beta$ (1-42), and the heightened inflammation observed in microglia surrounding the AD senile plaques may in part be due to the contribution of A $\beta$  interaction with TLR2 and TLR4 that are expressed on microglia, as well as the infiltrating macrophages that may be present in the site of injury. This study has thus opened new venues for understanding the mechanism of A $\beta$ -induced inflammatory response and may be a new therapeutic target for AD.

## VITA

Maria Lourdes Dichoso Udan is the daughter of Ofelio Udan and Rosalina (Dichoso) Udan. She was born in the city of Santa Rosa, Laguna in the Philippines on January 1, 1979. She graduated high school from Canossa School of Santa Rosa in 1995 and went on to attend college at the University of the Philippines in Los Baños, Laguna. In 2000, she earned a Bachelors degree in Agricultural Chemistry. Immediately after graduation, she took and passed the Chemistry licensure examination given by the Philippine Regulatory Commission. She worked as a quality control chemist in an electronics company for two years before going back to the University of the Philippines Los Baños to work as an analytical chemist and university research associate.

She joined the Department of Chemistry and Biochemistry at University of Missouri-Saint Louis to pursue graduate studies, majoring in Biochemistry, in 2004. She joined the lab of Dr. Michael R. Nichols for her graduate research. She had done numerous poster and oral presentations in different conferences, such as the ACS Midwest Meetings, UMSL Graduate Poster Presentations, Berg Symposium and the Society for Neuroscience conferences. In 2008, she was awarded the prestigious UMSL Graduate Research Scholarship.